Thèse n° 10 746

From roots to canopy: Unraveling the influence of species diversity on tree water relations under warmer and drier climates

Présentée le 23 février 2024

Faculté de l'environnement naturel, architectural et construit
Laboratoire d'écologie végétale
Programme doctoral en génie civil et environnement

pour l'obtention du grade de Docteur ès Sciences

par

Eugénie Isabelle MAS

Acceptée sur proposition du jury

Prof. S. Bonetti, présidente du jury
Prof. C. Grossiord, Prof. F. Valladares, directeurs de thèse
Dr D. Bonal, rapporteur
Prof. E. Allan, rapporteur
Dr M. Levesque, rapporteur

École
polytechnique
fédérale
de Lausanne

2024

From roots to canopy: Unraveling the influence of species diversity on tree water relations under warmer and drier climates

Dissertation pour l'obtention du grade de Docteurès sciences par :

EUGÉNIE MAS

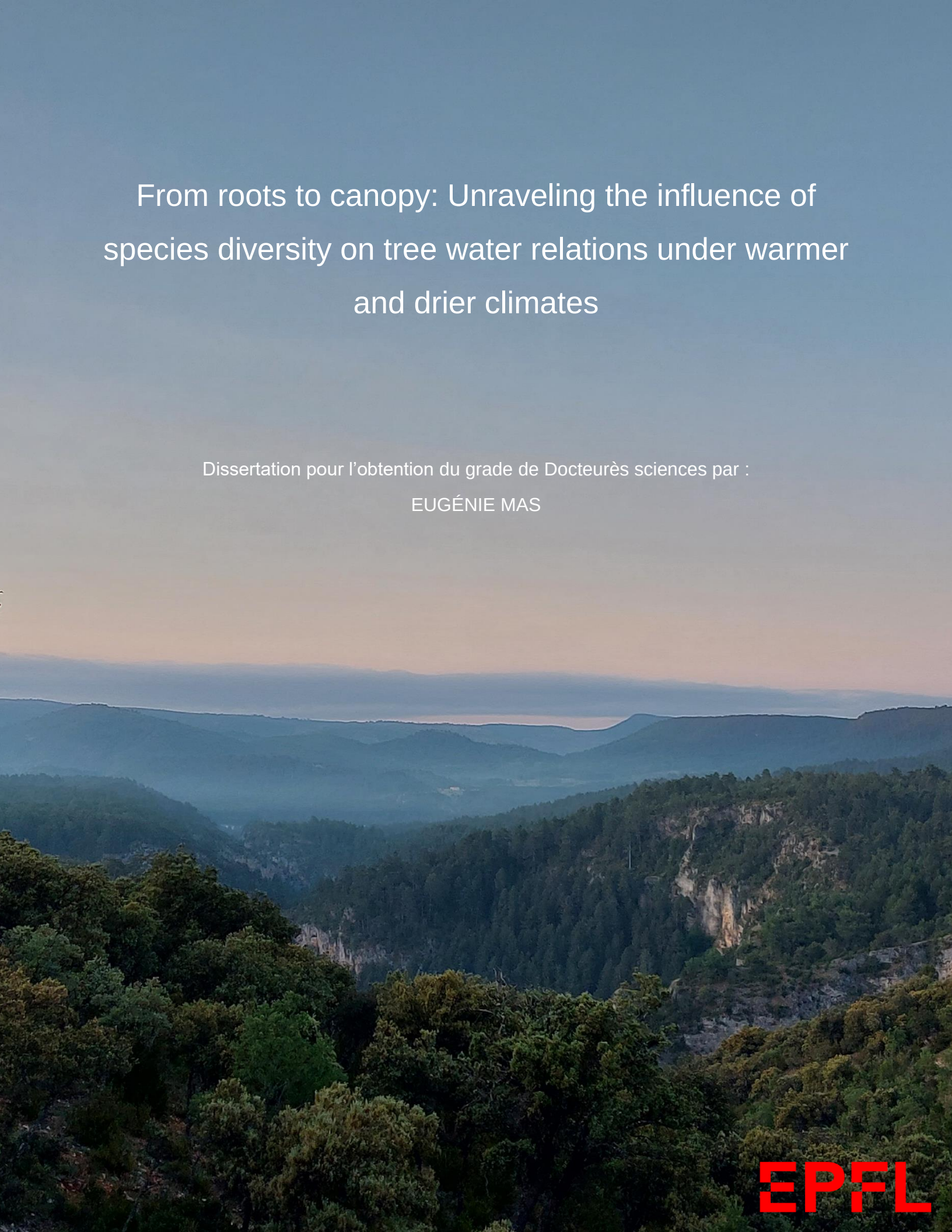

"We are only as strong as we are united, as weak as we are divided."

Albus Dumbledore

Harry Potter and the goblet of fire, JK Rowlings

Acknowledgments

"*The dark forest is strictly forbidden to all students*", said Albus Dumbledore but I dared to venture it with a great fellowship. Thus, I would like to thank my supervisors for their support during my thesis: Charlotte Grossiord and Fernando Valladares. I would like to especially thank Charlotte Grossiord who was always available to guide me in every single one of my projects. I am very grateful that you allowed me to continue my journey in the fascinating field of ecophysiology and forest ecology.

I would like to thank Mathieu Lévesque, Damien Bonal, and Eric Allan for agreeing to review this thesis and examine my defense. I hope you will enjoy reading it as much as I enjoyed writing it.

I am grateful to Alberto Vilagrosa and Luna Morcillo for welcoming me to the University of Alicante and introducing me to many Spanish traditions. Thanks for all your support, advice, and hard work, especially under the burning sun of Ayora. I hope we will collaborate again in the future.

I would also like to thank Hervé Cochard, Nicolas Martin-St Paul, and Matthias Saurer for their collaborations in this thesis; your advice was always useful and improve greatly this project.

Then, I am especially grateful to all my colleagues from the Plant Ecology Research Laboratory (PERL) at EPFL: Arianna Milano, Kate Johnson, Helena Vallicrosa, and Philipp Schuler. Christoph Bachofen, one of the original of the lab, we started it and I will always remember the first lab meetings in the Parc de Milan, the long and deep discussions at the coffee break, and all your advice on statistics to make it pretty. I also thank Sandra Levin Zurcher for your help with all the paperwork and bills coming from the fieldwork and trips. Thanks to Margaux Didion-Gency who introduced me to the MODOEK during my master, always with a smile. Thank you for your good mood, the beers, and the parties! I have also a special thank to Alice Gauthey who were always happy to hear my complaints about science around a glass of wine during our apero/gossip or shopping excursions. Finally, I would like to thank all the Ph.D. students in the lab with whom I shared an office: Thibaut Juillard, Janisse Deluigi, and Laura Merkani. I had a wonderful time in your company, all our discussions, Christmas parties, and beers at Sat were unforgettable and lighted up my time in the lab.

I am also grateful for all the help I have got during my thesis for the experiments in Switzerland with the civil services: Oskar Okaya, Arthur Royston, Stéphanne Jenni, Elias Ackermann, and the EPFL student Erwan Bellon. I would like to especially thank all the technicians and master students who helped me during my crazy fieldwork in Alto Tajo who spent hours driving, cutting and transporting branches and collecting soil cores: Karagan Smith, Omar Tomas, Luis Pizarro, Eric Breton, Giulia Casciano, David Lopez, and Francisco Fornieles. I would like to highlight Alex Tunas Corzon for his great energy and the many hours spent running with branches and driving around. I will always have

a place in my heart for little Terra, the real happiness manager of the lab. I would like to thank Paco and Carlos for their hospitality and great meals, and for accepting to transform the entrance of their hotel into a lab.

Finally, I would like to thank my family and friends. Un grand merci tout d'abord à Jeanne Fournier, Cécile Boulanger et Mélanie Dhinaut pour être de super amies depuis tellement longtemps (plus de 20 ans déjà pour toi, Mélanie). Merci pour m'avoir encouragé à me lancer dans la recherche et aidé à décompresser lors de super aventures avec les Morilles de la mort ou les JennyJeannes! Un grand merci à mon père et ma mère pour m'avoir permise de continuer mes études et encouragés lors de mes décisions. Merci à mon frère Adrien et ma sœur Camille pour leur soutien lors de cette thèse. Pour finir, merci Nola pour avoir supporté tous les séjours chez les uns et les autres pendant mes nombreux déplacements.

Abstract

The worsening of drought events with rising air temperature alters tree water relations causing severe hydraulic impairments and widespread forest mortality. Mixing tree species with contrasting hydraulic traits could reduce forest vulnerability to extreme events through positive species interactions, such as facilitation and niche partitioning. However, it remains unclear if and how species diversity modulates tree water relations as very few studies investigated such relationships mechanistically and in the field.

In this thesis, I aimed to evaluate how tree species diversity affects tree water relations in response to a drying and warming climate, from the roots up to the canopy. The first objective was to identify the physiological mechanisms driving species interaction effects on the leaf- and stem-level water relations in European trees exposed to chronically drier and warmer conditions. In a multi-year climatic manipulation using open-top chambers, I assessed how heat and drought affect the leaf hydraulic traits and time to hydraulic failure of juvenile *F. sylvatica* and *Q. pubescens* trees in monospecific and mixtures. Then, I investigated how tree species diversity alters the seasonal water dynamics in both belowground and aboveground compartments in natural dry forests subjected to seasonal variation in precipitation and temperature. In these mature forests, I studied the seasonal dynamics of *in-situ* hydraulic traits at the leaf, stem, and belowground compartments in four co-existing *Pinus* and *Quercus* species over two years in stands with increasing tree species diversity (from monospecific to four-species mixtures).

My work highlighted mainly adverse impacts of species diversity in mixed compared to monospecific stands for almost all tree species. This trend was observed both in experimental settings and in natural forests with adult trees. The work in open-top chambers showed that differences in canopy size and transpiration rates (driven mainly by contrasting stomatal regulation strategies between species) drove the observed leaf water dynamics. More specifically, higher water use rates and larger crowns in *Q. pubescens* exacerbated drought and heat impacts on *F. sylvatica* in mixtures. Similarly, I mainly observed adverse impacts of species diversity in mixed forests compared to monospecific stands for all tree species, including higher hydraulic impairments, especially for the two pines. However, I still observed important soil water source partitioning in more diverse stands, particularly as conditions became drier during the summer, suggesting that reduced competition for water in more diverse ecosystems is insufficient to buffer the adverse impacts of severe droughts.

To conclude, my work highlighted that diversity effects in forests are not systematically beneficial and highly depend on the species composition, especially the specific set of trait and degree

of acclimation of all interacting species to drier and warmer conditions. The drought vulnerability and competitiveness of tree species can vary in response to species interactions and are mainly driven by the species-specific canopy size, the stomatal regulation strategy, the maximum rooting depth, and local environmental conditions (i.e., heat and drought intensity) found in each forest stand. Hence, to combine forest multifunctionality and drought tolerance, my work provide key information to improve the selection of species combinations adapted to future climate.

Keywords: European forests, Drought vulnerability, Mortality risk, Plant-Plant interaction, Seasonal plasticity, Tree hydraulic

Résumé

Les sécheresses et les canicules altèrent les relations hydriques des arbres, provoquant de graves déficiences hydrauliques pouvant aboutir à la mort de l'arbre. Le mélange d'essence présentant des traits hydrauliques contrastés pourrait réduire la vulnérabilité des forêts aux événements extrêmes grâce à des interactions positives entre les espèces. Cependant, le role de la diversité d'essence sur les relations hydriques des arbres reste incertain, car très peu d'études les ont examinées mécanistiquement et sur le terrain.

Dans cette thèse, j'ai cherché à évaluer comment la diversité des essences affecte les relations hydriques des arbres en réponse à un climat plus sec et chaud, des racines jusqu'à la canopée. Le premier objectif était d'identifier les mécanismes physiologiques sous-jacents aux interactions entre espèces et leur impact sur les relations hydriques au niveau des feuilles et du bois chez des arbres soumis à des conditions constantes plus sèches et chaudes. Dans le cadre d'une manipulation climatique en serre, j'ai évalué l'impact de chaleur et sécheresse sur les traits hydrauliques des feuilles et la survie de jeunes plants de *F. sylvatica* et *Q. pubescens* en monocultures et en mélanges. Ensuite, j'ai étudié comment la diversité des essences modifie les dynamiques saisonnières de l'eau dans les feuilles, le bois et compartiments souterrains en mesurant des traits hydrauliques *in-situ* dans des forêts sèches présentant une diversité croissante d'essence (de monoculture à des mélanges de quatre essences) de *Pinus* et de *Quercus*.

Mon travail a révélé des impacts négatifs de la diversité des espèces pour presque toutes les essences. Cette tendance a été observée à la fois dans des conditions expérimentales et dans des forêts naturelles. L'expérience a montré que les différences de taille de la canopée et de transpiration (principalement dus à des stratégies de régulation stomatique contrastées entre espèces) ont influencé les relations hydriques foliaires. Plus précisément, une utilisation de l'eau plus élevé et de plus grande envergure chez *Q. pubescens* ont exacerbé les effets de la sécheresse et de la chaleur sur *F. sylvatica* en mélange. De manière similaire, j'ai principalement observé une augmentation du stress hydraulique dans les forêts mélangées par rapport aux monocultures pour toutes les essences mais surtout pour les deux pins. Cependant, j'ai tout de même trouvé un important partitionnement des ressources d'eau dans le sol dans les forêts mélangées, notamment lors des sécheresses estivales, suggérant que la réduction de la compétition pour l'eau dans des écosystèmes plus diversifiés est insuffisante pour atténuer les effets négatifs des sécheresses.

Pour conclure, mon travail a souligné que les effets de la diversité dans les forêts ne sont pas systématiquement bénéfiques et dépendent fortement de la composition en espèces, des traits physiologiques et du degré d'acclimatation des espèces à des conditions plus sèches et chaudes. La vulnérabilité à la sécheresse et la compétitivité des essences sont principalement influencées par la taille de la canopée, la stratégie de régulation stomatique, la profondeur maximale des racines et les conditions environnementales présentes dans chaque forêt. Ainsi, pour combiner la multifonctionnalité et la tolérance à la sécheresse des forêts, mon travail fournit des informations clés pour améliorer la sélection de combinaisons d'essence adaptées au climat futur.

Mots-clés: forêts européennes, hydraulique de l’arbre, interactions plante-plante, risque de mortalité des arbres, variations saisonnières, vulnérabilité à la sécheresse

Table of Contents

List of Figures

List of Supporting Figures

List of Supporting Tables

Chapter 1

Introduction

1.1 Context

1.1.1 Impact of global warming on forest functions and services

Along with the many consequences of global change, the combination of warmer air and low precipitation leading to severe droughts highly impact forest ecosystems (IPCC, 2018; Spinoni et al., 2018). Hotter droughts are characterized by rapid soil moisture evaporation due to increasing atmospheric drought, resulting from higher vapor pressure deficit (i.e., the difference between the saturation and actual vapor pressure in the air; VPD; Grossiord et al., 2020). The resulting worsening of drought events alter the water relations in trees, leading to severe hydraulic impairments (e.g., Fontes et al., 2018; Klein et al., 2022), widespread tree mortality (e.g., Anderegg et al., 2016; Hartmann et al., 2022; McDowell et al., 2018), and massive biodiversity loss (Archaux & Wolters, 2006; Zhang et al., 2023) with important feedback on the Earth's climate. Indeed, in addition to storing the majority of the worlds' terrestrial biodiversity (Peyre, 2021; Raft & Oliier, 2011), forests contribute to more than half of the terrestrial evapotranspiration (57.2%) (Wei et al., 2017) and are taking up about 25% of the total atmospheric CO_2 emissions (Keenan & Williams, 2018; Sha et al., 2022), thereby playing a crucial role in the global water and carbon cycles. Therefore, understanding how tree water relations respond to hotter droughts is essential to predict forests' future dynamics and for finding potential climate change and biodiversity loss mitigation strategies.

1.1.2 Tree-level responses to a drier and warmer climate

Water is pulled passively from the soil to the leaves along a negative water potential gradient (i.e., an increasing tension along the soil-plant-atmosphere water continuum, Smith & Smith, 2015) in the conductive tissues of the xylem. First, trees absorb water from the spaces between soil particles into the root hairs and the xylem of the root following a negative water potential. Then, cohesion and adhesion draw water up the tube-shaped xylem tissues due to the cohesion-tension theory (Dixon & Joly, 1895). Finally, water exits the xylem, enters the air space between mesophyll cells, and evaporates into the atmosphere through stomata (i.e., pores situated on foliar tissues) at the leaf-atmosphere interface (Fig. 1.1). This diffusion process at the leaf surface is called transpiration and is the driving force for water movement inside trees (Pickard, 1981). Hence, stomata are the control point for water loss but also for carbon uptake by driving the exchange of CO_2 with the atmosphere, thereby managing the challenge of assimilating carbon with minimum water loss (Raschke, 1976). Still, to

replace the water loss by transpiration and keep the stomata open for net carbon assimilation (A_{net}), uninterrupted water transport from the soil to the leaves is essential.

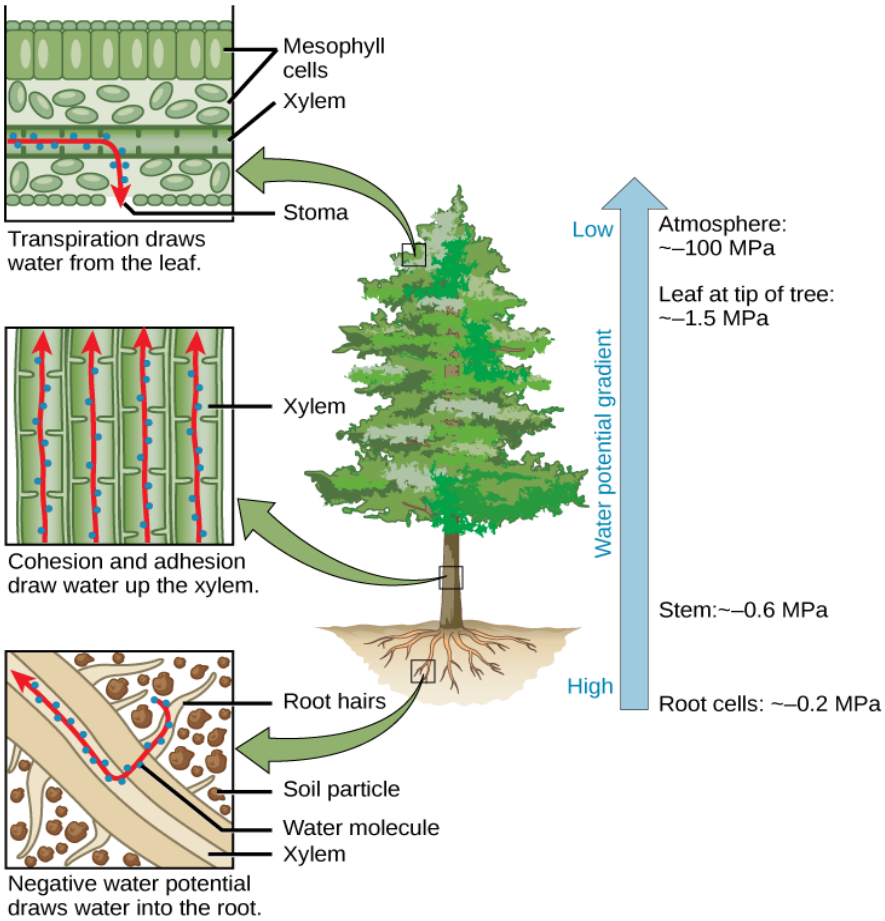

Figure 1.1: The water transport in trees according to the cohesion–tension theory. Evaporation through stomata produces a negative water potential gradient that causes water to move upwards from the roots through the xylem. (Figure extracted from https://openstax.org/books/biology/pages/30-5-transport-of-water-and-solutes-in-plants)

As the soil dries out during a drought, soil water potential decreases, resulting in a steeper gradient of tension in the plant, which will start a sequence of events that could lead to tree death (Fig.1.2). Following the drop in leaf water potential (Ψ_{leaf}), leaf relative water content decreases until trees will eventually close their stomata and reduce their stomatal conductance (g_s) to prevent excessive water loss. However, by reducing g_s, trees also limit their A_{net} (Brodribb & Holbrook, 2003; Martin-StPaul et al., 2017). As drought progresses, leaves lose their turgor after reaching a specific threshold of Ψ_{leaf} (i.e., the leaf water potential at turgor loss point, Ψ_{TLP}) where all physiological functions stop and stomata are closed (Bartlett et al., 2012). Nevertheless, water loss continues through the leaf cuticle and leaky stomata (i.e., the minimum stomatal conductance, g_{min}; Duursma et al., 2019), thereby contributing to progressive plant dehydration. As the drought intensifies, negative

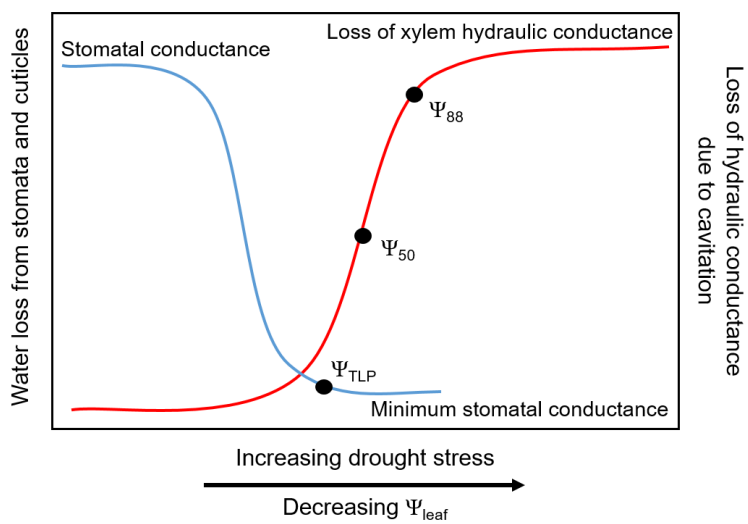

Figure 1.2: Water loss from stomata and cuticles (blue line) and loss of xylem hydraulic conductance due to cavitation (red line) as the xylem water potential decreases during a drought. (Figure extracted from Choat et al., 2018)

tensions in the vascular system will eventually surpass critical thresholds (e.g., the water potential leading to 50% loss of conductance, Ψ_{50}), leading to the formation of gas bubbles in the xylem conduits (i.e., cavitation) spreading in the conduits and breaking the water column (i.e., embolism) (Cochard, 2006; Tyree & Sperry, 1989). Ultimately, the xylem water potential will continue decreasing until the lethal threshold of 88% loss of hydraulic conductance (Ψ_{88}) is reached and runaway cavitation events occur leading to hydraulic failure and the whole tree desiccation (Choat et al., 2018).

Elevated temperature increases VPD, enhancing leaf transpiration (Grossiord et al., 2020; Teskey et al., 2015) and g_{min} (Riederer & Müller, 2008), which potentially increase the hydraulic conductance loss, even in well-watered conditions (Schönbeck et al., 2022). Furthermore, the increasing loss of water at the leaf-level accelerates soil moisture reductions, exacerbating the decrease of leaf and xylem water potential and ultimately amplifying cavitation and mortality risks (Cochard, 2021). Hence, the combination of high temperature and dry soil should exacerbate hydraulic dysfunctions experienced by trees under heat or drought alone (e.g., Fontes et al., 2018; Liu et al., 2020). However, while the sequence of events leading to drought-induced mortality has been well-studied, it remains unclear how tree species deal with an extended combination of high temperatures/VPD and low soil moisture (Brodribb et al., 2020).

In addition to the dynamic physiological responses allowing trees to deal rapidly with hotter droughts, they can also adjust their functional traits over the longer-term to improve their water-saving and carbon-gain strategies. This capacity of plants is known as phenotypic plasticity and can occur over short and/or extended periods (Nicotra et al., 2010). For instance aboveground, prolonged drought exposure could reduce whole-tree leaf area (e.g., DeLucia et al., 2000; Markesteijn & Poorter, 2009; Martin-Stpaul et al., 2013), g_{min} (e.g., Duursma et al., 2019; James et al., 2008), and Ψ_{TLP} (e.g., Bartlett et al., 2012; Limousin et al., 2022; Tordoni et al., 2022) to ensure the maintenance of CO_2 assimilation with limited water loss. Additionally, narrower xylem conduits and denser sapwood could be developed to improve cavitation resistance but at the expense of less efficient water transport

(Saadaoui et al., 2017; Sperry et al., 2006). Belowground, to maintain access to sufficient water resources, trees can shift their active zone of water uptake to deeper water sources as the superficial soil progressively dries out during drought (Brinkmann et al., 2019; Nie et al., 2011; Yang et al., 2015). Nevertheless, hydraulic acclimation to drought and heat is highly species-specific and context-dependent, making it hard to predict which species or functional group will be able to sufficiently acclimate to a progressively changing climate.

Species from different functional groups have diverse strategies to deal with water and heat stress depending on many factors including genetic and trait plasticity. For instance, the control of water flow by the stomata during drought is often ranked along a gradient from isohydric to anisohydric behaviors (Hochberg et al., 2018; Martínez-Vilalta & Garcia-Forner, 2017; McDowell et al., 2008; Tardieu & Simonneau, 1998). Anisohydric species, like some oak species, will track the decrease in soil water potential by keeping their stomata open, making them potentially more efficient in terms of carbon assimilation but more sensitive to cavitation. On the other hand, isohydric species, like some pines, will close stomata rapidly during stress to avoid hydraulic failure and adopt a safer strategy against drought (Aguadé et al., 2015; Garcia-Forner et al., 2016; Roman et al., 2015; Fig. 1.3a).

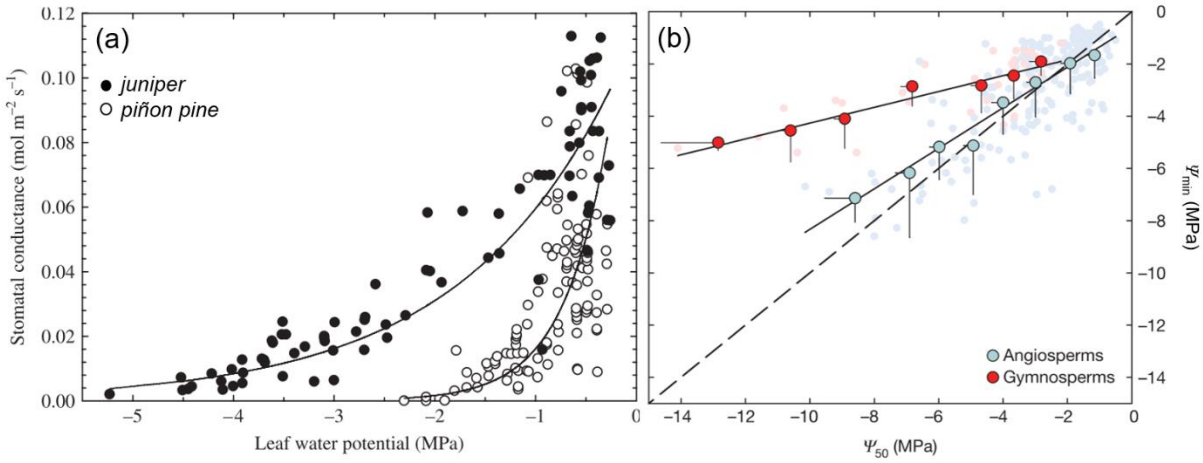

Figure 1.3: (a) Relationship between stomatal conductance and leaf water potential for isohydric piñon pine trees (open circles), and anisohydric juniper trees (closed circles). As drought progressed, piñon pine closes its stomata faster than juniper. (b) Relationship between minimum xylem pressure and embolism resistance for angiosperm and gymnosperm species. Gymnosperm have larger safety margin compared to angiosperm due to their higher wood cavitation resistance. (Figure extracted from McDowell et al., 2008 & Choat et al, 2012)

Furthermore, the xylem anatomy differs drastically between functional groups. Conifers' xylem is composed of short, narrow tracheids inter-connected with pores equipped with torus preventing cavitation, leading to safer xylem structure during drought. In contrast, broadleaves' xylem is defined by large and long vessels, highly efficient for water transport but at the expense of higher cavitation vulnerability (Sperry et al., 2006; Tyree & Ewers, 1991; Fig.1.3b). Finally, overall, trees can present

contrasting architecture and morphology aboveground (e.g., needle *vs.* leaves) or belowground (e.g., shallow *vs.* deep rooting systems) that can respond differently to drought and heat (Förster et al., 2021). Hence, mixing tree species with different functional traits could affect the forest's vulnerability to drought due to positive or negative species interactions.

1.1.3 Impact of tree species interactions on forest drought resistance

The co-occurrence of functionally contrasting tree species in natural forests could lead to either positive, neutral, or negative interactions due to niche partitioning, facilitation, selection or competition processes. The selection effect describes the dominance of one species with particular functional trait, causing a slow shift in the species composition as some species are promoted over others (Fox, 2005; Grossiord, 2020a). In dry environments, this selective process will favor drought-tolerant species over drought-sensitive ones, leading to a globally more drought-resistant ecosystem (e.g., Gea-Izquierdo et al., 2021). Niche partitioning occurs when two or more individuals with different functional traits share resources and thereby decrease the plants' stress by reducing tree-tree competition (Hooper, 1998; Silvertown, 2004). For instance, plants with different rooting depths such as pines and oaks will extract water from different soil layers resulting in belowground water source partitioning, which reduces water stress and can enhance productivity in semi-arid ecosystems (e.g., Grossiord et al., 2018; Rog et al., 2021; Fig. 1.4a). Facilitation processes can also mitigate the water stress of trees due, for example, to different timing in water use (i.e., iso- *vs.* anisohydric behaviors or conifers *vs.* broadleaf) (e.g., Aguadé et al., 2015; Martín-Gómez et al., 2017) or improved microclimate reducing

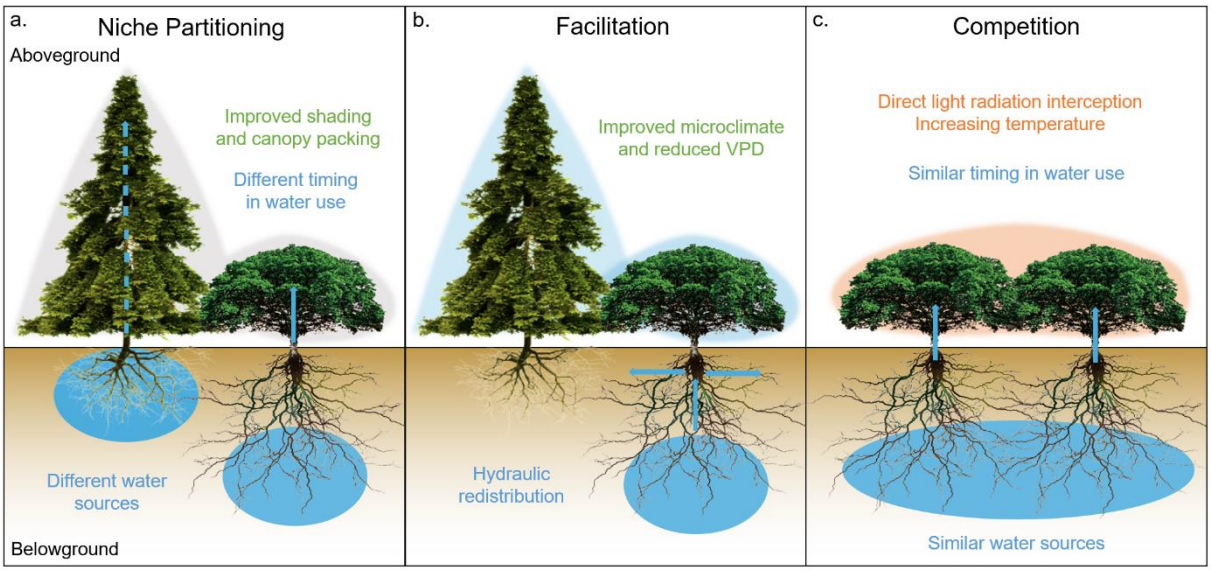

Figure 1.4: Conceptual representation of positive (i.e., niche partitioning and facilitation; a & b) and negative (i.e., competition; c) interaction mechanisms between two tree species from different functional groups with contrasting functional traits (e.g., canopy structure, tree height and rooting depth). The selection effect, which is a longer process taking place over the forest stand development is not depicted in the figure.

canopy's heat stress (i.e., reduced VPD) (e.g., Aguirre et al., 2021; Wright et al., 2015; Zhang et al., 2022). Similarly, belowground, trees with deep roots can further release the water absorbed at deeper and wetter soil layers to the superficial layers, increasing the soil moisture for shallow-rooted trees (i.e., a process known as hydraulic redistribution) (e.g., Zapater et al., 2011; Fig. 1.4b).

In contrast, when individuals share the same functional traits, they are "functionally redundant" in the ecosystem and thereby will compete for the same resources at the same time (i.e., negative species interactions) (Ford, 1975; Fig. 1.4c). For instance, in monospecific forests (i.e., forests composed of a single dominant tree species), all individuals may extract water from the same water source at the same time, resulting in faster exhaustion of the soil moisture and increasing water stress (e.g., Lutter et al., 2021; Rodríguez-Robles et al., 2020). Thus, as soil water resources diminish during drought, trees in monospecific forests are expected to be more negatively impacted than the ones in diverse forests where positive interactions could occur, highlighting the importance of tree species diversity for forest drought resistance.

Mixing contrasting tree species in natural forest has been shown to bring numerous positive effects on forest ecosystems such as increasing tree primary productivity (e.g., Jucker et al., 2014; Kambach et al., 2019; Liang et al., 2016), reducing herbivory by forest insects (e.g., Guo et al., 2019; Jactel et al., 2021), and stimulating forest multifunctionality (e.g., Manning et al., 2018; Van Der Plas et al., 2016). However, while some studies confirmed mitigation of the adverse effects of drought on tree physiology (e.g., Anderegg et al., 2018; Liu et al., 2022; Steckel et al., 2020), increasing species diversity does not systematically improve drought resistance in forests, leading sometimes even to enhanced mortality risk (Bonal et al., 2017; Grossiord et al., 2014; Searle et al., 2022). For instance, species interactions can shift from positive to negative due to enhanced competition (i.e., belowground niche overlapping) during intense drought (Ratcliffe et al., 2017; Rodríguez-Robles et al., 2020). Furthermore, beneficial niche partitioning and facilitation interactions may not be enough during severe water stress to overcome the extreme water depletion experienced by trees (e.g., Grossiord, 2020; Haberstroh & Werner, 2022). Hence, whether tree species diversity reduces or enhances forest vulnerability to drought is still unclear due to our lack of knowledge of the underlying mechanisms driving these responses in mixed forests.

1.2 Thesis objectives

The overall aim of this thesis was to evaluate how tree species diversity could modulate tree water relations during hotter and drier climatic conditions. Hydraulic traits in aboveground and belowground plant compartments were measured on tree seedlings under controlled conditions and on mature trees in natural dry forests with different species composition and diversity. The following detailed objectives were addressed:

(i) Identify the physiological mechanisms driving species interaction effects on the leaf-level water relations of European temperate trees under chronic multi-year warming and drought acting alone or combined, and their implication for the onset of hydraulic failure. The study related to this objective is presented in **Chapter 2**.

(ii) Assess the effect of tree species diversity on wood hydraulic traits in natural pine-oak mixed Mediterranean forests and its implication for tree vulnerability to cavitation during drought. The results of this study are reported in **Chapter 3**.

(iii) Investigate how tree species diversity alters the seasonal tree internal water dynamics by linking the belowground and aboveground hydraulic compartments in mature pine-oak forests. The study addressing this objective is discussed in **Chapter 4**.

1.3 Thesis outline

This thesis was based on two main approaches where tree species diversity effect was assessed for different hydraulic traits at the leaf, stem, and root levels. The first experiment presented in **Chapter 2** was conducted at the Model Ecosystem Facility of the Swiss Federal Research Institute for Forest, Snow, and Landscape WSL, Birmensdorf (Switzerland) where measurements were conducted over three years (2020-2022). The experimental set-up consisted of 16 open-top chambers where *Fagus sylvatica* and *Quercus pubescens* seedlings in monospecific and mixtures were exposed to chronic warming and drought acting alone or simultaneously since 2019. The second approach, used for **Chapters 3 & 4**, focused on mature trees in natural Mediterranean forests in the Alto Tajo Natural Park (Spain). Using a network of permanent plots with increasing tree species diversity (from monospecific to four-species mixtures), I measured leaf, wood, and belowground hydraulic traits on mature *Pinus* and *Quercus* trees at the beginning, middle, and end of the growing season in 2021 and 2022. I first assessed the species diversity effect on xylem hydraulic traits in monospecific and four-species mixture stands (**Chapter 3**). Then, I investigated how belowground species interactions could modulate the seasonal variability of leaf hydraulic traits in monospecific, two-species, and four-species mixture stands (**Chapter 4**). Finally, **Chapter 5** integrates the findings from the previous chapters and discusses the contributions of this work to our understanding of tree species diversity's effect on forest drought vulnerability in the broader context of climate change.

1.4 Supplementary studies

Besides the work stated above, three additional studies where I contributed to the data collection and paper writing are included in the Appendix. The first one highlights the effect of VPD and temperature on tree hydraulic traits at the leaf- and wood-level on three European tree species in climatic chambers (Schönbeck et al., 2022). The second study looks at the impact of heat and drought on the phenology and carbon gain of European trees (same setup as in **Chapter 2**) (Grossiord et al., 2022). The third study concerns the thermal acclimation of *Pinus sylvestris* under long-term drought exposure in natural forests in Valais (Switzerland) (Gauthey et al., 2023).

Chapter 2

Interactions between beech and oak seedlings can modify the effects of hotter droughts and the onset of hydraulic failure

Eugénie Mas[1,2]*, Hervé Cochard[3], Janisse Deluigi[1,2], Margaux Didion-Gency[1,2], Nicolas Martin-StPaul[4], Luna Morcillo[5], Fernando Valladares[6], Alberto Vilagrosa[5], Charlotte Grossiord[1,2]

[1]Plant Ecology Research Laboratory PERL, School of Architecture, Civil and Environmental Engineering, EPFL, CH-1015 Lausanne, Switzerland

[2]Community Ecology Unit, Swiss Federal Institute for Forest, Snow and Landscape WSL, CH-1015 Lausanne, Switzerland

[3]Université Clermont Auvergne, INRAE, PIAF, 63000 Clermont-Ferrand, France

[4]Unité Ecologie des Forêts Méditerranéennes (UR629), INRAE 84914 Avignon Cedex 9, DomaineSaint Paul, Site Agroparc, France

[5]CEAM Foundation, Joint Research Unit University of Alicante-CEAM, Department of Ecology, University of Alicante, PO Box 99, C. San Vicente del Raspeig, s/n, 03080 Alicante, Spain

[6]Depto de Biogeografía y Cambio Global, LINCGlobal, Museo Nacional de Ciencias Naturales (MNCN-CSIC), 28006 Madrid, España and Área de Biodiversidad y Conservación, Univ. Rey Juan Carlos, Móstoles, 28933 Madrid, España

This chapter has been published in the peer-reviewed journal "*New Phytologist*"

Mas, E., Cochard, H., Deluigi, J., Didion-Gency, M., Martin-StPaul, N., Morcillo, L., Valladares, F., Vilagrosa, A., & Grossiord, C. Interactions between beech and oak seedlings can modify the effects of hotter droughts and the onset of hydraulic failure. *New Phytologist*. https://doi.org/10.1111/nph.19358

Author's contribution:

Charlotte Grossiord (CG), Margaux Didion-Gency (MD-G) and I conceived and designed the study. This included decisions regarding the sampling design and field logistics. I specifically focused on preparing the sampling campaign by aquiring all necessary materials, and ensuring field protocols and logisitics could run smoothly. Janisse Deluigi (JD), MD-G, Luna Morcillo (LM), Alberto Vilagrosa (AV), CG and I collected the data. I measured all the hydraulic traits at the leaf- and stem- levels while JD and MD-G collected the gas exchange and leaf area data. Hervé Cochard (HC) and Nicolas Martin StPaul (NM) conducted the model simulations. I analyzed the data, produced all figures and tables, and led the writing of the manuscript. All authors (i.e., CG, MD-G, JD, LM, AV, HC, NM, Fernando Valladares, and I) critically contributed to the manuscript and gave final approval for publication.

Abstract

- Mixing species with contrasting resource use strategies could reduce forest vulnerability to extreme events. Yet, how species diversity affects seedling hydraulic responses to heat and drought, including mortality risk, is largely unknown.
- Using open-top chambers, we assessed how, over several years, species interactions (monocultures *vs.* mixtures) modulate heat and drought impacts on the hydraulic traits of juvenile European beech and pubescent oak. Using modelling, we estimated species interaction effects on timing to drought-induced mortality and the underlying mechanisms driving these impacts.
- We show that mixtures mitigate adverse heat and drought impacts for oak (less negative leaf water potential, higher stomatal conductance, and delayed stomatal closure) but enhance them for beech (lower water potential and stomatal conductance, narrower leaf safety margins, faster tree mortality). Potential underlying mechanisms include oak's larger canopy and higher transpiration, allowing for quicker exhaustion of soil water in mixtures.
- Our findings highlight that diversity has the potential to alter the effects of extreme events, which would ensure that some species persist even if others remain sensitive. Among the many processes driving diversity effects, differences in canopy size and transpiration associated to the stomatal regulation strategy seem the primary mechanisms driving mortality vulnerability in mixed seedling plantations.

Keywords: functional diversity, hydraulic failure, hydraulic safety margins, stomatal conductance, SurEau, turgor loss point.

2.1 Introduction

The worsening of drought events with rising air temperature alters tree water relations and causes one of the most critical environmental stresses for forests. Hotter droughts can lead to severe hydraulic impairments (e.g., Fontes et al., 2018; Klein et al., 2022) and more rapid and widespread tree mortality (e.g., Anderegg et al., 2016; Hartmann et al., 2022; McDowell et al., 2018). In this context, finding mitigation strategies to lessen tree vulnerability to hot droughts has become a critical research area in plant ecology. Interactions between species have a strong potential to alleviate drought impacts and forest die-off events (e.g., Anderegg et al., 2018; Grossiord, 2020). Yet, how diversity modulates the hydraulic responses of trees to hotter droughts is largely misunderstood and not accounted for in climate-vegetation models.

The interactions between functionally contrasting species can lead to facilitation processes and complementarity for resources, inducing higher water availability (e.g., Schwendenmann et al., 2015; Jing *et* al., 2021) and a potential delay in the onset of hydraulic dysfunctions during drought (Hajek et al., 2022). Cohabiting tree species often exhibit distinct hydraulic strategies to deal with drought, enabling such beneficial interactions (Grossiord, 2020). For instance, mixing juvenile trees can improve the microclimate and diminish atmospheric drought impacts due to a cooler, more humid atmosphere reducing the vapor pressure deficit (VPD) (Watson et al., 2023; Wright et al., 2021). Many studies in various plant communities from herbaceous to forests have reported such facilitative processes (e.g., Wright et al., 2015; Aguirre et al., 2021; Zhang et al., 2022). Similarly, complementarity between species may arise from a better sharing of belowground resources. In mixed beech and oak forests, beech (*Fagus sylvatica* L.) rooting system is not as effective in exploring deep soil layers as oak (*Quercus* spp.), suggesting that the two species partition water resources by relying on different soil depths (Zapater et al., 2011). Similar processes could be expected for these species at a younger development stage (Moreno et al., 2023). Juvenile trees may further benefit from the presence of adult ones because of enhanced shading and hydraulic redistribution, improving forest regeneration (Andivia et al., 2018; Warren et al., 2008). However, most studies conducted on juvenile trees focused on potted seedlings where root growth is extremely limited, leading potentially to belowground competition that outweigh facilitative processes (Prieto et al., 2011). Similarly, species interactions can shift from beneficial to negative due to spatial and temporal differences in resource availability (e.g., when moving from mild to extreme droughts) (Haberstroh & Werner, 2022) or during stand development (e.g., De Groote et al., 2018). During hotter droughts, moisture reductions may be too intense for these complementarity mechanisms to overcome, and plasticity in functional traits during the plant development (e.g., shift in water sources and/or canopy size) might affect the occurrence of resource partitioning (Grossiord et al., 2018). A crucial starting point for gaining process

knowledge on how functional diversity can lessen tree vulnerability to hotter droughts is to clarify the impacts of species interactions on tree hydraulic responses to extreme events.

Drought effects on tree hydraulics have been well-studied over the past 50 years, allowing us to gain a significant understanding of the sequence of events leading to tree decline (Choat et al., 2018). When exposed to decreasing soil moisture, leaf relative water content and Ψ_{leaf} decrease, leading to stomatal closure to prevent water loss (Brodribb & Holbrook, 2003; Martin-StPaul et al., 2017). As the drought intensifies, leaves lose their turgor after reaching a specific threshold of Ψ_{leaf} (i.e., the leaf turgor loss point, Ψ_{TLP}; Bartlett et al., 2012). Following stomatal closure, water loss continues through the leaf cuticle and leaky stomata (i.e., the minimum stomatal conductance, g_{min}; Duursma et al., 2019), thereby contributing to progressive plant dehydration. Consequently, plants with larger canopies might be subjected to earlier stomatal closure, higher global residual water loss because of the stronger evaporative demand of the crown, but also increased microclimate offset (Jucker et al., 2014; Lüttschwager & Jochheim, 2020; Zhang et al., 2022). Once a species-specific xylem water potential has been reached, embolism will start occurring and progressively decrease the stem hydraulic conductivity until reaching dangerous thresholds that induce hydraulic failure (e.g., the water potential leading to 50% loss of conductivity, P_{50}) and, ultimately, tree mortality (Choat et al., 2018; Cochard, 2006; Tyree & Sperry, 1989). Hydraulic indicators using the Ψ_{TLP} have been widely used to provide quantitative measures of a species' capacity to tolerate drought (Bartlett et al., 2012; Blackman, 2018; Meinzer et al., 2009). For instance, the leaf safety margin (SM_{leaf}) is the difference between the Ψ_{TLP} (i.e., often used as a proxy for the Ψ_{leaf} at stomatal closure; Rodriguez-Dominguez et al., 2016) and the minimum leaf water potential (Ψ_{min}, reflecting the midday water potential). Hence, SM_{leaf} represents the range of Ψ_{leaf} a plant can experience before stomatal closure (Fontes et al., 2018). Similarly, the difference between xylem P_{50} and Ψ_{TLP}, defined as the stomatal safety margin (SM_{P50}), determines the range of Ψ_{leaf} across which plants control the risk of hydraulic failure through stomatal closure (Martin-StPaul et al., 2017). Trees usually operate with narrow safety margins, regardless of the climatic conditions in which they occur (Choat et al., 2012). Still, sub-Mediterranean species such as pubescent oak (*Quercus pubescens* Willd.) may present wider safety margins than temperate species such as beech, reflecting their higher drought tolerance (Fuchs et al., 2021). Previous work often considered these margins as relatively static *(e.g., Meinzer et al., 2009; Choat et al.*, 2012; but see Tomasella et al., 2018). However, prolonged drought exposure has been shown to reduced whole-tree leaf area (e.g., DeLucia et al., 2000; Markesteijn & Poorter, 2009; Martin-Stpaul et al., 2013), g_{min} (e.g., James et al., 2008; Duursma et al., 2019), and Ψ_{TLP} (e.g., Bartlett et al., 2012; Limousin et al., 2022; Tordoni et al., 2022), resulting in narrower SM_{leaf}, and SM_{P50} to ensure the maintenance of CO_2 assimilation (Tyree & Sperry, 1988). Hence, long-term drought acclimation of

multiple leaf hydraulic traits can reduce tree evaporative demand and delay the time to hydraulic failure (THF) (e.g., Lemaire et al., 2021).

During hot droughts, elevated temperature increases the vapor pressure deficit (VPD; Grossiord et al., 2020), exacerbating hydraulic dysfunctions (e.g., Jagadish et al., 2021; Liu et al., 2020). High VPD increases leaf-level transpiration, which accelerates soil moisture reductions (Teskey et al., 2015). Higher air temperature further instantaneously amplifies g_{min} (Riederer & Müller, 2008), which can increase hydraulic conductivity losses (Schönbeck et al., 2022), especially if high temperature is combined with low soil moisture (Cochard, 2021). Furthermore, exposure to prolonged warming can produce larger and thinner leaves (e.g., Hudson et al., 2011; Wu et al., 2020), lower the stomatal sensitivity to VPD (e.g., Ameye et al., 2012; Drake et al., 2018; Teskey et al., 2015), decrease g_{min} (e.g., Duursma et al., 2019; Schönbeck et al., 2022) and reduce Ψ_{TLP} (via osmoregulation, e.g., Loik & Harte, 1997; Tordoni et al., 2022), thereby possibly limiting the adverse impacts of hotter droughts. Moreover, high VPD decreases steady-state stomatal aperture and g_s (Buckley et al., 2011), which could also ease drought impacts on hydraulic functions (Fontes et al., 2018). Overall, significant uncertainties remain on how tree species deal with an extended combination of high temperatures, VPD, and low soil moisture (Brodribb et al., 2020). Nonetheless, whether interactions between tree species with different hydraulic strategies and long-term acclimation to these extreme conditions could slow the events leading to tree mortality has never been addressed experimentally.

The main objective of this study is to investigate how species interactions alter the hydraulic responses and timing to hydraulic failure during hot droughts. We studied pubescent oak and European beech, two widely-distributed and co-habiting European tree species. Pubescent oak grows in warm sub-Mediterranean to temperate regions and is more tolerant to drought and heat than European beech, a temperate species growing in rather moist and cool environments (Didion-Gency et al., 2022). We exposed oak and beech seedlings planted in intra- or inter-specific combinations for four years to chronic air warming and soil drought acting alone or together in open-top chambers. We expected chronic drought to reduce g_s and Ψ_{leaf} and to lead to the development of smaller and thicker leaves with lower g_{min} and Ψ_{TLP}. These responses should result in narrower SM_{leaf} and SM_{P50} and faster hydraulic failure compared to the control when subsequently exposed to comparable drought conditions. We expected that under multi-year heating, the trees could produce larger and thinner leaves with less sensitive stomata, allowing higher g_s and Ψ_{leaf} but with lower g_{min} and $\Psi_{TLP,}$ leading to narrower hydraulic safety margins and faster onset of hydraulic failure compared to the control. The combination of drought and heat should exacerbate the effects observed under drought alone. The individual tree response to climatic treatments should be amplified for beech compared to oak, an already more drought tolerant species. Besides, inter-specific interactions are expected to mitigate the degree of soil moisture or atmospheric drought stress (through improved water resource partitioning

and reduced VPD), leading to lower adverse impacts of the climatic treatments than intra-specific interactions.

2.2 Material and methods

2.2.1 Site description

The study was conducted at the model ecosystem facility Modoek located at the Swiss Federal Research Institute WSL in Birmensdorf (47°21'48" N, 8°27'23" E, 545 m a.s.l). Sixteen hexagonal glass-walled open-top chambers of 6m², 3m height and 1.5m deep were filled with a 1 m-deep layer of gravel for fast drainage, covered with a fleece layer to avoid root proliferation past the soil layer, and topped by a 50 cm layer of artificial acidic sandy forest soil (Ökohum, DE; pH 6.3) that allows fast drainage. A shallow soil depth was selected to promote soil drying in the treatments and promote aboveground growth more rapidly. Nevertheless, this design also reduces the potential role of belowground complementarity in water uptake depth between species. The glass walls and roofs reduced photosynthetic active radiation (PAR) inside the chambers by about 50% compared to the outside (but still reached up to 1700 µmol m^{-2} s^{-1} PAR during sunny days). Each chamber was divided into eight compartments (i.e., 0.75 m^2 each), irrigated from April to November every two days and every two weeks during winter (Fig. 2.1c, d). Air temperature and humidity at 50 cm and 2 m above the ground were monitored inside each chamber every 10 min (Atmos 14; Meter Group Inc., Pullman, WA, USA). Soil temperature and moisture were measured in four compartments at 25 cm depth every 10 min (5TM Decagon Devices, Pullman, WA, USA). In October 2018, two-year-old tree seedlings of European beech (*Fagus sylvatica* L.) and pubescent oak (*Quercus pubescens* Willd.) were planted in two species combinations: monocultures (i.e., four trees of the same species) and mixtures (i.e., two trees of each species). Each chamber included all the possible species combinations. Grossiord et al. (2022) provide more details on the experimental design.

In April 2019, we started applying four climatic treatments in the chambers: 1) control (C), with ambient air temperature and soil moisture maintained at field capacity (i.e., approx. 10% considering the sandy soil composition); 2) heating (H), where the air temperature inside the chambers was maintained at approx. 5°C above the temperature of the control and soil moisture at field capacity; 3) drought (D), where the soil moisture was reduced by about 45% relative to the control and ambient air temperature; and 4) hot drought (HD), where both treatments were applied simultaneously (Fig. 2.1a,b). Our study aimed to understand the physiological mechanisms under chronic warming and reduced soil moisture rather than predict the response of trees to periodic extreme events. The selected conditions have been chosen at our facility to match a possible future shift in mean air temperature leading also to constantly drier soils (Lyon et al., 2022). Each combination of climatic treatment (n=4 chambers), species (n=2), and species combinations (n=2) was repeated six times. One tree per species was randomly selected in each species combination for repetitive measurements leading to 96 trees in total (i.e., 48 per species). Leaf-level hydraulic traits were measured in all trees

once per year at the end of the growing season in September (i.e., before the first sign of senescence) for three years from 2020 (i.e., one year after the treatments started) to 2022.

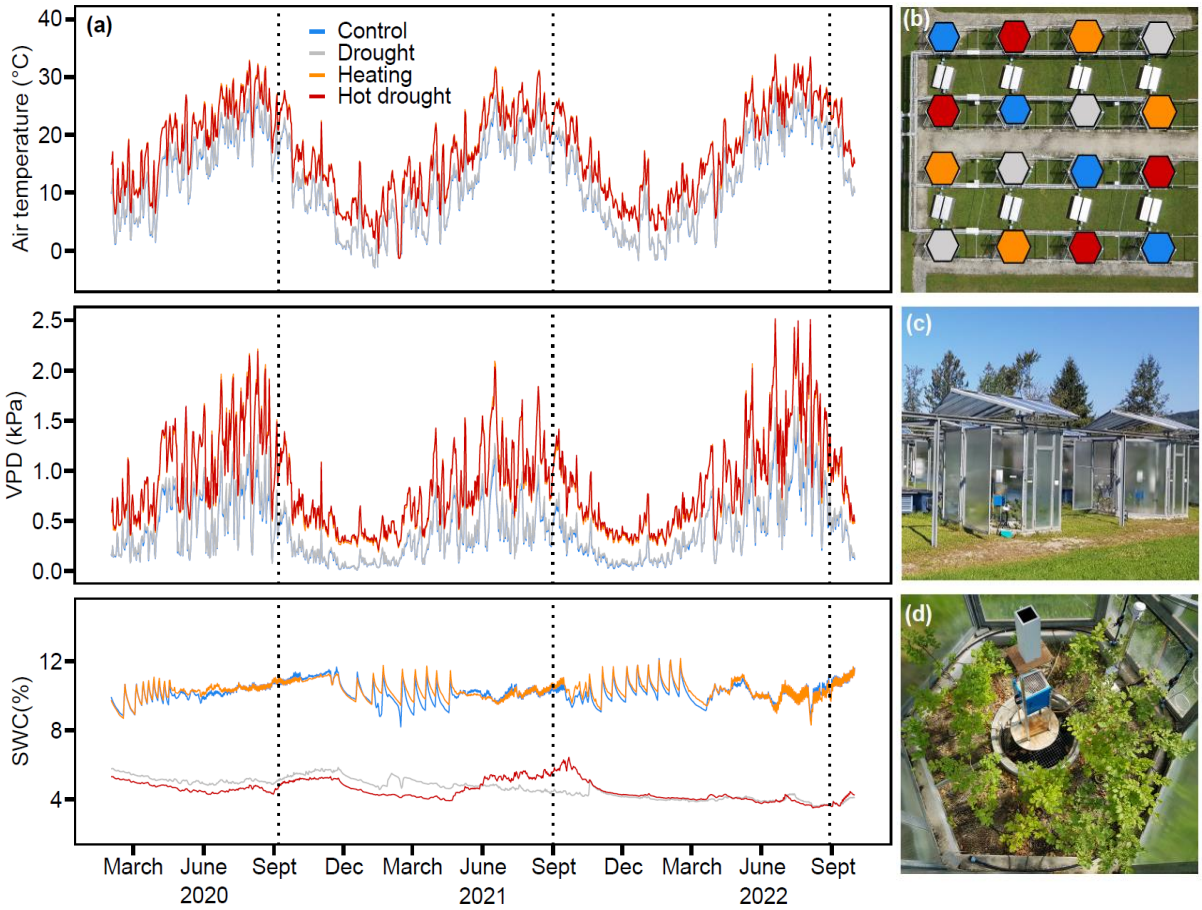

Figure 2.1: Mean daily air temperature, vapor pressure deficit (VPD), and soil water content (SWC) (a) under control (blue), drought (grey), heating (orange), and hot drought (red) conditions in the open-top chambers (n=4 chambers per treatment). Dashed vertical lines indicate the measurement campaigns. Aerial picture of the 16 open-top chambers with the four treatments (b), picture showing the side of the open-top chambers (c), and aerial picture from a heated chamber including a central heating system and eight compartments with different European beech and pubescent oak combinations (d).

2.2.2 Leaf-level stomatal conductance and water potential

We measured the leaf-level light-saturated stomatal conductance (g_s, mol m^{-2} s^{-1}) on one leaf from the highest part of the crown of each selected tree. Gas exchange measurements were conducted between 9 am and 3 pm (local time) using two LI-6800 infrared gas exchange analyzers (LI-6800, LICOR Biosciences, USA). The relative humidity was set to 50% (to match the average daily environmental conditions inside the chambers), the CO_2 concentration to 400 ppm, the photosynthetic photon flux density (PPFD) to 1500 µmol m^{-2} s^{-1} (to ensure saturating light conditions), and the air temperature inside the cuvette to 20°C in the non-heated chambers and 25°C in the heated ones (to fit the mean midday air temperature during the measurements). On the same day as stomatal

conductance measurements, one leaf per tree was collected before sunrise ($\Psi_{predawn}$) and at midday (Ψ_{midday}) to measure the leaf water potential (MPa) with a Scholander-type pressure chamber (M1505D, PMS Instruments, USA).

2.2.3 Minimum conductance and specific leaf area

Minimum conductance (g_{min}, mmol m^{-2} s^{-1}) was measured as described in Sack et al., (2003). One leaf per individual was cut before dawn when stomata were assumed to be still closed. The cut petiole was immediately sealed with melted candle wax, and the leaf area was scanned using a flatbed scanner (CanoScan LiDE 300, CANON, UK), followed by analysis with Fiji from ImageJ (Schindelin et al., 2019). The leaves were stuck to a lab tape run between two lab stands, standing in a small dark climatic chamber with stable air temperature (22 ± 2°C) and humidity (55 ± 12%). Every 15 minutes, the leaves were taken from the climatic chamber and stored in a closed black plastic bag while waiting to be weighed using a high-precision scale (MS104, Mettler Toledo, CH). This procedure was repeated eight times. g_{min} was obtained from the slope of the linear relationship between leaf mass and its drying time, corresponding to the cuticular transpiration per mole fraction VPD, assuming the leaf's internal air to be fully saturated (Pearcy et al., 2000).

Five fully-expanded mature leaves were collected for each tree and scanned using a flatbed scanner (CanoScan LiDE 300, CANON, UK), followed by analysis with ImageJ to extract the mean individual leaf area (LA_{leaf}, cm^2). Then, the leaves were dried at 60°C for 24h and weighed using a high precision scale (MS104, Mettler Toledo, CH) to calculate the specific leaf area (SLA, cm^2 g^{-1}). In June 2022, we further estimated the whole-canopy leaf area (LA_{total}, cm^2) for modeling purposes (see below and Notes S2.1).

2.2.4 Pressure-Volume Curves

Pressure-volume curves were determined using the bench-dehydration method (Koide et al., 2000). One fully-expanded mature leaf per tree was cut the evening preceding the measurement. The petiole was recut under water, and the leaf was stored with the petiole submerged in water in the darkness for the night, ensuring that full hydration was reached before the start of the measurements the following morning. Leaf water potential and weight were measured using a Scholander-type pressure bomb (M1505D, PMS Instruments, USA) and a high-precision scale (MS104, Mettler Toledo, CH). Different levels of water potential were reached by letting the leaves dry progressively in an open plastic bag on a lab bench. For oak, the procedure of measuring water potential, weighing, and drying was repeated with increasing drying time intervals (from 10s to 1h) until achieving water potentials of about -4 MPa or until water potential reached a plateau. For beech, the procedure was repeated continuously without letting the leaves dry on the bench due to the rapid water loss and the

corresponding drop in leaf water potential. After the measurements, the leaf was dried for 24h at 60°C to determine the dry mass. The pressure-volume curves were constructed by plotting the reciprocal of the water potential *vs*. the relative water deficit. Leaf water potential at turgor loss point (Ψ_{TLP}, MPa), the osmotic potential at full turgor (Ψ_o, MPa), modulus of elasticity (ε, MPa), and relative water content (RWC, %) were calculated following Koide et al*.,* (2000).

We calculated the stomatal safety margin (SM_{P50}, MPa) as the difference between the Ψ_{TLP} and the water potential at 50% of xylem conductivity loss (P_{50}, MPa) (Martin-StPaul et al., 2017). Because of the destructiveness of P_{50} measurements, we extracted the P_{50} of each species from a database (Choat et al., 2012) with a value of -3.2 MPa and -3.3 MPa for beech and oak, respectively. Although we acknowledge that using the same P_{50} values for all trees does not account for the potential acclimation of this trait to the climatic treatments, previous work has shown limited P_{50} plasticity to drought in our species (e.g., Matzner et al., 2001; Torres-Ruiz et al., 2013). However, Tomasella et al., (2018) observed a decrease of up to 0.4 MPa for beech under repetitive drought. Hence, care must be taken with result interpretation. We further calculated the leaf safety margin (SM_{leaf}, MPa) for each tree and year as the difference between Ψ_{midday} (proxy of Ψ_{min}) and Ψ_{TLP} (Fontes et al., 2018).

2.2.5 Timing to hydraulic failure and mechanisms of species interactions

The soil–plant hydraulic model SurEau (Cochard et al., 2021; Martin-StPaul et al., 2017; Ruffault et al., 2022) was applied to understand the impact of species interactions and trait plasticity to the different treatments on the overall plant performances. In brief, SurEau simulates water fluxes and water potential through a plant hydraulic scheme including different symplasmic and apoplasmic resistances. The model computes leaf stomatal and cuticular transpiration as the product between leaf-to-air VPD and stomatal and cuticular conductance. Then, stomatal and cuticular fluxes are used to compute the water potential in the different plant compartments (the symplasm and the apoplasm of leaves, stems, and roots), while accounting for (i) the symplasmic capacitance, (ii) water released by cavitation and (iii) the potential hydraulic conductance losses due to xylem embolism (if any). The soil water potential (Ψ_{soil}) and the soil hydraulic conductance are also computed from soil water content at each time step using water retention curves. A peculiarity of the SurEau model is the explicit representation of what occurs beyond the point of stomatal closure, under extreme water stress, when g_{min} leads to plant dehydration and hydraulic failure (i.e., 100% conductivity loss). The model can be parameterized with ecophysiological traits measured empirically and can be run using different environmental conditions and species composition to estimate their overall effect on plant performances (time with open stomata or time until total hydraulic failure). Here we used the detailed version coded in C (Cochard et al., 2021) which works at a time step of 0.01s and was adapted to allow two individuals to compete for the same stock of water (Moreno et al., 2023). In this case, the

model allows two trees to absorb water in the same soil volume. Technically, two codes corresponding to two trees with their own set of traits were run in parallel, withdrawing the water from the same volume.

We aimed to test the effect of trait plasticity in the different treatments (due to species interactions and climatic treatments) on the risk of hydraulic failure at the seedling stage. The model was parameterized with species-specific plant traits in each treatment for the year 2022 (due to LA_{total} missing in previous years). We used key measured plant traits that are known to influence the time to hydraulic failure (Ruffault et al., 2022) and that were affected by the treatments. These traits include soft traits: (i) height and diameter of the main stem (used to compute the wood volume and area, and thus, the water storage in the plant and bark), which influence g_{min}, (ii) LA_{total} (Notes S2.1), which influences tree transpiration, and (iii) LA_{leaf}, which influences the boundary layer conductance. In addition, we included hard traits: (iv) g_{min} and the maximum stomatal conductance, which defines tree transpiration, and (v) the pressure volume curve parameters, which influence the symplasm capacitance and are used to compute turgor-mediated stomatal closure (Martin-StPaul et al., 2017) (see Table S2.4 for a detailed description of the parameters). P_{50} was assumed constant at the species level in agreement with the low plasticity previously found for this trait (Matzner et al., 2001; Torres-Ruiz et al., 2013). However, it is important to acknowledge that P_{50} acclimation to drought was also reported in adult beech trees (Tomasella et al., 2018), which could alter the simulated responses in the model. To assess the impact of P_{50} acclimation on our results, four scenarios were run: (1) no acclimation of P_{50} to D and HD in both species (i.e., -3.2 and -3.3MPa for beech and oak, respectively in all treatments), (2) acclimation of P_{50} to D and HD in all species (i.e., -3.6 and -3.7MPa for beech and oak, respectively; only for the D and HD treatments), (3) acclimation of P_{50} to D and HD only for beech, and (4) acclimation of P_{50} to D and HD only for oak. Acclimation was estimated to be maximum 0.4 MPa based on published observations for *F. sylvatica* (Tomasella et al., 2018). In all treatments, the root area was assumed proportional to the leaf area. The model was run for the different trait combinations with constant atmospheric conditions (air temperature at 20°C, 0.7 kPa VPD, and PPFD at 500 µmol m^{-2} s^{-1}) and an initial soil water content at saturation. Hence, the model does not account for potential mitigating impacts of the microclimate in mixtures. Then the model was run until the plants reach total hydraulic failure (100% embolism in branches). Two integrative metrics of plant performance during drought were estimated: (i) the time to stomatal closure (TSC), which indicates the time over which the plant can be productive, and (ii) the time to hydraulic failure (THF), which indicates the survival time during drought. First, we compared monocultures and mixtures (i.e., the trees in mixtures share the same water pool) accounting for the measured trait plasticity (i.e., in soft and hard traits). Then, to isolate the influence of soft traits (related to tree size and leaf area) from hard

traits, we performed the same test with soft traits set constant on the monocultures only to simplify the simulations.

2.2.6 Statistical analysis

All analyses were performed using the R v.4.2.2 statistical software (R Development Core Team, Vienna, Austria, 2022). The effects of the climatic treatments and species combinations on $\Psi_{predawn}$, Ψ_{midday}, g_s, g_{min}, Ψ_{TLP}, SLA, LA_{leaf}, SM_{leaf}, and SM_{P50} were determined through linear mixed-effects models for each species using the package *lmer*. The interactive effects of heating (yes/no), drought (yes/no), and species combination (monocultures/mixtures) were used as fixed effects. The year in which the measurements were done (i.e., 2020, 2021, and 2022) and the individual open-top chambers were treated as random effects as no significant differences were found between them. The effects of climatic treatments and species combinations on TSC and THF were determined through a simple linear model for each species. To reveal significant differences between treatments for each measurement, post hoc analyses were performed with a Tukey's HSD test, with FDR correction for multiple testing. Linear and non-linear regressions were used to test the relationships between g_s, $\Psi_{predawn}$, g_{min}, SLA, SM_{leaf}, SM_{P50}, soil water content, and VPD. The significance of these relationships and the differences between species combinations were revealed using ANOVA. Before performing each model, the homogeneity of variances and the normality of residuals were assessed, and data were log-transformed if necessary.

2.3 Results

2.3.1 Species interaction effects on leaf hydraulic traits under heating and drought

Drought (D and HD) significantly reduced predawn leaf water potential ($\Psi_{predawn}$) and light-saturated stomatal conductance (g_s) for both species and reduced midday leaf water potential (Ψ_{midday}) for oak (Fig. 2.2 & Table S2.1). For both species, heat (H) significantly reduced $\Psi_{predawn}$ but had no significant impact on Ψ_{midday} and g_s. Indeed, while we found a significant increase of g_s with soil moisture for both species, we found a positive relationship with VPD only for beech, suggesting a lower sensitivity to atmospheric drought in oak (Fig. S2.1). For beech, species interactions modulated the responses of Ψ_{midday} to D and HD, with an increase in Ψ_{midday} in monocultures whereas no change was observed in mixtures (Fig. S2.2, Tables S2.1 & S2.2). On the contrary, for oak, lower reduction in Ψ_{midday} and g_s were found in monocultures compared to mixtures under D and HD (Fig. S2.2, Tables S2.1 & S2.3).

We found a significant reduction of the minimal stomatal conductance (g_{min}), the mean leaf area (LA_{leaf}), and the specific leaf area (SLA) under D and HD for both species. In contrast, no effect of heat was observed on these traits (Fig. 2.2, Table S2.1). When mixed, both species had significantly lower LA_{leaf} and SLA (for beech only), independently of the climatic treatment. We did not find a significant impact of species interactions on g_{min} (Fig. 2.2, Table S2.1).

We observed a significant increase in the water potential at the turgor loss point (Ψ_{TLP}) under D and HD for both species, independently of species combinations (Fig. 2.2, Table S2.1). Under D and HD, the stomatal safety margin (SM_{P50}) significantly increased only for beech, and the leaf safety margin (SM_{leaf}) decreased in both species. No significant impact of H and species combinations on Ψ_{TLP}, SM_{leaf}, or SM_{P50} was detected (Fig. S2.3, Table S2.1).

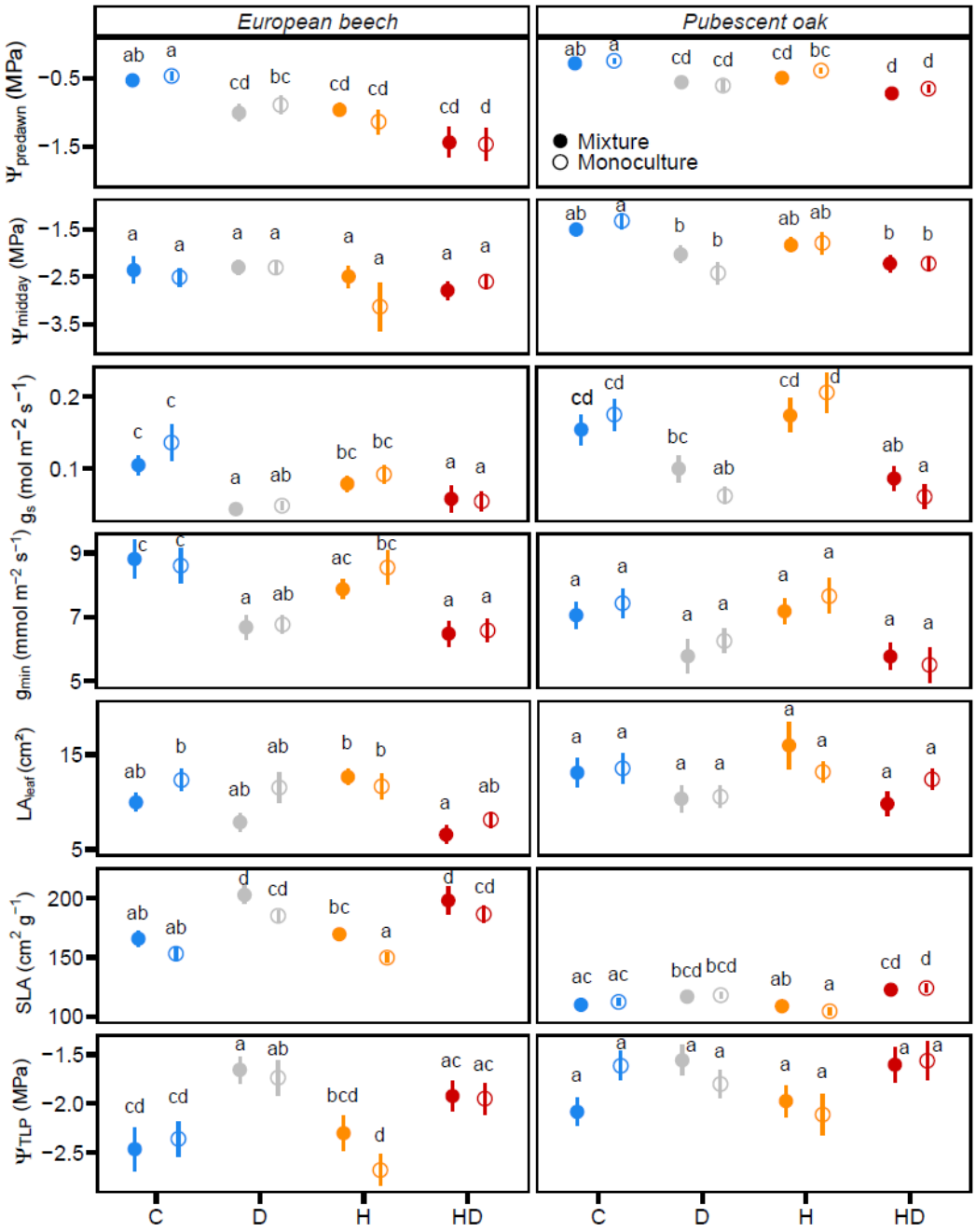

Figure 2.2: Leaf water potential at predawn ($\Psi_{predawn}$) and midday (Ψ_{midday}), light-saturated stomatal conductance (g_s), minimal stomatal conductance (g_{min}), mean individual leaf area (LA_{leaf}), specific leaf area (SLA), and water potential at turgor loss point (Ψ_{TLP}) for all years (i.e., 2020, 2021, 2022, mean ± SE, n=18 trees) for European beech and pubescent oak in control (C, blue), drought (D, grey), heating (H, orange) and hot drought conditions (HD, red) in monocultures (empty circles) and mixtures (full circles). The letters indicate significant differences between climatic treatments and species combinations.

2.3.2 Imact of species interactions on the relationships between hydraulic traits

With decreasing $\Psi_{predawn}$, g_s exponentially decreased for both species (Fig. 2.3). While no modulating effect of the species combination was observed on this relationship for beech, oak exhibited a steeper relationship (i.e., earlier stomatal closure) in monocultures compared to mixtures (Fig. 2.3).

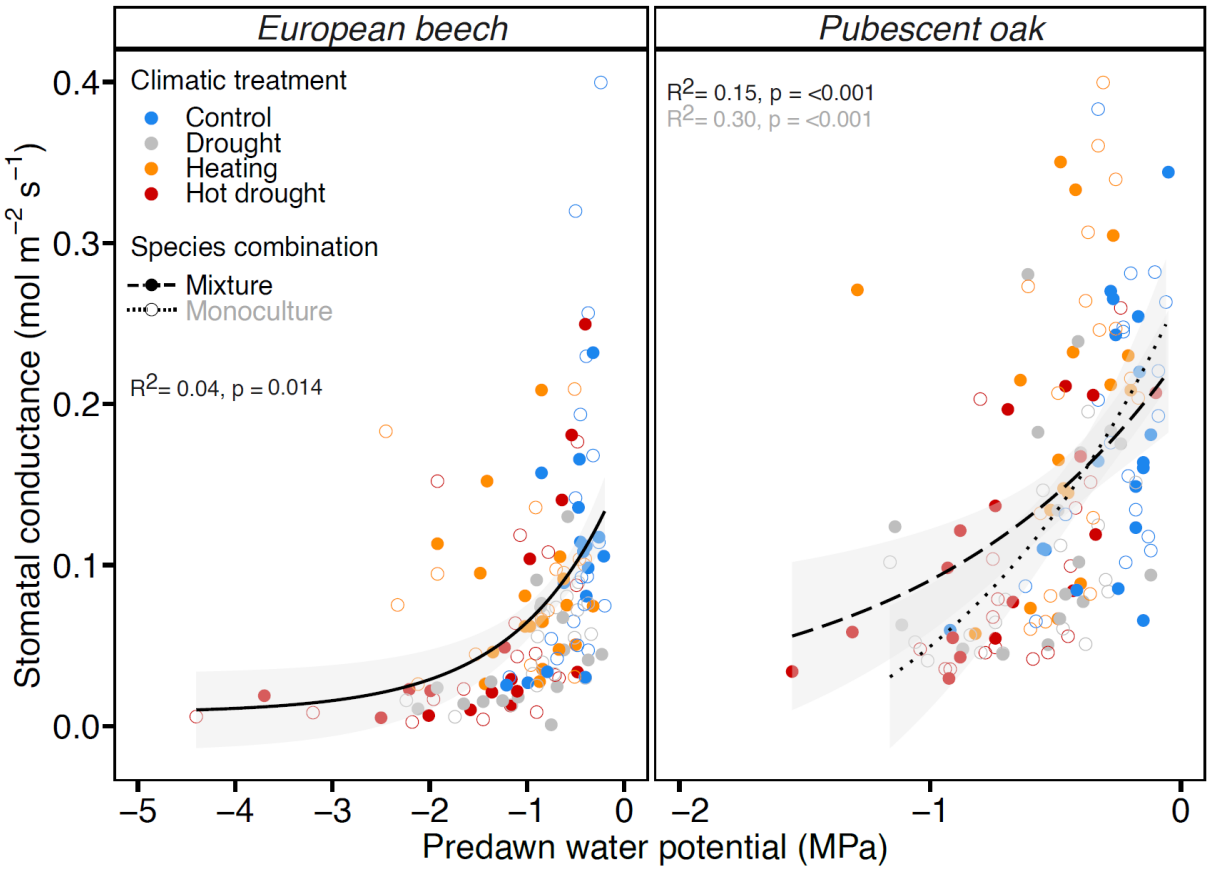

Figure 2.3: Relationships between the light-saturated stomatal conductance (g_s) and the leaf water potential at predawn ($\Psi_{predawn}$) for European beech and pubescent oak in control (blue), drought (grey), heating (orange), and hot drought conditions (red) in monocultures (empty circles) and mixtures (full circles). Lines (±CI 95%) represent exponential relationships, with dotted and solid lines standing for significant ones within a given species combination or across all species combinations, respectively. R^2 and p-value are given in the upper left corner, when significant.

With increasing g_{min}, g_s significantly increased, and SLA decreased for both species, independently of the species combination (Fig. 2.4).

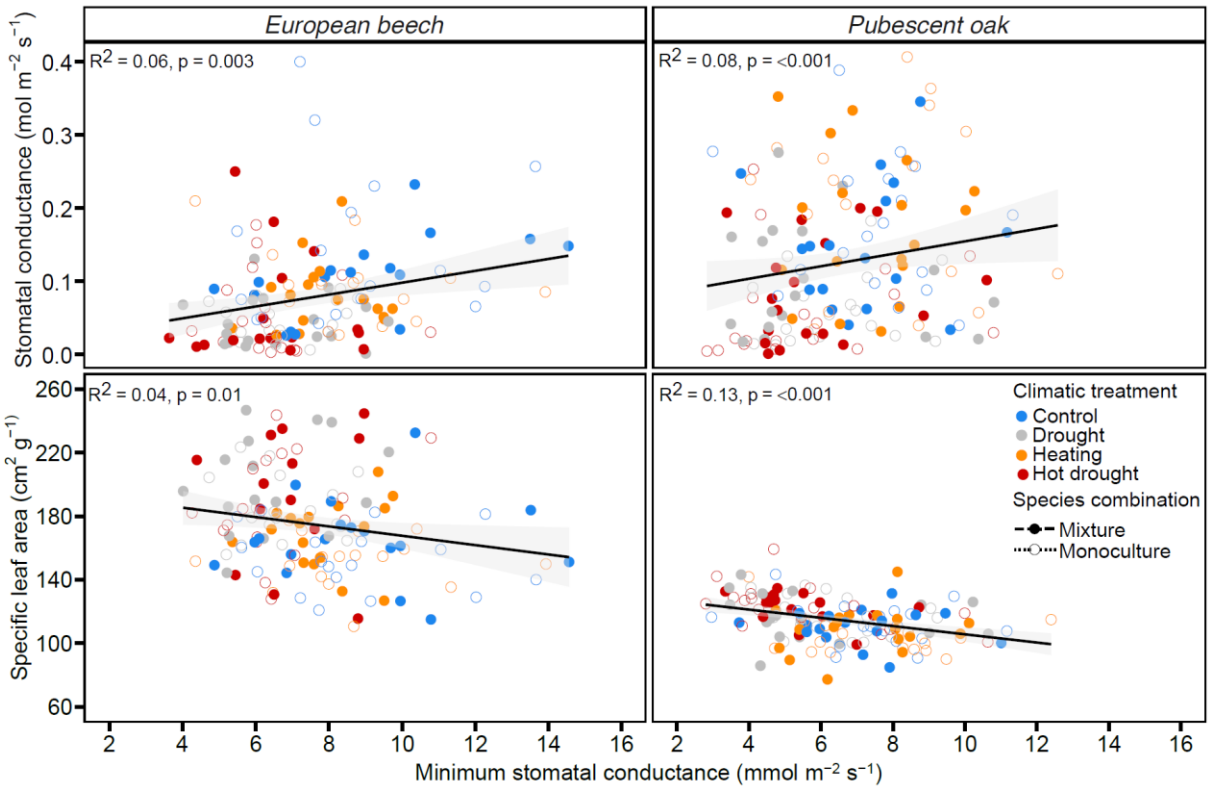

Figure 2.4: Relationships between the light-saturated stomatal conductance (g_s), the specific leaf area (SLA), and the minimal stomatal conductance (g_{min}) for European beech and pubescent oak in control (blue), drought (grey), heating (orange), and hot drought conditions (red) in monocultures (empty circles) and mixtures (plain circles). Lines represent linear regressions (±CI 95%) with solid lines standing for significant relationships across all species combinations. R^2 and p-value are given on the upper left corner, when significant.

We found a significant negative correlation between SM_{P50} and SM_{leaf} for both species (Fig. 2.5). The species combination affected this relationship for beech (P=0.01) with a steeper decrease (i.e., narrower SM_{leaf} for the same SM_{P50}) in mixtures than monocultures (Fig. 2.5).

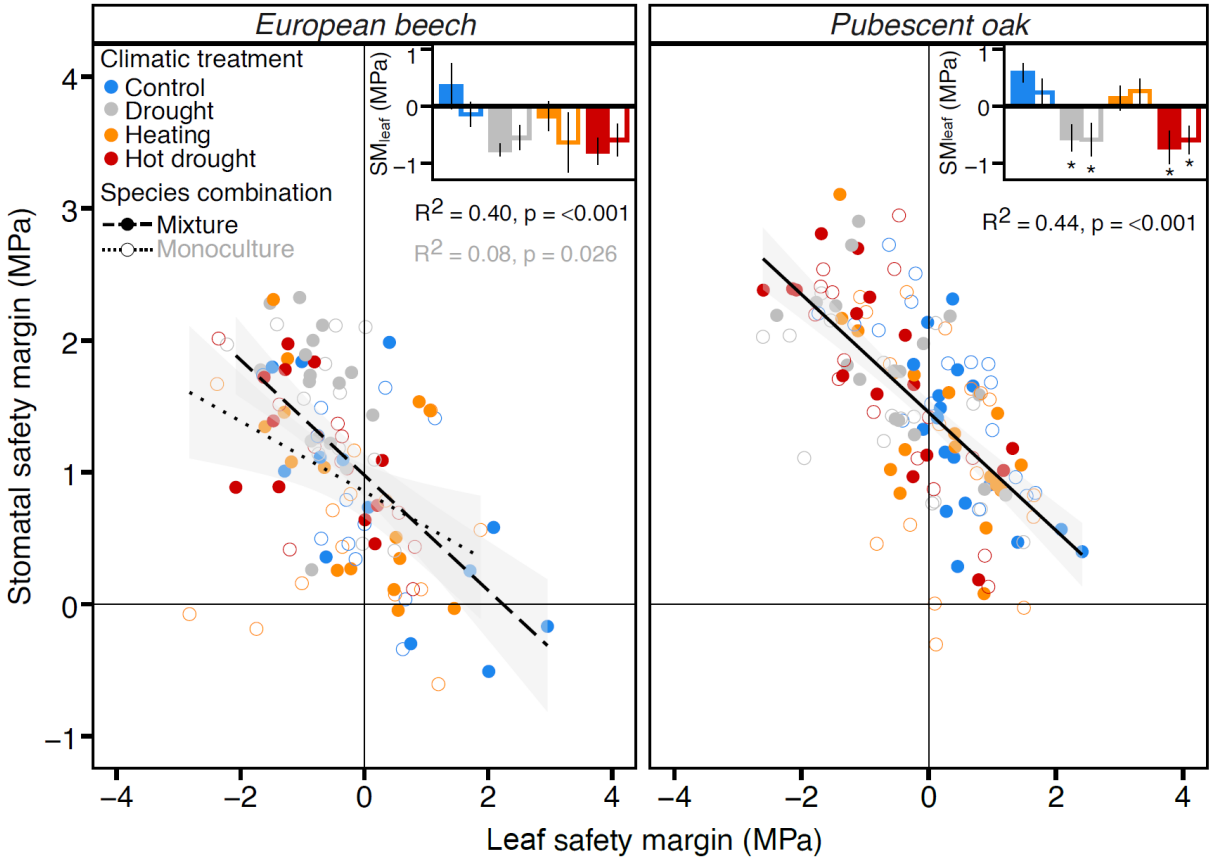

Figure 2.5: Relationships between the stomatal safety margin ($\Psi_{TLP} - P_{50}$; SM_{P50}) and the leaf safety margin ($\Psi_{midday} - \Psi_{TLP}$; SM_{leaf}) for European beech and pubescent oak in control (blue), drought (grey), heating (orange), and hot drought conditions (red) in monocultures (empty circles) and mixtures (full circles). Lines represent linear regressions (±CI 95%) with dotted and solid lines standing for significant relationships within a given species combination or across all species combinations, respectively. R^2 and p-value are given on the upper right corner, when significant. The captions in the upper right corners represent the mean SM_{leaf} for each climatic treatment and species combination for all years (i.e., 2020, 2021, 2022, mean ± SE, n= 18 trees). The stars indicate significant difference with the control (*, 0.05≥P>0.01; **, 0.01≥P>0.001; ***, P≥0.001).

2.3.3 Timing to hydraulic failure and mechanisms of species interactions

During a simulated drying cycle and under standardized climatic conditions, the time to stomatal closure (TSC) was consistently very close to hydraulic failure (THF) across all climatic treatments and for both species (6 days difference on average for beech and oak). THF was significantly longer under D and HD compared to the control for oak and beech in monocultures (+31 days and + 321 days on average for oak and beech, respectively; Fig. 2.6). With the inclusion of P_{50} acclimation in the model, THF slightly varied from +1day in the monoculture to -2 days in the mixture on average for both species in D and HD, suggesting that potential acclimation of P_{50} to drought is negligible in the THF simulation (Fig. S2.4). Moreover, the inclusion of soft traits in the simulation increased THF by 35% and 89% on average for the monoculture of oak and beech, respectively in HD

(Fig. S2.5), suggesting that THF was mainly explained by the smaller LA_{total} (Fig. S2.6) rather than the lower g_{min}, and higher Ψ_{TLP} (Fig. 2.2) in the D and HD treatments compared to the control for both species. Inter-specific interactions significantly reduced THF for beech in the D and HD treatments (by 84% and 95%, respectively), leading to similar values as oak. For oak, THF in mixtures was not significantly affected by species interactions in all climatic treatments (Fig. 2.6).

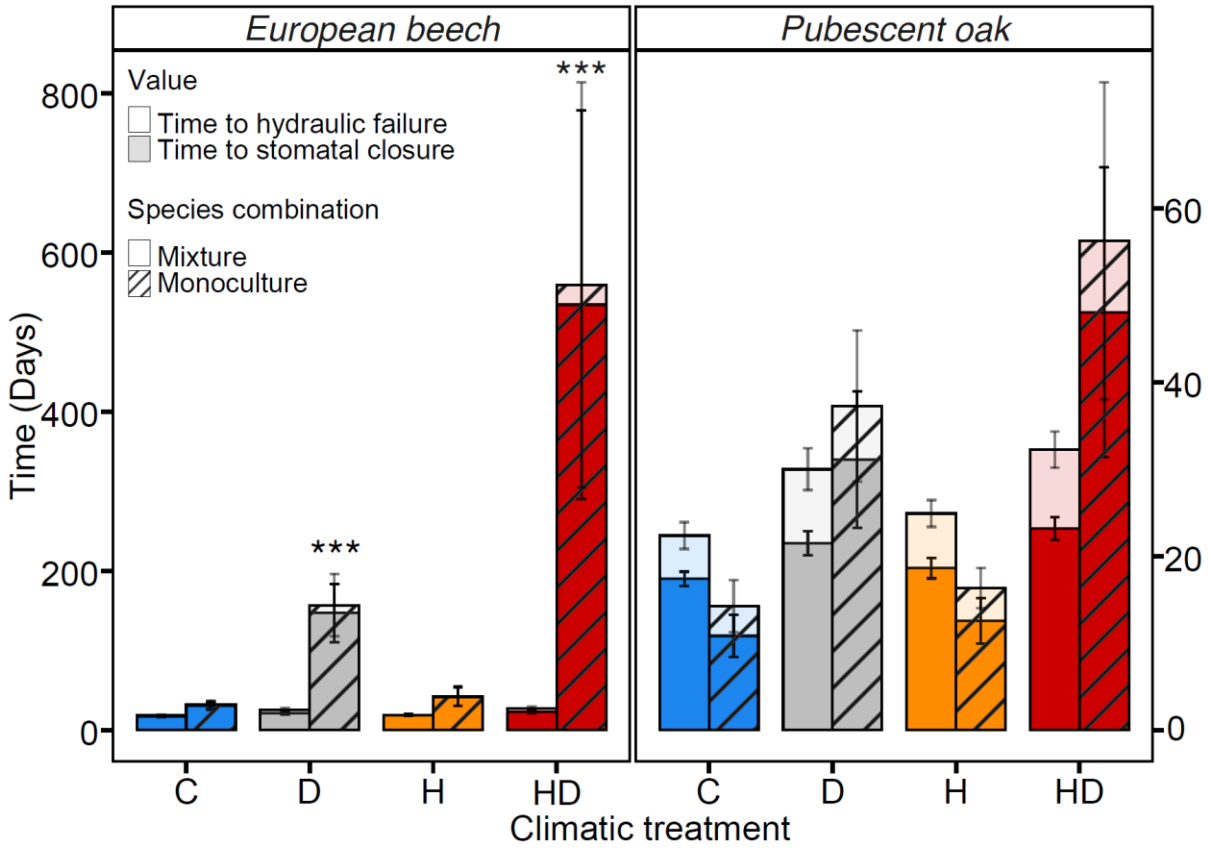

Figure 2.6: Time to hydraulic failure and stomatal closure (mean ± SE) modelled with SurEau for European beech and pubescent oak using constant P_{50} and the traits measured (Tab. S2.4) in control (C; blue), drought (D; grey), heating (H; orange), and hot drought conditions (HD; red) in monocultures (dashed bar) and mixtures (empty bar), simulated under a constant climate (i.e., mean air temperature at 20°C, VPD at 0.7, PPFD at 500 µmol m^{-2} s^{-1}, and no rain) starting with soil water at saturation. The interspecific competition was accounted for in the simulations. The stars indicate significant differences in time to hydraulic failure between species combinations within each climatic treatment and for each species (*, 0.05≥P>0.01; **, 0.01≥P>0.001; ***, P≥0.001).

2.4 Discussion

The broad screening of leaf hydraulic traits conducted in this study over multiple years allows us to shed light on how species interactions affect the events leading to drought-induced tree decline. As widely observed in temperate forests (e.g., Arend et al., 2013; Bolte et al., 2016), drought and heat increased hydraulic stress by altering multiple water-related traits, starting with decreasing the leaf water potential at predawn ($\Psi_{predawn}$) for both species (Fig. 2.2). However, we found more negative $\Psi_{predawn}$ for beech than oak, independently of the species combination (Fig. 2.3), suggesting that beech experienced stronger soil moisture limitation under the same climate manipulation. A lower tolerance to high VPD (e.g., Schönbeck et al., 2022) as highlighted by the significant reduction in stomatal conductance (g_s) with increasing VPD (Fig. S2.1), associated with a lower drought resistance (e.g., Klein, 2014; Meyer et al., 2020) could explain this response. With decreasing $\Psi_{predawn}$, both species similarly reduced g_s to limit water loss. Still, the mixture delayed stomatal closure for oak, allowing a higher g_s and less negative leaf water potential at midday (Ψ_{midday}) (Figs. 2.2 & 2.3). In contrast, for beech, the significant interaction between drought and species combination (Table S2.1) indicates a larger reduction in Ψ_{midday} in mixtures than monocultures in response to D and HD, and hence, exacerbated soil moisture stress (Fig. S2.2). These findings point to mixtures diminishing or enhancing water stress for oak and beech, respectively, potentially due to the more efficient water uptake and use of oak compared to beech. Alternatively, an improved microclimate in mixtures could benefit oak seedlings through reduced VPD (Aguirre et al., 2021; Wright et al., 2021), although, we found no indication of lower g_s sensitivity to VPD in this species (Fig. S2.1). Additional microclimate measurements would be needed to confirm this mechanism. Moreover, as previously observed (Bussotti et al., 1995; Cavender-Bares et al., 2007; Grossoni et al., 1998; Watson et al., 2023), both species reduced their minimum stomatal conductance (g_{min}), individual and whole-tree leaf area (LA_{leaf} and LA_{total}) (Fig. S2.5), and specific leaf area (SLA) under D and HD, thereby showing a long-term acclimation strategy to limit water loss. However, a more substantial reduction in LA_{leaf} (for both species) and increasing SLA (for beech only) under D and HD was found in mixtures compared to monocultures, indicating smaller and thinner leaves (Fig. 2.2 & Tab. S2.1). These findings contradict LA_{leaf} reductions in monocultures *vs*. mixtures observed in grasslands (Watson et al., 2023), which could be related to differences between grasses and trees or the relative young age of our seedlings. Nevertheless, these anatomical adjustments were insufficient for beech to overcome the higher competitiveness of oak.

These morphological shifts probably lead to a higher sensitivity to drought and heat in beech in mixtures compared to monocultures. These findings are corroborated by the steeper response of stomatal safety margins (SM_{P50}) to leaf safety margins (SM_{leaf}) in beech mixtures (Fig. 2.5). However, SM_{P50} calculations were based on a constant P_{50}, which excludes potential acclimation of this trait to

the treatments. Yet, previous study reported lower P_{50} under drought in beech (Tomasella et al., 2018) and if similar acclimation would occur in our study, SM_{P50} could increase further under drought (Fig. S2.7), leading to an even steeper relationship. Future work would be needed to determine how acclimation of P_{50} could alter this threshold in our study. Nevertheless, the observed trade-off highlights that beech in mixtures close their stomates earlier to extend the point of critical hydraulic failure. However, by reducing SM_{leaf}, beech also limits carbon uptake that could deplete carbohydrate reserves, especially under hot droughts (Grossiord et al., 2022), and minimize allocation of carbon resources belowground (e.g., Hagedorn et al., 2016). Numerous studies observed a decrease of Ψ_{TLP} under experimental drought (e.g., Serrano et al., 2005; Deligoz & Gur, 2015; Binks et al., 2016), extending the water potential range over which the leaf can remain turgid and functional. However, contrary to previously reported, Ψ_{TLP} increased under drought for both species in our experiment (Fig. 2.2), resulting in earlier stomatal closure as the soil progressively dries out. One potential explanation for higher Ψ_{TLP} could be that the smaller and thinner leaves and possible depletion of carbohydrates under prolonged hot drought may prevent osmoregulation processes from taking place (Sevanto et al., 2014). In addition, as suggested by Juenger & Verslues (2022), increasing Ψ_{TLP} could lead to slower soil water depletion, which could prove favorable under prolonged drought where water conservation and increased water use efficiency would be more valuable. From our knowledge, few works have monitored Ψ_{TLP} under chronic drought over multiple years (e.g., Tomasella et al., 2018; Hesse et al., 2023). Hence, our current understanding of Ψ_{TLP} acclimation remains limited and would need to be addressed more extensively in future studies.

An earlier stomatal closure (TSC) for beech under chronic drought when mixed with oak due to higher Ψ_{TLP} (Fig. 2.5) could reflect a more conservative strategy to delay hydraulic dysfunctions in mixtures. However, this acclimation response did not significantly broaden hydraulic safety margins and appeared insufficient to delay hydraulic failure. Indeed, we found earlier hydraulic failure (THF) for beech mixtures compared to monocultures by up to 95% under hot droughts with a standardized drying cycle and regardless of the potential acclimation of P_{50} (Fig. 2.6 & Fig. S2.4). THF was primarily driven by the total leaf area of the tree (Fig. S2.5 & S2.6), especially for oak that exhausted water resources more rapidly in mixtures. Consequently, oak's onset of hydraulic failure was not impacted by the presence of beech, whereas beech extensively shortened its TSC and THF due to increasing competition with oak compared to monocultures. Several studies highlighted the role of canopy size in drought-induced mortality with lower leaf area reducing water loss and local water stress (e.g., Greenwood et al., 2017; Anderegg et al., 2019; Rosas et al., 2019; Trugman et al., 2019). In our study, tree leaf area played a stronger role for THF than treatment acclimation in leaf hydraulic traits (i.e., g_{min} and Ψ_{TLP}) for both species. For example, this led to delayed mortality in beech compared to oak in monocultures under drought conditions (Fig. 2.6). However, when mixed with oak, the lower

evaporative demand in beech due to wider SM_{leaf} supports higher g_s in oak without decreasing soil moisture availability (as shown by the higher Ψ_{midday}). As observed here, previous work highlighted that mixtures often do not benefit the most vulnerable species to drought (i.e., beech) because the stronger competitors (i.e., oak) can exhaust water resources more rapidly or efficiently (e.g., Forrester et al., 2016; Didion-Gency et al., 2021). Here we show that this mechanism would also increase the probability of drought-induced mortality for less competitive species. However, it is important to consider that our model simulations did not include facilitative effects associated with microclimate amelioration (i.e., the simulations were run under similar climate in mixtures and monocultures), a process that would be particularly important in natural ecosystems (Aguirre et al., 2021; Wright et al., 2015). Hence, future work should further investigate how VPD may change within the different species combinations and how it could modify the THF in natural systems.

Overall, our results on tree seedlings are consistent with previous work that showed a higher growth resilience of oak in natural mixed stands with beech (e.g., Jourdan et al., 2020). Our model simulations further suggest that lower drought stress in oak could be driven by belowground competition reduction because of the lesser ability of beech to rapidly take up water resources (i.e., smaller leaf area and g_s in mixtures). However, our experiment was conducted on trees at an early development stage (i.e., six years old), and interactions between trees could take multiple years to establish (Domisch et al., 2015). Indeed, potential aboveground facilitation processes as microclimate feedbacks could be more dominant in mature forests (Zhang et al., 2022). Studies in old-growth forests have also reported lower g_s sensitivity to soil moisture and competitive dominance of beech when mixed with oak (Jacobs et al., 2022; Jonard et al., 2011), suggesting that the initial detrimental interaction observed here at the seedling stage could become beneficial as trees grow older. Moreover, although reduced drought stress in mixtures could be due to water partitioning by the deeper roots in mature stands (Früchtenicht et al., 2018), it is very unlikely that it occurred in our study as the trees were restricted to a 50-cm soil depth. Instead, belowground competition for water may have been predominant in our study. Work in more diverse forests using experimental drought or temperature manipulation would be needed to unravel how interaction processes may shift with tree ontogeny and tree diversity in natural conditions.

2.5 Conclusions

Our results show for the first time that species interactions affect the sequence of events leading to tree seedling decline and the risk of drought-induced mortality. Chronic and prolonged (i.e., more than four years) hot and dry conditions led to tighter stomatal control (lower $\Psi_{predawn}$, lower g_s, and higher turgor loss), smaller leaf area, and shorter leaf safety margins in juvenile beech. Similarly, oak acclimated to hot and dry conditions mainly by reducing leaf area and shortening the time to

stomatal closure. Nevertheless, these physiological adjustments to chronic heat and drought proved insignificant compared to differences in canopy size and transpiration rates between species during a fatal drought. Indeed, larger canopies and more rapid exhaustion of soil moisture for oak increased the simulated mortality risk of beech. Hence, this work highlights that leaf area (individual and total) and water use as proxy of plant functional strategy are important drivers of tree competitiveness and species mortality risk in mixed forests. Overall, this study pointed out the greater sensitivity of beech seedlings to projected climate scenarios mainly when mixed with more competitive species such as oak, whilst oak seedlings seemed to be more resilient to these scenarios in mixtures.

2.6 Acknowledgments

EM, JD, MD-G, and CG were supported by the Swiss National Science Foundation (310030_204697) and the Sandoz Family Foundation. We thank Jonas Gisler for help with the site installation and maintenance, and Alex Tunas for support with the field measurements. AV thanks Generalitat Valenciana for the grant CIBEST 2021/005 and INERTIA project (PID2019-111332RB-C22). CEAM is funded by Generalitat Valenciana. The authors has no competing interests to declare. Data used in this manuscript will be available from the Dryad Digital Repository, https://doi.org/10.5061/dryad.1ns1rn918.

2.7 Supporting information

2.7.1 Supporting figures

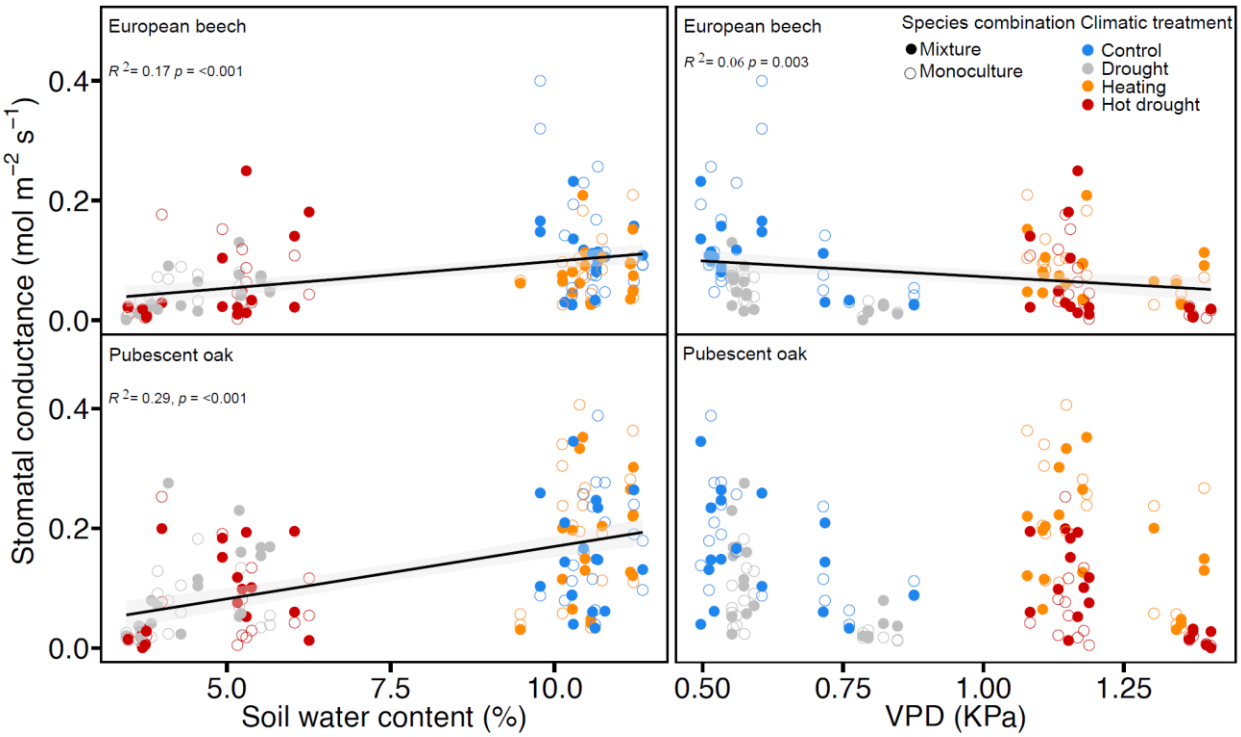

Figure S2.1: Relationships between the light-saturated stomatal conductance (g_s) and the soil water content or vapor pressure deficit (VPD) for beech and oak in control (blue), drought (grey), heating (orange), and hot drought conditions (red) in monocultures (empty circles) and mixtures (plain circles). Lines represent linear regressions with solid lines standing for significant relationships across all species combinations and climatic treatments, respectively. R^2 and p-value are given on the upper left corner, when significant.

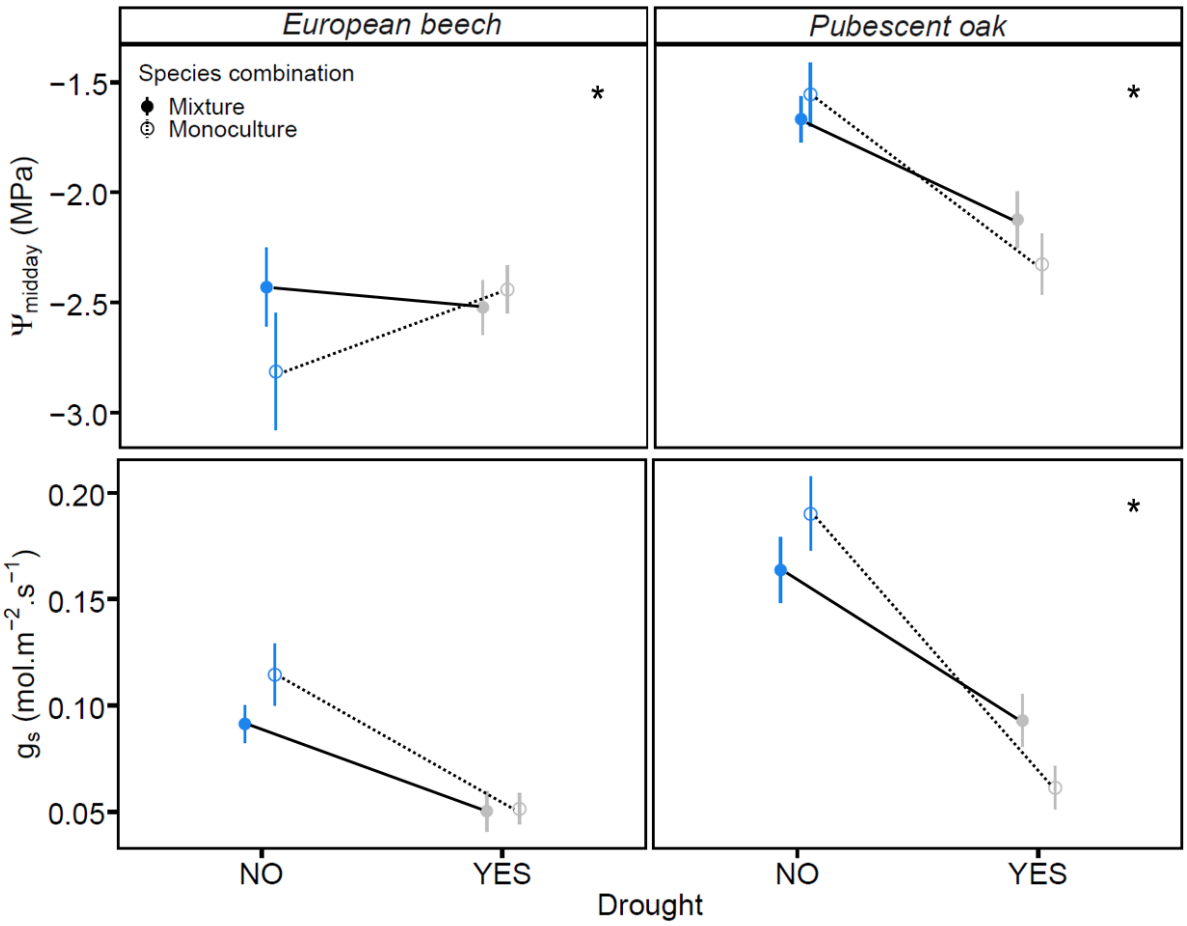

Figure S2.2: Mean leaf water potential at midday (Ψ_{midday}) and light-saturated stomatal conductance (g_s) of all years (i.e., 2020, 2021, 2022, mean ± SE, n=36 trees) for European beech (left panel) and pubescent oak (right panel) without drought treatment (i.e., Control and Heating, blue) and with drought treatment (i.e., Drought and Hot drought, gray) in mixtures (full circle) and monocultures (empty circle). Lines represent the interactions between drought and species combination, with dotted and solid lines standing for monoculture and mixture, respectively. The stars indicate significant interactions extracted from linear mixed-effects models (*, 0.05≥P>0.01; **, 0.01≥P>0.001; ***, P≥0.001).

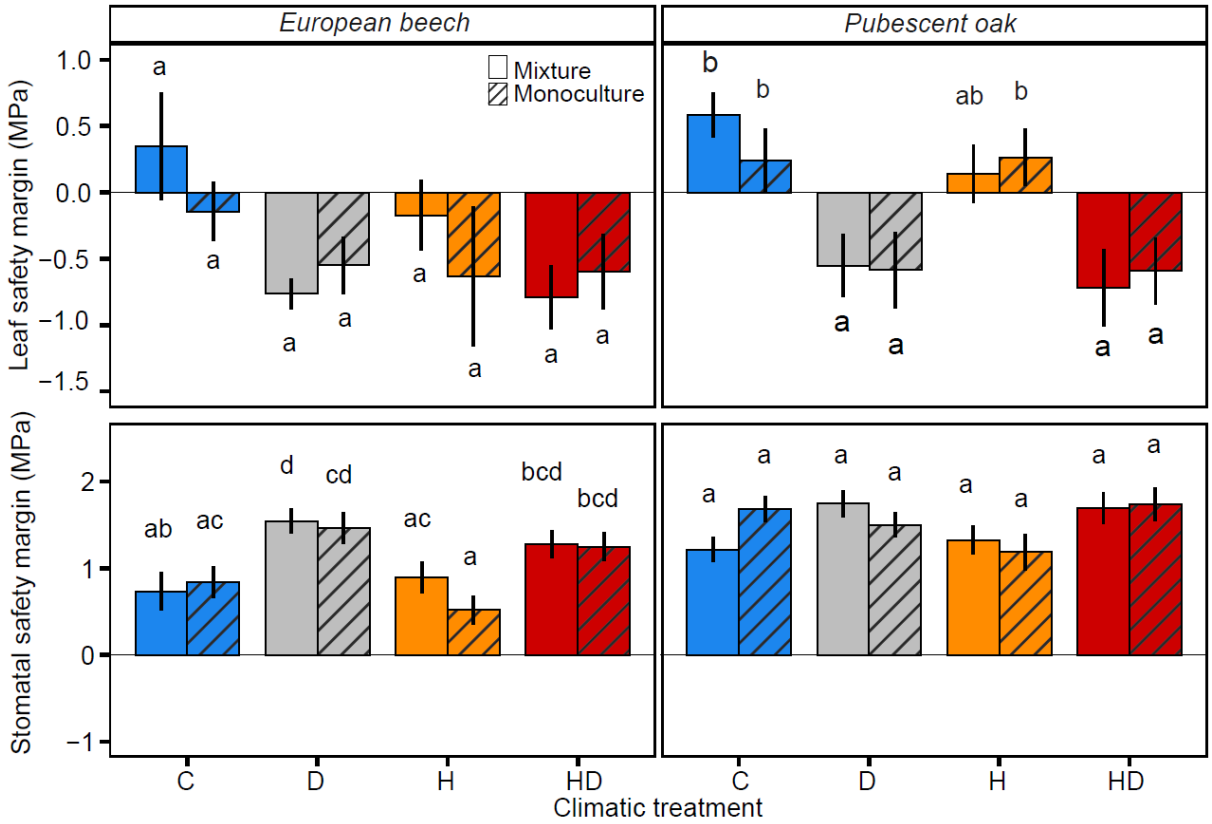

Figure S2.3: Mean leaf safety margins and stomatal safety margins of all years (i.e., 2020, 2021, 2022, mean ± SE, n=18 trees) for European beech (left panel) and pubescent oak (right panel) in control (C, blue), drought (D, gray), heating (H, orange) and hot drought treatments (HD, red) in mixtures (empty case) and monocultures (dashed case). The letters indicate significant differences between climatic and species combination treatments extracted from linear mixed-effects models followed by a Tukey-type post hoc test.

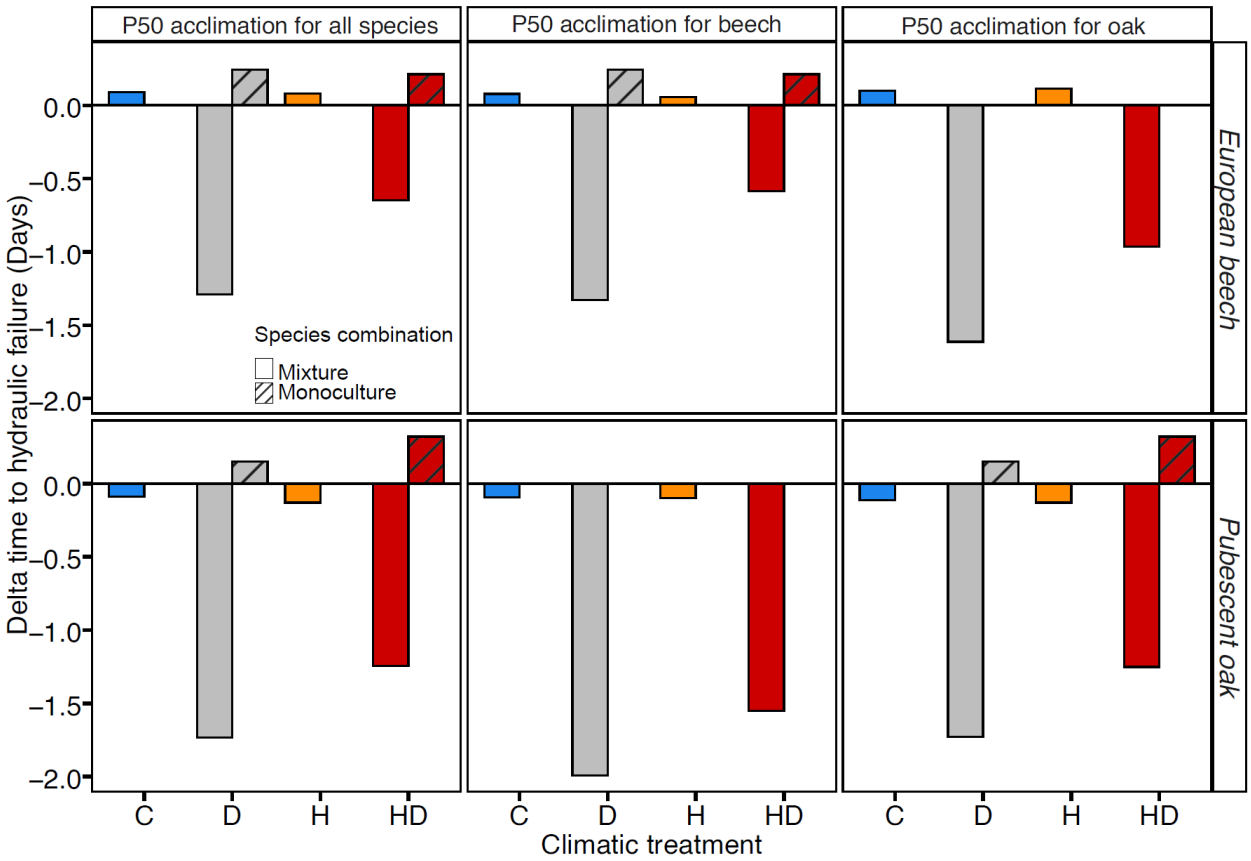

Figure S2.4: Difference of the time to hydraulic failure modelled with SurEau for beech and oak using the traits measured (Tab. S2.4) in control (C; blue), drought (D; grey), heating (H; orange), and hot drought conditions (HD; red) in monocultures (dashed bar) and mixtures (empty bar), simulated under a constant climate (i.e., mean air temperature at 20°C, VPD at 0.7, PPFD at 500 µmol m^{-2} s^{-1}, and no rain) starting with soil water at saturation; between rather acclimation of P_{50} to D and HD for all species; acclimation of P_{50} to D and HD only for beech; acclimation of P_{50} to D and HD only for oak and no acclimation of P_{50} to D and HD for all species. The interspecific competition was accounted for in the simulations.

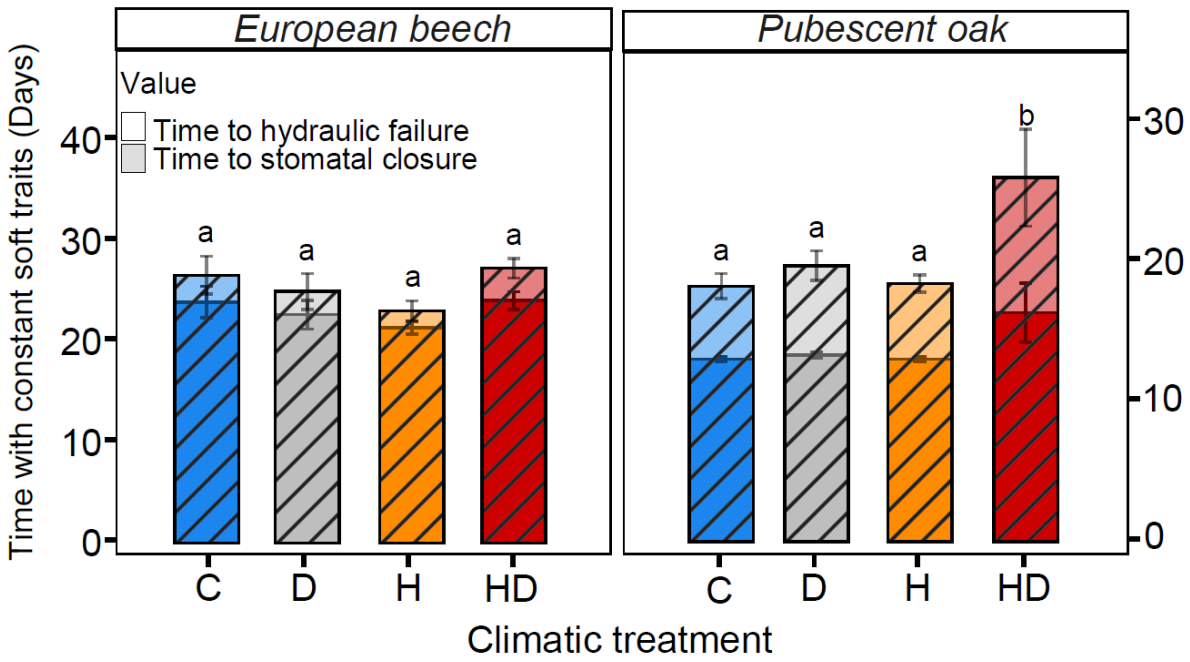

Figure S2.5: Time to hydraulic failure and stomatal closure (mean ± SE) modelled with SurEau for beech and oak using the traits measured (Tab.S2.4) in control (blue), drought (grey), heat (orange), and hot drought conditions (red) in monocultures simulated under a constant climate (i.e., mean air temperature at 20°C, VPD at 0.7, PAR 500, and no rain) starting with a soil water at saturation and with standardized soft traits across all treatments (i.e., LA_{total}, height and DBH). The letters indicate significant differences in time to hydraulic failure between climatic treatments and species combinations for each species.

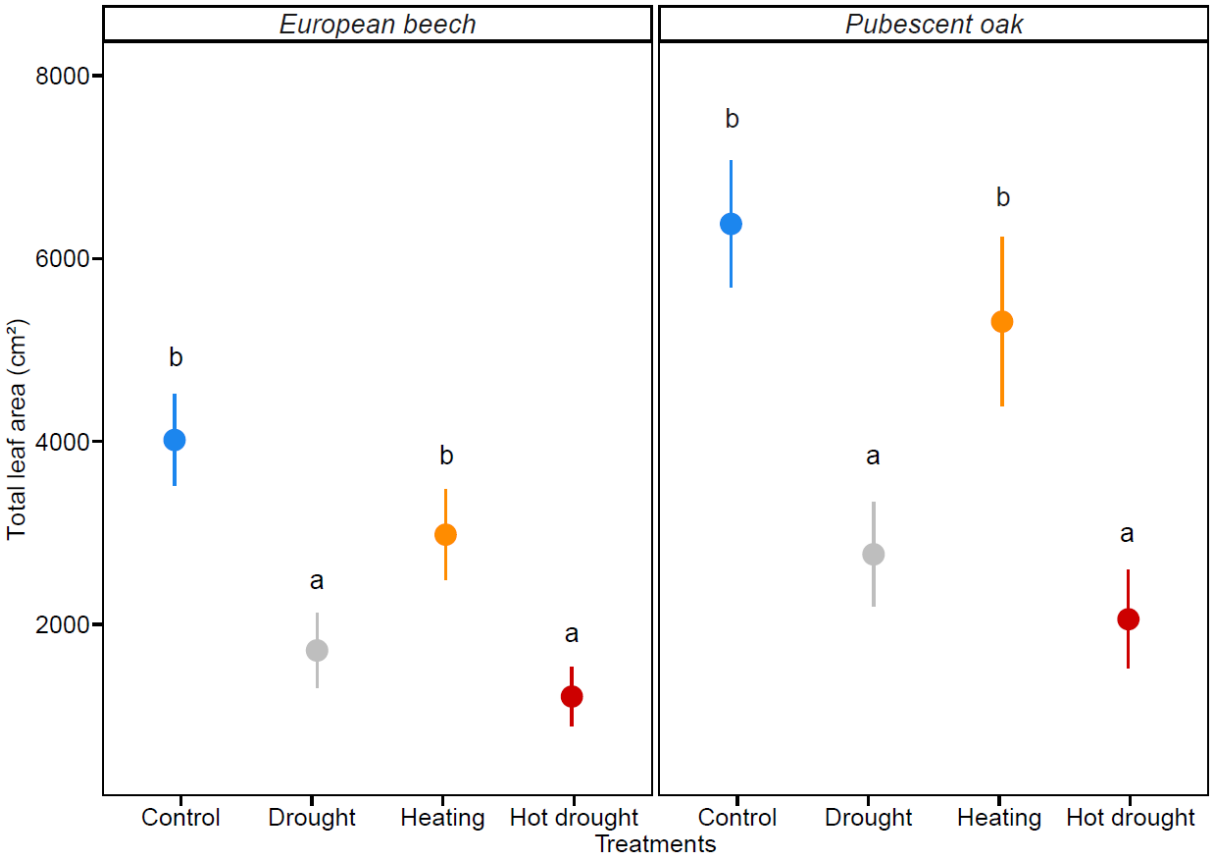

Figure S2.6: Total leaf area of the canopy (LA_{total}) for the year 2022 and all species combinations (i.e., mixture and monoculture, mean ± SE, n=12 trees) for European beech and pubescent oak in control (blue), drought (grey), heating (orange) and hot drought conditions (red). The letters indicate significant differences between climatic treatments.

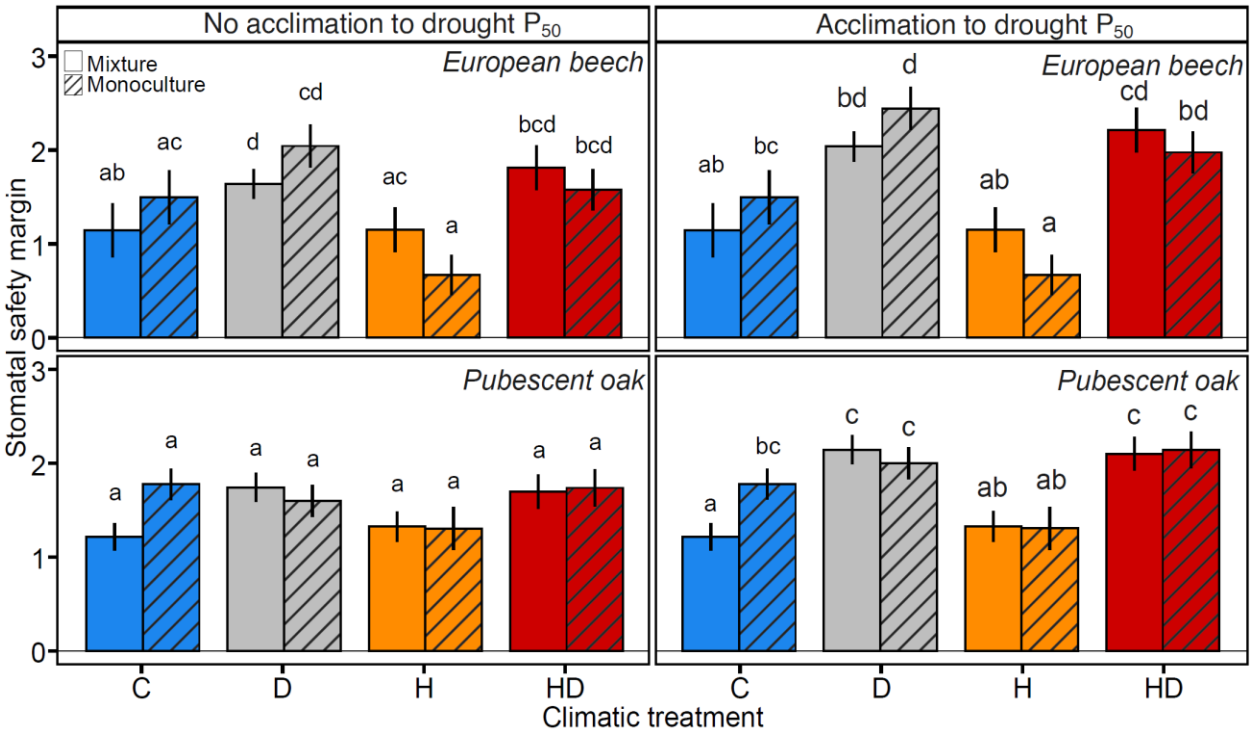

Figure S2.7: Mean stomatal safety margins of all years (i.e., 2020, 2021, 2022, mean ± SE, n=18 trees) for European beech (left panel) and pubescent oak (right panel) in control (C, blue), drought (D, gray), heating (H, orange) and hot drought treatments (HD, red) in mixtures (empty case) and monocultures (dashed case), and with or without acclimation of P_{50} to D and HD for beech and oak taking into account. The letters indicate significant differences between climatic and species combination treatments extracted from linear mixed-effects models followed by a Tukey-type post hoc test.

2.7.2 Supporting tables

Table S2.1: Statistical outputs of the mixed linear models where heating, drought, and species combination (i.e., mixture *vs*. monoculture) were used as fixed effects, and chamber and year were used as random effects for European beech and pubescent oak on leaf water potential predawn ($\Psi_{predawn}$) and midday (Ψ_{midday}), stomatal conductance (g_s), minimal stomatal conductance (g_{min}), leaf-level leaf area (LA_{leaf}), specific leaf area (SLA), water potential at the turgor loss point (Ψ_{TLP}), leaf safety margin (SM_{leaf}) and the stomatal safety margin (SM_{P50}) (*, 0.05≥P>0.01; **, 0.01≥P>0.001; ***, P≥0.001).

		European beech	Pubescent oak
$\Psi_{predawn}$	**Heating**	**>0.001*** **	**0,002** **
	Drought	**0,001** **	**>0.001*** **
	Mixture	0,454	0,703
	Heating:Drought	0,224	0,077
	Heating:Mixture	0,227	0,925
	Drought:Mixture	0,706	0,239
Ψ_{midday}	Heating	0,201	0,223
	Drought	0,606	**0,001** **
	Mixture	0,535	0,229
	Heating:Drought	0,945	0,296
	Heating:Mixture	0,693	0,976
	Drought:Mixture	**0,033***	**0,036***
g_s	Heating	0,513	0,476
	Drought	**>0.001*** **	**>0.001*** **
	Mixture	0,068	0,335
	Heating:Drought	0,711	0,264
	Heating:Mixture	0,392	0,791
	Drought:Mixture	0,901	**0,019**
g_{min}	Heating	0,442	0,746
	Drought	**0,001** **	**0,011** *
	Mixture	0,650	0,818
	Heating:Drought	0,841	0,595
	Heating:Mixture	0,634	0,545
	Drought:Mixture	0,926	0,522

LA_{leaf}	Heating	0,632	0,654
	Drought	**0,023***	**0,026***
	Mixture	**0,010***	**0,045***
	Heating:Drought	0,218	0,948
	Heating:Mixture	0,145	0,621
	Drought:Mixture	0,078	0,079
SLA	Heating	0,773	0,894
	Drought	**>0.001*** **	**>0.001*** **
	Mixture	**0,001** **	0,888
	Heating:Drought	0,689	0,056
	Heating:Mixture	0,890	0,420
	Drought:Mixture	0,538	0,283
Ψ_{TLP}	Heating	0,243	0,778
	Drought	**>0.001*** **	**0,040***
	Mixture	0,266	0,802
	Heating:Drought	0,511	0,320
	Heating:Mixture	0,489	0,707
	Drought:Mixture	0,558	0,349
SM_{P50}	Heating	0,273	0,731
	Drought	**<0,001*** **	**0,039***
	Mixture	0,322	0,702
	Heating:Drought	0,611	0,317
	Heating:Mixture	0,356	0,517
	Drought:Mixture	0,633	0,326
SM_{leaf}	Heating	0,210	0,482
	Drought	**0,040***	**<0,001*** **
	Mixture	0,707	0,945
	Heating:Drought	0,429	0,720
	Heating:Mixture	0,934	0,390
	Drought:Mixture	0,109	0,713

Table S2.2: European beech mean leaf water potential at predawn and midday ($\Psi_{predawn}$ and Ψ_{midday} in MPa, respectively), light-saturated stomatal conductance (g_s, mol m^{-2} s^{-1}), minimal stomatal conductance (g_{min}, mmol m^{-2} s^{-1}), individual leaf area (LA_{leaf}, cm²), specific leaf area (SLA, cm² g^{-1}), water potential at the turgor loss point (Ψ_{TLP}, MPa), stomatal safety margin (SM_{P50}, MPa) and leaf safety margin (SM_{leaf}, MPa) for each year (i.e., 2020, 2021, 2022) in control (C), drought (D), heating (H) and hot drought (HD) conditions in monocultures and mixtures (mean±sd, n=6 trees)

		Monoculture				Mixture			
		C	D	H	HD	C	D	H	HD
$\Psi_{predawn}$	2020	-0,34 ± 0,11	-0,58 ± 0,19	-1,41 ± 0,94	-1,02 ± 0,58	-0,48 ± 0,22	-0,71 ± 0,12	-0,84 ± 0,41	-1,07 ± 0,65
	2021	-0,40 ± 0,09	-0,64 ± 0,25	-0,64 ± 0,18	-1,13 ± 0,54	-0,39 ± 0,09	-0,82 ± 0,45	-0,95 ± 0,37	-1,18 ± 0,55
	2022	-0,67 ± 0,28	-1,45 ± 0,61	-1,28 ± 0,66	-2,26 ± 1,30	-0,71 ± 0,35	-1,51 ± 0,50	-1,11 ± 0,48	-2,39 ± 0,99
Ψ_{midday}	2020	-2,75 ± 0,48	-2,38 ± 0,32	-5,02 ± 2.00	-2,77 ± 0,72	-3,31 ± 0,61	-2,60 ± 0,64	-2,76 ± 0,79	-2,92 ± 0,88
	2021	-2,99 ± 0,36	-2,51 ± 0,68	-2,63 ± 0,39	-2,35 ± 0,28	-2,29 ± 0,68	-2,12 ± 0,65	-2,92 ± 0,45	-2,63 ± 0,72
	2022	-1,84 ± 0,91	-2,04 ± 0,76	-1,59 ± 0,97	-2,67 ± 0,81	-1,05 ± 0,95	-2,16 ± 0,50	-1,67 ± 1,11	-2,90 ± 0,28
g_s	2020	0,12 ± 0,08	0,07 ± 0,01	0,10 ± 0,05	0,10 ± 0,06	0,11 ± 0,03	0,07 ± 0,04	0,09 ± 0,06	0,08 ± 0,09
	2021	0,22 ± 0,12	0,05 ± 0,02	0,12 ± 0,05	0,06 ± 0,05	0,15 ± 0,04	0,05 ± 0,03	0,08 ± 0,04	0,07 ± 0,07
	2022	0,07 ± 0,04	0,02 ± 0,01	0,05 ± 0,02	0,01 ± 0,01	0,05 ± 0,04	0,02 ± 0,01	0,06 ± 0,03	0,01 ± 0,01
g_{min}	2020	8,98 ± 3,67	7,11 ± 1,42	8,63 ± 1,14	7,13 ± 2,09	7,74 ± 3,08	6,30 ± 1,43	8,05 ± 1,52	6,90 ± 1,72
	2021	9,02 ± 1,79	6,63 ± 1,56	8,76 ± 3,43	6,15 ± 1,34	10,72 ± 1,98	7,38 ± 1,78	7,94 ± 1,05	5,80 ± 1,48
	2022	7,79 ± 0,90	6,54 ± 0,61	8,18 ± 1,36	6,45 ± 0,75	7,97 ± 1,23	6,35 ± 1,62	7,55 ± 1,34	6,86 ± 1,54
LA_{leaf}	2020	9,21 ± 4,63	6,93 ± 3,67	8,73 ± 2,32	7,78 ± 3,81	7,32 ± 4,15	7,11 ± 3,85	11,08 ± 3,28	6,08 ± 2,12
	2021	15,37 ± 4,41	13,66 ± 6,56	16,44 ± 7,73	9,01 ± 3,68	11,25 ± 3,61	8,40 ± 2,87	11,60 ± 2,94	7,99 ± 4,92
	2022	12,34 ± 3,49	13,96 ± 8,12	9,78 ± 2,11	7,58 ± 3,36	11,29 ± 3,68	8,06 ± 5,30	15,23 ± 3,75	5,09 ± 3,57
SLA	2020	152,19 ± 17,94	171,54 ± 10,11	159,92 ± 12,56	174,99 ± 30,04	169,59 ± 14,66	210,82 ± 34,84	166,21 ± 31,65	187,17 ± 54,37
	2021	155,26 ± 24,78	192,09 ± 18,37	138,96 ± 16,65	185,21 ± 31,12	159,33 ± 41,47	196,47 ± 22,80	166,9 ± 14,71	202,7 ± 47,26
	2022	151,66 ± 21,19	191,43 ± 24,03	150,20 ± 20,87	198,94 ± 34,51	168,11 ± 19,10	200,62 ± 40,93	175,29 ± 12,81	206,5 ± 33,23
Ψ_{TLP}	2020	-2,46 ± 0,62	-1,88 ± 0,54	-2,85 ± 0,87	-2,17 ± 0,59	-2,50 ± 0,33	-1,61 ± 0,76	-2,82 ± 0,42	-2,11 ± 0,64
	2021	-2,57 ± 0,75	-1,51 ± 0,52	-2,86 ± 0,57	-2,09 ± 0,70	-2,50 ± 1,03	-1,75 ± 0,56	-2.00 ± 0,92	-2,10 ± 0,45
	2022	-2.00 ± 0,51	-1,95 ± 1,20	-2,26 ± 0,37	-1,47 ± 0,25	-2,41 ± 0,97	-1,59 ± 0,36	-2,14 ± 0,49	-1,31 ± 0,24

SM_{P50}	2020	0,75 ± 0,62	1,32 ± 0,54	0,35 ± 0,87	1,03 ± 0,59	0,70 ± 0,33	1,59 ± 0,76	0,38 ± 0,42	1,09 ± 0,64
	2021	0,63 ± 0,75	1,69 ± 0,52	0,34 ± 0,57	1,11 ± 0,70	0,70 ± 1,03	1,45 ± 0,56	1,2 ± 0,92	1,10 ± 0,45
	2022	1,20 ± 0,51	1,25 ± 1,20	0,94 ± 0,37	1,73 ± 0,25	0,79 ± 0,97	1,61 ± 0,36	1,06 ± 0,49	1,89 ± 0,24
SM_{leaf}	2020	-0,24 ± 0,79	-0,49 ± 0,35	-2,16 ± 2,44	-0,65 ± 0,93	-0,61 ± 0,68	-0,99 ± 0,28	0,32 ± 0,80	-0,85 ± 1.00
	2021	-0,29 ± 0,83	-0,93 ± 0,91	0,21 ± 0,60	-0,03 ± 0,67	0,21 ± 1,48	-0,54 ± 0,70	-0,92 ± 0,82	-0,52 ± 0,80
	2022	0,12 ± 0,82	0,25 ± 0,33	0,52 ± 0,96	-1,86 ± 0,69	1,28 ± 1,51	-0,72 ± 0,23	0,34 ± 1,03	-1,45 ± 0,24

Table S2.3: Pubescent oak mean leaf water potential at predawn and midday ($\Psi_{predawn}$ and Ψ_{midday} in MPa, respectively), light-saturated stomatal conductance (g_s, mol m^{-2} s^{-1}), minimal stomatal conductance (g_{min}, mmol m^{-2} s^{-1}), individual leaf area (LA_{leaf}, cm²), specific leaf area (SLA, cm² g^{-1}), water potential at the turgor loss point (Ψ_{TLP}, MPa), stomatal safety margin (SM_{P50}, MPa) and leaf safety margin (SM_{leaf}, MPa) for each year (i.e., 2020, 2021, 2022) in control (C), drought (D), heating (H) and hot drought (HD) conditions in monocultures and mixtures (mean±sd, n=6 trees).

		Monoculture				Mixture			
		C	D	H	HD	C	D	H	HD
$\Psi_{predawn}$	2020	-0,21 ± 0,10	-0,47 ± 0,20	-0,36 ± 0,11	-0,51 ± 0,23	-0,24 ± 0,07	-0,43 ± 0,10	-0,56 ± 0,37	-0,58 ± 0,20
	2021	-0,15 ± 0,08	-0,52 ± 0,34	-0,32 ± 0,14	-0,68 ± 0,14	-0,16 ± 0,07	-0,51 ± 0,36	-0,39 ± 0,19	-0,51 ± 0,33
	2022	-0,38 ± 0,20	-0,88 ± 0,15	-0,49 ± 0,12	-0,80 ± 0,23	-0,46 ± 0,29	-0,74 ± 0,26	-0,52 ± 0,18	-1,05 ± 0,31
Ψ_{midday}	2020	-1,86 ± 0,67	-2,74 ± 0,41	-2,37 ± 0,57	-2,60 ± 0,37	-1,72 ± 0,52	-2,47 ± 0,29	-2,54 ± 0,32	-1,95 ± 0,30
	2021	-1,24 ± 0,57	-2,61 ± 1,15	-2,12 ± 1,16	-1,87 ± 0,47	-1,72 ± 0,48	-2,08 ± 0,82	-1,70 ± 0,38	-2,44 ± 0,42
	2022	-0,87 ± 0,49	-1,88 ± 0,77	-0,87 ± 0,09	-2,20 ± 0,80	-1,07 ± 0,57	-1,55 ± 0,75	-1,26 ± 0,40	-2,27 ± 1,10
g_s	2020	0,26 ± 0,07	0,06 ± 0,03	0,25 ± 0,10	0,12 ± 0,09	0,18 ± 0,08	0,13 ± 0,08	0,27 ± 0,08	0,15 ± 0,06
	2021	0,15 ± 0,06	0,11 ± 0,05	0,25 ± 0,10	0,05 ± 0,04	0,17 ± 0,11	0,13 ± 0,08	0,15 ± 0,06	0,09 ± 0,06
	2022	0,11 ± 0,07	0,02 ± 0,01	0,12 ± 0,11	0,01 ± 0,01	0,10 ± 0,06	0,04 ± 0,02	0,10 ± 0,07	0,02 ± 0,01
g_{min}	2020	7,42 ± 2,68	6,53 ± 0,87	7,56 ± 3,37	6,29 ± 3,14	6,11 ± 1,60	5,75 ± 1,68	7,07 ± 1,87	6,82 ± 2,51
	2021	7,67 ± 0,85	6,15 ± 1,85	8,22 ± 1,74	5,59 ± 2,01	8,16 ± 1,55	6,32 ± 2,84	7,60 ± 1,72	5,53 ± 1,19
	2022	7,20 ± 1,94	6,07 ± 1,98	7,15 ± 1,83	4,63 ± 1,48	6,72 ± 1,56	5,26 ± 2,51	6,86 ± 1,41	4,94 ± 0,66
LA_{leaf}	2020	10,90 ± 2,64	7,11 ± 2,91	10,97 ± 2,62	9,42 ± 2,53	7,13 ± 1,60	4,50 ± 1,91	8,09 ± 3,55	7,32 ± 4,17
	2021	18,79 ± 9,88	10,98 ± 4,95	14,10 ± 4,35	14,47 ± 4,71	19,76 ± 5,27	14,65 ± 5,43	19,30 ± 8,57	9,06 ± 5,36
	2022	10,93 ± 1,34	13,53 ± 3,97	14,43 ± 5,41	13,24 ± 5,17	12,38 ± 4,26	11,86 ± 4,74	20,49 ± 13,03	13,02 ± 5,50
SLA	2020	105,92 ± 8,74	112,08 ± 15,31	111,64 ± 16,62	126,58 ± 19,21	100,30 ± 11,04	105,54 ± 13,25	105,52 ± 16,67	115,27 ± 13,42
	2021	109,63 ± 7,89	118,80 ± 9,02	101,40 ± 8,32	120,68 ± 13,55	115,15 ± 10,87	114,38 ± 7,09	112,59 ± 17,09	124,42 ± 5,08
	2022	121,24 ± 17,29	123,09 ± 11,74	99,35 ± 7,08	124,65 ± 7,80	114,17 ± 5,09	130,26 ± 10,03	108,01 ± 10,27	127,19 ± 6,22
Ψ_{TLP}	2020	-1,30 ± 0,44	-1,49 ± 0,60	-2,14 ± 1,09	-1,61 ± 0,74	-2,07 ± 0,55	-1,48 ± 0,39	-1,80 ± 0,57	-1,79 ± 0,85
	2021	-1,75 ± 0,79	-2,21 ± 0,57	-2,38 ± 0,90	-1,81 ± 0,93	-2,32 ± 0,42	-1,49 ± 1.00	-2,08 ± 1,07	-1,54 ± 0,90
	2022	-1,83 ± 0,47	-1,67 ± 0,36	-1,76 ± 0,45	-1,27 ± 0,85	-1,86 ± 0,81	-1,71 ± 0,49	-2,05 ± 0,26	-1,48 ± 0,61

SM_{P50}	2020	2.00 ± 0,44	1,81 ± 0,60	1,16 ± 1,09	1,69 ± 0,74	1,23 ± 0,55	1,82 ± 0,39	1,50 ± 0,57	1,51 ± 0,85
	2021	1,55 ± 0,79	1,09 ± 0,57	0,92 ± 0,90	1,49 ± 0,93	0,98 ± 0,42	1,81 ± 1.00	1,22 ± 1,07	1,76 ± 0,90
	2022	1,48 ± 0,47	1,63 ± 0,36	1,54 ± 0,45	2,03 ± 0,85	1,44 ± 0,81	1,59 ± 0,49	1,25 ± 0,26	1,82 ± 0,61
SM_{leaf}	2020	-0,56 ± 0,64	-1,19 ± 0,91	-0,23 ± 0,95	-0,85 ± 1.00	0,35 ± 0,36	-0,99 ± 0,58	-0,74 ± 0,40	-0,19 ± 0,68
	2021	0,52 ± 1,21	-0,40 ± 1,59	0,25 ± 0,86	-0,11 ± 1,04	0,60 ± 0,43	-0,87 ± 1,19	0,38 ± 1.00	-1,15 ± 0,73
	2022	0,88 ± 0,14	-0,21 ± 0,61	0,87 ± 0,51	-0,81 ± 0,87	0,79 ± 1,15	0,16 ± 0,81	0,79 ± 0,47	-0,79 ± 1,66

Table S2.4: Pubescent oak and European beech hard and soft traits used to parameterize the SurEAU model in 2022 in the control (C), drought (D), heating (H), and hot drought (HD) conditions in monocultures and mixtures (mean±SD, n=6 trees). The hard traits are: light-saturated maximal assimilation (A_{max}, µmol m^{-2} s^{-1}) and stomatal conductance (g_s, mol m^{-2} s^{-1}), evapotranspiration (E, mol m^{-2} s^{-1}), minimal stomatal conductance (g_{min}, mmol m^{-2} s^{-1}), water potential at the turgor loss point (Ψ_{TLP}, MPa), osmotic potential at full turgor (Ψ_o, MPa), modulus of elasticity (ε, MPa), relative water content (RWC, %), and water potential at 50% of xylem conductivity loss (P_{50}, MPa). The soft traits are: individual leaf area (LA_{leaf}, cm²), total leaf area (LA_{total}, cm²), specific leaf area (SLA, cm² g^{-1}), leaf dry matter content (LDMC, g g^{-1}), height (cm), and stem diameter at 15cm (DBH, mm).

			Monoculture				Mixture			
			C	D	H	HD	C	D	H	HD
Hard trait	A_{max}	Beech	2,59±0,91	0,89±0,65	2,59±1,56	0,27±0,47	2,32±1,34	0,91±0,82	2,64±1,4	0,81±0,89
		Oak	6,50±3,41	2,68±1,14	6,00±4,8	1,17±0,76	6,46±2,66	3,48±2,42	6,33±4,17	1,78±1,35
	g_s	Beech	0,07± 0,04	0,02 ± 0,01	0,05 ± 0,02	0,01 ± 0,01	0,05± 0,04	0,02± 0,01	0,06± 0,03	0,01 ± 0,01
		Oak	0,11 ± 0,07	0,02 ± 0,01	0,12± 0,11	0,01 ± 0,01	0,10 ± 0,06	0,04 ± 0,02	0,10± 0,07	0,02 ± 0,01
	E	Beech	0,0010±0,0005	0,0003±0,0002	0,0018±0,0015	0,0003±0,0002	0,0603±0,1461	0,0003±0,0002	0,0016±0,0008	0,0003±0,0002
		Oak	0,0015±0,0008	0,0003±0,0001	0,0024±0,0019	0,0003±0,0002	0,0014±0,0008	0,0007±0,0005	0,0022±0,0014	0,0005±0,0003
	g_{min}	Beech	7,79± 0,9	6,54 ± 0,61	8,18± 1,36	6,45± 0,75	7,97 ± 1,23	6,35 ± 1,62	7,55± 1,34	6,86 ± 1,54
		Oak	7,2± 1,94	6,07± 1,98	7,15± 1,83	4,63 ± 1,48	6,72 ± 1,56	5,26± 2,51	6,86 ± 1,41	4,94± 0,66
	Ψ_{TLP}	Beech	-2,00± 0,51	-1,95 ± 1,2	-2,26± 0,37	-1,47± 0,25	-2,41± 0,97	-1,59 ± 0,36	-2,14 ± 0,49	-1,31± 0,24
		Oak	-1,83± 0,47	-1,67 ± 0,36	-1,76 ± 0,45	-1,27± 0,85	-1,86± 0,81	-1,71± 0,49	-2,05± 0,26	-1,48 ± 0,61
	Ψ_0	Beech	-1,31±0,84	-1,78±1,19	-1,51±0,55	-1,23±0,22	-1,81±1,18	-0,94±0,41	-1,07±0,14	-1,03±0,35
		Oak	-1,63±0,33	-1,38±0,31	-1,47±0,47	-0,86±0,75	-1,53±0,83	-1,40±0,46	-1,73±0,37	-1,29±0,64
	ε	Beech	7,65±8,26	6,38±0,97	9,69±10,18	6,07±1,19	7,60±7,21	5,40±3,89	1,08±0,91	6,78±4,56
		Oak	10,79±1,55	8,04±1,66	10,45±5,89	4,64±3,04	8,73±4,24	10,01±3,14	11,46±2,86	9,75±5,2
	RWC	Beech	74,23±14,63	73,97±0,18	70,85±16,71	80,08±4,79	68,80±16,72	75,83±15,25	56,34±9,63	80,18±4,92
		Oak	87,87±2,57	87,47±4,51	87,54±2,5	87,57±5,38	90,00±1,45	88,65±4,05	87,62±2,91	90,30±1,44
	P_{50}	Beech	-3,20	-3,20	-3,20	-3,20	-3,20	-3,20	-3,20	-3,20
		Oak	-3,30	-3,30	-3,30	-3,30	-3,30	-3,30	-3,30	-3,30

Soft trait	LA_{leaf}	Beech	12,34±3,49	13,96±8,12	9,78±2,11	7,58±3,36	11,29±3,68	8,06±5,3	15,23±3,75	5,09±3,57
		Oak	10,93±1,34	13,53±3,97	14,43±5,41	13,24±5,17	12,38±4,26	11,86±4,74	20,49±13,03	13,02±5,5
	LA_{total}	Beech	4419,50±1642,39	2468,33±1716,71	2588,67±1233,5	1824,67±1062,2	3611,00±1874,82	957,67±305,14	3370,67±2149,01	470,20±376,84
		Oak	5137,83±700,88	2562,50±2387,81	3706,33±855,64	1317,83±687,31	7620,17±2923,14	2967,00±1682,75	6913,17±3933,08	2791,33±2427,87
	SLA	Beech	151,66± 21,19	191,43± 24,03	150,20 ± 20,87	198,94± 34,51	168,11 ± 19,1	200,62± 40,93	175,29± 12,81	206,5± 33,23
		Oak	121,24± 17,29	123,09 ± 11,74	99,35 ± 7,08	124,65 ± 7,8	114,17± 5,09	130,26 ± 10,03	108,01 ± 10,27	127,19± 6,22
	LDMC	Beech	0,46±0,04	0,46±0,03	0,50±0,03	0,49±0,04	0,46±0,04	0,44±0,05	0,48±0,03	0,47±0,06
		Oak	0,43±0,05	0,45±0,03	0,42±0,02	0,44±0,02	0,43±0,04	0,44±0,02	0,43±0,03	0,46±0,03
	Height	Beech	98,67±14,51	85,58±22,44	102,08±32,81	68,92±16,95	96,67±14,56	75,33±15,32	102,33±27,28	65,20±7,69
		Oak	155,33±40,59	72,58±12,91	114,17±30,38	76,67±13,22	131,50±54,55	75,83±16,74	136,00±115,08	81,00±13,19
	DBH	Beech	10,21±1,15	8,64±2,63	9,38±0,93	8,29±2,83	10,14±1,45	6,82±0,63	9,92±2,36	5,93±0,1
		Oak	13,32±2,24	6,65±1,56	9,31±2,71	6,32±1,07	11,96±2,68	7,60±1,19	10,27±5	7,61±2,41

2.7.3 Supporting notes

Notes S1: Total leaf area

We estimated the whole-canopy leaf area (LA_{total}, cm^2) by counting for each tree the number of leaves and measuring the average leaf area of ten representative leaves (i.e., of different sizes and canopy levels) from photographs. For this, we took a photograph of individual leaves placed on a clipboard next to a reference of 4 cm^2 at a fixed distance. We further analyzed the images and calculate the leaf area as follows: leaf area (cm^2) = (reference area (cm^2)/number of pixels reference) * number of pixels per leaf. Analyses were performed using the R software (R Core Team, 2022). LA_{total} was estimated by multiplying the total number of leaves with the average leaf area of the ten representative leaves.

Chapter 3

Mixing oak and pine trees in Mediterranean forests increases aboveground hydraulic dysfunctions

Eugénie Mas[1,2]*, Alberto Vilagrosa[3], Luna Morcillo[3], Fernando Valladares[4], Charlotte Grossiord[1,2]

[1]Plant Ecology Research Laboratory PERL, School of Architecture, Civil and Environmental Engineering, EPFL, Lausanne, Switzerland

[2]Community Ecology Unit, Swiss Federal Institute for Forest, Snow and Landscape WSL, Lausanne, Switzerland

[3]CEAM Foundation, Joint Research Unit University of Alicante-CEAM, Department of Ecology, University of Alicante, PO Box 99, C. San Vicente del Raspeig, s/n, Alicante 03080, Spain

[4]Depto de Biogeografía y Cambio Global, LINCGlobal, Museo Nacional de Ciencias Naturales (MNCN-CSIC), Madrid, España and Área de Biodiversidad y Conservación, Univ. Rey Juan Carlos, Móstoles, Madrid, España

This chapter has been submitted to the peer-reviewed journal "*Plant Biology*".

Author’s contribution

Charlotte Grossiord (CG) and I conceived and designed the study. This included decisions regarding the plots and trees selection, the sampling design and field logistics. I specifically focused on preparing the sampling campaign by aquiring all necessary materials, and ensuring field protocols and logisitics could run smoothly. Luna Morcillo (LM), Alberto Vilagrosa (AV) performed the wood hydraulic measurements in the laboratory. CG and I collected the samples and measured the water potentials at the leaf level. I analyzed the data, produced all figures and tables, and led the writing of the manuscript. All authors (i.e., CG, LM, AV, Fernando Valladares, and I) critically contributed to the manuscript and gave final approval for publication.

Abstract:

- Increasing tree species diversity in Mediterranean forests could reduce drought-induced hydraulic impairments through improved microclimate and reduced competition for water. However, it remains unclear if and how species diversity modulates tree hydraulic functions and how impacts may shift during the growing season.
- Using natural Mediterranean forest stands composed of one (i.e., monospecific) or four (i.e., multispecific) tree species, we examined the seasonal dynamics of *in-situ* hydraulic traits (predawn and midday leaf water potential – Ψ_{pd} and Ψ_{md}, xylem- and leaf-specific hydraulic conductivity - K_S and K_L, percentage loss of conductivity – PLC, hydraulic safety margin – HSM, and Huber value - HV) in four co-existing *Pinus* and *Quercus* species over two years.
- We mainly observed adverse impacts of species diversity with lower Ψ_{pd}, Ψ_{md}, K_S, K_L, and HSM and higher PLC in multispecific compared to monospecific stands for all tree species, especially the two pines. These impacts were observed all along the growing season but were stronger during the driest periods of the summer. Beneficial impacts of diversity were rare and only occurred for oaks (*Q. faginea*) after a prolonged and intense water stress.
- Our findings reveal that mixing oaks and pines enhances hydraulic impairments for all species, suggesting a potential decline in the survival of mixed Mediterranean forests under future climate. However, diversity could mitigate extreme and long-lasting drought stress for some species by preserving xylem integrity and helping species avoid critical mortality-inducing cavitation.

Keywords: hydraulic conductivity, hydraulic safety margin, *P. nigra, P. sylvestris, Q. ilex, Q. faginea*, tree-tree interactions

3.1 Introduction

Mediterranean forests are defined by a sharp temperature and precipitation seasonality, going from cold and wet winters to hot and dry summers (Aschmann, 1984; Polade et al., 2017). These iconic biodiversity hotspots host a rich plant community with co-existing coniferous and broadleaved tree species adapted to this substantial seasonal variation (Lavorel, 1999; Myers et al., 2000). However, the worsening of summer droughts associated with more extreme heatwaves alters the water dynamics within these systems, resulting in severe hydraulic impairments (e.g., Fontes et al., 2018; Klein et al., 2022) and widespread tree mortality (Hartmann et al., 2022; McDowell et al., 2018). Promoting tree species diversity, especially the co-existence of plants with contrasting hydraulic traits, has been advocated as a solution to mitigate the adverse impacts of intense summer droughts (Anderegg et al., 2018; Liu et al., 2022; Steckel et al., 2020). Yet, the underlying physiological mechanisms driving diversity's mitigation effect during drought are poorly understood, making it unclear if more diverse Mediterranean forests tolerate better extreme dry events (e.g., Bonal et al., 2017; Searle et al., 2022).

Tree species with contrasting functional traits (e.g., broadleaved and coniferous trees) naturally co-occur in Mediterranean forests, leading to complementary and facilitation mechanisms that could improve access to resources (Loreau & Hector, 2001; Meiner et al., 2012; Zapater et al., 2011). For instance, denser canopies in mixed broadleaved and coniferous forests (i.e., also referred to as "canopy packing") (Jucker et al., 2015) improve forest microclimate by buffering temperature extremes and reducing the evaporative demand (i.e., the vapor pressure deficit or VPD), especially in drier regions (e.g., De Frenne et al., 2021). Complementarity may also arise because of contrasting species-specific stomatal sensitivity to drought (which rank along a gradient from isohydric to anisohydric; Klein, 2014) that can modulate the competition intensity and timing as water resources are used differently throughout the year by co-existing species (Martínez-Vilalta et al., 2014; Tardieu & Simonneau, 1998). For example, conifers like *Pinus sylvestris L.* close their stomata more rapidly as the soil water potential drops during a drought (i.e., a rather isohydric behavior; Klein et al., 2011) to prevent increasing tension in the vascular system that could lead to embolism and reductions in xylem-specific hydraulic conductivity (K_s) (e.g., Aguadé et al., 2015; Fontes et al., 2018; Ladjal et al., 2005). This will be reflected by a stable midday leaf water potential (Ψ_{md}) as the predawn water potential decreases (Ψ_{pd}) (Hochberg et al., 2018; Martínez-Vilalta & Garcia-Forner, 2017). In contrast, co-existing broadleaved species like *Quercus ilex L.* keep their stomata open as they track soil moisture reductions (i.e., a rather anisohydric behavior; Roman et al., 2015), thereby also increasing the risk of xylem embolism and reductions in K_s. Consequently, conifers present wider hydraulic safety margins (HSM; i.e., the difference between the water potential that induces 50% conductivity loss - P_{50} and the minimum water potential) than some broadleaves, indicating a disparity in their drought vulnerability (Choat et al., 2012). Moreover, conifers can develop a more drought-resistant xylem structure with narrower and shorter tracheids

with a torus on the pit membranes to prevent embolism from spreading to neighboring water-filled cells (Delzon et al., 2010; Pittermann et al., 2006). On the other hand, the xylem in broadleaved trees is composed of large vessels that are highly efficient for water transport (resulting in higher K_s) but with higher embolism risk in some species (Gleason et al., 2016; Sperry et al., 2006). In addition to these contrasting aboveground water use strategies, trees with different rooting depths can rely on separate water sources in the soil (i.e., belowground water source partitioning), which could improve plant water status and drought resistance (Grossiord et al., 2018; Silvertown, 2004). For instance, mixing rather anisohydric oak trees with a deep rooting system (Moreno et al., 2005) and more isohydric pines with overall shallower roots (Čermák et al., 2008) could delay the onset of hydraulic dysfunctions because of reduced belowground tree-tree competition, as observed in various forest ecosystems (e.g., Hajek et al., 2022; Muñoz-Gálvez et al., 2021; Pretzsch et al., 2013). In addition, processes of facilitation such as hydraulic redistribution whereby deep-rooted species passively transfer water from deep, moist soils to dry superficial ones can provide additional moisture to shallow-rooted species (e.g., Rodríguez-Robles et al., 2015; Schwendenmann et al., 2015).

In contrast, species with similar water use strategies and water source preferences would strongly compete for the same resources, thereby increasing plant water stress despite higher species diversity (e.g., Grossiord et al., 2014; Rodríguez-Robles et al., 2020). If competition leads to increased water stress, Mediterranean species could, for instance, reduce their evaporative surfaces by developing smaller and thicker leaves (i.e., higher specific leaf area; SLA), ultimately increasing their leaf-specific hydraulic conductivity (i.e., the ratio of hydraulic conductivity over leaf area; K_L) and their Huber value (i.e., the ratio of sapwood over leaf area; HV). Such strategies have been observed in Mediterranean forests during extreme drought events (e.g., Bongers et al., 2017; Limousin et al., 2010; Moreno et al., 2021) or as a result of intensified plant-plant competition (e.g., Ferrio et al., 2021; Grossiord et al., 2014). Moreover, previous work highlighted that beneficial complementarity and facilitation interactions may not be enough during severe water stress to overcome the extreme water depletion experienced by trees (e.g., Haberstroh & Werner, 2022; Ratcliffe et al., 2017). Indeed, numerous studies conducted in mixed Mediterranean forests concluded that increasing tree species diversity is not systematically beneficial in terms of soil water availability for all the interacting species, which can favor one species at the expense of the others (e.g., Aguadé et al., 2015; Grossiord et al., 2015; Martín-Gómez et al., 2017; Moreno et al., 2021). Yet, whether tree species diversity, especially the mixing of coniferous and broadleaved species in Mediterranean forests experiencing intense summer droughts, reduces or enhances tree water stress and hydraulic impairments is still unclear.

In this study, we investigated how increasing tree species diversity modulates the seasonal water dynamics during drought by mixing coniferous and broadleaved trees. We worked with four co-existing Mediterranean tree species with contrasting water use strategies, wood anatomy, and rooting habits: two shallow-rooted isohydric conifers, i.e., *Pinus nigra* and *Pinus sylvestris*, and two

deep-rooted anisohydric broadleaves, i.e., *Quercus faginea* and *Quercus ilex* (Aguadé et al., 2015; Čermák et al., 2008; Moreno et al., 2005). Over two years, we monitored the seasonal dynamics in aboveground hydraulic traits (Ψ_{pd}, Ψ_{md}, K_s, K_L) in 15 monospecific and multispecific mature forest stands. Because of complementarity and facilitation processes, we expected a lesser decrease in Ψ_{pd}, Ψ_{md}, K_s, and K_L, resulting in wider HSM during the summer and more rapid recovery in the fall in multispecific than monospecific stands. In addition, due to enhanced canopy packing that should reduce the evaporative demand and buffer extreme heat, we expected larger and thinner leaves (i.e., larger SLA) and smaller HV in multispecific stands compared to monospecific ones.

3.2 Material & Methods

3.2.1 Study site

The study was conducted in Mediterranean forests in the Alto Tajo natural park (Guadalajara, Castilla La Mancha, 40.66°N, 02.27°W) in central Spain, where 15 stands (30m x 30m) within a 20 km^2 area were selected from the FunDivEUROPE Exploratory Platform (Fig. 3.1a, Baeten et al., 2013). To assess the effect of tree species diversity, the stands were established in 2011 in non-managed, mature, and even-aged (i.e., more than 50 years old) forests with limited variation in altitude (i.e., from 980 to 1300 m a.s.l.), topography, soil type, and density (see Table S3.1 and Baeten et al. (2013) for more details on plot selection). The soils in all stands were shallow (from 20 to 40 cm) calcic cambisol soils (FAO/UNESCO soil classification) on a cracked limestone bedrock but with plant roots that may extend down to several meters through the fractured bedrock (Peñuelas & Filella, 2003). This area has a continental Mediterranean climate with hot and dry summers and cold and snowy winters. The long-term annual precipitation sum was 416 mm (2011-2022), with 516 and 367 mm in 2021 and 2022 (during the measurements), respectively. The long-term mean annual temperature was 11°C (2011-2022), with 12°C and 11°C in 2021 and 2022, respectively. Maximum daily temperatures were 31°C and 33°C for 2021 and 2022, respectively (Fig. S3.1).

The area is characterized by the natural dominance of four tree species, i.e., two coniferous species (*Pinus nigra subsp. salzmannii (Dunal) Franco* and *Pinus sylvestris L.*) and two broadleaved ones (*Quercus faginea Lam.* and *Quercus ilex L.*), which were selected for this study. We selected stands where the target species represents more than 90% of the total basal area (i.e., for monospecific stands; Fig. 3.1b-e) and where the four tree species were mixed in similar abundances (i.e., multispecific stands; Fig. 3.1f). Each species richness level (monospecific *vs*. multispecific) was replicated three times for all species (Table S3.1; Baeten et al., 2013), leading to a total of 15 stands (three monospecific stands per species and three multispecific ones). The understory vegetation (representing less than 10% of the total basal area) was mainly composed of shrub species (*Arctostaphylos uva-ursi, Buxus sempervirens,* and *Genista scorpius*) and juveniles of the dominant tree species.

We randomly selected five dominant or co-dominant trees per species in each plot, leading to 120 trees. To assess the seasonal dynamics of aboveground hydraulic traits, we conducted *in-situ* measurements (detailed below) on each tree in 2021 and 2022 at the beginning (i.e., in May when soil moisture was high), middle (i.e., in July, corresponding to the driest and hottest period), and the end of the growing season (i.e., in September, representing the recovery transition from dry to wet soils).

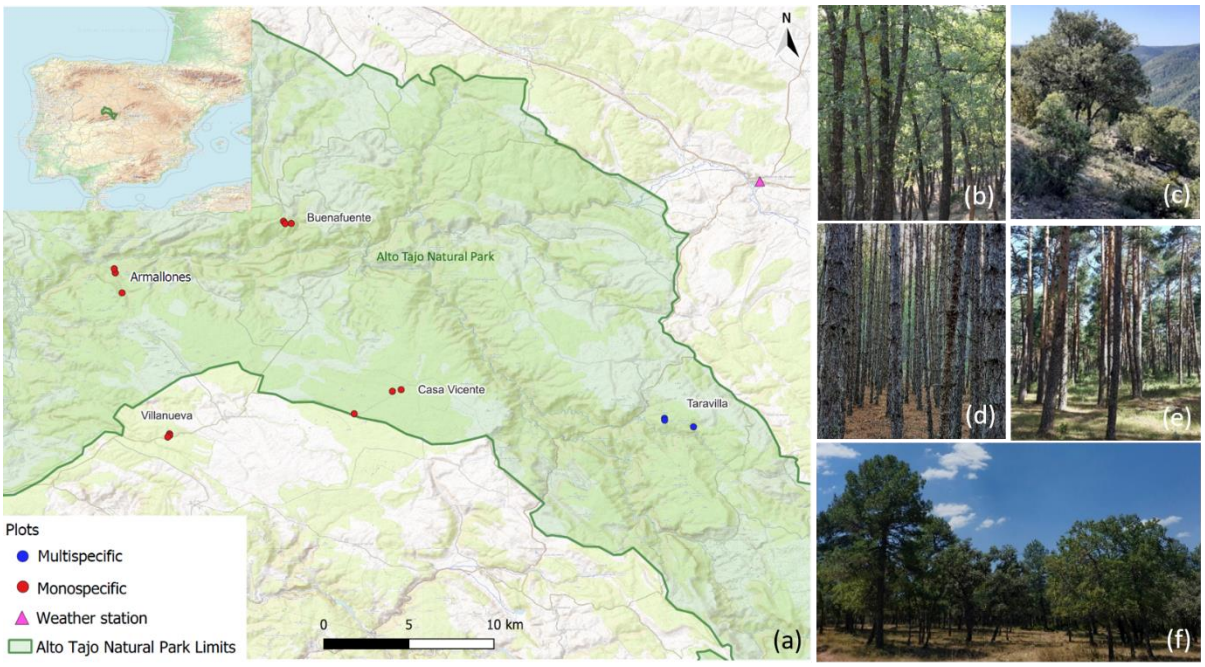

Figure 3.1: (a) Map of the Alto Tajo natural park (Central Spain) with the localization of the monospecific (red) and multispecific stands (dark blue) stands. The weather station is highlighted by a pink triangle. (b – e) Pictures of monospecific stands of *Q. faginea*, *Q. ilex*, *P. nigra*, and *P. sylvestris*, respectively. (f) Picture of a multispecific stand with all species.

3.2.2 Leaf water potential

One twig per tree was collected before sunrise (Ψ_{pd}) and at midday (Ψ_{mid}) to measure the leaf water potential (MPa) with a Scholander-type pressure chamber (M1505D, PMS Instruments, USA). We calculated the hydraulic safety margin (HSM, MPa) as the difference between the Ψ_{mid} (i.e., a proxy of the minimum water potential) and the water potential at 50% of xylem conductivity loss (P_{50}, MPa) (Choat et al., 2012). Because of the destructiveness of P_{50} measurements, we extracted the P_{50} of each species from a database (Choat et al., 2012; Esteso-Martínez et al., 2006) with a value of -2.8 MPa, -3.61 MPa, -3.3 MPa, and -3.9 MPa for *P. nigra*, *P. sylvestris*, *Q. ilex* and *Q. faginea*, respectively. Although we acknowledge that using the same P_{50} values for all trees does not account for the potential acclimation of this trait to the specific environment of our study, most work found little to no variability in this trait for our species (e.g., Gauthey et al., 2023; Matzner et al., 2001; Torres-Ruiz et al., 2013). However, previous work has shown some variability in P_{50} in response to drought varying between -0.4MPa and -0.2MPa for *Q. ilex* and *P. sylvestris*, respectively (e.g., Corcuera et al., 2011; Limousin et al., 2010; Martínez-Vilalta & Piñol, 2002; see Fig. S3.2 for the potential effect on HSM if P_{50} was shifted by ±0.4MPa for the *Quercus* species and ±0.2MPa for *Pinus* species).

3.2.3 Xylem hydraulic conductivity

On the same day as the leaf water potential measurements, one 1.5m and 50cm-long sun-exposed branch for broadleaves and conifers, respectively (to cut branches that were longer than the longest vessels or tracheids), was cut on four from the five selected trees (n=4) and placed in sealed black plastic bags with wet tissues to keep a humid atmosphere. Within the next two days, the samples were processed using a commercial conductivity meter (XYL'EM, Bronkhorst, France), according to Cochard et al., (2005). Three 3- to 5 cm-long segments were cut underwater from the terminal part of each branch, corresponding to the current and previous year (due to the slow growth of Mediterranean species). The proximal end of each segment was connected to the tubing system of the XYL'EM, which was filled with deionized filtered water with 10mM KCl and 1mM $CaCl_2$ that had been previously degassed. A low-pressure (70kPa) flow was applied to measure the initial hydraulic conductivity of each shoot (K_{ini}, kg m MPa^{-1} s^{-1}). Due to the high resin content in pines, only the segments of oak species were flushed at 0.15MPa for 1.30 min to measure their maximum hydraulic conductivity (K_{max}, kg m MPa^{-1} s^{-1}). A second flush at 0.15MPa for 30s was performed to confirm the maximal conductivity value. The K_{ini}/K_{max} ratio was used to compute the percentage loss conductivity for oaks (PLC, %). Xylem-specific conductivity (K_s, kg m^{-1} MPa^{-1} s^{-1}) was calculated for every shoot by dividing K_{ini} by the sapwood area, estimated as the cross-section area without bark.

In addition, all distal leaves and needles of each segment were scanned using a flatbed scanner (CanoScan LiDE 300, CANON, UK), followed by analysis with ImageJ (Schindelin et al., 2019) to extract the total leaf area per segment (LA, m^2). The leaf-specific hydraulic conductivity (K_L, kg m^{-1} MPa^{-1} s^{-1}) was calculated by dividing K_{ini} by LA, and the Huber value (HV, m^2 m^{-2}) was estimated as the sapwood area:LA ratio. The mature leaves and needles collected in July 2021 and 2022 were dried at 60°C for 24h and weighed using a high precision scale (MS104, Mettler Toledo, CH) to calculate the specific leaf area (SLA, m^2 g^{-1}).

3.2.4 Statistical analyses

The effects of tree species diversity on Ψ_{pd}, Ψ_{md}, K_s, K_L, PLC, HSM, HV, and SLA were determined through linear mixed-effects models for each species using the package *lmer*. The effect of the season (i.e., spring, summer, fall), year (i.e., 2021, 2022), and species diversity (i.e., monospecific/multispecific) were used as fixed effects, and the individual plot was treated as a random effect. To reveal significant differences between species diversity levelsfor each measurement at each sampling date and each species, post hoc analyses were performed with Tukey's HSD test, with FDR correction for multiple testing. Non-linear and linear regressions were used to test the relationships between Ψ_{pd}, K_L, PLC, and HSM. All analyses were performed using the R v.4.2.2 statistical software (R Development Core Team, Austria, 2022). Before performing each model, the homogeneity of variances and the normality of residuals were assessed, and data were log-transformed if necessary.

3.3 Results

3.3.1 Seasonal dynamics in aboveground hydraulic traits

As the drought intensified during the summer, the leaf water potential at predawn and midday (Ψ_{pd} and Ψ_{mid}, respectively) significantly decreased for all species in both years. A recovery in Ψ_{pd} and Ψ_{mid} was observed in September but only in 2021 (Figs. 3.2 & S3.3; Table S3.2), probably because of the late rain events in 2022 that prolonged and intensified the summer drought (Fig. S3.1). The same seasonal pattern was observed for the hydraulic safety margins (HSM; i.e., $\Psi_{mid} - P_{50}$) for all species (Fig. 3.2).

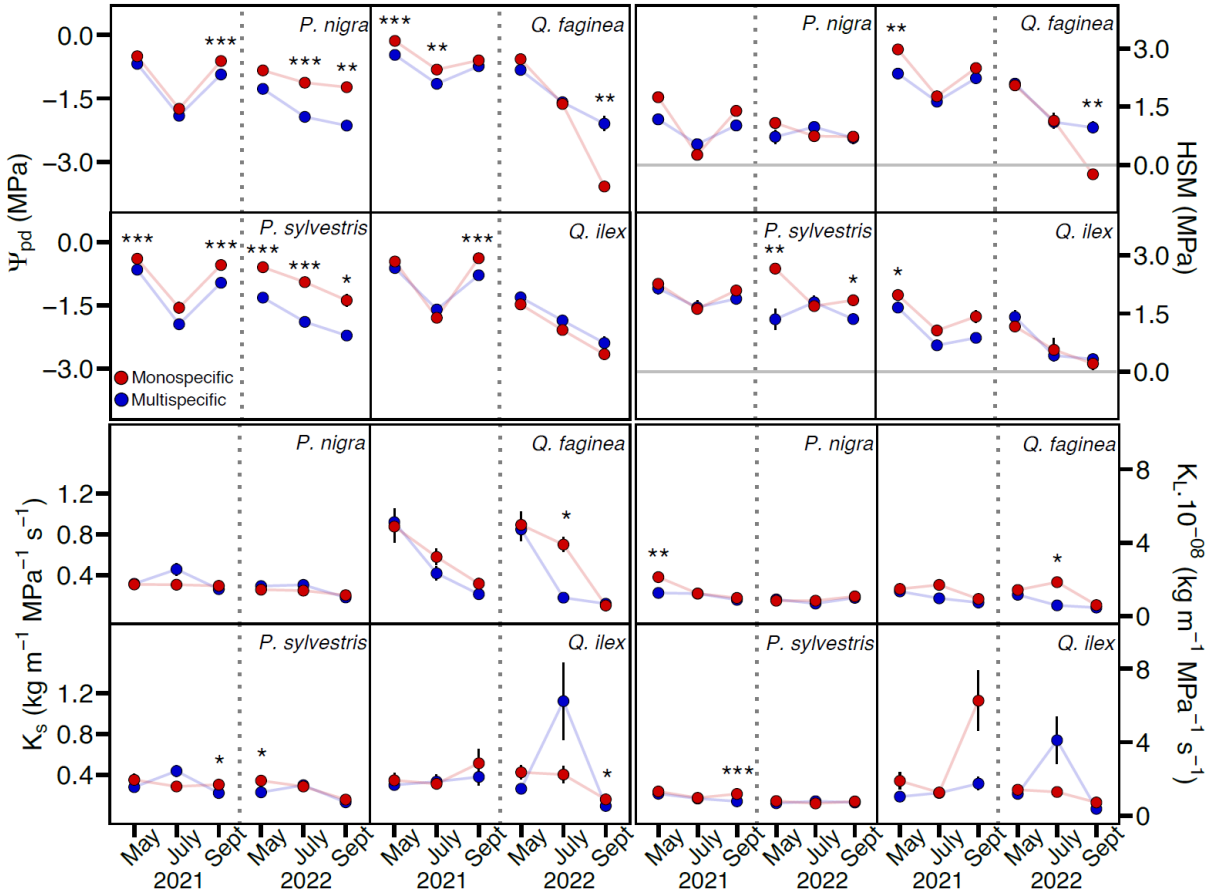

Figure 3.2: Mean (±SE) leaf water potential at predawn (Ψ_{pd}), hydraulic safety margin (HSM), sapwood-specific hydraulic conductivity (K_S), and leaf-specific hydraulic conductivity (K_L) for each sampling date in 2021 and 2022 for *P. nigra*, *P. sylvestris*, *Q. faginea*, and *Q. ilex* in monospecific (red) and multispecific stands (blue). The stars indicate significant differences between multispecific and monospecific stands for each sampling date (*0.05≥P>0.01; **0.01≥P>0.001; ***P≥0.001).

Differences in hydraulic traits between broadleaves and conifers emerged, with a relatively constant Ψ_{mid} and HSM in pines throughout the summer (Figs. 3.2 & S3.3). In contrast, for oaks, we found Ψ_{mid} and HSM following the reduction in Ψ_{pd} as the drought intensified in the middle of the summer. Further, while we observed no seasonal variability in the xylem- and leaf-specific

hydraulic conductivities (K_S and K_L, respectively) for both pines and *Q. ilex*, they significantly decreased in the middle of the summer for *Q. faginea*, with no recovery in the fall (Table S3.2, Fig. 3.2). Still, we observed an exponential decrease in K_L with decreasing Ψ_{pd} for all species, suggesting reduced conductivity with increasing water stress (Fig. 3.3). *Q. faginea* had a higher specific leaf area (SLA) than all the other species (i.e., 56% bigger on average), suggesting larger and thinner leaves (Fig. 3.4). Interestingly, we observed similar Huber value (HV) for all species (i.e., around 4.10^{-4} m^2 m^{-2} on average), indicating similar ratio of sapwood area:evaporative surfaces between conifers and broadleaves.

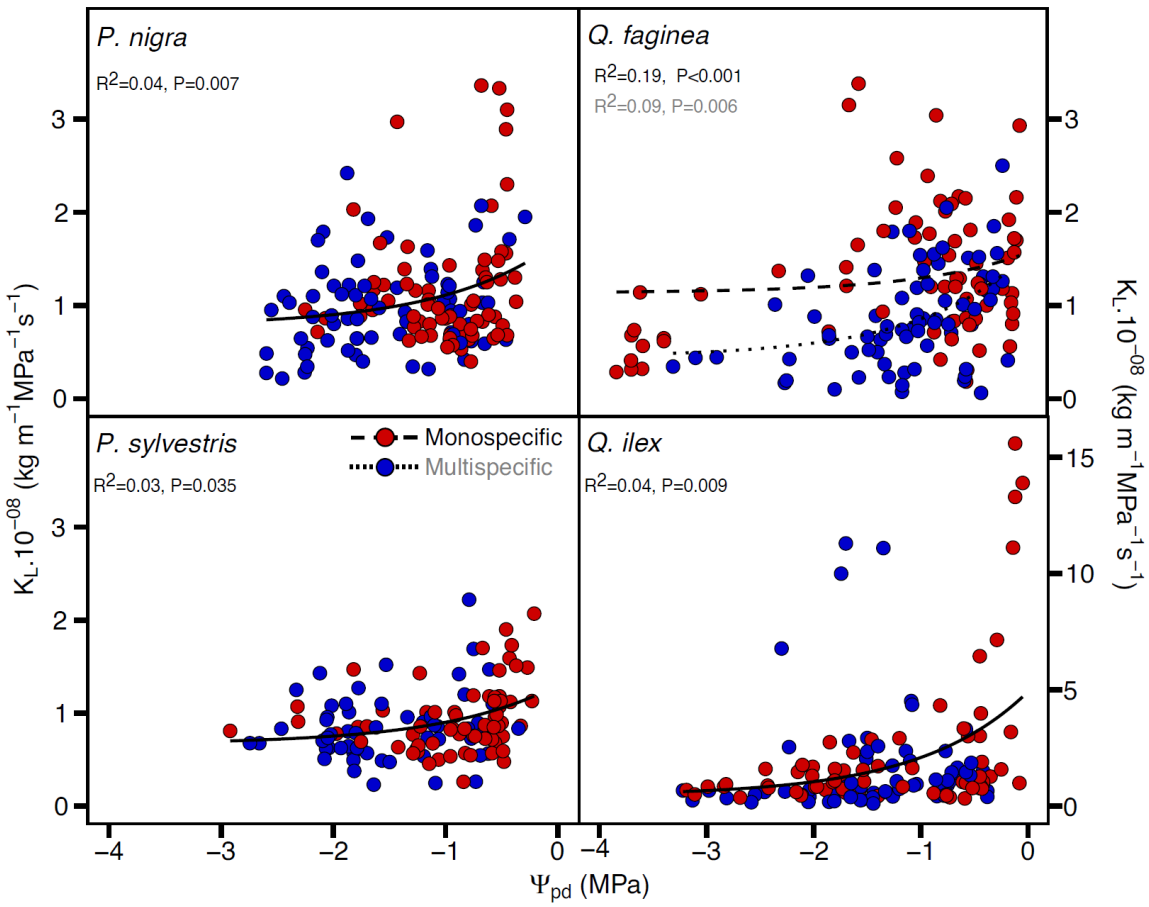

Figure 3.3: Relationships between the leaf-specific hydraulic conductivity (K_L) and the predawn leaf water potential (Ψ_{pd}) for *P. nigra*, *P. sylvestris*, *Q. faginea,* and *Q. ilex* in monospecific (red) and multispecific stands (blue). Lines represent exponential relationships, with dotted and solid lines standing for significant ones within a given species diversity level or across all species diversity levels, respectively. R^2 and p-value are given in the upper left corner.

For the oaks, the percentage loss of conductivity (PLC) significantly increased in the summer for *Q. faginea*, especially in the summer of 2022. In contrast, we found no significant differences between seasons or years for *Q. ilex* (Fig. 3.5b, Table S3.2). We further observed a significant negative relationship between PLC and HSM for both species (Fig. 3.5a), indicating higher critical cavitation risk (i.e., by crossing the P_{50} threshold) as hydraulic conductivity drops.

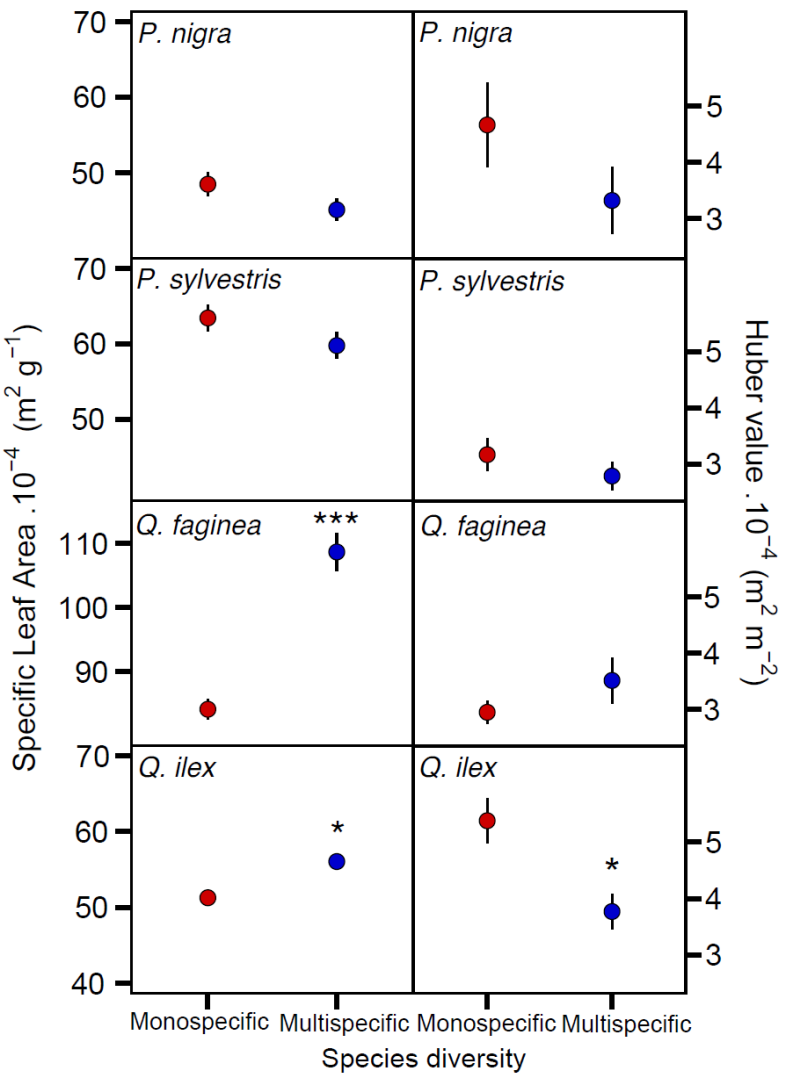

Figure 3.4: Mean (±SE) specific leaf area (SLA) and Huber value (HV) for all years (i.e., 2021, 2022) for *P. nigra*, *P. sylvestris*, *Q. faginea*, and *Q. ilex* in monospecific (red) and multispecific stands (blue). The stars indicate significant differences between diversity levels (*0.05≥P>0.01; **0.01≥P>0.001; ***P≥0.001).

3.3.2 Species diversity effects on the seasonal dynamics in aboveground hydraulic traits

Overall, we found no or adverse effects of species diversity on all aboveground hydraulic traits for all species. The only exception was for *Q. faginea* after the prolonged drought of 2022, where Ψ_{pd} was more negative and HSM were narrower in monospecific compared to multispecific stands in September (Fig. 3.2). For pines, regardless of the season, we found a significantly lower Ψ_{pd} in multispecific compared to monospecific stands, indicating higher water stress, especially during the extensive drought of 2022. Similarly, we observed lower Ψ_{pd} in the summer of 2021 for *Q. faginea* in multispecific stands. For *Q. ilex*, while we observed no change in Ψ_{pd} between monospecific and multispecific stands overall, we found a lower recovery in Ψ_{pd} after the summer of 2021 in multispecific stands (Fig. 3.2, Table S3.2), also indicating enhanced water stress.

For *P. sylvestris,* we further observed a reduction in K_S and K_L in September 2021 and May 2022 (only for K_S) in the multispecific stands compared to monospecific ones. Moreover, narrower

HSM in the spring and fall of 2022 were found for *P. sylvestris* in the multispecific than monospecific stands. For *Q. faginea* and *Q. ilex*, K_S and K_L were significantly lower in the multispecific compared to the monospecific stands in the summer and fall of 2022, respectively. Similarly, the HSM was narrower in the multispecific stands in May 2021 compared to monospecific ones for both oaks (Fig. 3.2; Table S3.2).

Q. faginea presented lower K_L for the same Ψ_{pd} in multispecific compared to monospecific stands, suggesting stronger conductivity loss under similar drought stress (Fig. 3.3). We further measured significantly higher PLC in multispecific stands compared to monospecific ones for both oaks, suggesting potentially more embolism events (Fig. 3.5b, Table S3.2). However, for *Q. faginea* we found higher PLC for the same HSM in multispecific stands compared to monospecific ones (Fig. 3.5a), indicating higher conductivity loss under similar critical cavitation risk with increasing species diversity.

While we found no significant diversity effects on SLA and HV for pines, we observed significantly smaller HV for *Q. ilex* and larger SLA for both oaks in the multispecific compared to the monospecific stands (Fig. 3.4), indicating larger and thinner leaves with increasing diversity.

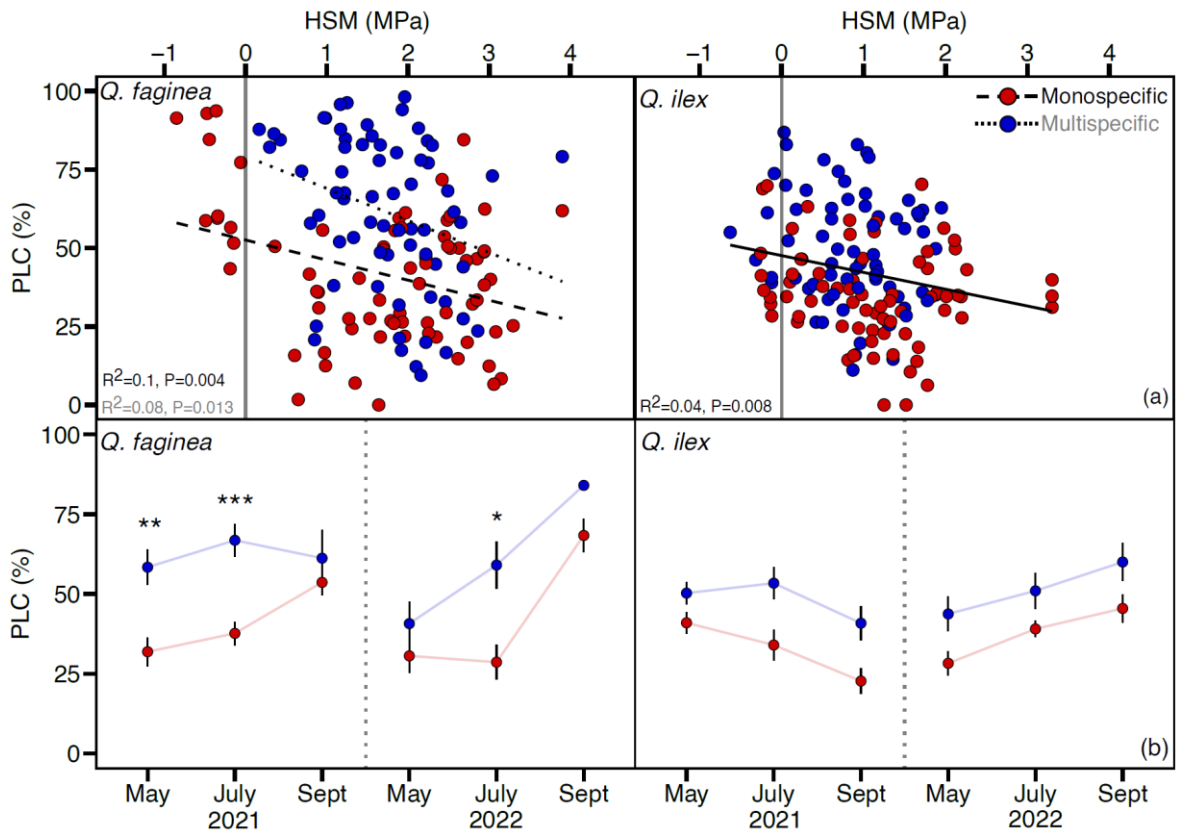

Figure 3.5: (a) Relationships between the percentage loss of conductivity (PLC) and the hydraulic safety margin (HSM) for *Q. faginea* and *Q. ilex* in monospecific (red) and multispecific stands (blue). Lines represent linear relationships, with dotted and solid lines standing for significant ones within a given species diversity level or across all diversity levels, respectively. (b) Mean (±SE) PLC for each sampling date in 2021 and 2022 for *Q. faginea* and *Q. ilex* in monospecific (red) and multispecific stands (blue). The stars indicate significant differences between diversity levels at each sampling date (*0.05≥P>0.01; **0.01≥P>0.001; ***P≥0.001). R^2 and p-value are given in the lower left corner. *Note*: PLC was not measured for the pine species.

3.4 Discussion

Our findings confirmed the well-known seasonality in plant water relations in Mediterranean forests with an important increase in drought stress during the summer, as highlighted by the lower Ψ_{pd}. Higher drought stress induced lower Ψ_{mid} and reduced xylem hydraulic conductivity (K_S and K_L) for all species, regardless of the species diversity (Figs. 3.2, 3.3 & S3.2; Table S3.2). However, contrary to our expectations and previous studies (e.g., Moreno et al., 2023; Muñoz-Gálvez et al., 2021), species diversity did not mitigate drought impacts and, instead, exacerbated it.

We found higher water stress for all species (i.e., lower Ψ_{pd}) in the multispecific compared to the monospecific stands (Fig. 3.2; Table S3.2). This adverse impact was particularly strong in the two pines in 2022, where Ψ_{pd} was, on average, 0.8 MPa lower in the multispecific stands. In contrast, we found no significant differences between diversity levels for the two oaks. This finding was consistent with previous observations in the same study area, where more substantial water stress was found for pines compared to oaks in mixed forests (Grossiord et al., 2015). A similar diversity effect as for Ψ_{pd} was observed for $\Psi_{mid,}$ but the lowest leaf water potential observed was still significantly higher than ones inducing critical embolism (i.e., P_{50}) for all species, highlighting the important drought resistance of Mediterranean tree species (Nardini et al., 2014). Overall, although pines keep a tighter stomatal control compared to oaks (Aguadé et al., 2015; Martín-Gómez et al., 2017), both functional groups, apart from *P. nigra*, had narrower HSM in multispecific compared to monospecific stands (Fig. 3.2), leading to higher embolism risk. In contrast, Moreno et al. (2023) observed narrower HSM in monocultures compared to mixtures for *Q. ilex* mixed in pots with pines during an experimental drought. Differences between the two studies could stem from the contrasting approach and plant development stage (i.e., field measurements on mature trees *vs*. pot experiment on young seedlings with limited root volume). Nevertheless, HSM in our study stayed mainly above zero for both diversity levels (Fig. 3.2 & S3.2), suggesting low mortality risk (Delzon & Cochard, 2014). Hence, independent of the intensity of competition, the stomatal regulation strategy of Mediterranean tree species seems sufficient to protect the xylem from hydraulic failure and allow them to cope with intense summer droughts (Forner et al., 2018).

Still, higher water stress in multispecific stands further resulted in higher conductivity loss (reduced K_S and K_L), but the impacts were less intense (26% drop on maximum for K_S in *Q. faginea*) and frequent (maximum once over the whole measurement period per species). In addition, both oaks experienced higher embolism (as shown by the higher PLC) in the multispecific compared to the monospecific stands (Fig. 3.5b). Interestingly, *Q. ilex* seems less adversely impacted by species diversity than *Q. faginea*, probably because of its higher tolerance to leaf dehydration due to its lower SLA (Fig. 3.4) and its higher resistance to wood cavitation due to its narrower vessels compared to *Q. faginea* (Alonso-Forn et al., 2021; Corcuera et al., 2004; Forner et al., 2018). Yet, these findings follow those of Aguadé et al. (2015), who found higher PLC in *Q. ilex* in mixed pine-

oak stands compared to pure ones despite no change in Ψ_{pd} and higher Ks. This effect could be due to secondary growth in summer that increases the xylem hydraulic conductivity at the risk of higher cavitation levels (Martínez-Sancho et al., 2021). Interestingly, in the work of Aguadé et al. (2015), the PLC of *P. sylvestris* was lower than that of *Q. ilex* and did not change with species diversity. Even if we could not measure PLC in the two pines because of the abundant resin and potential pit aspiration (Hietz et al., 2008), we can assume that species diversity should have a limiting effect for conifers. Indeed, the absence of species diversity effect on K_S and K_L for both pines (Fig. 3.2, Table S3.2) and the high resistance of the conifers' xylem to cavitation (Lens et al., 2013) could be sufficient to preserve the xylem integrity despite increasing water stress in multispecific stands (i.e., lower Ψ_{pd} and Ψ_{mid}). Still, regardless of the species diversity, *P.nigra* had a higher vulnerability to xylem cavitation with P_{50} at -2.8 MPa compared to -3.61 MPa for *P.sylvestris*, leading to narrower HSM and potential higher mortality risk for *P.nigra*.

The underlying mechanisms driving the overall adverse responses to diversity found in our study could be multiple. Larger and thinner leaves of *Q. faginea* and *Q. ilex* (i.e., higher SLA) found in the multispecific stands could increase water loss through transpiration and exhaust soil moisture faster (Figs. 3.4b & 3.5), thereby contributing to the negative impact of species diversity. Hence, the apparent higher efficiency in water transport due to larger evaporative surfaces and sapwood area (i.e., larger HV for *Q. faginea*) in more diverse stands could come at the risk of more frequent embolism (i.e., lower PLC) during dry periods. Indeed, Searle et al., (2022) found increasing mortality risk in more diverse forests due to the indirect effect of species diversity on wood productivity. The resulting increase in stem densities in mixed and more productive forests could cause higher competition for accessing site resources when they scarified (e.g., light, nutrients, or water). However, the mechanisms leading to the production of leaves with higher SLA and larger HV remain unclear but could be driven by a more favorable microclimate. Higher water use of oaks could reduce soil water availability for pines quicker than in monospecific plots, thereby driving the observed responses for pines. This study seems to be the first to observe mainly adverse effects of species diversity on hydraulic traits for all interacting species. Hence, future work should address the underlying processes (e.g., belowground water source competition, changed microclimate, increasing shading) driving diversity effects in mixed Mediterranean forests.

Nevertheless, it is essential to mention that we observed beneficial mixing effects for *Q. faginea* after a prolonged drought. Indeed, in monospecific stands, *Q. faginea* experienced stronger water stress in September 2022 (i.e., lower Ψ_{pd}) compared to multispecific stands, crossing the critical threshold (i.e., P_{50}) and inducing acute loss of hydraulic conductivity (Fig. 3.2). The 2022 drought was particularly long and intense with 70% less precipitation than 2021 and very late rain leading to dry conditions in September (34% lower than 2021). As a result, we observed lower drought stress for oaks in multispecific stands compared to monospecific ones, probably due to reduced belowground competition when mixed with drought-sensitive shallow-rooted pines (del Castillo et al., 2016; Gea-Izquierdo et al., 2021). Hence, *Q. faginea* in monospecific stands reached

a very low Ψ_{pd} of -4 MPa, which is lower than its P_{50} at -3.9 MPa, leading to negative HSM. Potential underlying drivers could include the higher critical cavitation risks for *Q. faginea* in monospecific compared to multispecific stands (narrower HSM for the same PLC; Fig. 3.5a), enhanced water competition in monospecific stands when soil moisture decreases (Bello et al., 2019), and reduction in evaporative demand for the oaks growing under the canopy of pines (Ferrio et al., 2021). Therefore, the effect of species diversity on tree water relations could shift from negative to positive depending on the drought intensity and the species. Thus, while mixing functionally contrasting species could exacerbate hydraulic dysfunctions under mild drought due to potentially enhanced transpiration rates, the potential reduced belowground competition for water under severe drought could preserve the xylem integrity in more diverse forests, avoiding critical cavitation levels. However, the underlying mechanisms of these effects remain unclear and should be further investigated to better conserve those critical ecosystems.

3.5 Acknowledgments

EM and CG were supported by the Swiss National Science Foundation (310030_204697) and the Sandoz Family Foundation. We thank Alex Tunas, David Lopez, Eric Breton, Francisco Fornieles, and Giulia Casciano for their support with the field measurements. Data used in this manuscript will be available from the Dryad Digital Repository after acceptance.

3.6 Supporting information

3.6.1 Supporting figures

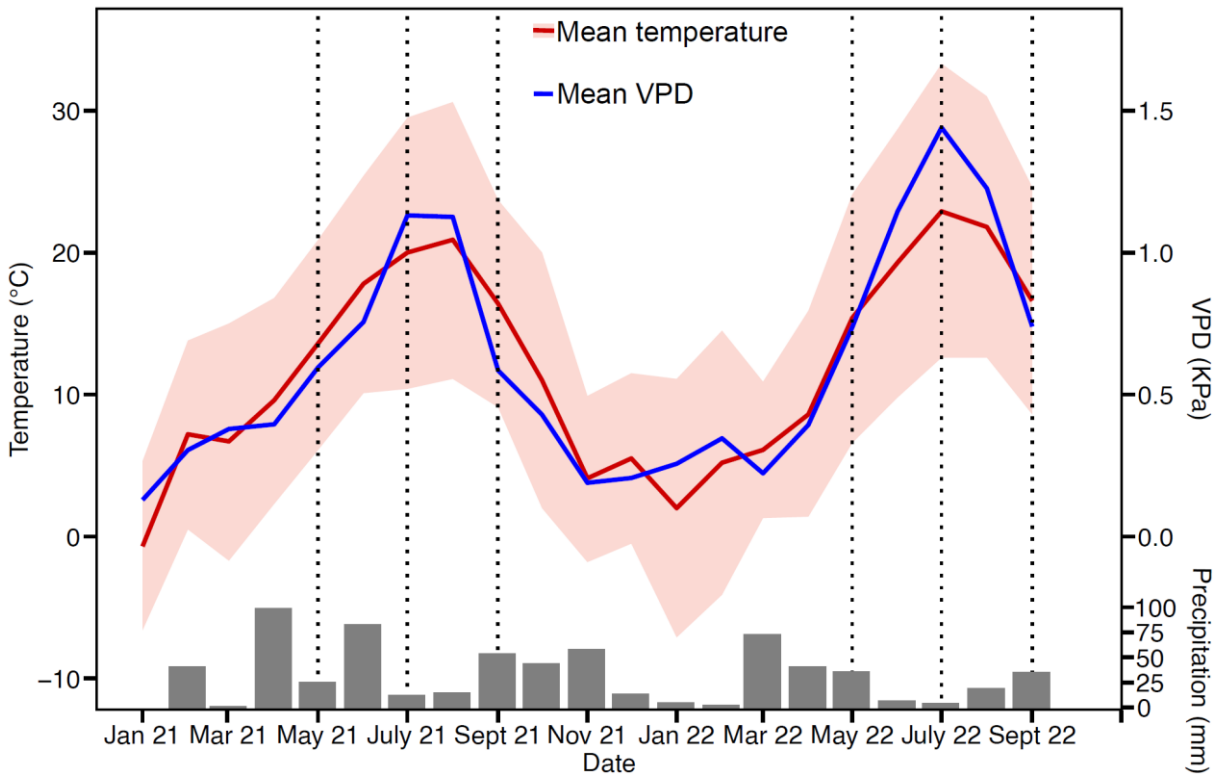

Figure S3.1: Mean monthly air temperature (± minimal and maximal temperature, °C), vapor pressure deficit (VPD, kPa), and total monthly precipitation (mm) in 2021 and 2022. Dashed vertical lines indicate the measurement campaigns.

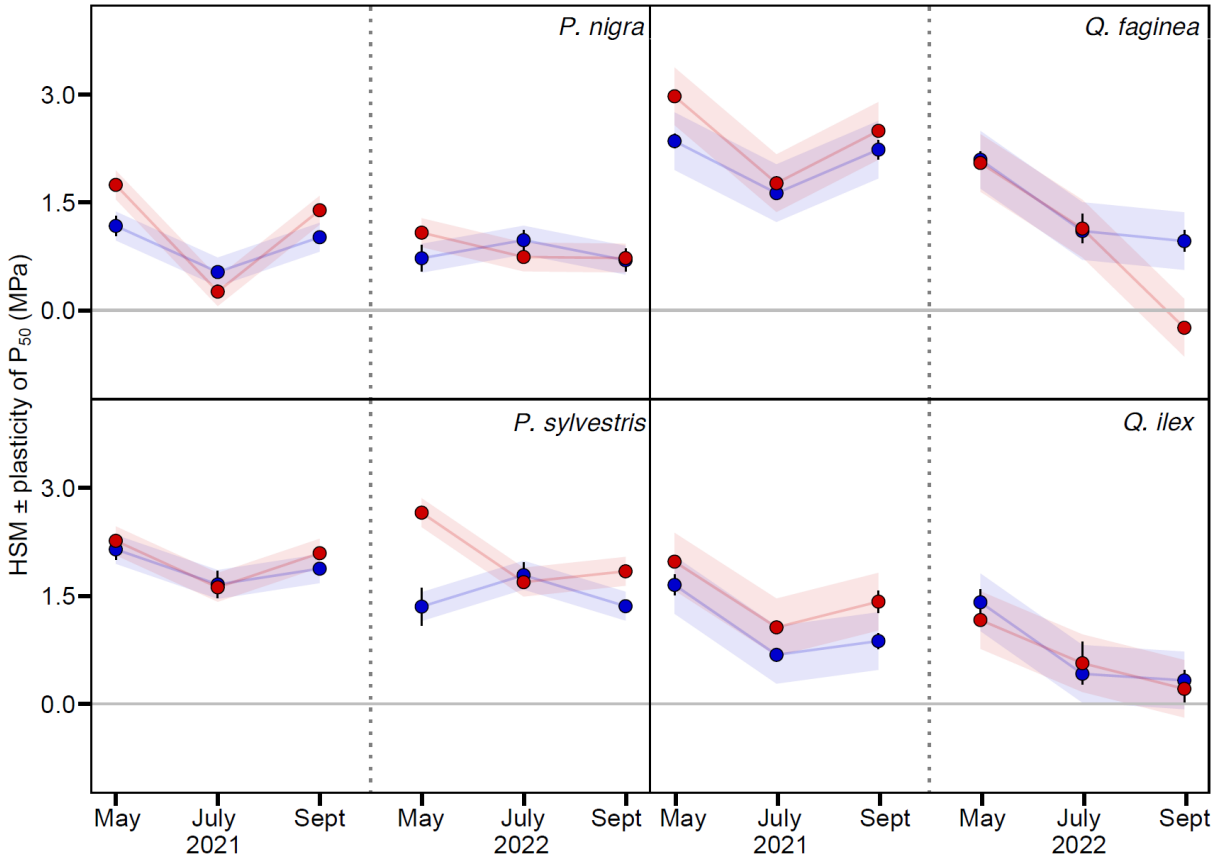

Figure S3.2: Mean (±SE) hydraulic safety margin (HSM) for each sampling date in 2021 and 2022 for *P. nigra*, *P. sylvestris*, *Q. faginea*, and *Q. ilex* in monospecific (red) and multispecific stands (blue). The ribbon indicates the potential variation in HSM if P_{50} varied with local environmental conditions (i.e., ±0.4 and ±0.2MPa for *Quercus* and *Pinus* species, respectively).

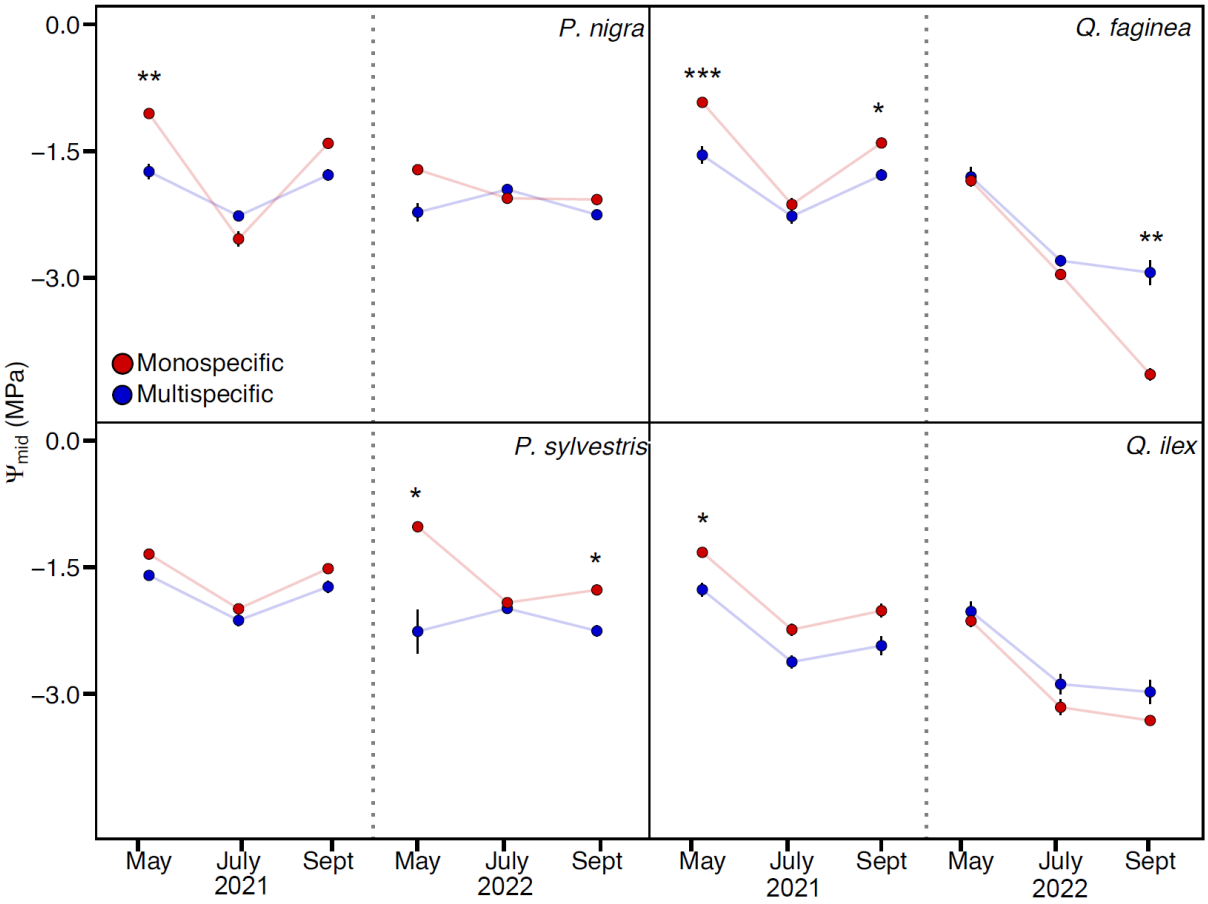

Figure S3.3: Mean (±SE) leaf water potential at midday (Ψ_{mid}) for each sampling date in 2021 and 2022 for *P. nigra*, *P. sylvestris*, *Q. faginea*, and *Q. ilex* in monospecific (red) and multispecific stands (blue). The stars indicate significant differences between multispecific and monospecific stands at each sampling date (*0.05≥P>0.01; **0.01≥P>0.001; ***P≥0.001).

3.6.2 Supporting tables

Table S3.1: Description of the 15 selected stands, including the plot-level leaf area index (LAI), the mean diameter at breast height (DBH), and mean tree height (±SD)

Plot	Latitude	Longitude	Altitude (m)	Exposition	Soil depth(cm)	LAI(m²/m²)	Species richness	Species composition	DBH (cm)	Height (m)
9	40.66814851	-2.292657672	1211	S	20	1.33	Monospecific	*Q. faginea*	61.4 ± 14	12.1 ± 1.3
10	40.66707271	-2.292521806	1270	SE/S	70	0.938	Monospecific	*Q. faginea*	56.4 ± 5.4	8.4 ± 1.6
11	40.66589427	-2.293874762	1187	SE	20	1.4	Monospecific	*Q. faginea*	66.1 ± 9.5	10.1 ± 1.9
12	40.7659242	-2.32553588	1073	NE		1.57	Monospecific	*P. nigra*	91.6 ± 28.1	14.5 ± 4.5
15	40.77979254	-2.330305941	980	W	20	1.39	Monospecific	*P. nigra*	77.8 ± 16.6	11.5 ± 1.5
17	40.78267786	-2.331021184	960	NA	20	1.93	Monospecific	*P. nigra*	91.0 ± 20.7	12.8 ± 1
18	40.68204502	-2.164579218	1403	NA	70	1.55	Monospecific	*P. sylvestris*	134.8 ± 15	16.8 ± 0.8
19	40.69764993	-2.138101195	1310	NA	50	1.31	Monospecific	*P. sylvestris*	108.8 ± 15.8	13.7 ± 1.2
20	40.69874911	-2.132025477	1311	NA	20	1.07	Monospecific	*P. sylvestris*	120.4 ± 30.9	13.5 ± 2
32	40.81556405	-2.213577194	1236	SW	30	0.686	Monospecific	*Q. ilex*	52.4 ± 13.9	6.3 ± 2.2
33	40.81397399	-2.212467962	1251	SW	20	1.48	Monospecific	*Q. ilex*	50.6 ± 16.7	5.8 ± 1.8
34	40.81408609	-2.208205077	1250	SW	20	2.42	Monospecific	*Q. ilex*	60.8 ± 8.6	6.9 ± 1.5
24	40.67891682	-1.949361418	1377	SW	50	1.72	Multispecific	*P. nigra*	105.8 ± 29.6	13.6 ± 2.2
								P. sylvestris	127.6 ± 24.1	14.7 ± 1.7
								Q. faginea	60.8 ± 13.3	10.1 ± 1.5
								Q. ilex	76.6 ± 13.1	9.0 ± 0.9
26	40.677634	-1.949266987	1387	N	30	1.88	Multispecific	*P. nigra*	130.0 ± 42.3	14.2 ± 2.5
								P. sylvestris	128.2 ± 26	16.8 ± 1.6
								Q. faginea	59.6 ± 15.2	10.8 ± 1.4

								Q. ilex	87.2 ± 16.7	9.1 ± 1.8
29	40.67299394	-1.929263151	1354	SE	30	2.1	Multispecific	*P. nigra*	124.4 ± 24	13.8 ± 1.8
								P. sylvestris	126.5 ± 38.9	14.9 ± 0.4
								Q. faginea	44.6 ± 16.8	6.3 ± 0.9
								Q. ilex	61.4 ± 21.8	6.7 ± 1.7

Table S3.2: Statistical outputs of the mixed linear models where season (i.e., Spring, Summer, Fall), year (i.e., 2021 and 2022), and species diversity referred as to as “Mixture” (i.e., monospecific and multispecific stands) were used as fixed effects, and stands were used as random effects for *P. nigra, P. sylvestris, Q. faginea,* and *Q. ilex* (*0.05≥P>0.01; **0.01≥P>0.001; ***P≥0.001).

		P. nigra	*P. sylvestris*	*Q. faginea*	*Q. ilex*
Ψ_{pd}	Season	< 0,001***	< 0,001***	< 0,001***	< 0,001***
	Year	< 0,001***	< 0,001***	< 0,001***	< 0,001***
	Mixture	0,0097**	0,0031**	0,6433	0,7892
	Season:Year	<0,001***	<0,001***	<0,001***	<0,001***
	Season:Mixture	0,0413*	0,1937	<0,001***	0,0012**
	Year:Mixture	<0,001***	0,0018**	<0,001***	<0,001***
Ψ_{md}	Season	< 0,001***	< 0,001***	< 0,001***	< 0,001***
	Year	< 0,001***	0,0046**	< 0,001***	< 0,001***
	Mixture	0,0226*	0,0132*	0,7963	0,4812
	Season:Year	<0,001***	<0,001***	<0,001***	0,0216*
	Season:Mixture	<0,001***	<0,001***	<0,001***	0,2842
	Year:Mixture	0,0019**	<0,001***	<0,001***	<0,001***
K_S	Season	<0,001***	<0,001***	<0,001***	0,006**
	Year	<0,001***	<0,001***	0,0197*	0,0545
	Mixture	0,4554	0,2219	0,05*	0,3883
	Season:Year	0,3406	0,0199*	0,1449	<0,001***
	Season:Mixture	0,0142*	0,0028**	0,0016**	0,227
	Year:Mixture	0,6465	0,3391	0,2179	0,4808
K_L	Season	0,0063**	0,0789	<0,001***	0,759
	Year	<0,001***	<0,001***	0,0187*	0,0036**
	Mixture	0,1832	0,0397*	<0,001***	0,1206
	Season:Year	<0,001***	0,1203	0,5679	<0,001***
	Season:Mixture	0,4577	0,1356	<0,001***	0,0264*
	Year:Mixture	0,2308	0,1283	0,2641	0,2624
PLC	Season			<0,001***	0,5512
	Year			0,9249	0,1148
	Mixture			0,0097**	<0,001***
	Season:Year			<0,001***	<0,001***
	Season:Mixture			0,0698	0,7665
	Year:Mixture			0,7056	0,7947
HSM	Season	<0,001***	<0,001***	<0,001***	<0,001***
	Year	<0,001***	0,0158*	<0,001***	<0,001***
	Mixture	0,1774	<0,001***	0,8233	0,1812
	Season:Year	<0,001***	0,0169*	<0,001***	0,0583
	Season:Mixture	<0,001***	<0,001***	<0,001***	0,538
	Year:Mixture	0,1273	<0,001***	<0,001***	0,0055**
SLA	Mixture	0,454	0,3686	<0,001***	0,0451*
HV	Mixture	0,0615	0,4336	0,6986	0,0397*

Chapter 4

Droughts in Mediterranean forests are not alleviated by diversity-driven water source partitioning

Eugénie Mas[1,2]*, Alberto Vilagrosa[3], Luna Morcillo[3], Matthias Saurer[5], Fernando Valladares[4], Charlotte Grossiord[1,2]

[1]Plant Ecology Research Laboratory PERL, School of Architecture, Civil and Environmental Engineering, EPFL, Lausanne, Switzerland

[2]Community Ecology Unit, Swiss Federal Institute for Forest, Snow and Landscape WSL, Lausanne, Switzerland

[3]CEAM Foundation, Joint Research Unit University of Alicante-CEAM, Department of Ecology, University of Alicante, PO Box 99, C. San Vicente del Raspeig, s/n, Alicante 03080, Spain

[4]Depto de Biogeografía y Cambio Global, LINCGlobal, Museo Nacional de Ciencias Naturales (MNCN-CSIC), Madrid, España and Área de Biodiversidad y Conservación, Univ. Rey Juan Carlos, Móstoles, Madrid, España

[5]Forest Dynamics, Swiss Federal Research Institute (WSL), Birmensdorf, Switzerland.

This chapter has been submitted to the peer-reviewed journal of "*Journal of Ecology*"

Author’s contributions

Charlotte Grossiord (CG) and I conceived and designed the study. This included decisions regarding the plots and trees selection, the sampling design and field logistics. I specifically focused on preparing the sampling campaign by aquiring all necessary materials, and ensuring field protocols and logisitics could run smoothly. Luna Morcillo (LM), Alberto Vilagrosa (AV), CG and I collected the branche and soil samples and measured the hydraulic traits at the leaf level. I extracted in the laboratory the water from the samples collected. Matthias Saurer (MS) analyzed the water extracted for stable isotope. I run the MixSIAR model to calculate the water source contribution and I calculated the water source partitioning. I analyzed the data, produced all figures and tables, and led the writing of the manuscript. All authors (i.e., CG, LM, AV, MS, Fernando Valladares, and I) critically contributed to the manuscript and gave final approval for publication.

Abstract

- Tree species diversity in forest ecosystems could reduce their vulnerability to extreme droughts through improved microclimate and reduced competition driven by contrasting species-specific water use patterns, especially belowground water source partitioning. However, little is known about the seasonal dynamics of belowground water uptake that determine whether diversity positively or negatively impacts tree carbon and water exchange.
- Using a network of 30 permanent plots in Mediterranean forests with increasing tree species diversity (from monospecific to four-species mixtures), we examined the seasonal patterns of *in-situ* aboveground and belowground carbon and water relations on 260 trees from four pine and oak species over two years using hydraulic and stable isotope approaches.
- We found that increasing functional diversity in broadleaf and conifer mixtures induced strong soil water source partitioning between oak and pine species. As the functional diversity was enhanced and conditions became drier during the summer, oak species took up water from deeper soil sources, while pines were systematically limited to shallow ones. Despite significant belowground moisture partitioning in mixed forests, drought-induced reductions in photosynthesis, stomatal conductance, leaf water potential, and stomatal regulation were still enhanced compared to monospecific stands for pines but with some benefits for oaks.
- Our findings reveal that although tree species diversity improved belowground water source partitioning in mixed oak and pine stands, reduced competition for water in more diverse ecosystems is insufficient to buffer the adverse impacts of severe droughts on aboveground carbon and water use.

Keywords: functional biodiversity, *Pinus nigra, Pinus sylvestris, Quercus faginea, Quercus ilex*, stable water isotopes, stomatal conductance, tree-tree interactions, water extraction depth.

4.1 Introduction

Mediterranean ecosystems are biodiversity hotspots and prime targets for conservation efforts (Myers et al., 2000). These iconic ecosystems count as a global change epicenter that is expected to experience stronger temperature rises compared to the global average (e.g., Giorgi & Lionello, 2008; Hoegh-Guldberg et al., 2018; Mariotti et al., 2015; Polade et al., 2017). More frequent and intense droughts with global warming will alter plant carbon and water exchange within these ecosystems, including leading to severe hydraulic impairments (e.g., Fontes et al., 2018; Klein et al., 2022) and amplified tree mortality (e.g., Anderegg et al., 2016; Breshears et al., 2005; Hartmann et al., 2022; McDowell et al., 2018). A strategy often advocated to mitigate adverse drought effects is to promote and restore tree species diversity via management efforts (e.g., reforestation and selective thinning; Vadell et al., 2022) (Anderegg et al., 2018; Liu et al., 2022; Steckel et al., 2020). Yet, the underlying mechanisms driving tree diversity effects on water dynamics are poorly understood. Therefore, it remains unclear if more diverse forests tolerate better extreme events (Grossiord, 2020).

The effect of drought on aboveground water use has been well studied, allowing us to gain a good understanding of the leaf- to tree-level processes leading to drought-induced tree decline. When soil moisture is reduced, the leaf predawn water potential (Ψ_{pd}) decreases. During the day, if trees continue to transpire, midday leaf water potential (Ψ_{md}) drops, which increases the difference between the predawn and midday water potentials ($\Delta\psi$, an index for stomatal regulation). Eventually, trees will close their stomata, reducing their net carbon uptake through photosynthesis (A_{net}) and their stomatal conductance (g_s) (e.g., Brodribb & Holbrook, 2003). As the drought progresses, negative tensions in the vascular system will eventually surpass critical thresholds (Choat et al., 2018; Cochard, 2006; Morcillo et al., 2022; Tyree & Sperry, 1989), leading to hydraulic failure and tree desiccation. However, compared to aboveground processes, we have limited knowledge of the belowground ones and their consequences for tree carbon and water relations, particularly the temporal and spatial dynamics of tree soil water uptake (Phillips et al., 2016). Mediterranean regions are often characterized by the duality of shallow soils where water quickly evaporates and a fractured deep bedrock that can store water for extended periods (Peñuelas & Filella, 2003; Rose et al., 2003). Consequently, Mediterranean plants tend to develop larger belowground biomass than aboveground ones, with roots reaching depths up to seven times the canopy projection (Moreno et al., 2005). Because of the prominence of dual root systems (i.e., shallow and vertical deep sinker roots; Devi et al., 2016) in dry regions, trees often transition their primary water source from superficial layers in the spring to water stored in the bedrock cracks in the summer (e.g., Barbeta et al., 2015; David et al., 2013; Eliades et al., 2018; Grossiord et al., 2017). Indeed, water from shallow soil layers is easier to extract due to its higher porosity, lower soil matric potential, and higher water storage than deeper layers (Dawson et al., 2020; Klos et al.,

2018; Or et al., 2002). Accessing water from deep horizons and the bedrock could allow maintenance of vital plant functions during extreme droughts (Hanson et al., 2007; Rempe & Dietrich, 2018). Yet, studies investigating the dynamics of tree water sources tend to focus on single species (e.g., Brinkmann et al., 2019), so the impacts of species interactions on water uptake are largely unknown. Moreover, because of technical challenges associated with belowground measurements, our knowledge of tree water uptake and its impact on tree carbon and water use is limited in natural ecosystems (but see Andrews et al., 2012; Ding et al., 2021; Grossiord et al., 2017; Kukowski et al., 2013). In this context, isotope profiling offers a non-destructive method, relating the stable isotopic signature of the plant water to that of the soil at different depths (Ehleringer & Dawson, 1992).

In forests, the co-existence of functionally contrasting species with distinct architectures (e.g., mixtures of broadleaf and conifer species) can lead to complementary aboveground structural traits, resulting in denser canopies (i.e., enhanced canopy packing) (e.g., Jucker et al., 2015) and stronger shading (Duarte et al., 2021; Ligot et al., 2016). Additionally, denser canopies improve the forest microclimate and buffer temperature extremes, especially in dry regions (e.g., De Frenne et al., 2021). Moreover, trees can differ in their aboveground water use strategy by ranking along a gradient from isohydric to anisohydric (Martínez-Vilalta et al., 2014; Tardieu & Simonneau, 1998), with some species tracking soil moisture reductions by dropping their leaf water potential (i.e., high $\Delta\psi$; anisohydric) while others maintain a relatively constant water potential by closing their stomata (i.e., low $\Delta\psi$; isohydric). Differences in species-specific stomatal sensitivity affect the competition intensity and timing as water resources are differently used throughout the year. On the contrary, species with similar water use strategies could severely compete during drought, increasing water stress (e.g., Grossiord et al., 2014). Nevertheless, belowground complementarity mechanisms are undoubtedly the ones that could play the most considerable role in Mediterranean systems. Indeed, interacting species may extend their roots at different depths to partition water sources and reduce tree-tree competition (Grossiord et al., 2018; Hooper, 1998; Rodríguez-Robles et al., 2020; Silvertown, 2004), inducing a slower reduction in water availability during drought and delaying the onset of hydraulic dysfunctions (Hajek et al., 2022). For instance, rather anisohydric oak species (Roman et al., 2015) are characterized by a deep dimorphic root system (i.e., deep taproot and secondary roots poorly developed horizontally) reaching up to 5.2 m depth (Moreno et al., 2005). In contrast, isohydric pines (Klein et al., 2011) tend to have more extended shallow root systems (Čermák et al., 2008; Moreno et al., 2005). Hence, when these two rooting habits coexist in mixed forests, they could, to some degree, exhibit water source partitioning. Additionally, processes of facilitation such as hydraulic redistribution whereby deep-rooted species passively transfer water from deep, moist soils to dry superficial ones can provide additional moisture to shallow-rooted species (e.g., Lubczynski, 2009; Rodríguez-Robles et al., 2020; Schwendenmann et al., 2015).

However, during extreme events, soil moisture reductions may be too severe for these mechanisms to overcome the water stress experienced by trees (e.g., Grossiord et al., 2018; Haberstroh & Werner, 2022). Species interactions can shift from positive to negative due to enhanced competition (i.e., belowground water niche overlapping) depending on environmental conditions (Ratcliffe et al., 2017), with most benefits observed at intermediate stress levels (Rodríguez-Robles et al., 2020). Still, the tree's functional characteristics and environmental conditions giving rise to beneficial or detrimental diversity effects remain unclear, mainly because the temporal belowground mechanisms have rarely been addressed.

The objective of this study is to investigate how tree species diversity modulates the seasonal dynamics of above- and belowground water use and carbon fixation in four co-existing Mediterranean tree species with contrasting water use strategies and rooting habit: two shallow-rooted isohydric conifers, i.e., *Pinus nigra* and *Pinus sylvestris*, and two deep-rooted anisohydric broadleaves, i.e., *Quercus faginea* and *Quercus ilex* (Čermák et al., 2008; Moreno et al., 2005). We monitored the seasonal dynamics in aboveground (Ψ_{pd}, Ψ_{md}, $\Delta\Psi$, A_{net}, g_s) and belowground (water uptake depth and water source partitioning determined by water stable isotope profiling) water dynamics over two years in 30 mature forest plots with increasing tree diversity (from monospecific to four-species mixtures). Because of complementarity and facilitation between functional groups, we expected a lesser decrease in Ψ_{pd}, Ψ_{md}, $\Delta\Psi$, A_{net}, and g_s during the summer drought and a more rapid recovery in the fall in mixed conifer-broadleaf stands. These responses should be driven by belowground moisture partitioning between the two functional groups.

4.2 Material and methods

4.2.1 Site description

The study was conducted in Mediterranean forests in the Alto Tajo natural park (Guadalajara, Castilla La Mancha, 40.66°N, 02.27°W) in central Spain, where 30 plots (30m x 30m) within a 20 km^2 area were selected from the FunDivEUROPE Exploratory Platform (Fig. S4.1, Baeten et al., 2013). To assess the effect of tree diversity, the plots were established in 2011 in non-managed mature even-aged (i.e., more than 50 years) forests with limited variation in altitude (i.e., from 980 to 1300 m a.s.l.), topography, soil type, and density (see Table S4.1 and Baeten et al. (2013) for more details on plot selection). The soils in all plots were shallow (from 20 to 40 cm) calcic cambisol soils (FAO/UNESCO soil classification) on a cracked limestone bedrock but with plant roots that may extend down to several meters through the fractured bedrock (Peñuelas & Filella, 2003). This area has a continental Mediterranean climate with hot and dry summers and cold and snowy winters. The long-term annual precipitation sum was 416 mm (2011-2022), with 516 and 367 mm in 2021 and 2022, respectively. The long-term mean annual temperature was 11°C (2011-2022), with 12°C and 11°C in 2021 and 2022, respectively. Maximum daily temperatures were 31°C and 33°C for 2021 and 2022, respectively (Fig. 4.1). The soil aridity index (P/PET) was calculated monthly using meteorological data from the nearest station (Molina De Aragon, Castilla La Mancha, ES; 20 km away, Fig. S4.1). We first computed the monthly potential evapotranspiration (PET) using the Thornthwaite equation (Yates & Strzepek, 1994) based on the average monthly temperature, daylight length, and heat index. P/PET was calculated by dividing the monthly precipitation sum by the monthly PET. P/PET varied from 0.34 and 0.38 in May (i.e., corresponding to wet soil conditions) to 0.11 and 0.05 in July (i.e., the driest and hottest period) for 2021 and 2022, respectively.

The area is characterized by the natural dominance of four tree species, i.e., two coniferous species (*Pinus nigra subsp. salzmannii (Dunal) Franco* and *Pinus sylvestris L.*) and two broadleaved ones (*Quercus faginea Lam.* and *Quercus ilex L.*), which were selected for this study. We selected plots with increasing tree species richness, including monospecific (where the target species represents more than 90% of the total basal area), monofunctional (i.e., two-species mixtures of either coniferous or broadleaved species), multifunctional (i.e., two-species mixtures of coniferous and broadleaved species) and mixtures of the four species. Each richness level was replicated three times for all species with all possible species combinations, except for the two-species mixture between *P. sylvestris* and *Q. ilex*, resulting in 30 plots (Table S4.1). In mixed plots, the target species had similar abundances with a lower limit of 60% of maximum evenness in the basal area (Baeten et al., 2013). The understory vegetation (representing less than 10% of the total basal area) was mainly composed of shrub species (*Arctostaphylos uvaursi, Buxus sempervirens,*

and *Genista scorpius*) and juveniles of the dominant tree species.

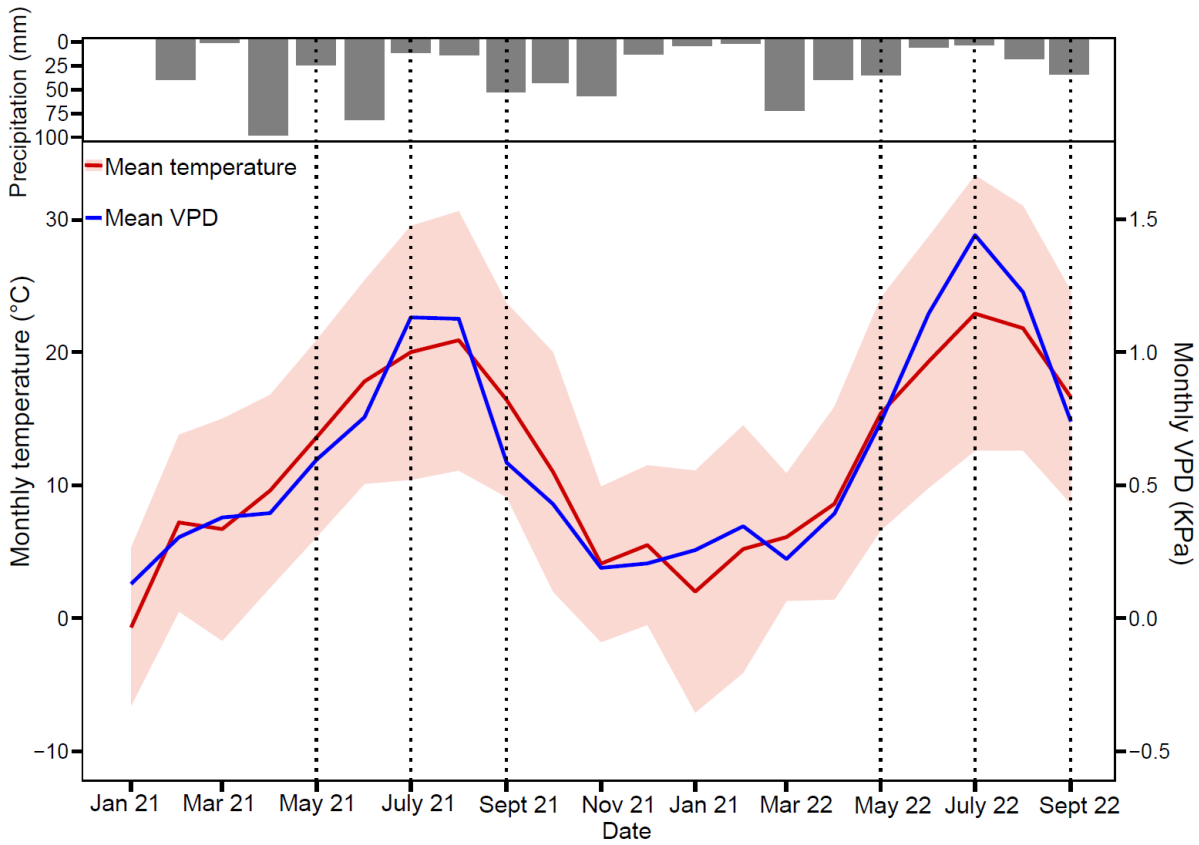

Figure 4.1: Mean monthly air temperature (± minimal and maximal temperature), vapor pressure deficit (VPD), and total monthly precipitation in 2021 and 2022. Dashed vertical lines indicate the measurement campaigns.

We randomly selected five dominant or co-dominant trees per species in each plot, leading to 265 trees. To assess the seasonal dynamics of aboveground and belowground tree water and carbon use, we conducted *in-situ* measurements (detailed below) on each tree in 2021 and 2022 at the beginning (i.e., in May when soil moisture was high), middle (i.e., in July, corresponding to the driest and hottest period), and the end of the growing season (i.e., in September, representing the recovery transition from dry to wet soils).

4.2.2 Leaf-level gas exchange and water potential

We measured the leaf-level light-saturated net photosynthesis (A_{net}, µmol m^{-2} s^{-1}) and stomatal conductance (g_s, mol m^{-2} s^{-1}) on one fully developed leaf (or multiple needles for conifers) per tree from a 50cm to 1m-long (for oak and pine species, respectively) sun-exposed branch. The branches were sampled using an extension pole, directly placed in a water bucket, and recutted under water to restore water flow (Lange et al., 1986). Within 15 min after sampling, A_{net} and g_s were measured using one infrared gas exchange analyzer (LI-6800 or LI-6400, LICOR Biosciences, USA). The measurements were done between 9 am and 1 pm (local time). The

relative humidity inside the chambers was set to 50% (to match the average daily ambient environmental conditions during the measurements), the CO_2 concentration to 400 ppm, the photosynthetic photon flux density (PPFD) to 1500 µmol m^{-2} s^{-1} (to ensure saturating light conditions), and the air temperature inside the cuvette from 20 to 30°C depending of the sampling dates (to fit the mean midday air temperature during the measurements; Fig. S4.2). Each leaf was measured when the gas exchange values were stable (i.e., after max. 5 minutes). On the same day as gas exchange measurements, one twig per tree was collected before sunrise (Ψ_{pd}) and at midday (Ψ_{md}) to measure the leaf water potential (MPa) with a Scholander-type pressure chamber (M1505D, PMS Instruments, USA). The difference between Ψ_{pd} and Ψ_{md} ($\Delta\psi$) was calculated to describe the tree's stomatal regulation strategy.

4.2.3 Water uptake patterns

On each sampling date, in the monospecific and four-species mixtures (n=15 plots), we collected three 10 cm-long twig samples across the canopy from each tree between 9 am and 3 pm (local time). After removing the bark, the samples were immediately sealed in airtight vials (Exetainer, Labco Limited, UK). The vial lid was wrapped with parafilm and placed in cool conditions to avoid evaporation. On the same day as the twig sampling, soil samples were collected every 10 cm at four depths (0–10, 10–20, 20–30, and 30-40 cm) and three random positions in each plot, using a manual soil corer or/and a pickaxe when the soil was too rocky. The soil samples were immediately placed in vials and stored like twigs. As the depth of the limestone bedrock varied within and between plots (between 20 and 70 cm; Table S4.1), the maximum depth of soil sample collection varied by date, plot, and position. Nevertheless, we could extract all the soil layers from 0 to 40 cm in every plot at each campaign, except for the *Q.ilex* monocultures in spring 2021, due to technical limitations. Precipitation water (used as a proxy of the groundwater isotopic values, see below) was collected by two Tube-dip-in-water collector types with pressure equilibration (RS1, Palmex, HR), spread into the study area (Fig. S4.1). Due to the unique design of the rain samplers avoiding evaporation for up to one year (Gröning et al., 2012), we collected the rainwater every two months during the growing season and once during the winter each year. The water was placed in vials and sealed with a lid and parafilm.

Water from xylem and soil samples was extracted using a custom-made cryogenic vacuum distillation system at the Swiss Federal Institute for Forest, Snow, and Landscape Research (WSL, Birmensdorf, CH) (Diao et al., 2022). The extraction system consisted of 20 tubes connected to 20 U-shaped collection tubes specifically designed for this system. A frozen sample was placed in the extraction tube and submerged in water at 80°C, while the associated collection tube was submerged in liquid nitrogen. The system was then evacuated to 5.10^{-2} mBar. The extraction was maintained for 2 h for both xylem and soil samples to achieve a complete extraction following the

recommendations of West et al. (2006) (i.e., a minimum of 60 min extraction time for a broad range of plant and soil materials). This process led to an extraction of 99.96% of the water in the samples, with more than 1 mL extracted for each sample, limiting the uncertainties in plant water isotopic composition due to cryogenic vacuum distillation (Diao et al., 2022). After the extraction, water samples were transferred into cap-crimp 2-ml vials and stored at −20 °C until the isotopic analysis. Uncertainties associated with bulk water extractions using cryogenic distillation systems could occur that would underestimate the contributions of soil water and overestimate the ones from groundwater (Barbeta et al., 2021). Yet, as all samples were treated similarly, the errors would only affect the actual values, not the comparison between mixtures and seasons.

The δ^2H and $\delta^{18}O$ of all water samples (i.e., twig, soil, and precipitation) were measured with a high-temperature conversion elemental analyzer coupled to a DeltaPlus XP isotope ratio mass spectrometer (TC/EA-IRMS; Thermo, DE). Isotope ratios were reported in per mil (‰) relative to Vienna Standard Mean Ocean Water (VSMOW). Calibration versus the international standards was achieved by analysis of a range of certified water of different isotope ratios, resulting in a precision of 2‰ for δ^2H and 0.3‰ for $\delta^{18}O$.

4.2.4 Water source contribution

From the natural abundance of δ^2H and $\delta^{18}O$ in plant xylem and soil water, we used a Bayesian stable isotope mixing model to quantify the contribution of potential tree water sources in each species in the monospecific and four-species mixtures for each sampling date. As the rainwater isotope ratio differs throughout the season (i.e., isotopically more depleted rainwater in winter compared to summer) and the water evaporation decreases with soil depth, each water source has a significantly different stable isotopic composition (Fig. S4.3). These distinct soil isotopic profiles allow us to determine the contribution of each water source to the tree xylem water under the assumption that there is no isotopic fractionation during water uptake by the roots (Dawson & Ehleringer, 1991). Therefore, the natural isotopic abundance of xylem sap should reflect the water sources used by the plant. We used the package *simmr* in R (Parnell, 2019), where the isotopic composition ($\delta^{18}O$ and δ^2H) for each potential source (i.e., 0-10 cm, 10-20 cm, 20-30 cm, 30-40 cm, rainwater) and each target tree were assigned into the model. We set the TEF (trophic enrichment factor) and the concentration dependence to 0 due to the absence of isotopic fractionation by the roots. We ran the model where 3600 iterations out of 10000 runs were produced over 4 Markov chain Monte Carlo (MCMC) for the isotopic values from each plant with the isotopic values from the soil water source of the corresponding plot in each date (Sun et al., 2022). To increase the clarity of presentation, the contributions from the water sources were grouped *a posteriori* into three layers: shallow (i.e., 0–20 cm), deep (i.e., 20–40 cm), and water stored in the fractured bedrock (i.e., rainwater). Indeed, the winter precipitation that penetrates deep soil layers

and bedrock cracks could be a substantial water source for trees in Mediterranean forests during summer droughts (Eliades et al., 2018). As the bedrock water is not subjected to evaporation (Ehleringer & Dawson, 1992), we used the precipitation collected at our site as a proxy, similar to Grossiord et al., (2017). The cumulative rainwater collected during the winter of 2021 (i.e., January-April) and 2022 (i.e., October-April) was considered bedrock water source for the May campaigns of 2021 and 2022, respectively. During the remaining growing season, the stable isotope composition of the precipitation until the sampling date was added to the winter precipitation (e.g., winter, May, and June for the campaigns in July).

4.2.5 Water source partitioning

To estimate the plot-level vertical water source distribution in the mixed forest plots, we calculated the belowground water source partitioning at the community level (P_W, unitless) from the sum of the differences in either the natural abundance of δ^2H or $\delta^{18}O$ in plant water between all interacting species in every four-species mixtures for each sampling date. As different water uptake depths between trees correspond to greater differences in the xylem water stable isotope within a tree cluster, higher P_W indicates that the trees are taking up water from more distant water sources from each other. Therefore, to calculate P_W based on δ^2H, we used the following equation developed by Grossiord et al. (2018):

$$P_W = |\delta^2H_{PN} - \delta^2H_{PS}| + |\delta^2H_{PN} - \delta^2H_{QF}| + |\delta^2H_{PN} - \delta^2H_{QI}| +$$

$$|\delta^2H_{PS} - \delta^2H_{QF}| + |\delta^2H_{PS} - \delta^2H_{QI}| + |\delta^2H_{QF} - \delta^2H_{QI}| \qquad \text{(Equ. 1)}$$

where δ^2H_{PN}, δ^2H_{PS}, $\delta^2H_{QF,}$ and δ^2H_{QI} correspond to δ^2H of *P. nigra, P. sylvestris, Q. faginea,* and *Q. ilex*, respectively. As the P_W resulted from $\delta^{18}O$ and δ^2H weighted similarly, only the P_W based on δ^2H was further used in this paper (Fig. S4.4).

4.2.6 Statistical analyses

The effects of tree species diversity on Ψ_{pd}, Ψ_{md}, Δ_{Ψ}, A_{net}, $g_{s,}$ xylem δ^2H and $\delta^{18}O$ were determined through linear mixed-effects models for each species using the package *lmer*. The effect of the season (i.e., spring, summer, fall), year (i.e., 2021, 2022), and species diversity (i.e., monospecific/monofunctional/multifunctional/four-species mixtures) were used as fixed effects, and the individual plot was treated as a random effect. Similar models were used to determine differences in soil water δ^2H and $\delta^{18}O$. Sampling dates, species diversity, species, and soil depth were used as explanatory factors in the fixed part of the model. Significant differences between depths for each species' diversity and sampling dates were found, allowing us to use the Bayesian isotope mixing model to determine the water source contribution of trees as described above (Fig. S4.3). The output of this model was analyzed similarly with linear mixed-effects models for each

species. First, the effect of soil depth (i.e., shallow, deep, bedrock), season, year, and species diversity (i.e., monospecific and four-species mixture) were set as fixed effects, and the individual plot as a random effect. Then, we ran similar models for each soil depth and species where the season, year, and species diversity were used as fixed effects and the plots as random effects. To reveal significant differences between species richness for each measurement at each sampling date and each species, post hoc analyses were performed with Tukey's HSD test, with FDR correction for multiple testing. Linear regressions were used to test the relationships between $\Delta\Psi$, Ψ_{pd}, g_s, xylem $\delta^{18}O$, P/PET, and P_W. All analyses were performed using the R v.4.2.2 statistical software (R Development Core Team, Vienna, Austria, 2022). Before performing each model, the homogeneity of variances and the normality of residuals were assessed, and data were log-transformed if necessary.

4.3 Results

4.3.1 Leaf-level gas exchange and water potential

In both years, as drought stress increased during the summer, predawn leaf water potential (Ψ_{pd}), net photosynthesis (A_{net}), and stomatal conductance (g_s) significantly decreased for all species (Fig. 4.2, Table S4.2). As precipitation increased soil water content in the early fall, Ψ_{pd}, A_{net}, and g_s recovered to similar values as in spring for all species in 2021. In contrast, Ψ_{pd} for all species and A_{net} and g_s for pines did not recover following the extreme summer drought in 2022 (Fig. 4.2). As Ψ_{pd} decreased, the difference between predawn and midday water potentials ($\Delta\psi$) significantly decreased for all species (P<0.001), with oaks reaching lower Ψ_{pd} while maintaining higher $\Delta\psi$ than pines (Fig. 4.3).

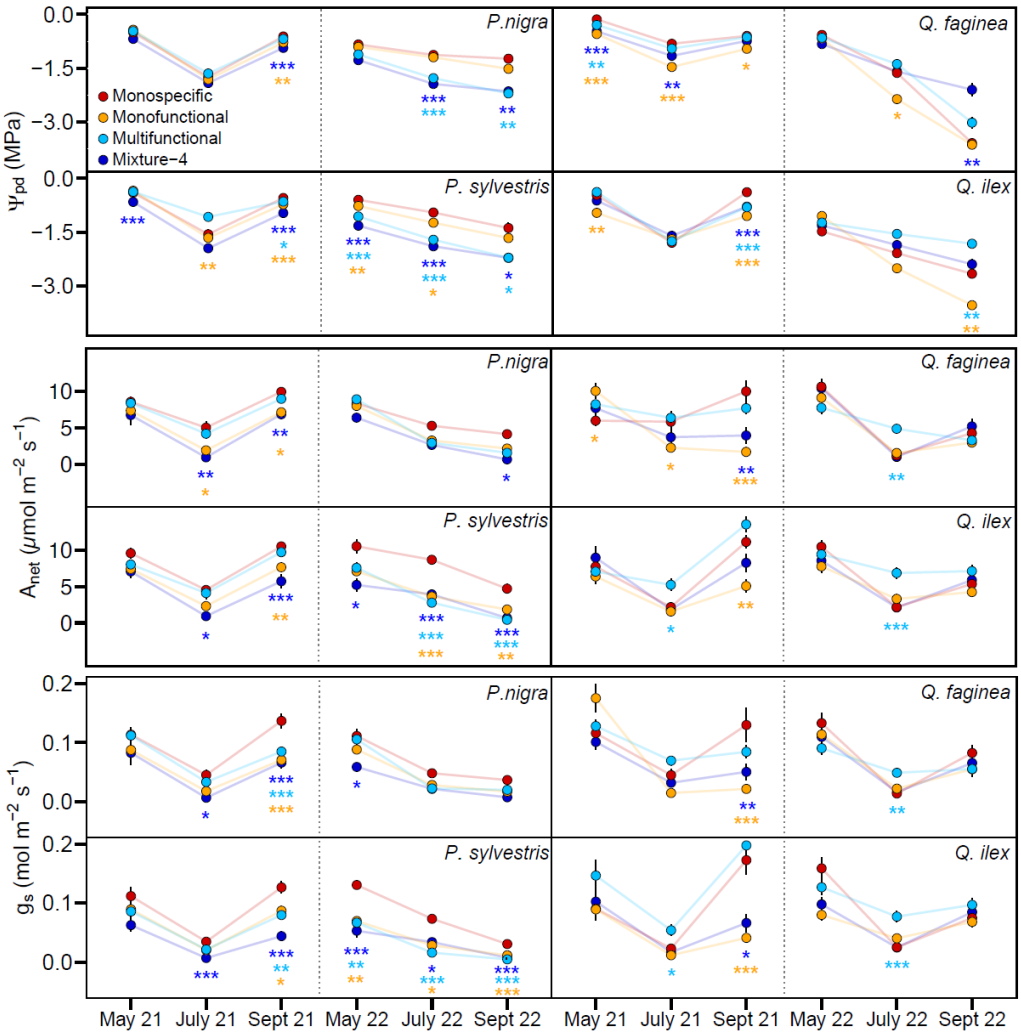

Figure 4.2: Mean (±SE) leaf water potential at predawn (Ψ_{pd}), light-saturated net photosynthesis (A_{net}), and stomatal conductance (g_s) for each sampling date in 2021 and 2022 for *P. nigra*, *P. sylvestris*, *Q. faginea*, and *Q. ilex* in monospecific (red), monofunctional (orange), multifunctional (light blue) and four-species mixture plots (dark blue). The stars indicate significant differences between mixed and monospecific plots at each sampling date (*0.05≥P>0.01; **0.01≥P>0.001; ***P≥0.001).

Throughout all seasons, we found lower Ψ_{pd}, A_{net}, and g_s in the four-species mixtures compared to the monospecific plots for *P. sylvestris* (Fig. 4.2 & Table S4.2). Similarly, in the two-species mixtures (i.e., monofunctional and multifunctional), significant reductions in Ψ_{pd}, A_{net}, and g_s compared to the monospecific plots were observed in the fall of 2021 and throughout 2022 for *P. sylvestris*. A similar pattern was found for *P. nigra* but with less significant diversity effects (Fig. 4.2 & Table S4.2). Indeed, for *P. nigra*, while Ψ_{pd} values were lower in the diverse plots compared to the monospecific ones in the summer and fall of 2022, A_{net} and g_s rates were only reduced in the four-species and monofunctional mixtures in the summer and fall of 2021. For oaks, the effect of species diversity was less consistent, with lower recovery of Ψ_{pd}, A_{net}, and g_s in the four-species mixtures compared to the monospecific plots following the summer of 2021. Further, in the fall of 2022, Ψ_{pd} was higher in multifunctional and four-species mixtures for *Q. ilex* and *Q. faginea,* respectively, compared to the monospecific plots. Similarly, A_{net} and g_s were higher for the multifunctional mixtures than the monospecific plots for both oak species (Fig. 4.2).

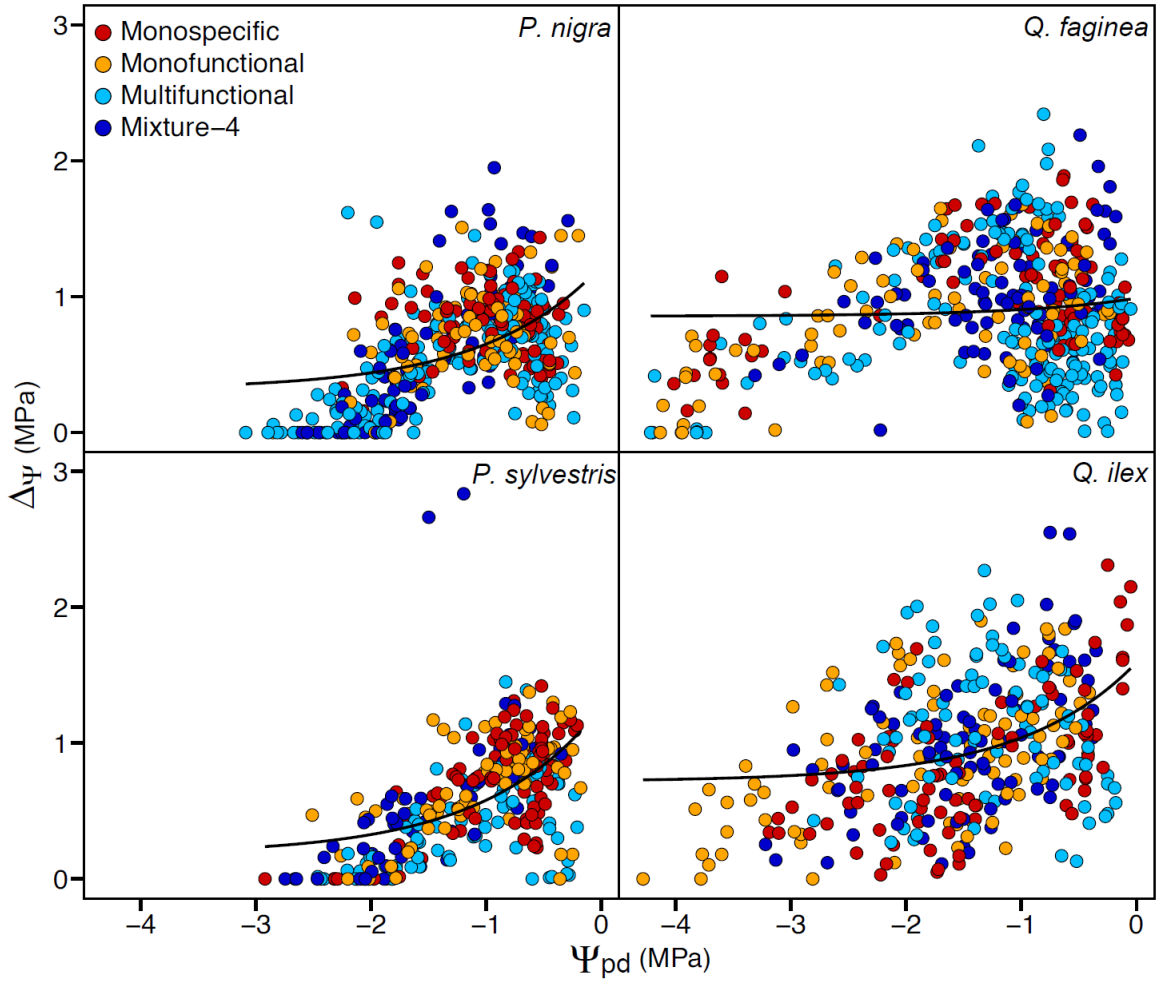

Figure 4.3: Relationships between the difference in predawn and midday leaf water potential ($\Delta\psi$) and the predawn leaf water potential (Ψ_{pd}) for *P. nigra*, *P. sylvestris*, *Q. faginea,* and *Q. ilex* in monospecific (red), monofunctional (orange), multifunctional (light blue) and four-species mixture plots (dark blue). Lines represent linear regressions with significant relationships across all species diversity levels.

4.3.2 Water source contribution and partitioning

As the soil dried out in the summer, all species, regardless of the diversity (i.e., monospecific and four-species mixtures), shifted their water uptake depth from shallow (i.e., 0-20 cm) in spring to deeper (i.e., >20 cm) layers in the summer (Fig. 4.4). In 2021, this trend was followed by a recovery to shallower layers in the fall. In contrast, the water uptake depth did not return to shallower sources in the fall of 2022 (Fig. 4.4 & Table S4.3), probably due to the reduced precipitation in fall 2022 (Fig. 4.1). The uptake of the water from the bedrock was consistently low for all species throughout the growing season (19±0.5%), except in the summer of 2021, where it increased by up to 23% compared to the springtime for the oaks in monospecific plots (Fig. 4.4).

However, we found no significant effect of species diversity on the water uptake depth for all species except for *Q. faginea*. In 2021, *Q. faginea* trees took up more water from the shallower layers in the spring and the deep layers in the summer in the four-species mixtures compared to monospecific plots (Fig. 4.4 & Table S4.3). We further observed a clear distinction in the seasonal variability between functional types (i.e., oaks and pines). Under wetter conditions (i.e., spring and fall), oaks took up a similar proportion of water from the shallowest layers as pines (44±11% and 39±6%, respectively). In the summer, oaks more sharply shifted towards deeper sources than pines (Fig. 4.4). This pattern resulted in less water extracted from the shallowest layers in summer than in spring, independently of the year (reduction of about 28% and 17% for oaks and pines, respectively).

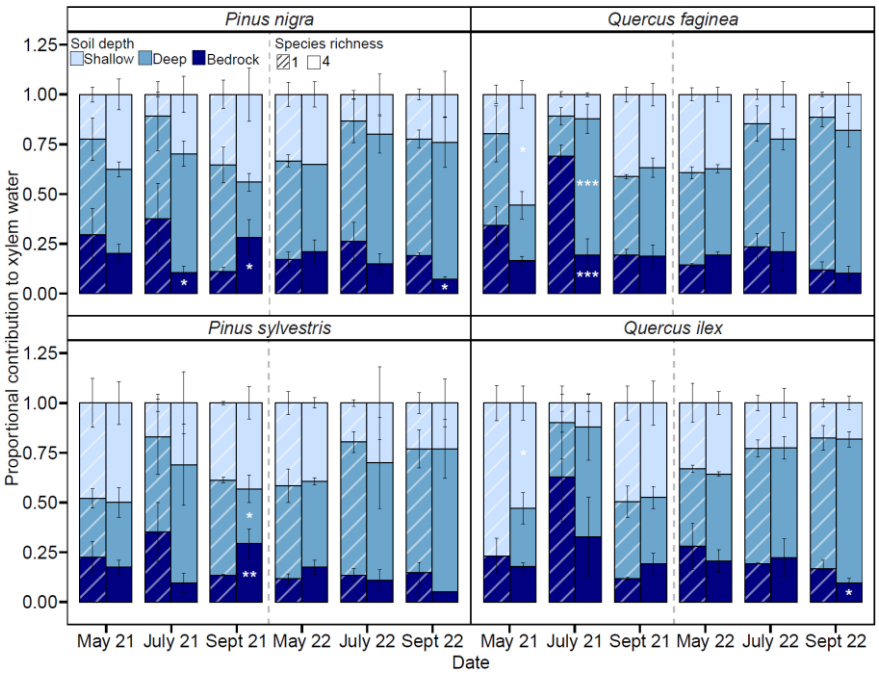

Figure 4.4: Proportional contribution to xylem water (mean ±SE) of the water in the fractured bedrock (bedrock; dark blue), deep (20-40 cm; medium blue), and shallow soil layers (0-20 cm; light blue) resulting from the mixing model, for *P. nigra, P. sylvestris, Q. faginea*, and *Q. ilex* in monospecific (dashed bars) and four-species mixtures (empty bars) for each sampling date. Asterisks denote significant differences between diversity levels for a given soil layers and date (*0.05≥P>0.01; **0.01≥P>0.001; ***P≥0.001).

We observed a significant negative relationship between water source partitioning (P_W), i.e., the average difference between water-uptake depths, and the soil aridity index (P/PET) (P<0.001; Fig. 4.5b). When the soil moisture decreased in the summer (i.e., decreasing P/PET), P_W consistently increased, indicating stronger water source partitioning. After the first rain replenished the soil in the fall of 2021, P_W decreased. In contrast, the intense 2022 drought delayed the recovery of P_W in the fall (Fig. 4.5a).

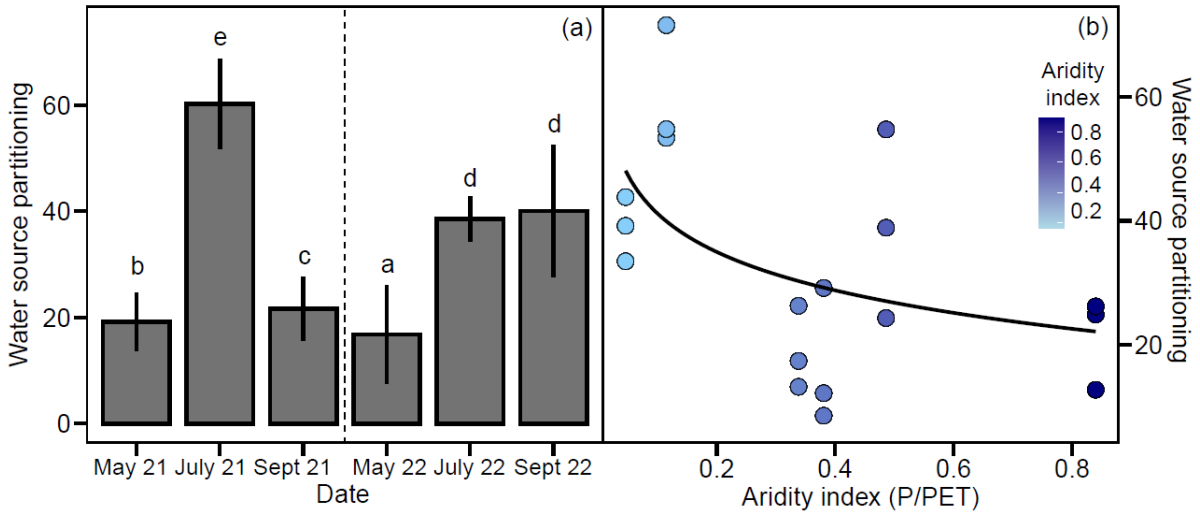

Figure 4.5: (a) Belowground community-level water source partitioning (mean ± SE, unitless) in the four-species mixtures for each sampling date. Letters denote significant differences between dates. (b) Relationship between the belowground community-level water source partitioning and the aridity index (P/PET) in the four-species mixtures. Colors represent the aridity index with a gradient from the driest (light blue) to the wettest (dark blue). The line represents the significant linear regression between water source partitioning and P/PET.

4.3.3 Relationship between leaf hydraulic traits and xylem water stable isotope

With increasingly dry conditions in the summer, the xylem $\delta^{18}O$ and $\delta^{2}H$ decreased for oaks and increased for pines in the four-species mixtures, leading to contrasting relationships between xylem $\delta^{18}O$ and the leaf hydraulic traits (Figs. 4.6 & S4.4; Table S4.2). With decreasing xylem $\delta^{18}O$, Ψ_{pd}, $\Delta\Psi$, and g_s significantly increased for pines, suggesting that deeper water uptake resulted in lower water stress and higher gas exchange. For oaks, decreasing xylem $\delta^{18}O$ led to lower Ψ_{pd}, $\Delta\Psi$, and g_s (P<0.001; Fig. 4.6), indicating lower gas exchange despite deeper water sources. These relationships were only significant in the four-species mixtures and not in the monospecific plots (Fig. 4.6).

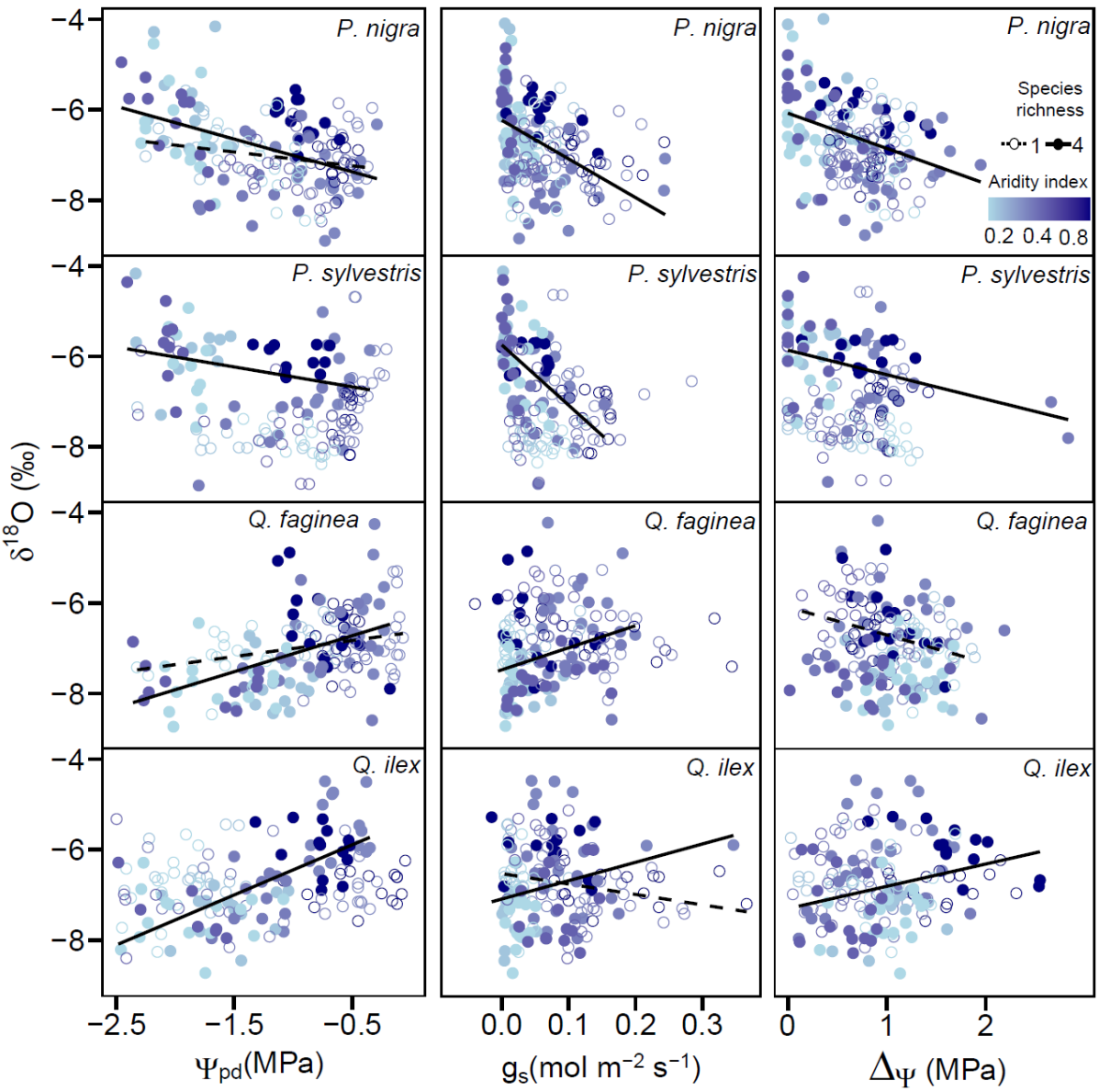

Figure 4.6: Relationships between the predawn leaf water potential ($\Psi_{predawn}$), the light-saturated stomatal conductance (g_s), the difference in predawn and midday leaf water potential ($\Delta\ \Psi_{predawn}$-Ψ_{midday}), and the xylem water oxygen isotopic composition ($\delta^{18}O$) for *P. nigra*, *P. sylvestris*, *Q. faginea* and *Q. ilex* in monospecific (empty circles), and four-species mixtures (plain circles). Colors represent the aridity index of all the measurement months with a gradient from the driest (light blue) to the wettest (dark blue) in 2021 and 2022. Lines represent significant linear regressions with dotted and solid lines standing for monospecific and four-species plots.

We found variable effects of P_W on the leaf hydraulic traits. For all species, we observed a decrease of Ψ_{pd} and g_s with increasing P_W ($P<0.001$), indicating reduced gas exchange with increased water source partitioning (mainly during the summer; Fig. 4.5). In addition, $\Delta\psi$ decreased with increasing P_W for pines but not oaks, highlighting the differential stomatal regulation strategies in the two functional groups (Fig. 4.7).

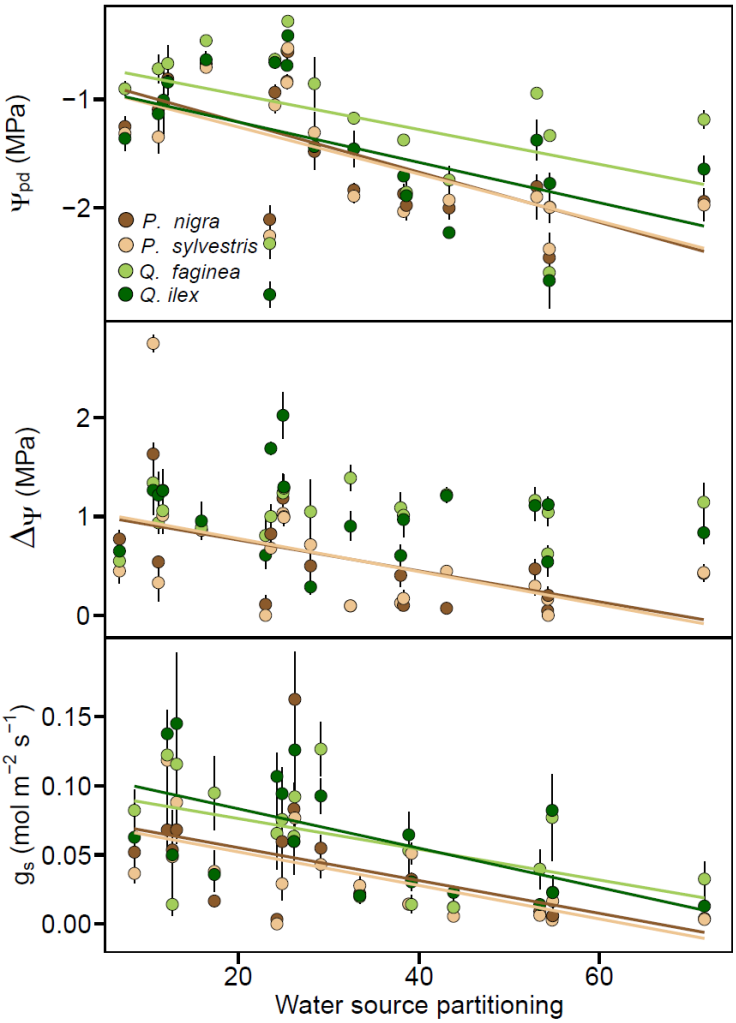

Figure 4.7: Relationships between the predawn leaf water potential (Ψ_{pd}), the difference in predawn and midday leaf water potential ($\Delta\psi$), the light-saturated stomatal conductance (g_s), and the belowground community-level water source partitioning for *P. nigra* (brown), *P. sylvestris* (beige), *Q. faginea* (light green) and *Q. ilex* (dark green) in the four-species mixtures (mean ± SE per plot and date). Lines represent significant linear regressions for each species.

4.4 Discussion

Understanding the environmental factors influencing drought vulnerability is crucial for effective forest management and conservation strategies. Our study indicates that while increasing tree diversity can promote water source partitioning and improve plant water availability to some extent, this mechanism alone is insufficient to overcome the adverse impacts of intense Mediterranean summer droughts. Indeed, we showed that the leaf hydraulic traits followed, as expected, the well-known seasonal variability in Mediterranean forests (Fotelli et al., 2019; Gulías et al., 2009). This trend is defined by increasing water stress (i.e., as shown by reduced Ψ_{pd}, $A_{net,}$ and g_s) when soil moisture decreases in the summer. Gas exchange then recovered in all species after the first rain replenished the soil in the fall of 2021 (Table S4.1 & Fig. 4.2). Interestingly, we observed lower or no recovery of gas exchange and hydraulic status in the fall of 2022 due to late precipitation events that kept soil moisture low at the end of the growing season (Fig. 4.1). However, tree species diversity modulated the magnitude of this seasonal variation with contrasting impacts on oaks and pines. Decreasing Ψ_{pd}, A_{net}, and g_s in pines in mixed plots compared to the monospecific ones indicates higher water stress during the summer. In contrast, oaks showed either no effect or a positive diversity effect (i.e., lower reduction in Ψ_{pd}, A_{net}, g_s in mixtures) (Fig. 4.2). Previous work conducted in the same area also found that tree diversity enhanced or reduced tree transpiration of *Q. faginea* and *P.sylvestris*, respectively (Grossiord et al., 2015). However, our work highlights the predominance of functional diversity effects rather than species richness *per se*, as similar seasonal variations in carbon and water dynamics were observed in monospecific and monofunctional mixtures for both functional groups (Díaz & Cabido, 2001). Hence, despite the general consensus and our initial hypothesis that diversity enhances drought resistance and resilience (e.g., Anderegg et al., 2018; Liu et al., 2022), we found that increasing functional diversity could benefit some species but also exacerbate the water stress for others. Aboveground, this response could be driven by the water–saving strategy of the more isohydric pines that maintain high water potential (i.e., low $\Delta\psi$) by closing their stomata earlier than the more anisohydric oaks (Fig. 4.3). As previously observed for *Q. ilex* and *P. sylvestris* in montane Mediterranean forests (Aguadé et al., 2015), contrasting stomatal regulations can result in faster exhaustion of soil moisture by oaks at the expense of pines.

Despite the essentially adverse impacts of drought on the aboveground carbon and water dynamics, all species shifted their water uptake depth from shallow to deep soil layers (>20cm) during the summer before going back to more superficial layers (0-20 cm) in the fall (Fig. 4.4). This finding supports the widely observed vertical plasticity of water sources in Mediterranean forests (e.g., Barbeta et al., 2015; David et al., 2013; Eliades et al., 2018; Grossiord et al., 2017). We further observed a constant contribution of water from the fractured bedrock (around 19%) (Fig. 4.4), supporting numerous studies that highlight the importance of such reservoirs in Mediterranean

regions (e.g., Barbeta et al., 2015; Eliades et al., 2018; Hanson et al., 2007). Contrary to our expectations, species diversity did not modify the water sources of the studied species in the four-species mixtures (Table S4.3). Nevertheless, contrasting water uptake depths in pines and oaks discriminated tree water sources along a vertical niche axis during drier periods (Rodríguez-Robles et al., 2020). Hence, increasing water source partitioning with reduced soil moisture was observed (Fig. 4.5), as previously found in various forests during drought (e.g., Bello et al., 2019; Grossiord et al., 2018; Meiner et al., 2012; Rodríguez-Robles et al., 2020; Schwendenmann et al., 2015). As expected, shallow-rooted pines took preferentially water from the more superficial soil layers throughout the year (Čermák et al., 2008). In contrast, oaks' deep and dual root systems facilitated access to significantly deeper water sources in the summer (Moreno et al., 2005). Whether the observed belowground niche partitioning could result from root growth competition remains unknown (del Castillo et al., 2016). Still, niche overlapping occurred when water was abundant, while niche partitioning ensued under dry conditions (e.g., Barbeta et al., 2015; Guo et al., 2018; Rodríguez-Robles et al., 2020; Rodríguez-Robles et al., 2015).

Belowground moisture partitioning (P_W; Figs. 4.4 & 4.5) had a limited beneficial impact on the aboveground carbon and water use dynamics. On the one hand, the shift to deeper sources in mixtures during the summer led to more negative xylem $\delta^{18}O$ (i.e., reduced P/PET leading to deeper water sources) that still resulted in lower Ψ_{pd}, g_s, and $\Delta\psi$ (Fig. 4.6) for oak. Thus, even if oaks maintained their water flux in mixed plots (i.e., no relationship between $\Delta\psi$ and P_W; Fig. 4.7), access to deeper water reservoirs was insufficient to fully overcome the water stress induced by drought. This finding contradicts previous work in *Quercus suber* L. trees in central Portugal, suggesting that shifts in water sources could maintain high transpiration rates during summer droughts (David et al., 2007). The discrepancy between these findings could stem from the lower groundwater contributions observed at our plots (19% *vs*. 30%) associated with shallower soils, high stoniness, and the lesser importance of hydraulic redistribution, representing up to 37% of transpired water in this work. Although we cannot exclude that hydraulic redistribution occurred in our study, the very low gas exchange observed during the summer (Fig. 4.2) suggests that it played a limited role. On the other hand, for pines, the continuous reliance on the shallowest soil layers (as shown by the more positive xylem $\delta^{18}O$; Fig. S4.3) lowered Ψ_{pd}, g_s, and $\Delta\psi$ during drought (Fig. 4.6). Hence, although water source partitioning increased as the soil dried out (mainly because of oak's deeper water uptake), it still resulted in decreased Ψ_{pd} and g_s in all species (Fig. 4.7). These findings contrast with previous studies highlighting the importance of belowground complementarity and water redistribution (e.g., David et al., 2007; Rodríguez-Robles et al., 2020). Overall, our findings feature the complex and multifaceted nature of forest responses to climate change by emphasizing that diversity-driven shifts in water sources can overcome water stress only up to a certain drought intensity (Figs. 4.2 & 4.6). Moreover, as species diversity effect on drought resistance depends on the environmental conditions (Grossiord et al., 2014; Liu et al., 2022), the

conclusions of this study could change in different forest ecosystems. Further research in multiple ecosystems is warranted to elucidate if other diversity-driven mechanisms (e.g., hydraulic lift, canopy packing, microclimate feedback) could play a pivotal role in these ecosystems and identify strategies to enhance forest tolerance to climate change.

4.5 Conclusion

Our results show that diversity-driven water source partitioning did not overcome the intense drought stress trees can experience in Mediterranean forests. When soil moisture decreases in the summer, oak species could shift their water sources to deeper soil layers. In contrast, the shallower-rooted pines were constrained to more superficial layers, leading to increasing water source partitioning. As a result, oaks mixed with pines could sustain slightly higher gas exchange rates than those in monospecific plots, probably because of the lower competition in deeper layers. On the contrary, pines' shallow root system and water-saving strategy induced earlier stomatal closure as the drought progressed, resulting in low gas exchange, especially in mixtures with oak. Thus, the combination of species with contrasting stomatal regulation strategies and root systems only benefited the most drought-tolerant species at the expense of drought-sensitive ones, highlighting that diversity could end up in a general decline of less competitive *Pinus* species (Gea-Izquierdo et al., 2021). While diversity may promote a range of services, promoting diverse forests may not prevent pine decline due to the worsening of droughts in Mediterranean areas. Over the long term, interactions between species could be further disrupted within mixed oak-pine forests, potentially leading to cascading effects on the entire ecosystem, including shifts in species composition and reduced biodiversity. Continued research is necessary to inform evidence-based management practices to foster the adaptability of those climate change hotspots.

4.6 Acknowledgments

EM and CG were supported by the Swiss National Science Foundation (310030_204697) and the Sandoz Family Foundation. AV and LM were supported by the INERTIA project (PID2019-111332RB-C22) and EVER_PROMETEU (CIPROM/2022/37). CEAM is funded by Generalitat Valenciana. We thank Alex Tunas, David Lopez, Eric Breton, Francisco Fornieles, and Giulia Casciano for their support with the field measurements. The authors declare no conflict of interest. The data supporting this study's findings are available in the paper and its Supplementary Information or from the corresponding author upon request. They will also be available from the Dryad Digital Repository after acceptance.

4.7 Supporting information

4.7.1 Supporting figures

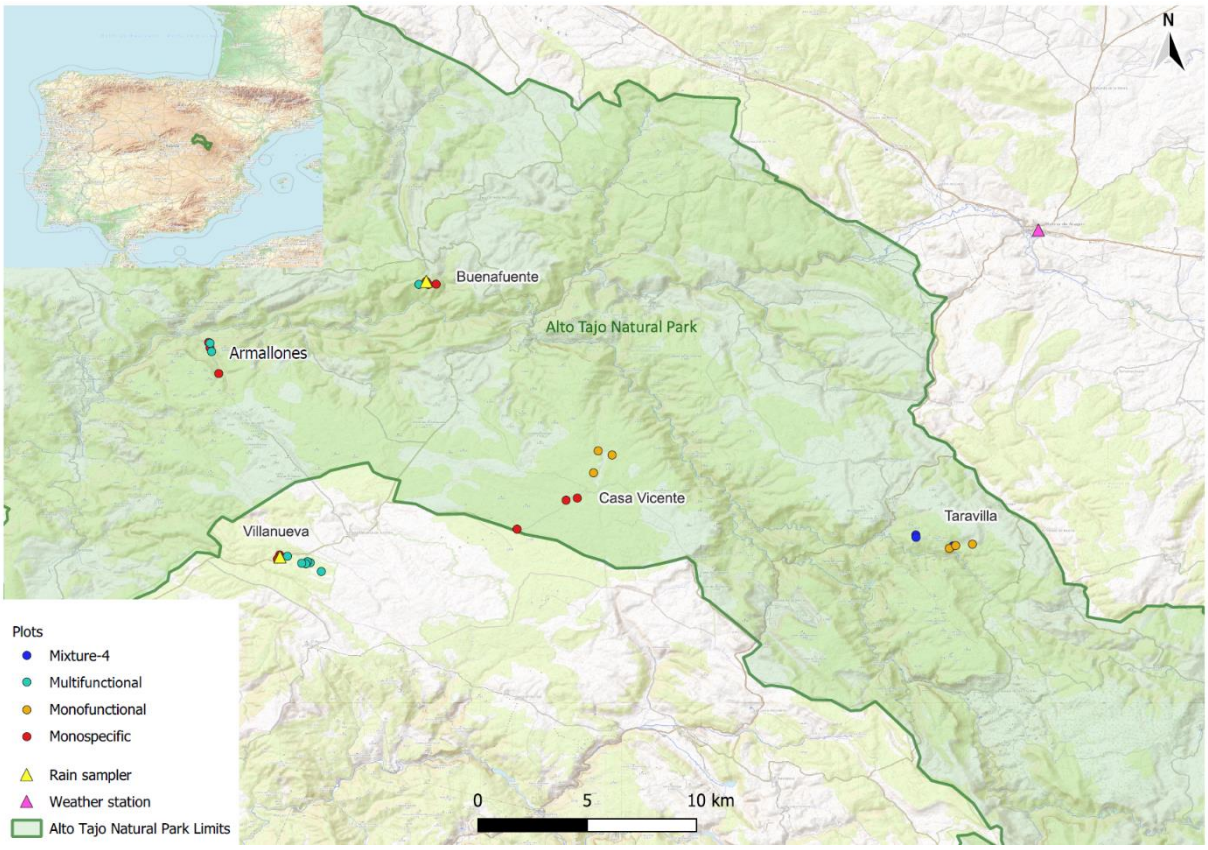

Figure S4.1: Map of the Alto Tajo natural park (Central Spain) with the localization of the studied plots of monospecific (red), monofunctional (orange), multifunctional (green) and four-species mixture plots (dark blue), the rain samplers (yellow triangle) and the weather station (pink triangle) (map lines delineate study areas and do not necessarily depict accepted national boundaries).

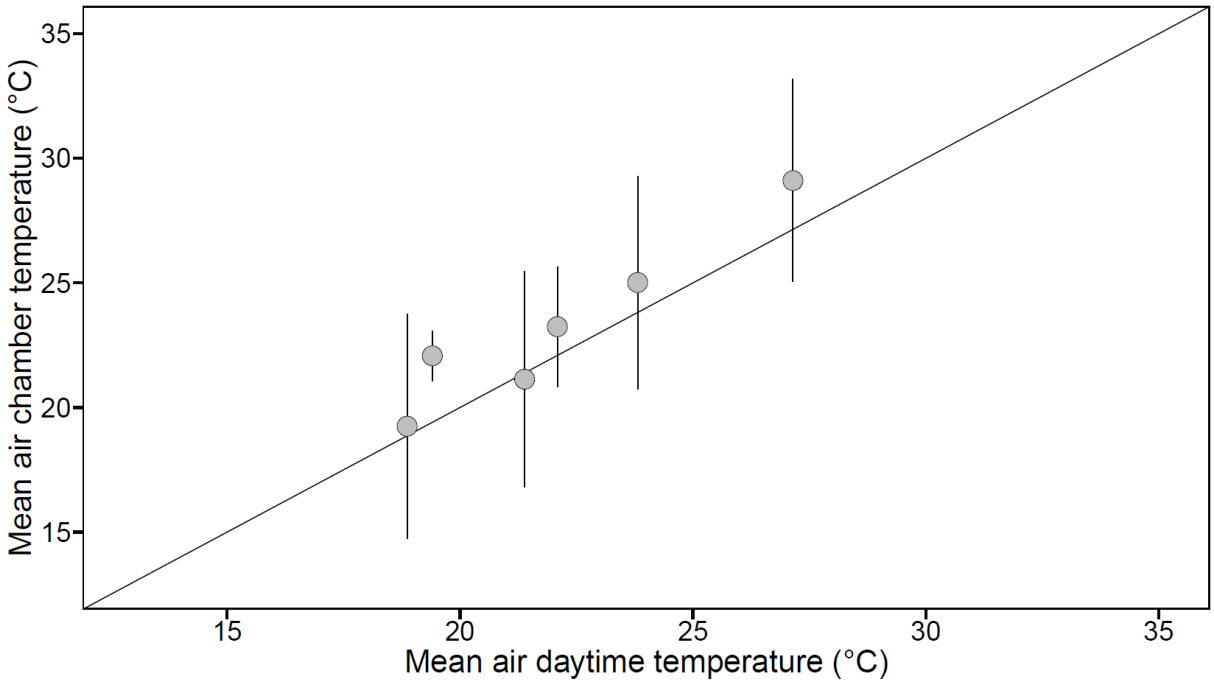

Figure S4.2: Relationship between the mean air daytime temperature and the mean air temperature inside the chamber of the gas exchange system (±sd) at each sampling date (n = 6 campaigns in total).

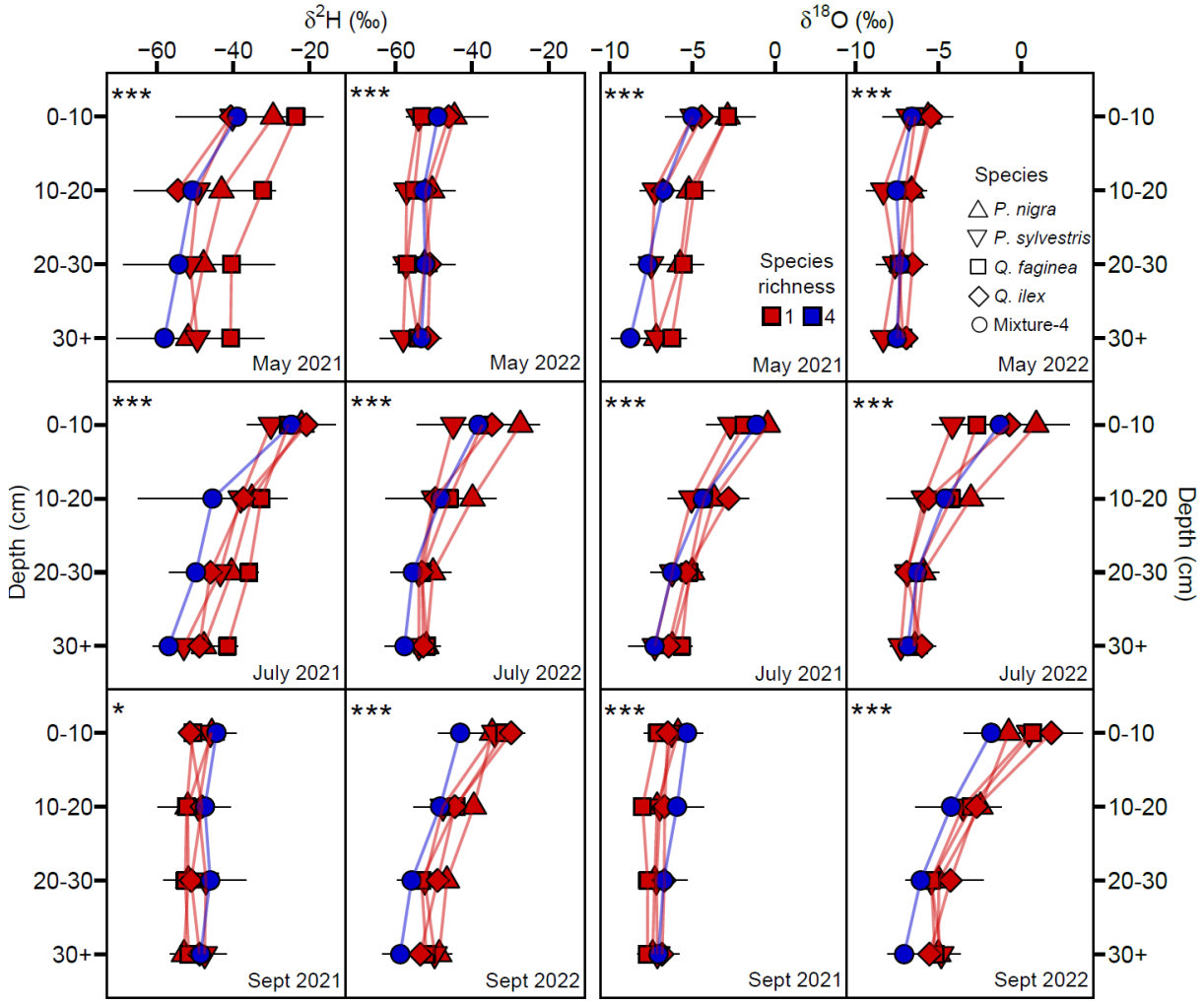

Figure S4.3: Soil water δ^2H and $\delta^{18}O$ (mean ± SD) at each depth (0-10 cm, 10-20 cm, 20-30 cm, >30 cm) and sampling date in 2021 and 2022 for the monospecific plots (red) of each species (*P. nigra*, *P. sylvestris*, *Q. faginea*, and *Q. ilex*), and the four-species mixtures (blue). The stars indicate significant differences between depths at each sampling date (*0.05≥P>0.01; **0.01≥P>0.001; ***P≥0.001).

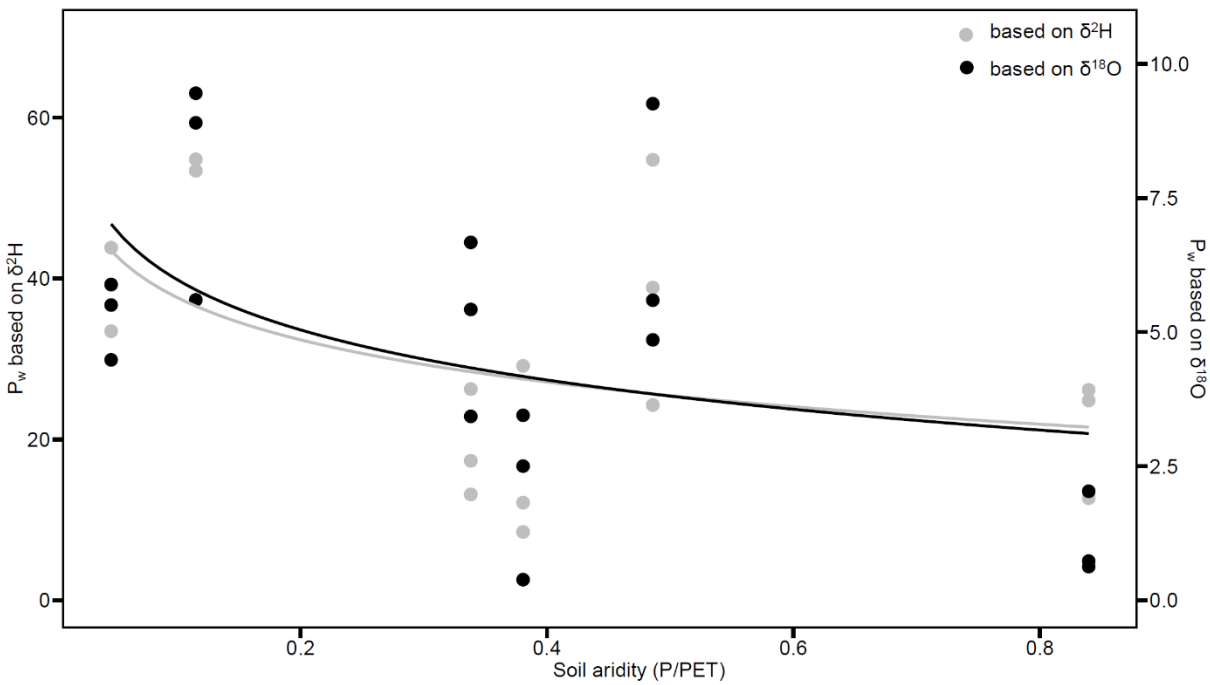

Figure S4.4: Relationship between the water source contribution (Pw, unitless) calculated based on the δ^2H (grey) or based on the $\delta^{18}O$ (black) and the soil aridity (P/PET). No significant interaction between the two relationships was found.

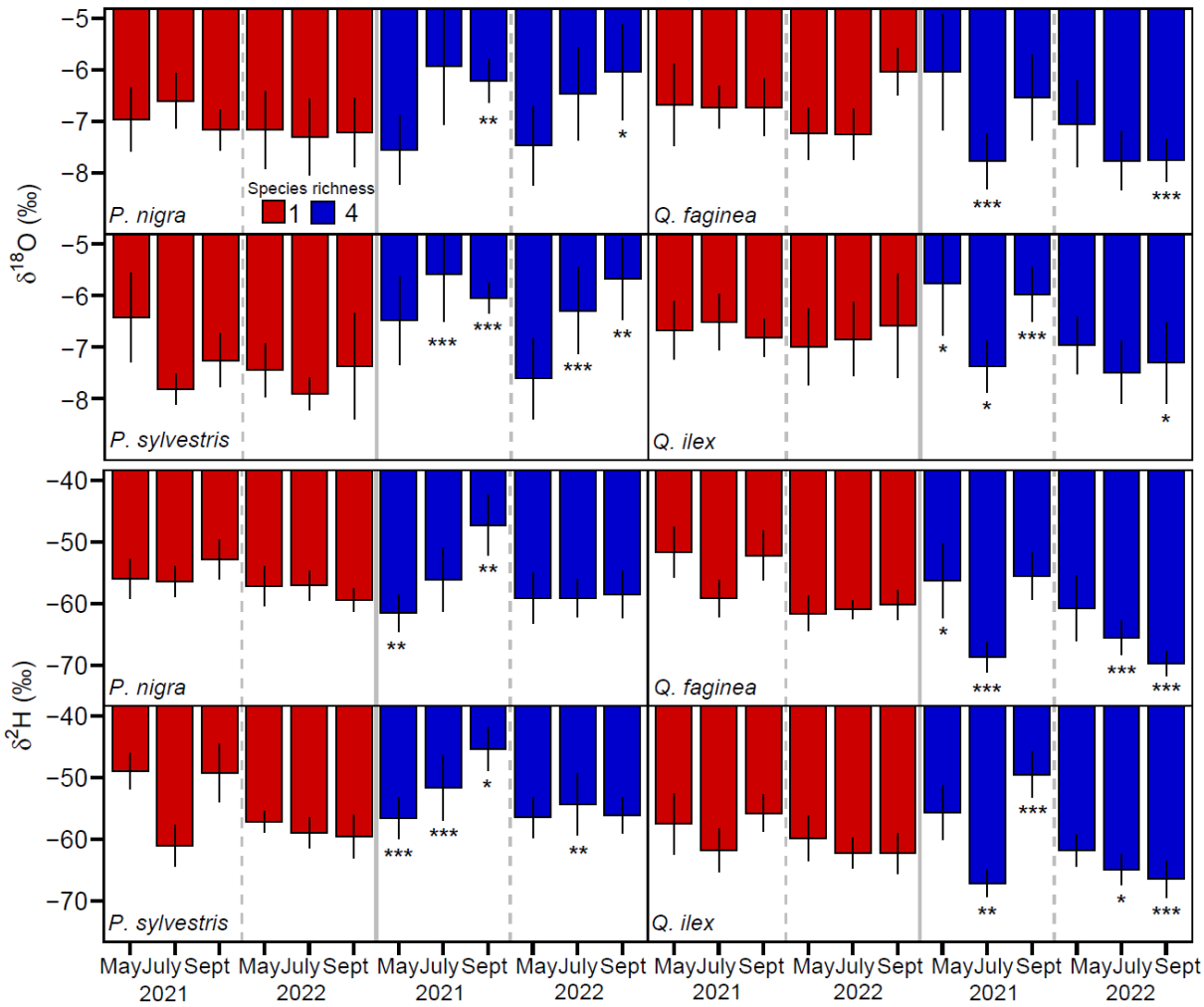

Figure S4.5: Xylem water δ^2H and $\delta^{18}O$ (mean ± SE) at each sampling date in 2021 and 2022 for *P. nigra*, *P. sylvestris*, *Q. faginea*, and *Q. ilex* in monospecific (red) and four-species mixtures (blue). The stars indicate significant differences between diversity levels (*0.05≥P>0.01; **0.01≥P>0.001; ***P≥0.001).

4.7.2 Supporting table

Table S4.1: Description of the 30 selected plots, including the plot-level leaf area index (LAI), the diameter at breast height (DBH), and tree height (mean ±SD).

Plot	Latitude	Longitude	Altitude (m)	Exposition	Soil depth (cm)	LAI (m²/m²)	Species richness	Species composition	DBH (cm)	Height (m)
9	40.66814851	-2.292657672	1211	S	20	1.33	Monospecific	*Q. faginea*	61.4± 14	12.1± 1.3
10	40.66707271	-2.292521806	1270	SE/S	70	0.938	Monospecific	*Q. faginea*	56.4± 5.4	8.4± 1.6
11	40.66589427	-2.293874762	1187	SE	20	1.4	Monospecific	*Q. faginea*	66.1± 9.5	10.1± 1.9
12	40.7659242	-2.32553588	1073	NE	NA	1.57	Monospecific	*P. nigra*	91.6± 28.1	14.5± 4.5
15	40.77979254	-2.330305941	980	W	20	1.39	Monospecific	*P. nigra*	77.8± 16.6	11.5± 1.5
17	40.78267786	-2.331021184	960	NA	20	1.93	Monospecific	*P. nigra*	91.0± 20.7	12.8± 1
18	40.68204502	-2.164579218	1403	NA	70	1.55	Monospecific	*P. sylvestris*	134.8± 15	16.8± 0.8
19	40.69764993	-2.138101195	1310	NA	50	1.31	Monospecific	*P. sylvestris*	108.8± 15.8	13.7± 1.2
20	40.69874911	-2.132025477	1311	NA	20	1.07	Monospecific	*P. sylvestris*	120.4± 30.9	13.5± 2
32	40.81556405	-2.213577194	1236	SW	30	0.686	Monospecific	*Q. ilex*	52.4± 13.9	6.3± 2.2
33	40.81397399	-2.212467962	1251	SW	20	1.48	Monospecific	*Q. ilex*	50.6± 16.7	5.8± 1.8
34	40.81408609	-2.208205077	1250	SW	20	2.42	Monospecific	*Q. ilex*	60.8± 8.6	6.9± 1.5
28	40.67163045	-1.931317871	1360	SE	30	1.51	Monofunctional	*Q. faginea* *Q. ilex*	41.6± 5.7 57.2± 17.6	5.5± 0.5 5.5± 0.7
30	40.67314834	-1.927862642	1350	SW	20	1.59	Monofunctional	*Q. faginea* *Q. ilex*	52.2± 8.9 48.2± 19.1	7.3± 0.9 6.3± 1
31	40.67396249	-1.91878851	1342	SW	30	2.22	Monofunctional	*Q. faginea* *Q. ilex*	59.8± 12.5 48.8± 27.6	8.4± 1.3 6.3± 1.7
21	40.71238926	-2.123322685	1404	N	70	1.21	Monofunctional	*P. nigra* *P. sylvestris*	107.8± 25.3 90.3± 12.3	15.0± 1.7 13.5± 2.5
22	40.72197039	-2.113274124	1325	NA	20	1.79	Monofunctional	*P. nigra* *P. sylvestris*	112.8± 34.8 106.7± 31.6	18.6± 2.2 17.3± 1.9
23	40.72421507	-2.120796695	1388	NE	50	1.73	Monofunctional	*P. nigra* *P. sylvestris*	104.6± 21.8 105.8± 22.5	13.7± 1.8 14.6± 2.1
1	40.65918475	-2.270218954	1224	NE	20	2.1	Multifunctional	*P. sylvestris* *Q. faginea*	97.6± 11.5 67.6± 13.9	16.0± 1.6 13.6± 2.3
4	40.6639185	-2.27621676	1286	NA	50	1.56	Multifunctional	*P. sylvestris* *Q. faginea*	119.2± 34.9 88.6± 18.8	15.3± 2.4 13.7± 4.6
5	40.66450616	-2.277687348	1283	NW	70	1.3	Multifunctional	*P. sylvestris* *Q. faginea*	88.6± 20.7 56.8± 9.8	11.0± 1.4 8.9± 2.5

3	40.66330164	-2.278531408	1228	SW	20	1.02	Multifunctional	*P. nigra* *Q. faginea*	118.0± 12.4 79.2± 11.3	12.4± 1.4 12.0± 2.6
6	40.66365811	-2.280742957	1306	NE	30	1.13	Multifunctional	*P. nigra* *Q. faginea*	113.2± 10.2 79.2± 7.5	12.9± 1.9 10.9± 2.7
8	40.66742444	-2.288461666	1207	SW	20	1.08	Multifunctional	*P. nigra* *Q. faginea*	119.2± 16.1 49.4± 15.5	14.4± 3.4 10.0± 1.4
14	40.77777338	-2.329420901	999	W	20	2.27	Multifunctional	*P. nigra* *Q. ilex*	103.2± 56 48.4± 16.3	12.0± 4.7 5.8± 1
16	40.78227813	-2.330269832	1032	NW	30	1.85	Multifunctional	*P. nigra* *Q. ilex*	91.6± 27.1 48.4± 19.1	13.2± 3.3 6.7± 1
36	40.81397776	-2.217555655	1211	S	30	1.46	Multifunctional	*P. nigra* *Q. ilex*	77.4± 37.1 45.4± 7.8	8.7± 2.2 5.8± 1.1
24	40.67891682	-1.949361418	1377	SW	50	1.72	Mixture-4	*P. nigra* *P. sylvestris* *Q. faginea* *Q. ilex*	105.8± 29.6 127.6± 24.1 60.8± 13.3 76.6± 13.1	13.6± 2.2 14.7± 1.7 10.1± 1.5 9.0± 0.9
26	40.677634	-1.949266987	1387	N	30	1.88	Mixture-4	*P. nigra* *P. sylvestris* *Q. faginea* *Q. ilex*	130.0± 42.3 128.2± 26 59.6± 15.2 87.2± 16.7	14.2± 2.5 16.8± 1.6 10.8± 1.4 9.1± 1.8
29	40.67299394	-1.929263151	1354	SE	30	2.1	Mixture-4	*P. nigra* *P. sylvestris* *Q. faginea* *Q. ilex*	124.4± 24 126.5± 38.9 44.6± 16.8 61.4± 21.8	13.8± 1.8 14.9± 0.4 6.3± 0.9 6.7± 1.7

Table S4.2: Statistical output of the mixed linear models where season (i.e., Spring, Summer, Fall), year (i.e., 2021 and 2022) and species diversity referred as the factor Mixture (i.e., monospecific, monofunctional, multifunctional, and four-species mixture) were used as fixed effects, and plots were used as random effects for *P. nigra, P. sylvestris, Q. faginea,* and *Q. ilex* (*0.05≥P>0.01; **0.01≥P>0.001; ***P≥0.001).

		P. nigra	*P. sylvestris*	*Q. faginea*	*Q. ilex*
Ψ_{pd}	Season	< 0,001***	< 0,001***	< 0,001***	< 0,001***
	Year	< 0,001***	< 0,001***	< 0,001***	< 0,001***
	Mixture	0,0124*	<0,001***	0,0191*	0,0205*
	Season:Year	<0,001***	<0,001***	<0,001***	<0,001***
	Season:Mixture	0,004**	0,0013**	<0,001***	<0,001***
	Year:Mixture	<0,001***	<0,001***	<0,001***	<0,001***
Ψ_{md}	Season	< 0,001***	< 0,001***	< 0,001***	< 0,001***
	Year	< 0,001***	< 0,001***	< 0,001***	< 0,001***
	Mixture	0,0266*	0,0027**	0,0012**	0,0317*
	Season:Year	<0,001***	<0,001***	<0,001***	<0,001***
	Season:Mixture	<0,001***	<0,001***	<0,001***	<0,001***
	Year:Mixture	<0,001***	<0,001***	<0,001***	<0,001***
$\Delta\psi$	Season	<0,001***	<0,001***	<0,001***	<0,001***
	Year	0,0023**	<0,001***	0,7819	<0,001***
	Mixture	0,007**	0,0126*	0,0268*	0,2127
	Season:Year	<0,001***	<0,001***	<0,001***	<0,001***
	Season:Mixture	<0,001***	<0,001***	<0,001***	<0,001***
	Year:Mixture	<0,001***	0,0331*	0,0213*	<0,001***
g_s	Season	<0,001***	<0,001***	<0,001***	<0,001***
	Year	<0,001***	<0,001***	0,0059**	0,5155
	Mixture	0,0685	<0,001***	0,0175*	0,0188*
	Season:Year	<0,001***	<0,001***	0,5941	<0,001***
	Season:Mixture	0,0533	0,8269	<0,001***	0,0056**
	Year:Mixture	0,0888	<0,001***	0,0247*	0,004**
A_{net}	Season	<0,001***	<0,001***	<0,001***	<0,001***
	Year	<0,001***	<0,001***	0,0101*	0,9499
	Mixture	0,0169*	<0,001***	0,0053**	0,0196*
	Season:Year	<0,001***	<0,001***	<0,001***	<0,001***
	Season:Mixture	0,0067**	0,8486	<0,001***	<0,001***
	Year:Mixture	0,001**	<0,001***	0,007**	0,1566
$\delta^{18}O$	Season	<0,001***	0,0128*	<0,001***	<0,001***
	Year	0,0353*	<0,001***	<0,001***	<0,001***
	Mixture	0,3081	0,003**	0,2593	0,7649
	Season:Year	0,0039**	<0,001***	0,0415*	0,1226
	Season:Mixture	<0,001***	<0,001***	<0,001***	<0,001***
	Year:Mixture	0,2179	0,7428	0,0024**	<0,001***
$\delta^{2}H$	Season	<0,001***	<0,001***	<0,001***	<0,001***
	Year	<0,001***	<0,001***	<0,001***	<0,001***
	Mixture	0,768	0,0587	0,0135*	0,46
	Season:Year	<0,001***	<0,001***	<0,001***	<0,001***
	Season:Mixture	<0,001***	<0,001***	<0,001***	<0,001***
	Year:Mixture	0,2232	0,3971	0,2027	<0,001***

Table S4.3: Statistical output of the mixed linear models where season (i.e., Spring, Summer, Fall), year (i.e., 2021 and 2022) and species diversity referred as the factor Mixture (i.e., monospecific, and four-species mixture) were used as fixed effects, and plots were used as random effects for the contribution to xylem water of each water source: shallow (i.e., 0-20 cm), deep (i.e., 20-40 cm) and water stored in the fractured bedrock (i.e., bedrock) for *P. nigra, P. sylvestris, Q. faginea,* and *Q. ilex* (*0.05≥P>0.01; **0.01≥P>0.001; ***P≥0.001).

		P. nigra	*P. sylvestris*	*Q. faginea*	*Q. ilex*
Shallow	Season	0,0015**	0,001**	< 0,001***	< 0,001***
	Year	0,086	0,0379*	0,1452	< 0,001***
	Mixture	0,3541	0,6684	0,0273*	0,6352
	Season:Year	0,0296*	0,1629	<0,001***	<0,001***
	Season:Mixture	0,5856	0,3972	0,2357	0,3430
	Year:Mixture	0,0805	0,6096	0,4338	0,1985
Deep	Season	0,1309	0,0265*	0,0379*	0,0746
	Year	0,0497*	0,0066**	< 0,001***	0,0023**
	Mixture	0,7155	0,9159	0,3258	0,2654
	Season:Year	0,2276	0,3619	0,5931	0,3976
	Season:Mixture	0,4867	0,865	0,0113*	0,6509
	Year:Mixture	0,2998	0,9125	0,1079	0,4826
Bedrock	Season	0,4334	0,9316	<0,001***	0,0188*
	Year	0,2113	0,032*	0,0011**	0,1196
	Mixture	0,4635	0,3943	0,1026	0,5215
	Season:Year	0,9496	0,8134	0,1867	0,0614
	Season:Mixture	0,1017	0,1797	0,0171*	0,5784
	Year:Mixture	0,979	0,7395	0,0031**	0,6117

Chapter 5

General discussion

Mixing functionally contrasting tree species has the potential to mitigate the adverse effect of drought on tree water relations and water dynamics, which could ultimately delay the onset of hydraulic failure and reduce the global tree mortality phenomenon. Throughout my work, I investigated the effect of tree species diversity on tree hydraulic acclimation to drought and heat at the leaf (**Chapter 2 & Chapter 4**), stem (**Chapter 3**), and in belowground (**Chapter 4**) compartments under chronic drought in open-top chambers and during summer droughts in natural dry forests. I compared the physiological responses to drought and heat in monospecific and mixtures of two or four functionally contrasting tree species from European forests. Overall, I investigated six tree species from different functional groups (conifer and broadleaves) ranked from drought-sensitive to drought-tolerant in the following order (using their isohydricity): *Pinus sylvestris, Pinus nigra*, *Fagus sylvatica*, *Quercus pubescens*, *Quercus faginea*, and *Quercus ilex*. These tree species are widespread in Europe and the Mediterranean basin with for instance *P. sylvestris* covering a range from Spain to Russia, making them prime targets for forest management and conservation options (San-Miguel-Ayanz et al., 2016). In the following parts, I will first discuss the functional diversity of hydraulic traits that I observed in European forests. Then, I will discuss how mixing these functionally contrasting tree species affects their water dynamics under drier and warmer conditions.

5.1 Functional diversity in water relations and responses to drought and heat

Each tree species is characterized by a unique set of functional traits that classify them into functional groups and induce specific responses to drier and warmer conditions. The combination of functionally contrasting species drives the community structure and dynamic during extreme events as numerous studies highlighted the predominance of functional diversity over species richness per se on ecosystem functioning (Díaz & Cabido, 2001)*. Hence, before discussing the effect of species diversity and interactions on forest drought vulnerability, I will describe the diversity of water-related functional traits and responses to heat and drought found in European tree species.*

European tree species display a large variety of hydraulic traits driving whole-tree water dynamics under drier and warmer conditions from root water uptake to leaf evaporation. Belowground, the maximum water uptake depth depend on a combination of the soil structure, depth, and the species-specific rooting system (Canadell et al., 1996; Dawson et al., 2020; Schenk & Jackson, 2005). In my work, I observed that water uptake was highly variable between interacting

species in natural forests, ranging from 10 cm to more than 40 cm during the driest conditions (**Chapter 4**), suggesting important diversity in water sources. Moreover, I observed that while pines (*P. nigra* & *P. sylvestris*) and oaks (*Q. faginea* & *Q. ilex*) shifted their water uptake depth as the soil dried out during the summer, the pines' shallow rooting system more strongly limited the accessibility to deep soil layers compared to deep-rooted oaks (**Chapter 4**), leading to a clearer belowground water source partitioning during drought.

However, shallower roots also suggests higher drought vulnerability in pines. Indeed, Kahmen et al. (2022) confirmed that a shallower rooting system in temperate European forests was directly linked to higher drought vulnerability, resulting in stronger stomatal regulation to avoid excessive water loss as drought stress increased (i.e., low water potential at predawn; Ψ_{pd}). Hence, pines close their stomata as soon as drought intensity increases (i.e., isohydric behaviors), leading to limited water loss at the expense of reduced carbon assimilation (Lévesque et al., 2014; Martínez-Sancho et al., 2017). In contrast, beech (not accessed in this work but shown in Meier et al., 2018) and oak trees that potentially access more abundant and deeper water sources maintain their water uptake and use for a longer time during drought (i.e., anisohydric), resulting in higher water consumption (Leuschner et al., 2019; Yi et al., 2017, Fig. 5.1). Such disparity in stomatal behaviors between conifers and broadleaves appeared during the summer drought in natural dry forests where *P. sylvestris* did not reach water potential at midday (Ψ_{md}) lower than -2.5 MPa, whereas *Q. ilex* exhibited Ψ_{md} at -4 MPa at the driest time point (**Chapter 4**). However, while pines (i.e., *P. nigra* and *P. sylvestris*) and oaks (i.e., *Q. pubescens, Q. ilex, Q. faginea*) presented clear iso *vs*. anisohydric stomatal behaviors, as widely observed previously in temperate and Mediterranean forests (e.g., Aguadé et al., 2015; Backes & Leuschner, 2000; Roman et al., 2015), *F. sylvatica* experienced higher reduction in stomatal conductance (g_s) compared to oaks species (**Chapter 2**, Fig. 5.1). Indeed, Leuschner et al. (2022) described *F. sylvatica* as strictly anisohydric but still less drought tolerant than oak species (Meyer et al., 2020), pointing out the wide range of drought tolerance and water use strategies between conifers and broadleaves, but also within broadleaves, in European forests (Klein, 2014; Martínez-Vilalta et al., 2014).

Moreover, European trees species differed largely in their leaf allometry depending of the functional group (needle *vs*. leaves) with specific leaf area (SLA) 75% smaller for *P. nigra* compared to *F. sylvatica*. In addition, I observed a strong correlation between SLA and drought tolerance for broadleaves across all my studies. Overall, SLA varied between 176 $cm^2\ g^{-1}$ and 53 $cm^2\ g^{-1}$ for *F. sylvatica* and *Q. ilex*, respectively, highlighting the large variability in leaf structure between the studied broadleaved species (Fig. 5.1). As previously observed in response to drier conditions (e.g., Martin-Stpaul et al., 2013; Valladares & Sánchez-Gómez, 2006), I found consistently smaller and thicker leaves for tree species from more arid climates (**Chapters 2 & 3**; Fig. 5.1). This large diversity in leaf structure can help characterize species tolerance to drought and point out species that may be at higher risk of mortality. For instance, the large and thin leaves of *F. sylvatica* with

high stomatal sensitivity to drought and high minimum stomatal conductance (g_{min}) (**Chapter 2**) could lead to higher risk of drought-induced mortality, especially on shallow soils with limited water retention capacity (Klesse et al., 2022; Leuschner, 2020). Similarly, oak species with their anisohydric behaviors (Forner et al., 2018) and large canopy (**Chapter 2**) maintained larger hydraulic conductivity during summer droughts at the risk of accumulating cavitation events leading to higher mortality risk (i.e., narrower hydraulic safety margin; HSM) (**Chapter 3**, Choat et al., 2012; Greenwood et al., 2017). On the contrary, by limiting the water loss through the needles during drought via reduced g_s and SLA, pines have a smaller stem hydraulic conductivity but also a smaller risk of wood cavitation (i.e., large HSM) (**Chapter 3**).

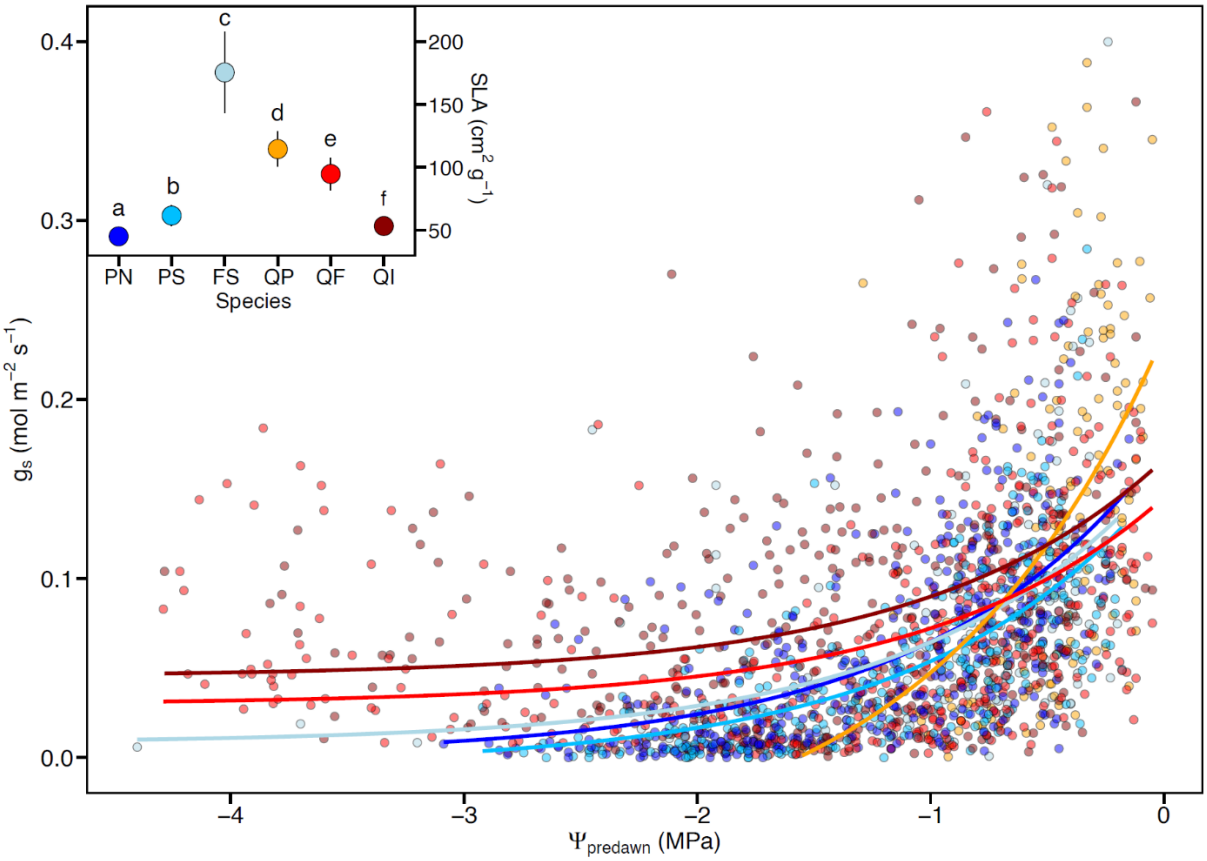

Figure 5.1: Relationships between the light-saturated stomatal conductance (g_s) and the leaf water potential at predawn (Ψ_{pd}) for *P. nigra* (PN; dark blue), *P. sylvestris* (PS; medium blue), *F. sylvatica* (FS; light blue), *Q. pubescent* (QP; orange), *Q. faginea* (QF; red), and *Q. ilex* (QI; dark red). Lines represent the exponential regressions with solid lines standing for significant relationships within given species and across all species richness and climatic treatments. The captions in the upper left corners represent the mean specific leaf area (SLA) for each species for all species richness and years (i.e., 2020, 2021, 2022, mean ± sd). Letters denote significant differences between species.

In addition, trees can acclimate their traits to better tolerate changing environmental conditions, thereby potentially broadening the diversity of functional strategies found in forests during extreme events. For instance, tree species can modulate their water potential at turgor loss point (Ψ_{TLP}) over the growing season (e.g., Bartlett et al., 2014; Serrano et al., 2005) or during chronic drought exposure (e.g., **Chapter 2**, Binks et al., 2016; Deligoz & Gur, 2015). In my work, I also found large variability in Ψ_{TLP} varying from control and hot drought conditions by 27% and 30% for *F. sylvatica* and *Q. pubescens*, respectively (**Chapter 2**). However, while most of the previous studies observed consistently low Ψ_{TLP} in arid conditions (e.g., Kunert et al., 2021; Zhu et al., 2018), I measured for oak and beech higher $\Psi_{TLP,}$ suggesting a shift to more conservative behaviors that could extend the stomatal safety margin, protect the xylem from cavitation, and potentially delay hydraulic failure (Martin-StPaul et al., 2017). Moreover, I also observed a strong acclimation in canopy size with a reduction by 59% and 74% for *F. sylvatica* and *Q. pubescens* in response to hot drought, in addition to decreased stomatal conductance (and hence total water use), which further broadened the range of water use strategies during drier conditions (**Chapter 2**).

Overall, these findings place the leaf water relations as key elements that modulate species drought resistance. Although I did not measure the vulnerability to xylem cavitation, i.e., defined as the water potential at 50% hydraulic conductance loss (P_{50}), in my studies, I observed low variability in P_{50} between species in the database extracted from Choat et al. (2012) with values ranking from -2.8 MPa for *P. nigra* to -3.9 MPa for *Q. faginea*. This highlights that even if leaf-level traits varied largely among the studied species, vulnerability to cavitation did not. Hence, even if P_{50} is a key hydraulic trait, widely used to describe tree drought vulnerability and diversity (Choat et al., 2012; Delzon & Cochard, 2014), it seems to be less relevant than the leaf water-relations such as LA and Ψ_{TLP}. Indeed, Rowland et al., (2023) concluded from a global data analysis that P_{50} shifted from a maximum of 1 MPa in response to drought, which could potentially not be enough to protect against severe hydraulic impairments. Rosas et al. (2019) further found that tree adjustments to drier conditions relied more on leaf adjustments through lower Ψ_{TLP} than the xylem safety with lower P_{50}. Furthermore, increasing air temperature enhances the evaporative demand due to higher VPD, which could ultimately cause numerous hydraulic impairments at the leaf and stem levels. Although, during my experiment, I didn't observe the direct effect of heat acting alone on the measured water-related traits (g_s, g_{min}, Ψ_{TLP}), probably due to the limited increase in mean VPD by 1KPa, Schönbeck et al. (2022) observed reduction of g_{min} and higher cavitation events due to increased VPD by 2.5 KPa on the same species. Hence, future work should focus especially on the diversity in leaf hydraulic traits, and how they may be driving the vulnerability of species to a worsening of drought events with global warming.

Key finding: European tree species have a large spectrum of water-related physiological traits, leading to a gradient of vulnerability to drought. In addition, I showed that acclimation to drought and heat can broaden this functional diversity even further. Furthermore, leaf hydraulic traits are also important indicators of the drought tolerance and mortality risks of species. My work showed that the leaf area and stomatal behavior are main drivers of drought-induced hydraulic impairments in European forests and may provide stronger indicators of mortality risks than P_{50}. This is particularly important for future work as the increasing VPD resulting from higher temperatures could exacerbate canopy water loss and tree mortality risk during drought. Hence, my work suggests that the warming-induced worsening of drought could potentially lead to the decline of the widely distributed European tree species such as *F. sylvatica* or *P. sylvestris*, which showed not only low drought tolerance but also limited acclimation potential.

5.2 Species diversity effect on tree water dynamics and tree tolerance to drier and warmer conditions

The combination of diverse tree species with contrasting functional traits has the potential to affect forest ecosystem dynamics due to positive but also negative species interactions. Numerous studies, mainly on grasslands, observed strong beneficial effects of increasing functional diversity on ecosystem functions and services, including multifunctionality (Hong et al., 2022; Manning et al., 2018), revealing that biodiversity is a key factor for ecosystem conservation and stability (Ampoorter et al., 2020). Hence, mixing functionally contrasting tree species has been widely advocated as a climate-smart forest management practice that could help alleviate the adverse effects of extreme droughts in forests. In the following section, I will discuss how mixing European tree species could modulate their in-situ water dynamics and tolerance to drier and warmer conditions.

In my work, I found mainly adverse effects of mixing tree species (on leaf and xylem functions) during chronic drought exposure and natural seasonal summer droughts. This observation contradicts the breath of work pointing to positive effects of functional diversity on forest drought resistance (e.g., Liu et al., 2022; Pretzsch et al., 2013). However, contrary to my work, most studies have focused largely on wood production and stem hydraulic traits until now (e.g., productivity, P_{50}, wood density) when assessing diversity effects (e.g., Anderegg et al., 2018; Liang et al., 2016). Indeed, I observed that when rather drought-sensitive pines (*P. nigra* and *P. sylvestris*) and *F. sylvatica* interacted with more drought-tolerant oaks (*Q. ilex*, *Q. faginea*, and *Q. pubescens*) under drier soil conditions, they experienced stronger drought stress (i.e., lower Ψ_{pd}) and tighter stomatal regulation (i.e., lower reduction in g_s) compared to their monocultures (**Chapters 2 & 4**, Fig. 5.2). However, these responses were not necessarily accompanied by lesser drought impacts for the other interacting species. Following the increasing xylem tension in more diverse stands, the xylem-specific hydraulic conductance (K_S) decreased more strongly in mixed compared to monospecific stands due to more frequent cavitation events for all species. Among other adverse consequences, this could lead to increasing mortality risk in mixed stands during drought (**Chapters 2 & 3**). Indeed, I observed advanced hydraulic failure for *F. sylvatica* mixed with oak when drought-induced mortality was simulated with the SurEau model (**Chapter 2**). The same pattern was observed by Searle et al. (2022) who found higher mortality risk in diverse temperate forests due to higher stem density and productivity. However, it is important to point out that in arid climates, none of the Mediterranean tree species, except *Q. faginea* in monospecific stands, were close to their critical mortality thresholds all along the growing season (i.e., positive HSM), revealing a large operational range of coping with water stress regardless of species strategy (i.e., iso-anisohydric) or species interactions (**Chapter 3,** Forner et al., 2018).

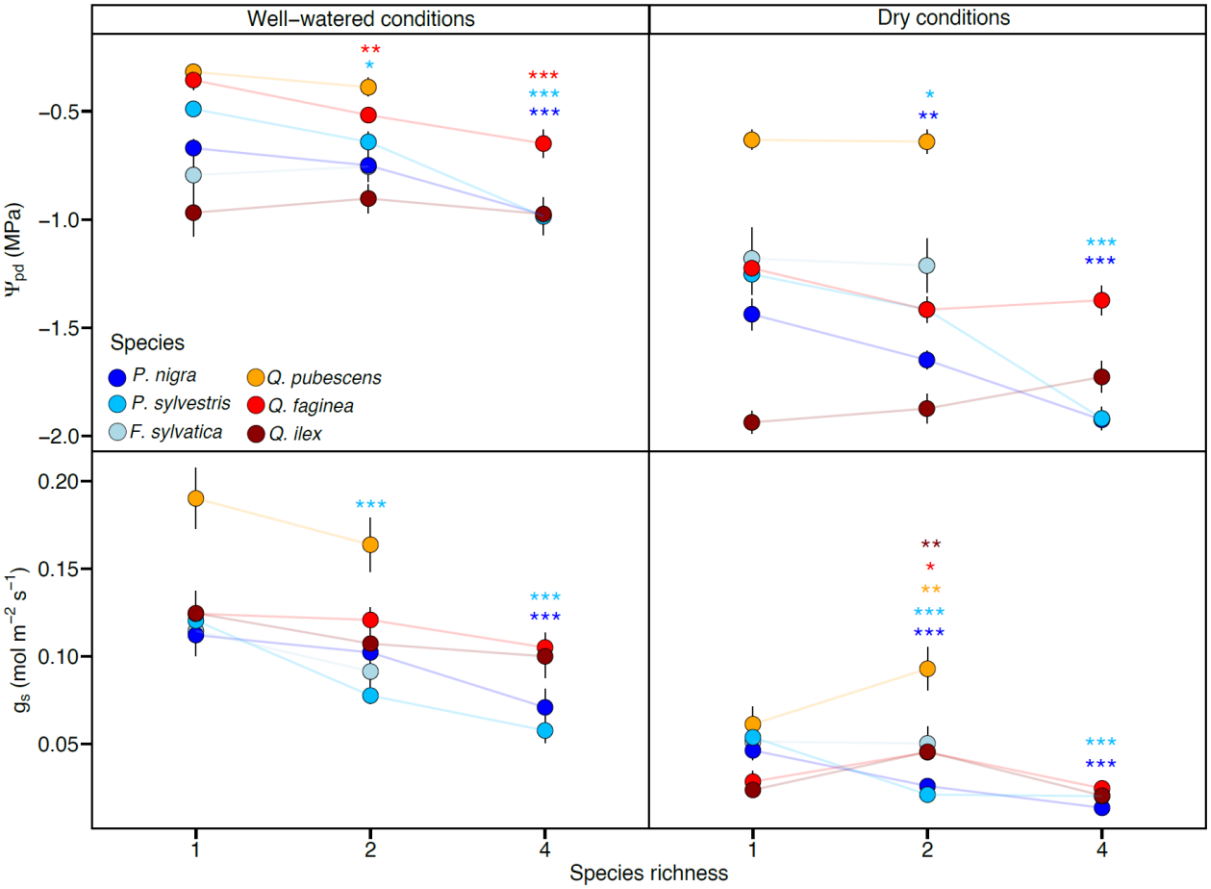

Figure 5.2: Mean (±SE) leaf water potential at predawn (Ψ_{pd}) and light-saturated stomatal conductance (g_s) for each species richness levels (i.e., 1, 2, 4) for *P. nigra* (dark blue), *P. sylvestris* (medium blue), *F. sylvatica* (light blue), *Q. pubescens* (orange), *Q. faginea* (red), and *Q. ilex* (dark red) in well-watered conditions (i.e., control and heating treatments in the open-chamber experiment, and Spring for natural forests) and dry conditions (i.e., drought and hot drought treatments, and Summer) for all years (i.e., 2020, 2021, 2022). Letters denote significant differences with the monospecific stands (i.e., species richness 1) for each species.

Nevertheless, my work highlighted still the occurrence of positive belowground species interactions mechanisms in more diverse forests. Indeed, I observed a strong belowground water source partitioning as the soil dried out in summer in mixed forests due to pines taking up water from shallower water sources than oaks. This reduction in water competition resulted in a slight increase in g_s for the oaks in mixtures of two species under dry conditions (Fig. 5.2). However, the apparent positive species interaction mechanism was not enough to overcome the adverse effects of drought on aboveground tree water relations for the more drought-sensitive species (**Chapter 4,** Fig. 5.2). Similarly, del Castillo et al. (2016) explained higher drought stress for pines compared to oaks in Mediterranean pine-oak mixed forests because of pine roots being limited to the upper soil layers that evaporate faster during drought. These findings highlight that belowground niche partitioning, although it may play an essential role in temperate forest drought tolerance (e.g., Weides et al., 2023), is insignificant when soil drought becomes too intense, probably due to niche

overlapping caused by a shift in water sources to deeper soils (Rodríguez-Robles et al., 2020). This is why in the same Mediterranean forests, Jucker et al. (2014) found larger crowns for pines due to improved water accessibility when mixed with oaks under well-watered conditions. However, during very dry years, pine's productivity declined more strongly in mixed than monospecific stands, confirming the limitation of niche partitioning to overcome drought stress. This shift in species diversity effect depending on the environmental conditions is following the "stress-gradient hypothesis" that states that under mild stress, facilitation and niche partitioning processes should increase plant tolerance but when conditions get too extreme, positive interactions between species may change to increasing competition for resources (Haberstroh & Werner, 2022; Michalet et al., 2014; Ratcliffe et al., 2017).

Overall, while I observed mainly adverse effects of species diversity on leaf and wood hydraulic traits for all species, those were consistently exacerbated for the most drought-sensitive species (i.e., *P. nigra*, *P. sylvestris*, and *F. sylvatica*) in European forests (Fig. 5.2). These results were confirmed by previous studies in Mediterranean and temperate forests that observed negative or neutral diversity effects on drought resistance or productivity, especially for the most drought-sensitive species (e.g., Aguadé et al., 2015; Bonal et al., 2017; Grossiord et al., 2014). The potential drivers of these diversity effects could be related to the differences in canopy size, isohydric strategy (i.e., iso *vs*. anisohydric behaviors), and maximum rooting depth, highlighting the importance of considering the physiological characteristics of the interacting species rather than the species richness *per se* (Forrester et al., 2016; Gillerot et al., 2021). Aboveground, trees with larger canopy and more tolerant to soil moisture reductions would exhaust faster the belowground water resources, even if the different rooting systems between species lead to water source partitioning. As a result, the unbalanced consumption of water and limitation to shallow soil layers more prone to evaporation lead to a general impairment of the most drought-sensitive species in mixed forests. These findings support the general shift from drought-sensitive to more drought-tolerant tree species in forest communities as observed in European dry forests where pines are slowly replaced by oaks in the understory (Wohlgemuth et al., 2018) or in temperate forests where oaks overtake beech (Rubio-Cuadrado et al., 2018). Hence, species at their dry limit of distribution like *P. sylvestris* in Spain (Durrant et al., 2016) are more sensitive to soil water deficit (Lévesque et al., 2013) and could be slowly replaced by more drought-adapted species, resulting in a general decline of the local maladapted species, and potentially of tree species diversity.

Key findings: Overall, tree species diversity has mainly a negative effect on individual tree water dynamics and tolerance during drought for all interacting species. However, these adverse effects were exacerbated for the most drought-sensitive tree species, resulting in their potential decline over the long-term. In my work, I further observed that the local environment but also the species-specific leaf area, water use rates, stomatal behaviors, and maximum rooting depths are the principal drivers of tree competitiveness and species interactions in forests subjected to drought. Indeed, tree species with higher leaf areas, transpiration rates, and deeper roots, exhaust water resources more rapidly in mixtures, thereby enhancing drought stress for the other species but not necessarily at their own benefit. Hence, although mixing contrasting tree species bring numerous positive effects for forest ecosystems, the warming-induced worsening of drought will not be offset by only favoring more diverse forests in Europe.

General conclusions & Perspectives

Improving the tolerance of European forests to climate-change is necessary to maintain all the vital functions and services they provide (Manning et al., 2018). Mixing tree species with contrasting functional traits was often described as an ideal solution to improve forest drought resistance (e.g., Grossiord, 2020). With my thesis, I improved our knowledge on the importance of tree species diversity in forests, and the underlying mechanisms driving diversity effects.

European trees exhibited a large range of leaf-, stem- and root-level strategies to cope with drier and warmer conditions from rather drought-sensitive species (i.e., *P. nigra*, *P. sylvestris*, and *F. sylvatica*) to more drought-tolerant ones (i.e., *Q. pubescens*, *Q. ilex*, and *Q. faginea*). This wide range of drought tolerance and physiological traits suggested a high potential for beneficial diversity effects during extreme events. Yet, under natural seasonal droughts and chronic experimental drought, I observed that mixing functionally contrasting species tended to enhance the drought stress for all species, especially for the most drought-sensitive tree species. Hence, the species-specific drought vulnerability and species diversity effects seem intrinsically related and could result in a potential decline of the most drought-sensitive species in mixed forests. Moreover, I observed that the drought vulnerability and diversity effects were mainly driven by specific traits of the interacting species, including species-specific evaporative surface and total leaf area, the water use strategy that is determined by species-specific stomatal behaviors, the maximum rooting depth, and the local environmental conditions (dry *vs*. wet conditions). Variability in these functional traits further highlighted the vulnerability to climate change and higher mortality risk of widely distributed and iconic European tree species such as *P. sylvestris* and *F. sylvatica*, inducing potential future massive changes in forest structure, composition, and diversity.

Nevertheless, although this work demonstrated that mixing contrasting tree species will not always improve forest drought resistance, it is important to point out that biodiversity can support multiple ecosystem services (Ampoorter et al., 2020; Messier et al., 2022). Moreover, the importance of diversity should highly depend on ontogeny, species characteristics, and other environmental conditions not assessed in this work (Kambach et al., 2019). Further investigations in different climates, species richness levels, and species compositions are necessary to improve predictions on forest dynamics under future climate. This includes assessing also other potential mechanisms of diversity effects such as the facilitation processes that may arise in more diverse forests and affect the canopy microclimate by mitigating effects of high VPD. Multiple studies have pointed out the rising role of VPD and high temperature in driving future forest dynamics (e.g., De Frenne et al., 2021; Zhang et al., 2022). Hence, mitigating these impacts will likely be dependent on environmental conditions in forests canopies.

References

Aguadé, D., Poyatos, R., Rosas, T., & Martínez-Vilalta, J. (2015). Comparative drought responses of Quercus ilex L. and Pinus sylvestris L. In a montane forest undergoing a vegetation shift. *Forests*, *6*(8), 2505–2529. https://doi.org/10.3390/f6082505

Aguirre, B. A., Hsieh, B., Watson, S. J., & Wright, A. J. (2021). The experimental manipulation of atmospheric drought: Teasing out the role of microclimate in biodiversity experiments. *Journal of Ecology*, *109*(5), 1986–1999. https://doi.org/10.1111/1365-2745.13595

Alonso-Forn, D., Peguero-Pina, J. J., Ferrio, J. P., Mencuccini, M., Mendoza-Herrer, Ó., Sancho-Knapik, D., & Gil-Pelegrín, E. (2021). Contrasting functional strategies following severe drought in two Mediterranean oaks with different leaf habit: Quercus faginea and Quercus ilex subsp. rotundifolia. *Tree Physiology*, *41*(3), 371–387. https://doi.org/10.1093/treephys/tpaa135

Ameye, M., Wertin, T. M., Bauweraerts, I., McGuire, M. A., Teskey, R. O., & Steppe, K. (2012). The effect of induced heat waves on Pinus taeda and quercus rubra seedlings in ambient and elevated co2 atmospheres. *New Phytologist*, *196*(2), 448–461. https://doi.org/10.1111/j.1469-8137.2012.04267.x

Ampoorter, E., Barbaro, L., Jactel, H., Baeten, L., Boberg, J., Carnol, M., Castagneyrol, B., Charbonnier, Y., Dawud, S. M., Deconchat, M., Smedt, P. De, Wandeler, H. De, Guyot, V., Hättenschwiler, S., Joly, F. X., Koricheva, J., Milligan, H., Muys, B., Nguyen, D., … Allan, E. (2020). Tree diversity is key for promoting the diversity and abundance of forest-associated taxa in Europe. *Oikos*, *129*(2), 133–146. https://doi.org/10.1111/oik.06290

Anderegg, W. R. L., Anderegg, L. D. L., Kerr, K. L., & Trugman, A. T. (2019). Widespread drought-induced tree mortality at dry range edges indicates that climate stress exceeds species' compensating mechanisms. *Global Change Biology*, *25*(11), 3793–3802. https://doi.org/10.1111/gcb.14771

Anderegg, W. R. L., Klein, T., Bartlett, M., Sack, L., Pellegrini, A. F. A., Choat, B., & Jansen, S. (2016). Meta-analysis reveals that hydraulic traits explain cross-species patterns of drought-induced tree mortality across the globe. *Proceedings of the National Academy of Sciences of the United States of America*, *113*(18), 5024–5029. https://doi.org/10.1073/pnas.1525678113

Anderegg, W. R. L., Konings, A. G., Trugman, A. T., Yu, K., Bowling, D. R., Gabbitas, R., Karp, D. S., Pacala, S., Sperry, J. S., Sulman, B. N., & Zenes, N. (2018). Hydraulic diversity of forests regulates ecosystem resilience during drought. *Nature*, *561*(7724), 538–541. https://doi.org/10.1038/s41586-018-0539-7

Andivia, E., Madrigal-González, J., Villar-Salvador, P., & Zavala, M. A. (2018). Do adult trees increase conspecific juvenile resilience to recurrent droughts? Implications for forest regeneration. *Ecosphere*, *9*(6). https://doi.org/10.1002/ecs2.2282

Andrews, S. F., Flanagan, L. B., Sharp, E. J., & Cai, T. (2012). Variation in water potential, hydraulic characteristics and water source use in montane Douglas-fir and lodgepole pine trees in southwestern Alberta and consequences for seasonal changes in photosynthetic capacity. *Tree Physiology*, *32*(2), 146–160. https://doi.org/10.1093/treephys/tpr136

Archaux, F., & Wolters, V. (2006). Impact of summer drought on forest biodiversity: What do we know? *Annals of*

Forest Science, *63*(6), 645–652. https://doi.org/10.1051/forest:2006041

Arend, M., Brem, A., Kuster, T. M., & Günthardt-Goerg, M. S. (2013). Seasonal photosynthetic responses of European oaks to drought and elevated daytime temperature. *Plant Biology*, *15*(SUPPL.1), 169–176. https://doi.org/10.1111/j.1438-8677.2012.00625.x

Aschmann, H. (1984). A restrictive definition of mediterranean climates. *Bulletin de La Societe Botanique de France. Actualites Botaniques*, *131*(2–4), 21–30. https://doi.org/10.1080/01811789.1984.10826643

Backes, K., & Leuschner, C. (2000). Leaf water relations of competitive Fagus sylvatica and Quercus petraea trees during 4 years differing in soil drought. *Canadian Journal of Forest Research*, *30*(3), 335–346. https://doi.org/10.1139/cjfr-30-3-335

Baeten, L., Verheyen, K., Wirth, C., Bruelheide, H., Bussotti, F., Finér, L., Jaroszewicz, B., Selvi, F., Valladares, F., Allan, E., Ampoorter, E., Auge, H., Avăcăriei, D., Barbaro, L., Bărnoaiea, I., Bastias, C. C., Bauhus, J., Beinhoff, C., Benavides, R., … Scherer-Lorenzen, M. (2013). A novel comparative research platform designed to determine the functional significance of tree species diversity in European forests. *Perspectives in Plant Ecology, Evolution and Systematics*, *15*(5), 281–291. https://doi.org/10.1016/j.ppees.2013.07.002

Barbeta, A., Burlett, R., Martín-Gómez, P., Fréjaville, B., Devert, N., Wingate, L., Domec, J., & Ogée, J. (2021). Evidence for distinct isotopic compositions of sap and tissue water in tree stems: consequences for plant water source identification. *New Phytologist*. https://doi.org/10.1111/nph.17857

Barbeta, A., Mejía-Chang, M., Ogaya, R., Voltas, J., Dawson, T. E., & Peñuelas, J. (2015). The combined effects of a long-term experimental drought and an extreme drought on the use of plant-water sources in a Mediterranean forest. *Global Change Biology*, *21*(3), 1213–1225. https://doi.org/10.1111/gcb.12785

Bartlett, M. K., Scoffoni, C., & Sack, L. (2012). The determinants of leaf turgor loss point and prediction of drought tolerance of species and biomes: A global meta-analysis. *Ecology Letters*, *15*(5), 393–405. https://doi.org/10.1111/j.1461-0248.2012.01751.x

Bartlett, M. K., Zhang, Y., Kreidler, N., Sun, S., Ardy, R., Cao, K., & Sack, L. (2014). Global analysis of plasticity in turgor loss point, a key drought tolerance trait. *Ecology Letters*, *17*(12), 1580–1590. https://doi.org/10.1111/ele.12374

Bello, J., Hasselquist, N. J., Vallet, P., Kahmen, A., Perot, T., & Korboulewsky, N. (2019). Complementary water uptake depth of Quercus petraea and Pinus sylvestris in mixed stands during an extreme drought. *Plant and Soil*, *437*(1–2), 93–115. https://doi.org/10.1007/s11104-019-03951-z

Binks, O., Meir, P., Rowland, L., da Costa, A. C. L., Vasconcelos, S. S., de Oliveira, A. A. R., Ferreira, L., Christoffersen, B., Nardini, A., & Mencuccini, M. (2016). Plasticity in leaf-level water relations of tropical rainforest trees in response to experimental drought. *The New Phytologist*, *211*(2), 477–488. https://doi.org/10.1111/nph.13927

Blackman, C. J. (2018). Leaf turgor loss as a predictor of plant drought response strategies. *Tree Physiology*, *38*(5), 655–657. https://doi.org/10.1093/treephys/tpy047

Bolte, A., Czajkowski, T., Cocozza, C., Tognetti, R., De Miguel, M., Pšidová, E., Ditmarová, L., Dinca, L., Delzon, S., Cochard, H., Ræbild, A., De Luis, M., Cvjetkovic, B., Heiri, C., & Müller, J. (2016). Desiccation and mortality dynamics in seedlings of different European beech (Fagus sylvatica L.) populations under extreme drought conditions. *Frontiers in Plant Science*, *7*(JUNE2016), 1–12. https://doi.org/10.3389/fpls.2016.00751

Bonal, D., Pau, M., Toigo, M., Granier, A., & Perot, T. (2017). Mixing oak and pine trees does not improve the functional response to severe drought in central French forests. *Annals of Forest Science*, *74*(4). https://doi.org/10.1007/s13595-017-0671-9

Bongers, F. J., Olmo, M., Lopez-Iglesias, B., Anten, N. P. R., & Villar, R. (2017). Drought responses, phenotypic plasticity and survival of Mediterranean species in two different microclimatic sites. *Plant Biology*, *19*(3), 386–395. https://doi.org/10.1111/plb.12544

Breshears, D. D., Cobb, N. S., Rich, P. M., Price, K. P., Allen, C. D., Balice, R. G., Romme, W. H., Kastens, J. H., Floyd, M. L., Belnap, J., Anderson, J. J., Myers, O. B., & Meyer, C. W. (2005). Regional vegetation die-off in response to global-change-type drought. *Proceedings of the National Academy of Sciences of the United States of America*, *102*(42), 15144–15148. https://doi.org/10.1073/pnas.0505734102

Brinkmann, N., Eugster, W., Buchmann, N., & Kahmen, A. (2019). Species-specific differences in water uptake depth of mature temperate trees vary with water availability in the soil. *Plant Biology*, *21*(1), 71–81. https://doi.org/10.1111/plb.12907

Brodribb, Tim J., & Holbrook, N. M. (2003). Stomatal closure during leaf dehydration, correlation with other leaf physiological traits. *Plant Physiology*, *132*(4), 2166–2173. https://doi.org/10.1104/pp.103.023879

Brodribb, Timothy J., Powers, J., Cochard, H., & Choat, B. (2020). Hanging by a thread? Forests and drought. *Science*, *368*(6488), 261–266. https://doi.org/10.1126/science.aat7631

Buckley, T. N., Sack, L., & Gilbert, M. E. (2011). The role of bundle sheath extensions and life form in stomatal responses to leaf water status. *Plant Physiology*, *156*(2), 962–973. https://doi.org/10.1104/pp.111.175638

Bussotti, F., Bottacci, A., Bartolesi, A., Grossoni, P., & Tani, C. (1995). Morpho-anatomical alterations in leaves collected from beech trees (Fagus sylvatica L.) in conditions of natural water stress. *Environmental and Experimental Botany*, *35*(2), 201–213. https://doi.org/10.1016/0098-8472(94)00040-C

Canadell, J., Jackson, R. B., Ehleringer, J. R., Mooney, H. A., Sala, O. E., & Schulze, E. D. (1996). Maximum rooting depth of vegetation types at the global scale. *Oecologia*, *108*(4), 583–595. https://doi.org/10.1007/BF00329030

Cavender-Bares, J., Sack, L., & Savage, J. (2007). Atmospheric and soil drought reduce nocturnal conductance in live oaks. *Tree Physiology*, *27*(4), 611–620. https://doi.org/10.1093/treephys/27.4.611

Čermák, J., Nadezhdina, N., Meiresonne, L., & Ceulemans, R. (2008). Scots pine root distribution derived from radial sap flow patterns in stems of large leaning trees. *Plant and Soil*, *305*(1–2), 61–75. https://doi.org/10.1007/s11104-007-9433-z

Choat, B., Brodribb, T. J., Brodersen, C. R., Duursma, R. A., López, R., & Medlyn, B. E. (2018). Triggers of tree mortality under drought. *Nature*, *558*(7711), 531–539. https://doi.org/10.1038/s41586-018-0240-x

Choat, B., Jansen, S., Brodribb, T. J., Cochard, H., Delzon, S., Bhaskar, R., Bucci, S. J., Feild, T. S., Gleason, S. M., Hacke, U. G., Jacobsen, A. L., Lens, F., Maherali, H., Martínez-Vilalta, J., Mayr, S., Mencuccini, M., Mitchell, P. J., Nardini, A., Pittermann, J., … Zanne, A. E. (2012). Global convergence in the vulnerability of forests to drought. *Nature*, *491*(7426), 752–755. https://doi.org/10.1038/nature11688

Cochard, H. (2006). Cavitation in trees. *Comptes Rendus Physique*, *7*(9–10), 1018–1026. https://doi.org/10.1016/j.crhy.2006.10.012

Cochard, H. (2021). A new mechanism for tree mortality due to drought and heatwaves. *Peer Community Journal*, *1*(e36). http://www.centre-mersenne.org/

Cochard, H., Pimont, F., Ruffault, J., & Martin-StPaul, N. (2021). SurEau: a mechanistic model of plant water relations under extreme drought. *Annals of Forest Science*, *78*(2), 55. https://doi.org/10.1007/s13595-021-01067-y

Corcuera, L., Camarero, J. J., & Gil-Pelegrín, E. (2004). Effects of a severe drought on Quercus ilex radial growth and xylem anatomy. *Trees - Structure and Function*, *18*(1), 83–92. https://doi.org/10.1007/s00468-003-0284-9

Corcuera, L., Cochard, H., Gil-Pelegrin, E., & Notivol, E. (2011). Phenotypic plasticity in mesic populations of Pinus pinaster improves resistance to xylem embolism (P50) under severe drought. *Trees - Structure and Function*, *25*(6), 1033–1042. https://doi.org/10.1007/s00468-011-0578-2

David, T S, Henriques, M. O., Nunes, J., Valente, F., Vaz, M., Pereira, J. S., Siegwolf, R., Chaves, M. M., Gazarini, L. C., & David, J. S. (2007). Water-use strategies in two co-occurring Mediterranean evergreen oaks : surviving the summer drought. *Tree Physiology*, *27*, 793–803.

David, Teresa S., Pinto, C. A., Nadezhdina, N., Kurz-Besson, C., Henriques, M. O., Quilhó, T., Cermak, J., Chaves, M. M., Pereira, J. S., & David, J. S. (2013). Root functioning, tree water use and hydraulic redistribution in Quercus suber trees: A modeling approach based on root sap flow. *Forest Ecology and Management*, *307*, 136–146. https://doi.org/10.1016/j.foreco.2013.07.012

Dawson, T. E., & Ehleringer, J. R. (1991). Streamside trees that do not use stream water. *Nature*, *350*, 335–337.

Dawson, T. E., Hahm, W. J., & Crutchfield-Peters, K. (2020). Digging deeper: what the critical zone perspective adds to the study of plant ecophysiology. *New Phytologist*, *226*(3), 666–671. https://doi.org/10.1111/nph.16410

De Frenne, P., Lenoir, J., Luoto, M., Scheffers, B. R., Zellweger, F., Aalto, J., Ashcroft, M. B., Christiansen, D. M., Decocq, G., De Pauw, K., Govaert, S., Greiser, C., Gril, E., Hampe, A., Jucker, T., Klinges, D. H., Koelemeijer, I. A., Lembrechts, J. J., Marrec, R., … Hylander, K. (2021). Forest microclimates and climate change: Importance, drivers and future research agenda. *Global Change Biology*, *27*(11), 2279–2297. https://doi.org/10.1111/gcb.15569

De Groote, S. R. E., Vanhellemont, M., Baeten, L., Van den Bulcke, J., Martel, A., Bonte, D., Lens, L., & Verheyen, K. (2018). Competition, tree age and size drive the productivity of mixed forests of pedunculate oak, beech and red oak. *Forest Ecology and Management*, *430*(July), 609–617. https://doi.org/10.1016/j.foreco.2018.08.050

del Castillo, J., Comas, C., Voltas, J., & Ferrio, J. P. (2016). Dynamics of competition over water in a mixed oak-pine Mediterranean forest: Spatio-temporal and physiological components. *Forest Ecology and Management*, *382*, 214–224. https://doi.org/10.1016/j.foreco.2016.10.025

Deligoz, A., & Gur, M. (2015). Morphological, physiological and biochemical responses to drought stress of Stone pine (Pinus pinea L.) seedlings. *Acta Physiologiae Plantarum*, *37*(11), 1–8. https://doi.org/10.1007/s11738-015-1998-1

DeLucia, E. H., Maherali, H., & Carey, E. V. (2000). Climate-driven changes in biomass allocation in pines. *Global Change Biology*, *6*(5), 587–593. https://doi.org/10.1046/j.1365-2486.2000.00338.x

Delzon, S., & Cochard, H. (2014). Recent advances in tree hydraulics highlight the ecological significance of the hydraulic safety margin. *New Phytologist*, *203*(2), 355–358. https://doi.org/10.1111/nph.12798

Delzon, S., Douthe, C., Sala, A., & Cochard, H. (2010). Mechanism of water-stress induced cavitation in conifers : bordered pit structure and function support the hypothesis of seal capillary-seeding. *Plant, Cell & Environment*, *33*, 2101–2111. https://doi.org/10.1111/j.1365-3040.2010.02208.x

Devi, S., Angrish, R., Madaan, S., Toky, O. P., & Arya, S. S. (2016). Sinker Root System in Trees with Emphasis on Soil Profile. In *Plant-Microbe Interaction: An Approach to Sustainable Agriculture* (pp. 463–474). Springer Singapore. https://doi.org/10.1007/978-981-10-2854-0_21

Diao, H., Schuler, P., Goldsmith, G. R., Siegwolf, R. T. W., Saurer, M., & Lehmann, M. M. (2022). Technical note: On uncertainties in plant water isotopic composition following extraction by cryogenic vacuum distillation. *Hydrology and Earth System Sciences*, *26*(22), 5835–5847. https://doi.org/10.5194/hess-26-5835-2022

Díaz, S., & Cabido, M. (2001). Vive la différence: Plant functional diversity matters to ecosystem processes. *Trends in Ecology and Evolution*, *16*(11), 646–655. https://doi.org/10.1016/S0169-5347(01)02283-2

Didion-Gency, M., Bachofen, C., Buchmann, N., Gessler, A., Morin, X., Vicente, E., Vollenweider, P., & Grossiord, C. (2021). Interactive effects of tree species mixture and climate on foliar and woody trait variation in a widely distributed deciduous tree. *Functional Ecology*, *35*(11), 2397–2408. https://doi.org/10.1111/1365-2435.13898

Didion-Gency, M., Gessler, A., Buchmann, N., Gisler, J., Schaub, M., & Grossiord, C. (2022). Impact of warmer and drier conditions on tree photosynthetic properties and the role of species interactions. *New Phytologist*, *236*(2), 547–560. https://doi.org/10.1111/nph.18384

Ding, Y., Nie, Y., Chen, H., Wang, K., & Querejeta, J. I. (2021). Water uptake depth is coordinated with leaf water potential, water-use efficiency and drought vulnerability in karst vegetation. *New Phytologist*, *229*(3), 1339–1353. https://doi.org/10.1111/nph.16971

Dixon, H. H., & Joly, J. (1895). On the Ascent of Sap. *Royal Society*, *186*, 563–576.

Domisch, T., Finér, L., Dawud, S. M., Vesterdal, L., & Raulund-Rasmussen, K. (2015). Does species richness affect fine root biomass and production in young forest plantations? *Oecologia*, *177*(2), 581–594. https://doi.org/10.1007/s00442-014-3107-3

Drake, J. E., Tjoelker, M. G., Vårhammar, A., Medlyn, B. E., Reich, P. B., Leigh, A., Pfautsch, S., Blackman, C. J., López, R., Aspinwall, M. J., Crous, K. Y., Duursma, R. A., Kumarathunge, D., De Kauwe, M. G., Jiang, M., Nicotra, A. B., Tissue, D. T., Choat, B., Atkin, O. K., & Barton, C. V. M. (2018). Trees tolerate an extreme heatwave via sustained transpirational cooling and increased leaf thermal tolerance. *Global Change Biology*, *24*(6), 2390–2402. https://doi.org/10.1111/gcb.14037

Duarte, M. M., Moral, R. de A., Guillemot, J., Zuim, C. I. F., Potvin, C., Bonat, W. H., Stape, J. L., & Brancalion, P. H. S. (2021). High tree diversity enhances light interception in tropical forests. *Journal of Ecology*, *109*, 2597–2611. https://doi.org/10.1111/1365-2745.13669

Duursma, R. A., Blackman, C. J., Lopéz, R., Martin-StPaul, N. K., Cochard, H., & Medlyn, B. E. (2019). On the minimum leaf conductance: its role in models of plant water use, and ecological and environmental controls. *New Phytologist*, *221*(2), 693–705. https://doi.org/10.1111/nph.15395

Ehleringer, J. R., & Dawson, T. E. (1992). Water uptake by plants: perspectives from stable isotope composition. *Plant, Cell and Environment*, *15*(9), 1073–1082. https://doi.org/10.1111/j.1365-3040.1992.tb01657.x

Eliades, M., Bruggeman, A., Lubczynski, M. W., Christou, A., Camera, C., & Djuma, H. (2018). The water balance components of Mediterranean pine trees on a steep mountain slope during two hydrologically contrasting years. *Journal of Hydrology*, *562*(May), 712–724. https://doi.org/10.1016/j.jhydrol.2018.05.048

Esteso-Martínez, J., Camarero, J. J., & Gil-Pelegrín, E. (2006). Competitive effects of herbs on Quercus faginea seedlings inferred from vulnerability curves and spatial-pattern analyses in a Mediterranean stand (Iberian System, northeast Spain). *Ecoscience*, *13*(3), 378–387. https://doi.org/10.2980/i1195-6860-13-3-378.1

Ferrio, J. P., Shestakova, T. A., Del Castillo, J., & Voltas, J. (2021). Oak competition dominates interspecific interactions in growth and water-use efficiency in a mixed pine–oak mediterranean forest. *Forests*, *12*(8). https://doi.org/10.3390/f12081093

Fontes, C. G., Dawson, T. E., Jardine, K., McDowell, N., Gimenez, B. O., Anderegg, L., Negrón-Juárez, R., Higuchi, N., Fine, P. V. A., Araújo, A. C., & Chambers, J. Q. (2018). Dry and hot: The hydraulic consequences of a climate change–type drought for Amazonian trees. *Philosophical Transactions of the Royal Society B: Biological Sciences*, *373*(1760). https://doi.org/10.1098/rstb.2018.0209

Ford, E. D. (1975). Competition and Stand Structure in Some Even-Aged Plant Monocultures. *The Journal of Ecology*, *63*(1), 311. https://doi.org/10.2307/2258857

Forner, A., Valladares, F., & Aranda, I. (2018). Mediterranean trees coping with severe drought: Avoidance might not be safe. *Environmental and Experimental Botany*, *155*(July), 529–540. https://doi.org/10.1016/j.envexpbot.2018.08.006

Forrester, D. I., Bonal, D., Dawud, S., Gessler, A., Granier, A., Pollastrini, M., & Grossiord, C. (2016). Drought responses by individual tree species are not often correlated with tree species diversity in European forests. *Journal of Applied Ecology*, *53*(6), 1725–1734. https://doi.org/10.1111/1365-2664.12745

Förster, A., Hertel, D., Werner, R., & Leuschner, C. (2021). Belowground consequences of converting broadleaf to conifer forest: Comparing the fine root systems of European beech and Scots pine. *Forest Ecology and Management*, *496*(May). https://doi.org/10.1016/j.foreco.2021.119457

Fotelli, M. N., Korakaki, E., Paparrizos, S. A., Radoglou, K., Awada, T., & Matzarakis, A. (2019). Environmental controls on the seasonal variation in gas exchange and water balance in a near-coastal Mediterranean Pinus halepensis forest. *Forests*, *10*(4). https://doi.org/10.3390/f10040313

Fox, J. W. (2005). Interpreting the “selection effect” of biodiversity on ecosystem function. *Ecology Letters*, *8*(8), 846–856. https://doi.org/10.1111/j.1461-0248.2005.00795.x

Früchtenicht, E., Neumann, L., Klein, N., Bonal, D., & Brüggemann, W. (2018). Response of Quercus robur and two potential climate change winners—Quercus pubescens and Quercus ilex—To two years summer drought in a semi-controlled competition study: I—Tree water status. *Environmental and Experimental Botany*, *152*(August 2017), 107–117. https://doi.org/10.1016/j.envexpbot.2018.01.002

Fuchs, S., Leuschner, C., Mathias Link, R., & Schuldt, B. (2021). Hydraulic variability of three temperate broadleaf tree species along a water availability gradient in central Europe. *New Phytologist*, *231*(4), 1387–1400. https://doi.org/10.1111/nph.17448

Garcia-Forner, N., Adams, H. D., Sevanto, S., Collins, A. D., Dickman, L. T., Hudson, P. J., Zeppel, M. J. B., Jenkins, M. W., Powers, H., Martínez-Vilalta, J., & Mcdowell, N. G. (2016). Responses of two semiarid conifer tree species to reduced precipitation and warming reveal new perspectives for stomatal regulation. *Plant Cell and Environment*, *39*(1), 38–49. https://doi.org/10.1111/pce.12588

Gauthey, A., Bachofen, C., Deluigi, J., Didion-Gency, M., D'Odorico, P., Gisler, J., Mas, E., Schaub, M., Schuler, P., Still, C. J., Tunas, A., & Grossiord, C. (2023). Absence of canopy temperature variation despite stomatal adjustment in Pinus sylvestris under multidecadal soil moisture manipulation. *New Phytologist*, *240*(1), 127–137. https://doi.org/10.1111/nph.19136

Gea-Izquierdo, G., Aranda, I., Cañellas, I., Dorado-Liñán, I., Olano, J. M., & Martin-Benito, D. (2021). Contrasting species decline but high sensitivity to increasing water stress on a mixed pine–oak ecotone. *Journal of Ecology*, *109*(1), 109–124. https://doi.org/10.1111/1365-2745.13450

Gillerot, L., Forrester, D. I., Bottero, A., Rigling, A., & Lévesque, M. (2021). Tree Neighbourhood Diversity Has Negligible Effects on Drought Resilience of European Beech, Silver Fir and Norway Spruce. *Ecosystems*, *24*(1), 20–36. https://doi.org/10.1007/s10021-020-00501-y

Giorgi, F., & Lionello, P. (2008). Climate change projections for the Mediterranean region. *Global and Planetary Change*, *63*(2–3), 90–104. https://doi.org/10.1016/j.gloplacha.2007.09.005

Gleason, S. M., Westoby, M., Jansen, S., Choat, B., Hacke, U. G., Pratt, R. B., Bhaskar, R., Brodribb, T. J., Bucci, S. J., Cao, K., Fan, Z., Feild, T. S., Jacobsen, A. L., Johnson, D. M., Domec, J., Mitchell, P. J., Morris, H., Nardini, A., Pittermann, J., … Zanne, A. E. (2016). Weak tradeoff between xylem safety and xylem-specific hydraulic efficiency across the world ' s woody plant species. *New Phytologist*, *209*, 123–136.

Greenwood, S., Ruiz-Benito, P., Martínez-Vilalta, J., Lloret, F., Kitzberger, T., Allen, C. D., Fensham, R., Laughlin, D. C., Kattge, J., Bönisch, G., Kraft, N. J. B., & Jump, A. S. (2017). Tree mortality across biomes is promoted by drought intensity, lower wood density and higher specific leaf area. *Ecology Letters*, *20*(4), 539–553. https://doi.org/10.1111/ele.12748

Gröning, M., Lutz, H. O., Roller-Lutz, Z., Kralik, M., Gourcy, L., & Pöltenstein, L. (2012). A simple rain collector preventing water re-evaporation dedicated for δ 18O and δ 2H analysis of cumulative precipitation samples. *Journal of Hydrology*, *448–449*, 195–200. https://doi.org/10.1016/j.jhydrol.2012.04.041

Grossiord, C., Granier, A., Ratcliffe, S., Bouriaud, O., Bruelheide, H., Checko, E., Forrester, D. I., Dawud, S. M., Finer, L., Pollastrini, M., Scherer-Lorenzen, M., Valladares, F., Bonal, D., & Gessler, A. (2014). Tree diversity does not always improve resistance of forest ecosystems to drought. *Proceedings of the National Academy of Sciences*, *111*(41), 14812–14815. https://doi.org/10.1073/pnas.1411970111

Grossiord, Charlotte. (2020). Having the right neighbors: how tree species diversity modulates drought impacts on forests. *New Phytologist*, *228*(1), 42–49. https://doi.org/10.1111/nph.15667

Grossiord, Charlotte, Bachofen, C., Gisler, J., Mas, E., Vitasse, Y., & Didion-Gency, M. (2022). Warming may extend tree growing seasons and compensate for reduced carbon uptake during dry periods. *Journal of Ecology*, *110*(7), 1575–1589. https://doi.org/10.1111/1365-2745.13892

Grossiord, Charlotte, Buckley, T. N., Cernusak, L. A., Novick, K. A., Poulter, B., Siegwolf, R. T. W., Sperry, J. S., & McDowell, N. G. (2020). Plant responses to rising vapor pressure deficit. *New Phytologist*, *226*(6), 1550–1566. https://doi.org/10.1111/nph.16485

Grossiord, Charlotte, Forner, A., Gessler, A., Granier, A., Pollastrini, M., Valladares, F., & Bonal, D. (2015). Influence of species interactions on transpiration of Mediterranean tree species during a summer drought. *European Journal of Forest Research*, *134*(2), 365–376. https://doi.org/10.1007/s10342-014-0857-8

Grossiord, Charlotte, Gessler, A., Granier, A., Pollastrini, M., Bussotti, F., & Bonal, D. (2014). Interspecific competition influences the response of oak transpiration to increasing drought stress in a mixed Mediterranean forest. *Forest Ecology and Management*, *318*, 54–61. https://doi.org/10.1016/j.foreco.2014.01.004

Grossiord, Charlotte, Sevanto, S., Bonal, D., Borrego, I., Dawson, T. E., Ryan, M., Wang, W., & McDowell, N. G. (2018). Prolonged warming and drought modify belowground interactions for water among coexisting plants. *Tree Physiology*, *39*(1), 55–63. https://doi.org/10.1093/treephys/tpy080

Grossiord, Charlotte, Sevanto, S., Dawson, T. E., Adams, H. D., Collins, A. D., Dickman, L. T., Newman, B. D., Stockton, E. A., & McDowell, N. G. (2017). Warming combined with more extreme precipitation regimes modifies the water sources used by trees. *New Phytologist*, *213*(2), 584–596. https://doi.org/10.1111/nph.14192

Grossoni, P., Bussotti, F., Tani, C., Gravano, E., Santarelli, S., & Bottacci, A. (1998). Morpho-anatomical alterations in leaves of Fagus Syl Vatica L. And Quercus Ilex L. in different environmental stress condition. *Chemosphere*, *36*(4–5), 919–924. https://doi.org/10.1016/S0045-6535(97)10148-5

Gulías, J., Cifre, J., Jonasson, S., Medrano, H., & Flexas, J. (2009). Seasonal and inter-annual variations of gas exchange in thirteen woody species along a climatic gradient in the Mediterranean island of Mallorca. *Flora: Morphology, Distribution, Functional Ecology of Plants*, *204*(3), 169–181. https://doi.org/10.1016/j.flora.2008.01.011

Guo, J. S., Hungate, B. A., Kolb, T. E., & Koch, G. W. (2018). Water source niche overlap increases with site moisture availability in woody perennials. *Plant Ecology*, *219*(6), 719–735. https://doi.org/10.1007/s11258-018-0829-z

Guo, Q., Fei, S., Potter, K. M., Liebhold, A. M., & Wen, J. (2019). Tree diversity regulates forest pest invasion. *Proceedings of the National Academy of Sciences of the United States of America*, *116*(15), 7382–7386. https://doi.org/10.1073/pnas.1821039116

Haberstroh, S., & Werner, C. (2022). The role of species interactions for forest resilience to drought. *Plant Biology*, *24*(7), 1098–1107. https://doi.org/10.1111/plb.13415

Hagedorn, F., Joseph, J., Peter, M., Luster, J., Pritsch, K., Geppert, U., Kerner, R., Molinier, V., Egli, S., Schaub, M., Liu, J. F., Li, M., Sever, K., Weiler, M., Siegwolf, R. T. W., Gessler, A., & Arend, M. (2016). Recovery of trees from drought depends on belowground sink control. *Nature Plants*, *2*(8). https://doi.org/10.1038/NPLANTS.2016.111

Hajek, P., Link, R. M., Nock, C. A., Bauhus, J., Gebauer, T., Gessler, A., Kovach, K., Messier, C., Paquette, A., Saurer, M., Scherer-Lorenzen, M., Rose, L., & Schuldt, B. (2022). Mutually inclusive mechanisms of drought-induced tree mortality. *Global Change Biology*, *28*(10), 3365–3378. https://doi.org/10.1111/gcb.16146

Hanson, P. J., Tschaplinski, T. J., Wullschleger, S. D., Todd Jr, D. E., & Augé, R. M. (2007). The resilience of upland-oak forest canopy trees to chronic and acute precipitation manipulations. *E-Gen. Tech. Rep. SRS*–

101. US Department of Agriculture, Forest Service, Southern Research Station: 3-2012 [CD-ROM]., 3–12.

Hartmann, H., Bastos, A., Das, A. J., Esquivel-Muelbert, A., Hammond, W. M., Martínez-Vilalta, J., Mcdowell, N. G., Powers, J. S., Pugh, T. A. M., Ruthrof, K. X., & Allen, C. D. (2022). Climate Change Risks to Global Forest Health: Emergence of Unexpected Events of Elevated Tree Mortality Worldwide. *Annual Review of Plant Biology*, *73*, 673–702. https://doi.org/10.1146/annurev-arplant-102820-012804

Hesse, B. D., Gebhardt, T., Hafner, B. D., Hikino, K., Reitsam, A., Gigl, M., Dawid, C., Häberle, K. H., & Grams, T. E. E. (2023). Physiological recovery of tree water relations upon drought release—response of mature beech and spruce after five years of recurrent summer drought. *Tree Physiology*, *43*(4), 522–538. https://doi.org/10.1093/treephys/tpac135

Hietz, P., Rosner, S., Sorz, J., & Mayr, S. (2008). Comparison of methods to quantify loss of hydraulic conductivity in Norway spruce. *Annals of Forest Science*, *65*(5), 502–502. https://doi.org/10.1051/forest:2008023

Hochberg, U., Rockwell, F. E., Holbrook, N. M., & Cochard, H. (2018). Iso/Anisohydry: A Plant–Environment Interaction Rather Than a Simple Hydraulic Trait. *Trends in Plant Science*, *23*(2), 112–120. https://doi.org/10.1016/j.tplants.2017.11.002

Hoegh-Guldberg, O., D. Jacob, M. Taylor, M. Bindi, S. Brown, I. Camilloni, A. Diedhiou, R. Djalante, K.L. Ebi, F. Engelbrecht, J. Guiot, Y. Hijioka, S. Mehrotra, A. Payne, S.I. Seneviratne, A. Thomas, R. Warren, G. Z. (2018). Impacts of 1.5°C global warming on natural and human systems. In: Global Warming of 1.5 °C. An IPCC special report on the impacts of global warming of 1.5 °C above preindustrial levels and related global greenhouse gas emission pathways, in the context of. *Special Report, Intergovernmental Panel on Climate Change*, *ISBN 978-92-9169-151-7*, 175–311.

Hong, P., Schmid, B., De Laender, F., Eisenhauer, N., Zhang, X., Chen, H., Craven, D., De Boeck, H. J., Hautier, Y., Petchey, O. L., Reich, P. B., Steudel, B., Striebel, M., Thakur, M. P., & Wang, S. (2022). Biodiversity promotes ecosystem functioning despite environmental change. *Ecology Letters*, *25*(2), 555–569. https://doi.org/10.1111/ele.13936

Hooper, D. U. (1998). The role of complementarity and competition in ecosystem responses to variation in plant diversity. *Ecology*, *79*(2), 704–719. https://doi.org/10.1890/0012-9658(1998)079[0704:TROCAC]2.0.CO;2

Houston Durrant, T., de Rigo, D., & Caudullo, G. (2016). Pinus sylvestris in Europe: Distribution, habitat, usage and treats. In A. San-Miguel-Ayanz, J., de Rigo, D., Caudullo, G., Houston Durrant, T., Mauri (Ed.), *European atlas of forest tree species.* (pp. 132–133). Publ. Off. EU.

Hudson, J. M. G., Henry, G. H. R., & Cornwell, W. K. (2011). Taller and larger: Shifts in Arctic tundra leaf traits after 16 years of experimental warming. *Global Change Biology*, *17*(2), 1013–1021. https://doi.org/10.1111/j.1365-2486.2010.02294.x

Jacobs, K., Jonard, M., Muys, B., & Ponette, Q. (2022). Shifts in dominance and complementarity between sessile oak and beech along ecological gradients. *Journal of Ecology*, *110*(10), 2404–2417. https://doi.org/10.1111/1365-2745.13958

Jactel, H., Moreira, X., & Castagneyrol, B. (2021). Tree Diversity and Forest Resistance to Insect Pests: Patterns, Mechanisms, and Prospects. *Annual Review of Entomology*, *66*, 277–296. https://doi.org/10.1146/annurev-ento-041720-075234

Jagadish, S. V. K., Way, D. A., & Sharkey, T. D. (2021). Plant heat stress: Concepts directing future research. *Plant Cell and Environment*, *March*, 1992–2005. https://doi.org/10.1111/pce.14050

James, A. T. A., Lawn, R. J. B., & Cooper, M. C. (2008). *Genotypic variation for drought stress response traits in soybean . I . Variation in soybean and wild Glycine spp . for epidermal conductance , osmotic potential , and relative water content*. *1986*, 656–669.

Jing, X., Muys, B., Bruelheide, H., Desie, E., Hättenschwiler, S., Jactel, H., Jaroszewicz, B., Kardol, P., Ratcliffe, S., Scherer-Lorenzen, M., Selvi, F., Vancampenhout, K., van der Plas, F., Verheyen, K., Vesterdal, L., Zuo, J., & Van Meerbeek, K. (2021). Above- and below-ground complementarity rather than selection drive tree diversity–productivity relationships in European forests. *Functional Ecology*, *35*(8), 1756–1767. https://doi.org/10.1111/1365-2435.13825

Jonard, F., André, F., Ponette, Q., Vincke, C., & Jonard, M. (2011). Sap flux density and stomatal conductance of European beech and common oak trees in pure and mixed stands during the summer drought of 2003. *Journal of Hydrology*, *409*(1–2), 371–381. https://doi.org/10.1016/j.jhydrol.2011.08.032

Jourdan, M., Kunstler, G., & Morin, X. (2020). How neighbourhood interactions control the temporal stability and resilience to drought of trees in mountain forests. *Journal of Ecology*, *108*(2), 666–677. https://doi.org/10.1111/1365-2745.13294

Jucker, T., Bouriaud, O., Avacaritei, D., & Coomes, D. A. (2014). Stabilizing effects of diversity on aboveground wood production in forest ecosystems: Linking patterns and processes. *Ecology Letters*, *17*(12), 1560–1569. https://doi.org/10.1111/ele.12382

Jucker, T., Bouriaud, O., Avacaritei, D., Dănilă, I., Duduman, G., Valladares, F., & Coomes, D. A. (2014). Competition for light and water play contrasting roles in driving diversity-productivity relationships in Iberian forests. *Journal of Ecology*, *102*(5), 1202–1213. https://doi.org/10.1111/1365-2745.12276

Jucker, T., Bouriaud, O., & Coomes, D. A. (2015). Crown plasticity enables trees to optimize canopy packing in mixed-species forests. *Functional Ecology*, *29*(8), 1078–1086. https://doi.org/10.1111/1365-2435.12428

Juenger, T. E., & Verslues, P. E. (2022). Time for a drought experiment: Do you know your plants' water status? *The Plant Cell*, 1–14. https://doi.org/10.1093/plcell/koac324

Kahmen, A., Basler, D., Hoch, G., Link, R. M., Schuldt, B., Zahnd, C., & Arend, M. (2022). Root water uptake depth determines the hydraulic vulnerability of temperate European tree species during the extreme 2018 drought. *Plant Biology*, *24*(7), 1224–1239. https://doi.org/10.1111/plb.13476

Kambach, S., Allan, E., Bilodeau-Gauthier, S., Coomes, D. A., Haase, J., Jucker, T., Kunstler, G., Müller, S., Nock, C., Paquette, A., van der Plas, F., Ratcliffe, S., Roger, F., Ruiz-Benito, P., Scherer-Lorenzen, M., Auge, H., Bouriaud, O., Castagneyrol, B., Dahlgren, J., … Bruelheide, H. (2019). How do trees respond to species mixing in experimental compared to observational studies? *Ecology and Evolution*, *9*(19), 11254–11265. https://doi.org/10.1002/ece3.5627

Keenan, T. F., & Williams, C. A. (2018). The terrestrial carbon sink. *Annual Review of Environment and Resources*, *43*, 219–243. https://doi.org/10.1146/annurev-environ-102017-030204

Klein, T. (2014). The variability of stomatal sensitivity to leaf water potential across tree species indicates a continuum between isohydric and anisohydric behaviours. *Functional Ecology*, *28*(6), 1313–1320. https://doi.org/10.1111/1365-2435.12289

Klein, T., Cohen, S., & Yakir, D. (2011). Hydraulic adjustments underlying drought resistance of Pinus halepensis. *Tree Physiology*, *31*, 637–648. https://doi.org/10.1093/treephys/tpr047

Klein, T., Torres-Ruiz, J. M., & Albers, J. J. (2022). Conifer desiccation in the 2021 NW heatwave confirms the role of hydraulic damage. *Tree Physiology*, *42*(4), 722–726. https://doi.org/10.1093/treephys/tpac007

Klesse, S., Wohlgemuth, T., Meusburger, K., Vitasse, Y., von Arx, G., Lévesque, M., Neycken, A., Braun, S., Dubach, V., Gessler, A., Ginzler, C., Gossner, M. M., Hagedorn, F., Queloz, V., Samblás Vives, E., Rigling, A., & Frei, E. R. (2022). Long-term soil water limitation and previous tree vigor drive local variability of drought-induced crown dieback in Fagus sylvatica. *Science of the Total Environment*, *851*(August). https://doi.org/10.1016/j.scitotenv.2022.157926

Klos, P. Z., Goulden, M. L., Riebe, C. S., Tague, C. L., O'Geen, A. T., Flinchum, B. A., Safeeq, M., Conklin, M. H., Hart, S. C., Berhe, A. A., Hartsough, P. C., Holbrook, W. S., & Bales, R. C. (2018). Subsurface plant-accessible water in mountain ecosystems with a Mediterranean climate. *Wiley Interdisciplinary Reviews: Water*, *5*(3), 1–14. https://doi.org/10.1002/WAT2.1277

Koide, R. T., Robichaux, R. H., Morse, S. R., & Smith, C. M. (2000). Plant water status, hydraulic resistance and capacitance. In *Plant Physiological Ecology: Field Methods and Instrumentation* (pp. 161–183). Springer Netherlands. https://doi.org/10.1007/978-94-009-2221-1_9

Kukowski, K. R., Schwinning, S., & Schwartz, B. F. (2013). Hydraulic responses to extreme drought conditions in three co-dominant tree species in shallow soil over bedrock. *Oecologia*, *171*(4), 819–830. https://doi.org/10.1007/s00442-012-2466-x

Kunert, N., Zailaa, J., Herrmann, V., Muller-Landau, H. C., Wright, S. J., Pérez, R., McMahon, S. M., Condit, R. C., Hubbell, S. P., Sack, L., Davies, S. J., & Anderson-Teixeira, K. J. (2021). Leaf turgor loss point shapes local and regional distributions of evergreen but not deciduous tropical trees. *New Phytologist*, *230*(2), 485–496. https://doi.org/10.1111/nph.17187

Ladjal, M., Huc, R., & Ducrey, M. (2005). Drought effects on hydraulic conductivity and xylem vulnerability to embolism in diverse species and provenances of Mediterranean cedars. *Tree Physiology*, *25*(9), 1109–1117. https://doi.org/10.1093/treephys/25.9.1109

Lange, O. L., Fiihrer, G., & Gebel, J. (1986). Rapid field determination of photosynthetic capacity of cut spruce twigs (Picea abies) at saturating ambient CO2. *Trees*, 70–77.

Lavorel, S. (1999). Ecological diversity and resilience of Mediterranean vegetation to disturbance. *Diversity and Distributions*, *5*(1–2), 3–13. https://doi.org/10.1046/j.1472-4642.1999.00033.x

Lemaire, C., Blackman, C. J., Cochard, H., Menezes-Silva, P. E., Torres-Ruiz, J. M., & Herbette, S. (2021). Acclimation of hydraulic and morphological traits to water deficit delays hydraulic failure during simulated drought in poplar. *Tree Physiology*, *41*(11), 2008–2021. https://doi.org/10.1093/treephys/tpab086

Lens, F., Tixier, A., Cochard, H., Sperry, J. S., Jansen, S., & Herbette, S. (2013). Embolism resistance as a key mechanism to understand adaptive plant strategies. *Current Opinion in Plant Biology*, *16*, 287–292. https://doi.org/10.1016/j.pbi.2013.02.005

Leuschner, C. (2020). Drought response of European beech (Fagus sylvatica L.)—A review. *Perspectives in Plant Ecology, Evolution and Systematics*, *47*(October), 125576. https://doi.org/10.1016/j.ppees.2020.125576

Leuschner, C., Schipka, F., & Backes, K. (2022). Stomatal regulation and water potential variation in European beech: Challenging the iso/anisohydry concept. *Tree Physiology*, *42*(2), 365–378. https://doi.org/10.1093/treephys/tpab104

Leuschner, C., Wedde, P., & Lübbe, T. (2019). The relation between pressure–volume curve traits and stomatal regulation of water potential in five temperate broadleaf tree species. *Annals of Forest Science*, *76*(2). https://doi.org/10.1007/s13595-019-0838-7

Lévesque, M., Saurer, M., Siegwolf, R., Eilmann, B., Brang, P., Bugmann, H., & Rigling, A. (2013). Drought response of five conifer species under contrasting water availability suggests high vulnerability of Norway spruce and European larch. *Global Change Biology*, *19*(10), 3184–3199. https://doi.org/10.1111/gcb.12268

Lévesque, M., Siegwolf, R., Saurer, M., Eilmann, B., & Rigling, A. (2014). Increased water-use efficiency does not lead to enhanced tree growth under xeric and mesic conditions. *New Phytologist*, *203*(1), 94–109. https://doi.org/10.1111/nph.12772

Liang, J., Crowther, T. W., Picard, N., Wiser, S., Zhou, M., Alberti, G., Schulze, E. D., McGuire, A. D., Bozzato, F., Pretzsch, H., De-Miguel, S., Paquette, A., Hérault, B., Scherer-Lorenzen, M., Barrett, C. B., Glick, H. B., Hengeveld, G. M., Nabuurs, G. J., Pfautsch, S., … Reich, P. B. (2016). Positive biodiversity-productivity relationship predominant in global forests. *Science*, *354*(6309). https://doi.org/10.1126/science.aaf8957

Ligot, G., Aitor, A., Benoît, C., Lluís, C., & Dan, K. (2016). Tree light capture and spatial variability of understory light increase with species mixing and tree size heterogeneity. *Canadian Journal of Forest Research*, *46*(7), 968–977. https://doi.org/10.1139/cjfr-2016-0061

Limousin, J. M., Longepierre, D., Huc, R., & Rambal, S. (2010). Change in hydraulic traits of Mediterranean Quercus ilex subjected to long-term throughfall exclusion. *Tree Physiology*, *30*(8), 1026–1036. https://doi.org/10.1093/treephys/tpq062

Limousin, J. M., Roussel, A., Rodríguez-Calcerrada, J., Torres-Ruiz, J. M., Moreno, M., Garcia de Jalon, L., Ourcival, J. M., Simioni, G., Cochard, H., & Martin-StPaul, N. (2022). Drought acclimation of Quercus ilex leaves improves tolerance to moderate drought but not resistance to severe water stress. *Plant Cell and Environment*, *45*(7), 1967–1984. https://doi.org/10.1111/pce.14326

Liu, D., Wang, T., Peñuelas, J., & Piao, S. (2022). Drought resistance enhanced by tree species diversity in global forests. *Nature Geoscience*, *15*(10), 800–804. https://doi.org/10.1038/s41561-022-01026-w

Liu, Y., Kumar, M., Katul, G. G., Feng, X., & Konings, A. G. (2020). Plant hydraulics accentuates the effect of atmospheric moisture stress on transpiration. *Nature Climate Change*, *10*(7), 691–695. https://doi.org/10.1038/s41558-020-0781-5

Loik, M. E., & Harte, J. (1997). Changes in water relations for leaves exposed to a climate-warming manipulation in the Rocky Mountains of Colorado. *Environmental and Experimental Botany*, *37*(2–3), 115–123. https://doi.org/10.1016/S0098-8472(96)01043-X

Loreau, M., & Hector, A. (2001). Partitioning selection and complementarity in biodiversity experiments. *Nature*, *412*(6842), 72–76. https://doi.org/10.1038/35083573

Lubczynski, M. W. (2009). The hydrogeological role of trees in water-limited environments. *Hydrogeology Journal*, *17*(1), 247–259. https://doi.org/10.1007/s10040-008-0357-3

Lutter, R., Henriksson, N., Lim, H., Blaško, R., Magh, R. K., Näsholm, T., Nordin, A., Lundmark, T., & Marshall, J. D. (2021). Belowground resource utilization in monocultures and mixtures of Scots pine and Norway spruce. *Forest Ecology and Management*, *500*(August). https://doi.org/10.1016/j.foreco.2021.119647

Lüttschwager, D., & Jochheim, H. (2020). Drought primarily reduces canopy transpiration of exposed beech trees and decreases the share of water uptake from deeper soil layers. *Forests*, *11*(5). https://doi.org/10.3390/F11050537

Lyon, C., Saupe, E. E., Smith, C. J., Hill, D. J., Beckerman, A. P., Stringer, L. C., Marchant, R., McKay, J., Burke, A., O'Higgins, P., Dunhill, A. M., Allen, B. J., Riel-Salvatore, J., & Aze, T. (2022). Climate change research and action must look beyond 2100. *Global Change Biology*, *28*(2), 349–361. https://doi.org/10.1111/gcb.15871

Manning, P., Van Der Plas, F., Soliveres, S., Allan, E., Maestre, F. T., Mace, G., Whittingham, M. J., & Fischer, M. (2018). Redefining ecosystem multifunctionality. *Nature Ecology and Evolution*, *2*(3), 427–436. https://doi.org/10.1038/s41559-017-0461-7

Mariotti, A., Pan, Y., Zeng, N., & Alessandri, A. (2015). Long-term climate change in the Mediterranean region in the midst of decadal variability. *Climate Dynamics*, *44*(5–6), 1437–1456. https://doi.org/10.1007/s00382-015-2487-3

Markesteijn, L., & Poorter, L. (2009). Seedling root morphology and biomass allocation of 62 tropical tree species in relation to drought- and shade-tolerance. *Journal of Ecology*, *97*(2), 311–325. https://doi.org/10.1111/j.1365-2745.2008.01466.x

Martín-Gómez, P., Aguilera, M., Pemán, J., Gil-Pelegrín, E., & Ferrio, J. P. (2017). Contrasting ecophysiological strategies related to drought: the case of a mixed stand of Scots pine (Pinus sylvestris) and a submediterranean oak (Quercus subpyrenaica). *Tree Physiology*, *37*(11), 1478–1492. https://doi.org/10.1093/treephys/tpx101

Martin-StPaul, N., Delzon, S., & Cochard, H. (2017). Plant resistance to drought depends on timely stomatal closure. *Ecology Letters*, *20*(11), 1437–1447. https://doi.org/10.1111/ele.12851

Martin-Stpaul, N. K., Limousin, J. M., Vogt-Schilb, H., Rodríguez-Calcerrada, J., Rambal, S., Longepierre, D., & Misson, L. (2013). The temporal response to drought in a Mediterranean evergreen tree: Comparing a regional precipitation gradient and a throughfall exclusion experiment. *Global Change Biology*, *19*(8), 2413–2426. https://doi.org/10.1111/gcb.12215

Martínez-Sancho, E., Gutiérrez, E., Valeriano, C., Ribas, M., Popkova, M. I., Shishov, V. V., & Dorado-Liñán, I. (2021). Intra-and inter-annual growth patterns of a mixed pine-oak forest under mediterranean climate. *Forests*, *12*(12), 1–15. https://doi.org/10.3390/f12121746

Martínez-Sancho, E., Navas, L. K. V., Seidel, H., Dorado-Liñán, I., & Menzel, A. (2017). Responses of contrasting tree functional types to air warming and drought. *Forests*, *8*(11). https://doi.org/10.3390/f8110450

Martínez-Vilalta, J., & Garcia-Forner, N. (2017). Water potential regulation, stomatal behaviour and hydraulic transport under drought: deconstructing the iso/anisohydric concept. *Plant Cell and Environment*, *40*(6), 962–976. https://doi.org/10.1111/pce.12846

Martínez-Vilalta, J., & Piñol, J. (2002). Drought-induced mortality and hydraulic architecture in pine populations of the NE Iberian Peninsula. *Forest Ecology and Management*, *161*(1–3), 247–256.

https://doi.org/10.1016/S0378-1127(01)00495-9

Martínez-Vilalta, J., Poyatos, R., Aguadé, D., Retana, J., & Mencuccini, M. (2014). A new look at water transport regulation in plants. *New Phytologist*, *204*(1), 105–115. https://doi.org/10.1111/nph.12912

Matzner, S. L., Rice, K. J., & Richards, J. H. (2001). Intra-specific variation in xylem cavitation in interior live oak (Quercus wislizenii A. DC.). *Journal of Experimental Botany*, *52*(357), 783–789. https://doi.org/10.1093/jexbot/52.357.783

McDowell, N., Allen, C. D., Anderson-Teixeira, K., Brando, P., Brienen, R., Chambers, J., Christoffersen, B., Davies, S., Doughty, C., Duque, A., Espirito-Santo, F., Fisher, R., Fontes, C. G., Galbraith, D., Goodsman, D., Grossiord, C., Hartmann, H., Holm, J., Johnson, D. J., … Xu, X. (2018). Drivers and mechanisms of tree mortality in moist tropical forests. *New Phytologist*, *219*(3), 851–869. https://doi.org/10.1111/nph.15027

McDowell, N., Pockman, W. T., Allen, C. D., Breshears, D. D., Cobb, N., Kolb, T., Plaut, J., Sperry, J., West, A., Williams, D. G., & Yepez, E. A. (2008). Mechanisms of plant survival and mortality during drought: Why do some plants survive while others succumb to drought? *New Phytologist*, *178*(4), 719–739. https://doi.org/10.1111/j.1469-8137.2008.02436.x

Meier, I. C., Knutzen, F., Eder, L. M., Müller-Haubold, H., Goebel, M. O., Bachmann, J., Hertel, D., & Leuschner, C. (2018). The Deep Root System of Fagus sylvatica on Sandy Soil: Structure and Variation Across a Precipitation Gradient. *Ecosystems*, *21*(2), 280–296. https://doi.org/10.1007/s10021-017-0148-6

Meiner, M., Köhler, M., Schwendenmann, L., & Hölscher, D. (2012). Partitioning of soil water among canopy trees during a soil desiccation period in a temperate mixed forest. *Biogeosciences*, *9*(8), 3465–3474. https://doi.org/10.5194/bg-9-3465-2012

Meinzer, F. C., Johnson, D. M., Lachenbruch, B., McCulloh, K. A., & Woodruff, D. R. (2009). Xylem hydraulic safety margins in woody plants: Coordination of stomatal control of xylem tension with hydraulic capacitance. *Functional Ecology*, *23*(5), 922–930. https://doi.org/10.1111/j.1365-2435.2009.01577.x

Meyer, B. F., Buras, A., Rammig, A., & Zang, C. S. (2020). Higher susceptibility of beech to drought in comparison to oak. *Dendrochronologia*, *64*(November), 125780. https://doi.org/10.1016/j.dendro.2020.125780

Michalet, R., Le Bagousse-Pinguet, Y., Maalouf, J. P., & Lortie, C. J. (2014). Two alternatives to the stress-gradient hypothesis at the edge of life: The collapse of facilitation and the switch from facilitation to competition. *Journal of Vegetation Science*, *25*(2), 609–613. https://doi.org/10.1111/jvs.12123

Morcillo, L., Muñoz-Rengifo, J. C., Torres-Ruiz, J. M., Delzon, S., Moutahir, H., & Vilagrosa, A. (2022). Post-drought conditions and hydraulic dysfunction determine tree resilience and mortality across Mediterranean Aleppo pine (Pinus halepensis) populations after an extreme drought event. *Tree Physiology*, *42*(7), 1364–1376. https://doi.org/10.1093/treephys/tpac001

Moreno, G., Obrador, J. J., Cubera, E., & Dupraz, C. (2005). Fine Root Distribution in Dehesas of Central-Western Spain. *Plant and Soil*, *277*(1–2), 153–162. https://doi.org/10.1007/s11104-005-6805-0

Moreno, M., Simioni, G., Cailleret, M., Ruffault, J., Badel, E., Carrière, S., Davi, H., Gavinet, J., Huc, R., Limousin, J. M., Marloie, O., Martin, L., Rodríguez-Calcerrada, J., Vennetier, M., & Martin-StPaul, N. (2021). Consistently lower sap velocity and growth over nine years of rainfall exclusion in a Mediterranean mixed pine-oak forest. *Agricultural and Forest Meteorology*, *308–309*(August 2020).

https://doi.org/10.1016/j.agrformet.2021.108472

Moreno, M., Simioni, G., Cochard, H., & Doussan, C. (2023). *Functional diversity reduces the risk of hydraulic failure in tree mixtures through hydraulic disconnection*. https://doi.org/https://doi.org/10.1101/2023.06.09.544345

Muñoz-Gálvez, F. J., Herrero, A., Esther Pérez-Corona, M., & Andivia, E. (2021). Are pine-oak mixed stands in Mediterranean mountains more resilient to drought than their monospecific counterparts? *Forest Ecology and Management*, *484*(January). https://doi.org/10.1016/j.foreco.2021.118955

Myers, N., Mittermeier, R. A., Mittermeier, C. G., da Fonseca, G. A. B., & Kent, J. (2000). Biodiversity hotspots for conservation priorities. *Nature*, *403*(6772), 853–858. https://doi.org/10.1038/35002501

Nardini, A., Lo Gullo, M. A., Trifilò, P., & Salleo, S. (2014). The challenge of the Mediterranean climate to plant hydraulics: Responses and adaptations. *Environmental and Experimental Botany*, *103*, 68–79. https://doi.org/10.1016/j.envexpbot.2013.09.018

Nicotra, A. B., Atkin, O. K., Bonser, S. P., Davidson, A. M., Finnegan, E. J., Mathesius, U., Poot, P., Purugganan, M. D., Richards, C. L., Valladares, F., & van Kleunen, M. (2010). Plant phenotypic plasticity in a changing climate. *Trends in Plant Science*, *15*(12), 684–692. https://doi.org/10.1016/j.tplants.2010.09.008

Nie, Y. peng, Chen, H. song, Wang, K. lin, Tan, W., Deng, P. yan, & Yang, J. (2011). Seasonal water use patterns of woody species growing on the continuous dolostone outcrops and nearby thin soils in subtropical China. *Plant and Soil*, *341*(1–2), 399–412. https://doi.org/10.1007/s11104-010-0653-2

Or, D., Wraith, J. M., & Warrick, A. W. (2002). *Soil water content and water potential relationships* (vol. 1). Soil physics companion.

Parnell, A. (2019). Simmr: A Stable Isotope Mixing Model. R package version 0.4.1. *CRAN. R-Project*. https://doi.org/10.1002/env.2221>.Depends

Pearcy, R. W., E.-D, S., & Zimmermann, R. (2000). Measurement of transpiration and leaf conductance. In R. W. Pearcy, J. R. Ehleringer, H. A. Mooney, & P. . Rundel (Eds.), *Plant Physiological Ecology: Field Methods and Instrumentation* (pp. 137–160). Kluwer Academic, Dordrecht, The Netherlands.

Peñuelas, J., & Filella, I. (2003). Deuterium labelling of roots provides evidence of deep water access and hydraulic lift by Pinus nigra in a Mediterranean forest of NE Spain. *Environmental and Experimental Botany*, *49*(3), 201–208. https://doi.org/10.1016/S0098-8472(02)00070-9

Peyre, G. (2021). Terrestrial Biodiversity Hotspots: Challenges and Opportunities. In W. Leal Filho (Ed.), *Life on Land, Encyclopedia of the UN Sustainable Development Goals* (pp. 1–20). Springer Nature Switzerland AG. https://doi.org/10.1007/978-3-319-71065-5_150-1

Phillips, R. P., Ibáñez, I., D'Orangeville, L., Hanson, P. J., Ryan, M. G., & McDowell, N. G. (2016). A belowground perspective on the drought sensitivity of forests: Towards improved understanding and simulation. *Forest Ecology and Management*, *380*, 309–320. https://doi.org/10.1016/j.foreco.2016.08.043

Pickard, W. F. (1981). The ascent of sap in plants. *Progress in Biophysics and Molecular Biology*, *37*(C), 181–229. https://doi.org/10.1016/0079-6107(82)90023-2

Pittermann, J., Sperry, J. S., Wheeler, J. K., Hacke, U. W. E. G., & Sikkema, E. H. (2006). Mechanical reinforcement of tracheids compromises the hydraulic efficiency of conifer xylem. *Plant, Cell & Environment*,

29, 1618–1628. https://doi.org/10.1111/j.1365-3040.2006.01539.x

Polade, S. D., Gershunov, A., Cayan, D. R., Dettinger, M. D., & Pierce, D. W. (2017). Precipitation in a warming world: Assessing projected hydro-climate changes in California and other Mediterranean climate regions. *Scientific Reports*, *7*(1), 1–10. https://doi.org/10.1038/s41598-017-11285-y

Pretzsch, H., Schütze, G., & Uhl, E. (2013). Resistance of European tree species to drought stress in mixed versus pure forests: Evidence of stress release by inter-specific facilitation. *Plant Biology*, *15*(3), 483–495. https://doi.org/10.1111/j.1438-8677.2012.00670.x

Pretzsch, Hans, Bielak, K., Block, J., Bruchwald, A., Dieler, J., Ehrhart, H. P., Kohnle, U., Nagel, J., Spellmann, H., Zasada, M., & Zingg, A. (2013). Productivity of mixed versus pure stands of oak (Quercus petraea (Matt.) Liebl. and Quercus robur L.) and European beech (Fagus sylvatica L.) along an ecological gradient. *European Journal of Forest Research*, *132*(2), 263–280. https://doi.org/10.1007/s10342-012-0673-y

Prieto, I., Padilla, F. M., Armas, C., & Pugnaire, F. I. (2011). The role of hydraulic lift on seedling establishment under a nurse plant species in a semi-arid environment. *Perspectives in Plant Ecology, Evolution and Systematics*, *13*(3), 181–187. https://doi.org/10.1016/j.ppees.2011.05.002

Raft, A., & Oliier, H. (2011). Forest restoration, biodiversity and ecosystem functioning. *BMC Ecology*, 1–21.

Raschke, K. . (1976). How Stomata Resolve the Dilemma of Opposing Priorities. *Philosophical Transactions of the Royal Society of London*, *273*(927), 551–560.

Ratcliffe, S., Wirth, C., Jucker, T., van der Plas, F., Scherer-Lorenzen, M., Verheyen, K., Allan, E., Benavides, R., Bruelheide, H., Ohse, B., Paquette, A., Ampoorter, E., Bastias, C. C., Bauhus, J., Bonal, D., Bouriaud, O., Bussotti, F., Carnol, M., Castagneyrol, B., … Baeten, L. (2017). Biodiversity and ecosystem functioning relations in European forests depend on environmental context. *Ecology Letters*, *20*(11), 1414–1426. https://doi.org/10.1111/ele.12849

Rempe, D. M., & Dietrich, W. E. (2018). Direct observations of rock moisture, a hidden component of the hydrologic cycle. *Proceedings of the National Academy of Sciences of the United States of America*, *115*(11), 2664–2669. https://doi.org/10.1073/pnas.1800141115

Riederer, M., & Müller, C. (Eds.). (2008). *Annual Plant Reviews Volume 23: Biology of the Plant Cuticle*. Blackwell Publishing.

Rodriguez-Dominguez, C. M., Buckley, T. N., Egea, G., de Cires, A., Hernandez-Santana, V., Martorell, S., & Diaz-Espejo, A. (2016). Most stomatal closure in woody species under moderate drought can be explained by stomatal responses to leaf turgor. *Plant Cell and Environment*, *39*(9), 2014–2026. https://doi.org/10.1111/pce.12774

Rodríguez-Robles, U., Arredondo, J. T., Huber-Sannwald, E., Yépez, E. A., & Ramos-Leal, J. A. (2020). Coupled plant traits adapted to wetting/drying cycles of substrates co-define niche multidimensionality. *Plant Cell and Environment*, *43*(10), 2394–2408. https://doi.org/10.1111/pce.13837

Rodríguez-Robles, U., Arredondo, J. T., Huber-Sannwald, E., & Vargas, R. (2015). Geoecohydrological mechanisms couple soil and leaf water dynamics and facilitate species coexistence in shallow soils of a tropical semiarid mixed forest. *New Phytologist*, *207*(1), 59–69. https://doi.org/10.1111/nph.13344

Rog, I., Tague, C., Jakoby, G., Megidish, S., Yaakobi, A., Wagner, Y., & Klein, T. (2021). Interspecific Soil Water

Partitioning as a Driver of Increased Productivity in a Diverse Mixed Mediterranean Forest. *Journal of Geophysical Research: Biogeosciences*, *126*(9), 1–22. https://doi.org/10.1029/2021JG006382

Roman, D. T., Novick, K. A., Brzostek, E. R., Dragoni, D., Rahman, F., & Phillips, R. P. (2015). The role of isohydric and anisohydric species in determining ecosystem - scale response to severe drought. *Oecologia*, *179*(3), 641–654. https://doi.org/10.1007/s00442-015-3380-9

Rosas, T., Mencuccini, M., Barba, J., Cochard, H., Saura-Mas, S., & Martínez-Vilalta, J. (2019). Adjustments and coordination of hydraulic, leaf and stem traits along a water availability gradient. *New Phytologist*, *223*(2), 632–646. https://doi.org/10.1111/nph.15684

Rose, K. L., Graham, R. C., & Parker, D. R. (2003). Water source utilization by Pinus jeffreyi and Arctostaphylos patula on thin soils over bedrock. *Oecologia*, *134*(1), 46–54. https://doi.org/10.1007/s00442-002-1084-4

Rowland, L., Ramírez-Valiente, J. A., Hartley, I. P., & Mencuccini, M. (2023). How woody plants adjust above- and below-ground traits in response to sustained drought. *New Phytologist*, *Box 1*, 1173–1189. https://doi.org/10.1111/nph.19000

Rubio-Cuadrado, Á., Camarero, J. J., del Río, M., Sánchez-González, M., Ruiz-Peinado, R., Bravo-Oviedo, A., Gil, L., & Montes, F. (2018). Drought modifies tree competitiveness in an oak-beech temperate forest. *Forest Ecology and Management*, *429*(April), 7–17. https://doi.org/10.1016/j.foreco.2018.06.035

Ruffault, J., Pimont, F., Cochard, H., Dupuy, J. L., & Martin-Stpaul, N. (2022). SurEau-Ecos v2.0: a trait-based plant hydraulics model for simulations of plant water status and drought-induced mortality at the ecosystem level. *Geoscientific Model Development*, *15*(14), 5593–5626. https://doi.org/10.5194/gmd-15-5593-2022

Saadaoui, E., Ben Yahia, K., Dhahri, S., Ben Jamaa, M. L., & Khouja, M. L. (2017). An overview of adaptative responses to drought stress in Eucalyptus spp. *Forestry Studies*, *67*(1), 86–96. https://doi.org/10.1515/fsmu-2017-0014

Sack, L., Cowan, P. D., Jaikumar, N., & Holbrook, N. M. (2003). The “hydrology” of leaves: Co-ordination of structure and function in temperate woody species. *Plant, Cell and Environment*, *26*(8), 1343–1356. https://doi.org/10.1046/j.0016-8025.2003.01058.x

San-Miguel-Ayanz, J., de Rigo, D., Caudullo G., Houston Durrant, T., Mauri, A., Tinner, W., Ballian, D., Beck, P., Birks, H. J. B., Eaton, E., Enescu, C. M., Pasta, S., Popescu, I., Ravazzi, C., Welk, E., Abad Viñas, R., Azevedo, J. C., Barbati, A., Barre, B. (2016). *European Atlas of Forest Tree Species* (A. San-Miguel-Ayanz, J., de Rigo, D., Caudullo, G., Houston Durrant, T., Mauri (Ed.); KJ-01-20-1). Publ. Off. EU. https://doi.org/10.2760/776635

Schenk, H. J., & Jackson, R. B. (2005). Mapping the global distribution of deep roots in relation to climate and soil characteristics. *Geoderma*, *126*(1-2 SPEC. ISS.), 129–140. https://doi.org/10.1016/j.geoderma.2004.11.018

Schindelin, J., Arganda-carreras, I., Frise, E., Kaynig, V., Longair, M., Pietzsch, T., Preibisch, S., Rueden, C., Saalfeld, S., Schmid, B., Tinevez, J., White, D. J., Hartenstein, V., Eliceiri, K., Tomancak, P., & Cardona, A. (2019). *Fiji : an open-source platform for biological-image analysis*. *9*(7). https://doi.org/10.1038/nmeth.2019

Schönbeck, L. C., Schuler, P., Lehmann, M. M., Mas, E., Mekarni, L., Pivovaroff, A. L., Turberg, P., & Grossiord, C. (2022). Increasing temperature and vapour pressure deficit lead to hydraulic damages in the absence of soil drought. *Plant Cell and Environment*, *45*(11), 3275–3289. https://doi.org/10.1111/pce.14425

Schwendenmann, L., Pendall, E., Sanchez-Bragado, R., Kunert, N., & Hölscher, D. (2015). Tree water uptake in a tropical plantation varying in tree diversity: Interspecific differences, seasonal shifts and complementarity. *Ecohydrology*, *8*(1), 1–12. https://doi.org/10.1002/eco.1479

Searle, E. B., Chen, H. Y. H., & Paquette, A. (2022). Higher tree diversity is linked to higher tree mortality. *Proceedings of the National Academy of Sciences of the United States of America*, *119*(19), 1–7. https://doi.org/10.1073/pnas.2013171119

Serrano, L., Peñuelas, J., Ogaya, R., & Savé, R. (2005). Tissue-water relations of two co-occurring evergreen Mediterranean species in response to seasonal and experimental drought conditions. *Journal of Plant Research*, *118*(4), 263–269. https://doi.org/10.1007/s10265-005-0220-8

Sevanto, S., Mcdowell, N. G., Dickman, L. T., Pangle, R., & Pockman, W. T. (2014). How do trees die? A test of the hydraulic failure and carbon starvation hypotheses. *Plant, Cell and Environment*, *37*(1), 153–161. https://doi.org/10.1111/pce.12141

Sha, Z., Bai, Y., Li, R., Lan, H., Zhang, X., Li, J., Liu, X., Chang, S., & Xie, Y. (2022). The global carbon sink potential of terrestrial vegetation can be increased substantially by optimal land management. *Communications Earth and Environment*, *3*(1), 1–10. https://doi.org/10.1038/s43247-021-00333-1

Silvertown, J. (2004). Plant coexistence and the niche. *Trends in Ecology & Evolution*, *19*(11), 605–611. https://doi.org/10.1016/j.tree.2004.09.003

Smith, T. M., & Smith, R. L. (2015). *Elements of ECOLOGY. Ninth Edition* (Global Edi). Pearson.

Sperry, J. S., Hacke, U. G., & Pittermann, J. (2006). Size and function in conifer tracheids and angiosperm vessels. *American Journal of Botany*, *93*(10), 1490–1500. https://doi.org/10.3732/ajb.93.10.1490

Spinoni, J., Vogt, J. V., Naumann, G., Barbosa, P., & Dosio, A. (2018). Will drought events become more frequent and severe in Europe? *International Journal of Climatology*, *38*(4), 1718–1736. https://doi.org/10.1002/joc.5291

Steckel, M., del Río, M., Heym, M., Aldea, J., Bielak, K., Brazaitis, G., Černý, J., Coll, L., Collet, C., Ehbrecht, M., Jansons, A., Nothdurft, A., Pach, M., Pardos, M., Ponette, Q., Reventlow, D. O. J., Sitko, R., Svoboda, M., Vallet, P., … Pretzsch, H. (2020). Species mixing reduces drought susceptibility of Scots pine (Pinus sylvestris L.) and oak (Quercus robur L., Quercus petraea (Matt.) Liebl.) – Site water supply and fertility modify the mixing effect. *Forest Ecology and Management*, *461*(November 2019), 117908. https://doi.org/10.1016/j.foreco.2020.117908

Sun, Q., Klaus, V. H., Wittwer, R., Liu, Y., Van Der Heijden, M. G. A., Gilgen, A. K., & Buchmann, N. (2022). Water uptake patterns of pea and barley responded to drought but not to cropping systems. *Biogeosciences*, *19*(6), 1853–1869. https://doi.org/10.5194/bg-19-1853-2022

Tardieu, F., & Simonneau, T. (1998). Variability among species of stomatal control under fluctuating soil water status and evaporative demand: modelling isohydric and anisohydric behaviours. *Journal of Experimental Botany*, *49*(Special), 419–432. https://doi.org/10.1093/jxb/49.special_issue.419

Teskey, R., Wertin, T., Bauweraerts, I., Ameye, M., McGuire, M. A., & Steppe, K. (2015). Responses of tree species to heat waves and extreme heat events. *Plant Cell and Environment*, *38*(9), 1699–1712. https://doi.org/10.1111/pce.12417

Tomasella, M., Beikircher, B., Häberle, K. H., Hesse, B., Kallenbach, C., Matyssek, R., & Mayr, S. (2018). Acclimation of branch and leaf hydraulics in adult Fagus sylvatica and Picea abies in a forest through-fall exclusion experiment. *Tree Physiology*, *38*(2), 198–211. https://doi.org/10.1093/treephys/tpx140

Tordoni, E., Petruzzellis, F., Di Bonaventura, A., Pavanetto, N., Tomasella, M., Nardini, A., Boscutti, F., Martini, F., & Bacaro, G. (2022). Projections of leaf turgor loss point shifts under future climate change scenarios. *Global Change Biology*, *28*(22), 6640–6652. https://doi.org/10.1111/gcb.16400

Torres-Ruiz, J. M., Diaz-Espejo, A., Morales-Sillero, A., Martín-Palomo, M. J., Mayr, S., Beikircher, B., & Fernández, J. E. (2013). Shoot hydraulic characteristics, plant water status and stomatal response in olive trees under different soil water conditions. *Plant and Soil*, *373*(1–2), 77–87. https://doi.org/10.1007/s11104-013-1774-1

Trugman, A. T., Anderegg, L. D. L., Wolfe, B. T., Birami, B., Ruehr, N. K., Detto, M., Bartlett, M. K., & Anderegg, W. R. L. (2019). Climate and plant trait strategies determine tree carbon allocation to leaves and mediate future forest productivity. *Global Change Biology*, *25*(10), 3395–3405. https://doi.org/10.1111/gcb.14680

Tyree, M T, & Sperry, J. S. (1989). Vunerability of Xylem to Cavitation and Embolism. *Annual Review of Plant Physiology and Plant Molecular Biology*, *40*, 19–38. https://doi.org/10.1146/annurev.pp.40.060189.000315

Tyree, Melvin T., & Ewers, F. W. (1991). The hydraulic architecture of trees and other woody plants. *New Phytologist*, *119*(3), 345–360. https://doi.org/10.1111/j.1469-8137.1991.tb00035.x

Tyree, Melvin T., & Sperry, J. S. (1988). Do Woody Plants Operate Near the Point of Catastrophic Xylem Dysfunction Caused by Dynamic Water Stress? *Plant Physiology*, *88*(3), 574–580. https://doi.org/10.1104/pp.88.3.574

Vadell, E., Pemán, J., Verkerk, P. J., Erdozain, M., & de-Miguel, S. (2022). Forest management practices in Spain: Understanding past trends to better face future challenges. *Forest Ecology and Management*, *524*(July). https://doi.org/10.1016/j.foreco.2022.120526

Valladares, F., & Sánchez-Gómez, D. (2006). Ecophysiological traits associated with drought in Mediterranean tree seedlings: Individual responses versus interspecific trends in eleven species. *Plant Biology*, *8*(5), 688–697. https://doi.org/10.1055/s-2006-924107

Van Der Plas, F., Manning, P., Allan, E., Scherer-Lorenzen, M., Verheyen, K., Wirth, C., Zavala, M. A., Hector, A., Ampoorter, E., Baeten, L., Barbaro, L., Bauhus, J., Benavides, R., Benneter, A., Berthold, F., Bonal, D., Bouriaud, O., Bruelheide, H., Bussotti, F., … Fischer, M. (2016). Jack-of-all-trades effects drive biodiversity-ecosystem multifunctionality relationships in European forests. *Nature Communications*, *7*, 1–11. https://doi.org/10.1038/ncomms11109

Warren, J. M., Brooks, J. R., Meinzer, F. C., & Eberhart, J. L. (2008). Hydraulic redistribution of water from Pinus ponderosa trees to seedlings: Evidence for an ectomycorrhizal pathway. *New Phytologist*, *178*(2), 382–394. https://doi.org/10.1111/j.1469-8137.2008.02377.x

Watson, S. J., Aguirre, B. A., & Wright, A. J. (2023). Soil versus atmospheric drought: A test case of plant functional trait responses. *Ecology*, *May*, 1–15. https://doi.org/10.1002/ecy.4109

Wei, Z., Yoshimura, K., Wang, L., Miralles, D. G., Jasechko, S., & Lee, X. (2017). Revisiting the contribution of transpiration to global terrestrial evapotranspiration. *Geophysical Research Letters*, *44*(6), 2792–2801. https://doi.org/10.1002/2016GL072235

Weides, S. E., Hájek, T., Liancourt, P., Herberich, M. M., Kramp, R. E., Tomiolo, S., Pacheco-Riaño, L. C., Tielbörger, K., & Májeková, M. (2023). Belowground niche partitioning is maintained under extreme drought. *Ecology*, *September*, 1–11. https://doi.org/10.1002/ecy.4198

West, A. G., Patrickson, S. J., & Ehleringer, J. R. (2006). Water extraction times for plant and soil materials used in stable isotope analysis. *Rapid Communications in Mass Spectrometry*, *20*(8), 1317–1321. https://doi.org/10.1002/rcm.2456

Wohlgemuth, T., Doublet, V., Nussbaumer, C., Feichtinger, L., & Rigling, A. (2018). Vegetation shift in Scots pine forests in the Valais accelerated by large disturbances. *Schweizerische Zeitschrift Für Forstwesen*, *169*(5), 260–268.

Wright, A. J., Barry, K. E., Lortie, C. J., & Callaway, R. M. (2021). Biodiversity and ecosystem functioning: Have our experiments and indices been underestimating the role of facilitation? *Journal of Ecology*, *109*(5), 1962–1968. https://doi.org/10.1111/1365-2745.13665

Wright, A., Schnitzer, S. A., & Reich, P. B. (2015). Daily environmental conditions determine the competition-facilitation balance for plant water status. *Journal of Ecology*, *103*(3), 648–656. https://doi.org/10.1111/1365-2745.12397

Wu, T., Tissue, D. T., Li, X., Liu, S., Chu, G., Zhou, G., Li, Y., Zheng, M., Meng, Z., & Liu, J. (2020). Long-term effects of 7-year warming experiment in the field on leaf hydraulic and economic traits of subtropical tree species. *Global Change Biology*, *26*(12), 7144–7157. https://doi.org/10.1111/gcb.15355

Yang, B., Wen, X., & Sun, X. (2015). Seasonal variations in depth of water uptake for a subtropical coniferous plantation subjected to drought in an East Asian monsoon region. *Agricultural and Forest Meteorology*, *201*, 218–228. https://doi.org/10.1016/j.agrformet.2014.11.020

Yates, D., & Strzepek, K. (1994). Potential Evapotranspiration Methods and their Impact on the Assessment of River Basin Runoff Under Climate Change. *IIASA Working Paper*, *WP-94-046*.

Yi, K., Dragoni, D., Phillips, R. P., Roman, D. T., & Novick, K. A. (2017). Dynamics of stem water uptake among isohydric and anisohydric species experiencing a severe drought. *Tree Physiology*, *37*(10), 1379–1392. https://doi.org/10.1093/treephys/tpw126

Zapater, M., Hossann, C., Bréda, N., Bréchet, C., Bonal, D., & Granier, A. (2011). Evidence of hydraulic lift in a young beech and oak mixed forest using 18O soil water labelling. *Trees - Structure and Function*, *25*(5), 885–894. https://doi.org/10.1007/s00468-011-0563-9

Zhang, S., Landuyt, D., Verheyen, K., & De Frenne, P. (2022). Tree species mixing can amplify microclimate offsets in young forest plantations. *Journal of Applied Ecology*, *59*(6), 1428–1439. https://doi.org/10.1111/1365-2664.14158

Zhang, T. Y., Di, D. R., Liao, X. L., & Shi, W. Y. (2023). Response of Forest Plant Diversity to Drought: A Review. *Water*, *15*(19). https://doi.org/10.3390/w15193486

Zhu, S. D., Chen, Y. J., Ye, Q., He, P. C., Liu, H., Li, R. H., Fu, P. L., Jiang, G. F., & Cao, K. F. (2018). Leaf turgor loss point is correlated with drought tolerance and leaf carbon economics traits. *Tree Physiology*, *38*(5), 658–663. https://doi.org/10.1093/treephys/tpy013

Appendix 1

Increasing temperature and vapour pressure deficit lead to hydraulic damages in the absence of soil drought

Leonie Schönbeck[1,2,3], Philipp Schuler[4,5], Laura Mekarni[1,2], Eugénie Mas[1,2], Alexandria Pivovaroff[6], Marco Lehmann[4], Charlotte Grossiord[1,2]

[1]Plant Ecology Research Laboratory PERL, School of Architecture, Civil and Environmental Engineering ENAC, EPFL, Lausanne, Switzerland

[2]Community Ecology Unit, Swiss Federal Institute for Forest, Snow and Landscape WSL, Lausanne, Switzerland

[3]Department of Botany & Plant Sciences, University of California, Riverside, Riverside, California, USA

[4]Forest Dynamics Unit, Swiss Federal Institute for Forest, Snow and Landscape WSL, Birmensdorf, Switzerland

[5]Institute of Agricultural Sciences, ETH Zurich, Zurich, Switzerland

[6]Biology Division, Glendale Community College, Glendale, California, USA

This appendix has been published in the peer-reviewed journal "*Plant, Cell & Environment*"

Schönbeck, L. C., Schuler, P., Lehmann, M. M., Mas, E., Mekarni, L., Pivovaroff, A. L., et al. (2022) Increasing temperature and vapour pressure deficit lead to hydraulic damages in the absence of soil drought. Plant, Cell & Environment, 45, 3275–3289. https://doi.org/10.1111/pce.14425

Abstract

Temperature (*T*) and vapour pressure deficit (VPD) are important drivers of plant hydraulic conductivity, growth, mortality, and ecosystem productivity, indepen- dently of soil water availability. Our goal was to disentangle the effects of T and VPD on plant hydraulic responses. Young trees of *Fagus sylvatica* L., *Quercus pubescens Willd*. and *Quercus ilex* L. were exposed to a cross-combination of a *T* and VPD manipulation under unlimited soil water availability. Stem hydraulic conductivity and leaf-level hydraulic traits (e.g., gas exchange and osmotic adjustment) were tracked over a full growing season. Significant loss of xylem conductive area (PLA) was found in *F. sylvatica* and *Q. pubescens* due to rising VPD and T, but not in *Q. ilex*. Increasing *T* aggravated the effects of high VPD in *F. sylvatica* only. PLA was driven by maximum hydraulic conductivity and minimum leaf conductance, suggesting that high transpiration and water loss after stomatal closure contributed to plant hydraulic stress. This study shows for the first time that rising VPD and *T* lead to losses of stem conductivity even when soil water is not limiting, highlighting their rising importance in plant mortality mechanisms in the future.

Keywords: *Fagus sylvatica*, hydraulic conductivity, PLA, PLC, *Quercus ilex*, *Quercus pubescens*, X-ray micro-CT

A1.1 Introduction

Rising temperatures (T) have caused exponential increases in atmospheric evaporative demand (i.e., vapour pressure deficit [VPD]) in many parts of the world (Dai, 2006; Grossiord, Buckley, et al., 2020), as the air humidity is not increasing at the same speed as the exponentially rising saturation vapour pressure of the atmosphere. As a result, T and VPD have been identified as increasingly important drivers of plant hydraulic conductivity losses (Olson et al., 2020), growth reduction (Trotsiuk et al., 2021), plant mortality (Adams et al., 2009; Allen et al., 2015) and reduced ecosystem productivity (Ciais et al., 2005). Many studies focus on plant responses to a combination of soil drought and either high T ('hot droughts') (Allen et al., 2015; Cochard, 2019; Grossiord et al., 2018; Rehschuh et al., 2021), or high VPD (Anderegg & Meinzer, 2015; Eamus et al., 2013; Fontes et al., 2018). For example, high VPD combined with soil drought leads to extreme xylem tensions and embolisms (Tardieu & Simonneau, 1998). VPD and soil water dynamics are generally closely coupled on timescales from months to seasons (Liu et al., 2020; Novick et al., 2016), but their individual contributions to plant hydraulics on the timescale from days to weeks are not well established. Disentangling T and VPD under field conditions is challenging because higher T inherently increases VPD (Urban et al., 2017). As a result, few studies have isolated the physiological effects of rising VPD versus T on plants without soil moisture stress, limiting our ability to anticipate future impacts on terrestrial ecosystems.

Higher VPD enhances the driving force for water loss from the leaves. When the water demand exceeds the supply, the water potential in the leaves and stems becomes more negative, which below a given threshold, can lead to embolisms in the xylem vessels, in turn causing a loss of hydraulic conductivity (K). Due to species differences in vessel pit structure and width, some species are more vulnerable to embolisms than others (Lens et al., 2011; Tixier et al., 2014). To prevent expensive and sometimes irreparable damages, leaves regulate water loss under high evaporative demand and/or low soil moisture by controlling stomatal opening, thereby regulating leaf and stem water potentials (Martínez-Vilalta et al., 2014). With increasing VPD, leaf stomata close gradually (Jarvis & McNaughton, 1986; Monteith, 1995). Although the exact sensing mechanism involved in stomatal closure to rising VPD is unclear, it is thought to involve changes in the water status in stomatal guard cells mediated by hormonal signals like abscisic acid (Buckley, 2005; McAdam & Brodribb, 2016). While it is generally thought that stomata close to prevent embolisms, the relationship between the two is still under discussion, and it is unknown whether and to what extent embolisms may occur before stomata are fully closed (Hochberg et al., 2017).

The rate at which stomatal closure occurs, that is, the stomatal sensitivity to VPD (m), differs per species and along climatic gradients, with plants adapted to more xeric biomes having lower stomatal sensitivity to changes in VPD (i.e., stomata close more slowly) than those adapted to mesic ones (Martínez-Vilalta et al., 2014; Novick et al., 2016). Yet, how stomatal sensitivity variation

between xeric and mesic species alters hydraulic damages without soil moisture limitation remains unclear. Moreover, stomatal sensitivity can be adjusted in response to enduring environmental stress. For instance, Cardoso et al. (2020) showed that stomatal closure in response to VPD was delayed in plants with lowered leaf osmotic potential. This reduction in osmotic potential is achieved, among others, by accumulating soluble sugars in the cells, which lowers the turgor loss point (ψ_{TLP}), that is, the leaf water potential below which the cells lose turgor and start to wilt. Such a response would allow extended stomatal opening and higher water losses before risking hydraulic failure under high VPD, thereby benefiting carbon assimilation. However, while adjustment of osmotic potential has been documented in roots and leaves in response to soil drought (Schönbeck et al., 2018), it is unknown whether similar mechanisms occur in response to high VPD and/or T under ample water supply.

Even after stomatal closure, water loss continues through incompletely closed stomata and the cuticle (i.e., minimum leaf conductance, g_{min}) (Duursma et al., 2019), representing a significant risk for plants, particularly in the context of rising VPD. The cuticle, meant to serve as a protective leaf shield against water loss, pathogens and UV damage (Kerstiens, 1996; Schuster et al., 2017), still provides a significant alternative pathway for water to exit the leaf, with its conductance even exceeding that of leaky stomata (Gardingen & Grace, 1992). The mechanisms behind g_{min} and the role of the cuticle are still poorly understood, as are the responses of g_{min} to environmental changes. A reduction in g_{min} was observed in response to soil drought and increasing VPD (Bengtson et al., 1978; Drake et al., 2018; Gardingen & Grace, 1992). In response to high T, both steep increases of g_{min} (Schuster et al., 2016) and reduction due to long-term heat stress have been demonstrated (Duursma et al., 2019). Nevertheless, the possible prominent role of g_{min} in total water loss indicates that the mechanism must be considered a final step to plant desiccation under plant stress conditions.

In addition to leaf hydraulic properties, leaf T control is essential to maintain photosynthetic capacity under high T because bio- chemical processes like photosynthesis and respiration have a certain T optimum, below and above which these enzymatic processes slow down (Berry & Bjorkman, 1980). Higher T can induce stomatal opening to provide leaf cooling by evaporation (Urban et al., 2017), and may thus induce opposite effects to high VPD. Thermal tolerance, that is, the ability to photosynthesise under a specific high T (Seemann et al., 1984), might be strongly connected to plant hydraulics and drought tolerance (Gimeno et al., 2009; Knight & Ackerly, 2002), with low thermal tolerance requiring more leaf cooling and resulting in a high water demand under warm conditions. Xeric species adapted to dry conditions may thus have the possibility for stronger leaf cooling without risking hydraulic failure compared to mesic species (Urban et al., 2017). Higher T also decreases water viscosity, allowing higher leaf transpiration rates and possibly exerting more substantial reductions in leaf and stem water potential in addition to high VPD (Cochard, Martin, et al., 2000; Yang et al., 2020).

In this study, our goal was to disentangle the effects of T and VPD on plant hydraulic responses. We exposed well-watered young trees from *Fagus sylvatica L., Quercus pubescens Willd.* and *Quercus ilex,* three species differing in hydraulic safety strategies (Supporting Information: Table SA1.1 and Figure SA1.1), to a cross-combination of a T and VPD manipulation under unlimited soil water availability. We tracked the response of stem hydraulic conductivity and the leaf- level mechanisms that may drive the loss of conductivity (g_s, m, g_{min}, ψ_{leaf}, ψ_{TLP}, leaf sugar concentrations). Specifically, we investigated whether increasing T and VPD would induce hydraulic stress in the form of a higher percentage loss of conductive area (PLA, %) of the stem xylem. We used microcomputed tomography (µCT) to deter- mine PLA and confirmed the method with pressure-flow techniques to assess loss of hydraulic conductance (PLC, %) (Sperry et al., 1988). We compared PLA responses with a range of plant traits (g_s, g_{min}, K_s leaf sugar concentrations, and ψ_{TLP}) to find potential drivers of PLA among all three species. We hypothesised that (1) increasing VPD, independent of T changes and in the absence of soil drought, causes tension on the hydraulic transport system as long as stomata remain open by reducing leaf water potential and inducing loss of xylem conductivity (PLC and PLA) with mesic species being more strongly affected than xeric ones; (2) higher T alone leads to higher foliar transpiration (and little to no stomatal regulation) thereby supporting leaf cooling but causing an aggravating effect on the loss of conductivity in combination with increasing VPD, especially in mesic species with a lower T optimum.

A1.2 Materials and Methods

A1.2.1 Species and experimental setup

Three ecologically and hydraulically contrasting tree species relevant to a wide range of European forest ecosystems were selected for the experiment. On a gradient from mesic to xeric species, these are: the maritime-temperate European beech (*Fagus sylvatica L.*, provenance Biberist, Switzerland, 440–490 m asl), the sub-Mediterranean pubes- cent oak (*Quercus pubescens Willd.*, provenance Leuk, Switzerland, 720–750 m asl), and the Mediterranean holm oak (*Quercus ilex*, provenance Veneto region, Italy, 0–50 m asl) (Supporting Information: Figure SA1.1, Table SA1.1 for ψ_{TLP}, K_{max} and ψ_{P50}). In March 2020, 108 even-sized 3-year-old trees per species were planted from quick-pots into 3 L pots filled with water-retaining soil (40% clay, 25% bark compost, 20% broken puffed clay, 15% peat replacement from wood fibres; Kübelpflanzenerde, RICOTER Erdaufbereitung AG, Aarberg, Switzerland). Quick-pots are tree propagation trays (650 cm3) which allow the roots to stay connected to the soil and not to be disturbed during transplanting. This study used six climate chambers (PGV36, Conviron) at the Phytotron facility of ETH, Zürich, Switzerland, to manipulate air T and VPD using a factorial design, each housing 18 individuals per species. The light roofs of the climate chambers were adjusted in height so that light intensity at canopy height was in all chambers ~390 µmol m−2 s−1. At this light intensity, all three species are at, or approach their light saturation point (Čater & Kobler, 2017; Pena-Rojas et al., 2004; Petersson et al., 2020; Staudt et al., 2003). All plants were regularly (i.e., every 2–3 days) watered by hand to ensure complete soil hydration, and soil volumetric water content (VWC) was manually measured bi-weekly to ensure no soil drought occurred (Supporting Information: Figure SA1.2).

Due to a lockdown during the global pandemic of 2020, the plants were kept in a cool climate chamber (4°C) with 6 h of day length during March and April 2020 to delay bud break until access to the climate chambers was possible in May 2020. The plants were first exposed to an acclimation period of 5 weeks to recover from the transport and leaf flush inside the climate chambers. During this period, all chambers were set to 16 daylight hours, T of 25°C, and relative humidity (RH) of 50%. Nighttime was 6h long with a T of 15°C and RH of 50%. One-hour dawn and dusk occurred between day and night. Air T and humidity were continuously (10 min resolution) measured at canopy height in each chamber with Onset HOBO MX T and RH loggers (Onset computer corporation).

After the acclimation period, three chambers were set to daytime T of 25°C and three to 30°C. Nighttime T was set to 10°C lower than during the day in all chambers (i.e., 15°C and 20°C). Within every T group, chambers were given a low (1 kPa ± 0.3), medium (1.6 kPa ± 0.3), or high (2.2 kPa ± 0.3) daytime VPD treatment by setting RH to reach the desired VPD levels. The highest

VPD level was selected based on the physical limitations of the climate chambers to reach a maximum temperature of 30°C and the minimum RH that could be reached with the addition of a dehumidifier. While a VPD of 2.2 kPa is not excessive compared to what the xeric species in this study experience during the dry season in their natural habitat (Tognetti, Longobucco, et al., 1998), we do believe the range of VPD was sufficient to induce plant hydraulic changes. Because of difficulties in regulating humidity levels in the chambers, RH was kept similar during day and night, even though such conditions are unlikely in real-world conditions. The goal RH was calculated by solving the equation for VPD using the Tetens formula (Monteith & Unsworth 2013). VPD was calculated as the difference between saturated and actual VPD:

$$actual\ VPD = \frac{(RH * VPD_{sat})}{100} \qquad (1),$$

$$VPD_{sat} = 0.6108 * e^{\frac{17.27*T}{T+237.3}} \qquad (2),$$

where VPsat is saturated VP at a given T in °C.

A humidifier was added to the chamber with 30°C + low VPD (to reach 78% RH), and dehumidifiers were used to increase VPD as high as possible in the 25°C and 30°C chambers + high VPD. While all chambers maintained stable T throughout the experiment, the difficulty in manipulating air humidity in the chambers led to slight VPD variation over time (Supporting Information: Figure SA1.2). Despite this, VPD levels were consistently within the set range (0.7–1.3 kPa for low, 1.3–1.9 kPa for medium, and 1.9–2.5 kPa for high VPD) (Figure A1.1 and Supporting Information: Figure SA1.2).

Six plants per chamber and species were randomly selected for repeated physiological measurements. The physiological measure- ments were carried out during four campaigns that were held at a ~5- week interval, with the first campaign just before the start of the treatments: 1–10 June (campaign 1, pretreatment); 13–23 July (campaign 2, +5 weeks); 26 August–4 September (campaign 3, +10 weeks); and 19–31 October (campaign 4, +15 weeks). Across all campaigns, physiological measurements were performed on the same leaf of each individual, unless the leaf wilted or dropped. During each campaign (apart from campaign 3), six randomly selected individuals per chamber and species were harvested for destructive measurements as described below (Supporting Information: Figure SA1.2). The individuals used for physiological measurements were harvested during the last campaign.

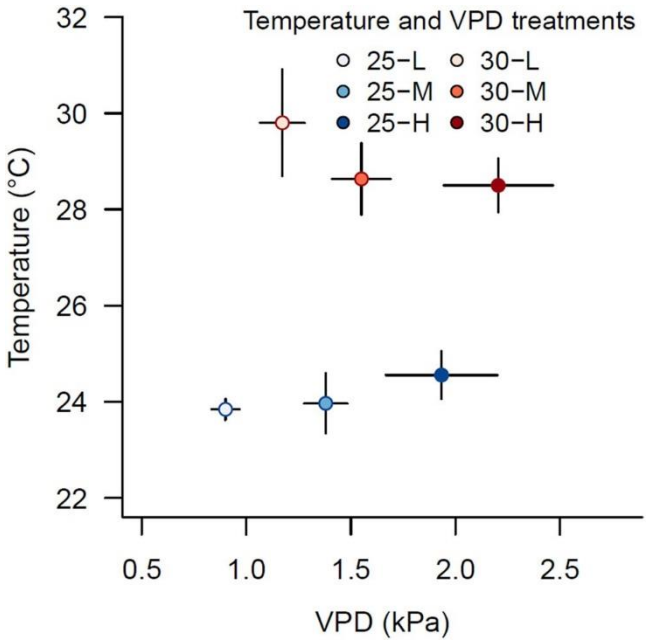

Figure A1.1: Average temperature and vapour pressure deficit (VPD) in the six climate chambers. Plants were exposed to two temperature treatments (25°C and 30°C) and three VPD levels that are defined by low (L), middle (M) and high (H) VPD. Symbols indicate the average (±SD) over the total treatment period (June 1st – November 8th, 2020).

A1.2.2 Stomatal conductance and VPD response

Stomatal conductance (g_s, mmol m−2 s−1) and transpiration (E, mmol m−2 s−1) were measured on each tree selected for repeated physiological measurements (six replicates per species) during each campaign using four LiCor LI-6800 (LiCor Inc.). One leaf was clipped in the cuvette, set to ambient chamber T and RH, with a light intensity of 1500 µmol m−2 s−1 PAR and flow at 500 µmol s−1. While 1500 µmol m−2 s−1 is well above the ambient light conditions in the chambers, using this standard light value during gas exchange measurements ensures cross-comparison with other studies and light-saturation of the trees. The leaf was left acclimating for 20 min or longer if needed to reach stable g_s. The g_s at 400 ppm CO2 was extracted from photosynthesis over CO_2 (A/Ci) measurements, including three log entries at 400 ppm CO_2. The three measurements were then averaged.

Response curves of g_s to VPD variation were measured on five replicates per species by measuring g_s at 75, 60, 45, 30, 15 and 5% RH, with similar light, CO_2, T, and flow as described above. RH was chosen to vary instead of VPD to ensure that the VPD would be solely controlled by RH in the LiCor instrument. Each step included a minimum waiting time of 15 min for *F. sylvatica* and 20 min for both *Quercus* species to allow for g_s stabilisation between each RH step. *F. sylvatica* reached stable g_s faster than the two *Quercus* species. In the chambers with the highest VPD (i.e., lowest humidity), the LiCor devices did not always reach 75% RH. Nonetheless, all g_s to VPD curves started at VPD values <1.1 kPa. The reference g_s at 1 kPa VPD ($g_{s,\,ref}$, mmol m−2 s−1) and

the stomatal sensitivity (m, mmol m−2 s−1 kPa−1) of each tree and each campaign was extracted by fitting logarithmic curves to the data (for detailed curve fitting methods, see Supporting Information: Methods SA1.1, Figures SA1.4 and SA1.5):

$$g_s = -m \times \log(\mathrm{VPD}) + g_{s,ref} \qquad (3)$$

The curve fits resulted in an m to g_s, ref ratio of 0.46, which is slightly lower but close to the suggested ratio of 0.5–0.6 suggested by Oren et al. (1999) (Supporting Information: Figure SA1.5). The g_s to VPD response curves differ from the point measurements in the climate chambers at the ambient VPD levels. The VPD response curves represent the response to rapid changes in VPD (over 2 h), while the point measurements represent the long-term acclimation of g_s to different VPD levels. In addition, the VPD response curves were done over a more extensive range of VPD levels (0.8–3.5 kPa) than the chambers could reach (1–2.2 kPa) (see also Supporting Information: Methods SA1.1).

A1.2.3 Minimum leaf conductance (g_{min})

Minimum leaf conductance (Kerstiens, 1996) was measured as described in Pearcy and Zimmermann (2000). One leaf per individual was cut before dawn when stomata were assumed to be still closed. The cut petiole was immediately sealed with melted candle wax, and the leaf area was scanned using a flatbed scanner, followed by analysis using Pixstat (Schleppi, 2021). The leaves were stuck to a lab tape run between two lab stands, standing in a small dark climate chamber with stable T (26°C) and humidity (60%) and the ventilation on. Every 15–20 min, the leaves were taken from the climate chamber and weighed in a dark room using a fine-precision scale (Mettler-Toledo). This procedure was repeated eight times. g_{min} (mmol m−2 s−1) was calculated as cuticular transpiration per mole fraction VPD, assuming the leaf internal air to be fully saturated (Pearcy & Zimmermann, 2000).

A1.2.4 Pressure volume curves and leaf water potential at predawn and midday

Pressure-volume curves were determined using the bench- dehydration method (Koide et al., 2000). Before dawn, a leaf from the top of the crown was cut off and immediately sealed in a plastic bag (Whirlpak) that was previously exhaled. Predawn water potential (kPa) was measured directly using a Scholander-type pressure chamber (PMS Instrument Company, Model 1505D). The same leaf was immediately weighed using a fine-precision scale (Mettler- Toledo), placed in a plastic bag, and allowed to dry progressively in the open plastic bag on a lab bench. The procedure of measuring water potential, weighing, and drying was repeated with increasing drying time intervals (from 10 s to 1 h) for the two *Quercus* species until achieving water potentials of about −4 MPa or until water potential reached a plateau. For *Fagus sylvatica*, the procedure was repeated continuously without letting the leaves dry on the bench due to the rapid water loss and a

corresponding drop in leaf water potential. Subsequently, the leaves were individually put in a paper bag and dried in an oven at 60°C for 24 h to determine the dry mass. Leaf water potential at turgor loss point (Ψ_{TLP}, MPa) was calculated after Koide et al. (2000). At midday, another leaf was cut off from the same individuals, and midday water potential (Ψ_{md}) was measured.

A1.2.5 Percent loss of conductive area (PLA)

On the three harvest dates (June, July and October), six trees per chamber and species were transported to the Interdisciplinary Platform for X-ray microcomputed tomography (µCT) (PIXE, EPFL) and stored in a cool room in the absence of direct light (to avoid transpirational water loss), until they were scanned. For the µCT scanning, the tree was fixed in a custom-built plant holder, and its branches were wrapped in cling film to prevent movements during the measurements that could alter the quality of the images. A 1 cm part of the stem to be scanned at approximately 40 cm height was marked with tape before starting the measurements. The tree was then moved onto the scanning platform and scanned at 80 keV and 87 µA in the RX-Solutions Ultratom X-ray scanner using a Hama- matsu 230 kV X-ray tube in reflection mode. The sapling rotated in0.22° increments during the scan, yielding between 1400 and 1600 two-dimensional projections with a ~5–7 mm pixel resolution. The acquired longitudinal projections were reconstructed (Filtered back- projection) into a ‘stack’ of multiple transverses TIF images using Xact (RX-Solutions, version 2.0 R9901). After scanning, the scanned part of the stem was cut and flushed with 1 bar air pressure for 1.5 min and subsequently scanned again to obtain a fully embolized stem cross-section as a reference that allowed us to visualise all vessels in the sapwood (Figure A1.2).Image analysis was done with the Avizo software (2019.4). The assessment was done on one image located in the middle of the scanned volume, as we found no significant differences between the bottom, top and middle of the 1 cm stem portion during preliminary tests. The area of interest was selected by excluding bark and phloem (Figure A1.2). Segmentation was performed by defining a selection threshold such that most of the air around the stem was chosen as a reference, without including any material on the bark and making sure that the concurrently selected void vessels did not merge due to a wide selection range. A visual assessment of each scan followed the automated threshold tool segmentation to assess scan quality, artifacts and white level. PLA (%) was calculated as the total embolized area in the intact stem divided by the total vessel area in the flushed stem (x100%). Due to flushing, some stem samples had shrunk. A correction factor was used to control the stem area of the shrunk sample. To estimate the impact of the treatments over time, we used the average PLA per species and chamber from the first harvest (i.e., to account for potential cavitation present before the treatments started) and deducted these values from the results of the second and third harvest (dPLA, %).

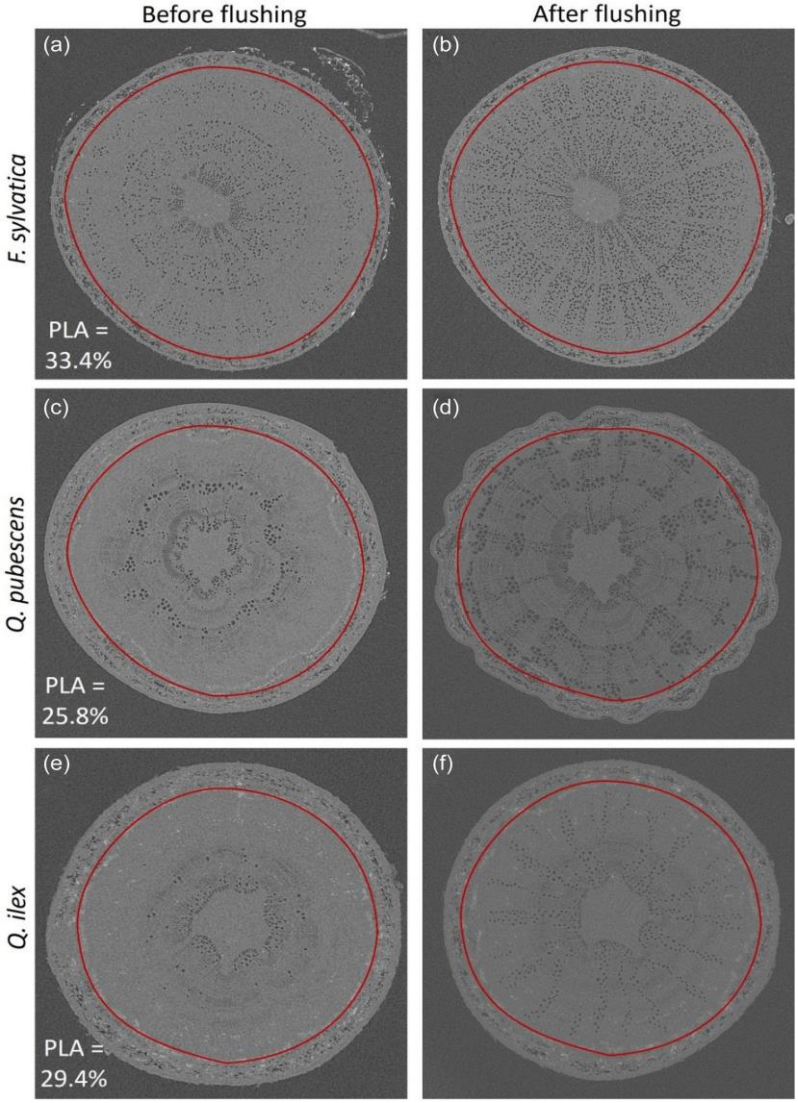

Figure A1.2: Microcomputed tomography images of stem sections of *Fagus sylvatica* (a, b), *Quercus pubescens* (c, d) and *Quercus ilex* (e, f) on the intact stems (a, c, e) and after flushing the stem segments with air at high pressure (b, d, f). Black areas indicate air-filled vessels. Grey areas indicate wood and water-filled sections. The red circles indicate the area of interest, including only the xylem and excluding bark and phloem. Percent loss of conductive area (PLA) was calculated as embolized vessel area/total vessel area × 100%. [Color figure can be viewed at wileyonlinelibrary.com]

A1.2.6 Percent loss of conductivity (PLC)

On the last harvest, after the trees were scanned by the µCT, the stem was cut immediately above the scanned part to measure the hydraulic conductivity. These measurements were done to confirm the methodology and results of the µCT scans. Hydraulic conductiv- ity (K, kg m s−1 MPa−1) was measured using a commercial XYL'EM Plus apparatus (Bronkhorst) according to the method described by Sperry et al. (1988). The branch was recut underwater and left in the water for at least 30 min to relax xylem tension in the branch segment. The segment was then cut to its final size. Its proximal end was connected to the tubing system of the XYL'EM, which was filled with deionized filtered and degassed water with 10 mM KCl and 1 mM CaCl2, flowing from an elevated

source. Initial hydraulic conductivity (K_i, kg m s−1 MPa−1) was recorded. The stem segment was then flushed with water at 1.5 bar for 1 min to remove emboli, and its maximum hydraulic conductivity (K_{max}, kg m s−1 MPa−1) was measured. A second flush at 1.5 bar for 30 s followed by a measurement was done to confirm the maximum hydraulic conductivity value. Percentage loss of conductivity (PLC, %), a direct estimate of the percentage of embolized vessels (Cochard, Bodet, et al., 2000), was calculated as

$$PLC(\%) = \frac{Km - Ki}{Km} \times 100\% \quad (4)$$

A1.2.7 Leaf sugar concentrations

At each destructive sampling campaign (i.e., first, second and last campaign), four leaves per individual were dried in an oven at 60°C until reaching stable weight. The leaf material was homogenised with a ball mill. Sugar concentrations were determined with an enzymatic extraction method described by Wong (1990) and adapted according to Hoch et al. (2002). The sugars measured using this method are defined as low molecular weight sugars (glucose, fructose and sucrose). 10–12 mg of ground material was boiled in 2 ml distilled water for 30 min. After centrifugation, an aliquot of 200 µl was treated with Invertase and Isomerase from baker's yeast (Sigma- Aldrich) to degrade sucrose and convert fructose into glucose. The total amount of glucose (sugars) was determined photometrically at 340 nm in a 96-well microplate photometer (HR 7000, Hamilton) after enzymatic conversion to gluconate-6-phosphate (hexokinase reaction, hexokinase from Sigma Diagnostics). Pure glucose-, fructose- and sucrose- solutions were used as standards, and standard plant powder (Orchard leaves, Leco) was included to control the reproducibility of the extraction. Sugar concentrations are expressed on a percent dry matter basis. Because all samples were run in a single laboratory with no change in protocol during the processing, issues with comparing results across methods or labs were obviated (Quentin et al., 2015).

A1.2.8 Statistical analysis

The similarities between PLA and PLC measurements were tested by fitting a linear model to the data with PLA explaining PLC. If the confidence interval of the slope includes 1, a 1:1 relationship between PLA and PLC is assumed.

Treatment differences

Data were analyzed for each species separately. A mixed-effect model was carried out for each parameter (excl. dPLA and PLC, see below) with T, VPD, and campaign (only the three measurement campaigns after the start of treatment) as fixed factors, including all interactions while controlling for repeated measures on the tree individual (included as a random factor). The model was then analyzed using a type-3 ANOVA using Satterthwaite’s estimation. The timepoint did not

show any significant interactions with the treatments. Thus, it was decided to pool all data of the three campaigns. A two-way ANOVA without mixed effects (no repeated measurements) was used for dPLA and PLC, with T and VPD, including their interaction, as explanatory variables.

Correlations between plant physiological parameters

To relate PLA to different leaf-level hydraulic characteristics that may drive the loss of conductivity, correlation analyses were carried out for PLA paired with all other parameters: E, g_s, g_{min}, m, ψ_{TLP}, ψ_{md}, $K_{s,max}$, and sugar concentration in the leaves. Data for all species were pooled. For significant correlations ($p < 0.05$), the parameters were plotted, and a regression line was added to illustrate the relationship between the two.

A1.3 Results

A1.3.1 Correlation between PLA and PLC

The percent loss of conductivity (PLC, %) measured with the pressure-flow technique and the percent loss of conductive area (PLA, %) measured using µCT were strongly correlated (Fig. A1.3). The regression line did not significantly deviate from the 1:1 line, indicating the µCT method is reliable and comparable to the pressure-flow technique (Nolf et al. 2017). We will focus mainly on the PLA results in the following sections because PLC was only measured in the last campaign, while PLA was measured during three campaigns.

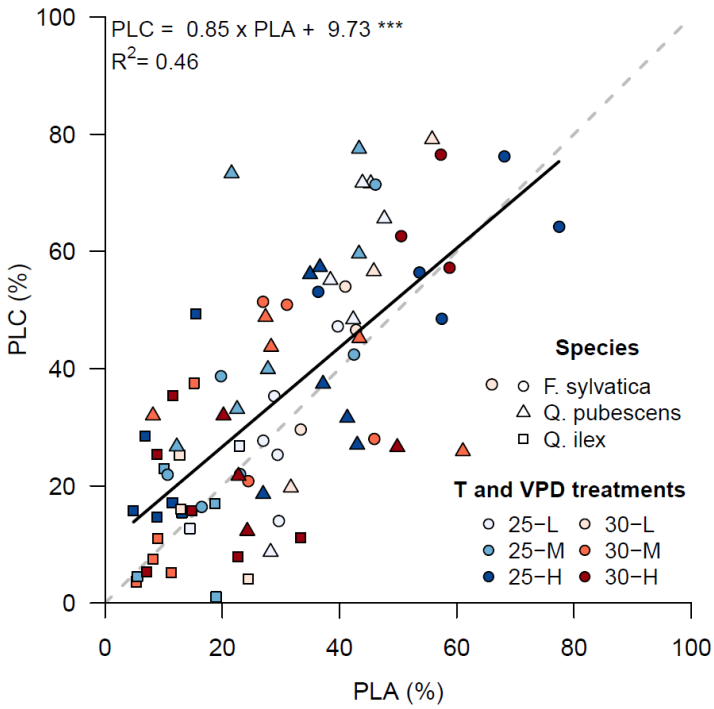

Figure A1.3: Relationship between the percentage loss of conductive area (PLA, %), measured using micro-computed tomography, and the percentage loss of conductivity (PLC, %), calculated using hydraulic conductivity measurements. Symbols indicate species and colors indicate temperature and VPD treatments. The dashed grey line indicates the 1:1 ratio. The black line indicates the fitted regression line. Confidence interval of the slope was 0.65 – 1.05, indicating no significant deviation from the 1:1 line.

A1.3.2 VPD and T effects on plant hydraulics

F. sylvatica: Increased VPD and T significantly raised the loss of hydraulic conductance (dPLA, the difference between pre-treatment and during-treatment PLA, and PLC) in *F. sylvatica* (Fig. A1.4, Table SA1.2). High VPD caused a decrease in $\psi_{leaf,pd}$, $\psi_{leaf,md}$, and g_{min} (Figs. A1.4 & A1.5, Table SA1.2 & SA1.3), but the latter only in the 30°C chambers. Higher T reduced $\psi_{leaf,md}$, and interacted with VPD, causing even stronger reductions of $\psi_{leaf,md}$ with higher VPD. Transpiration (E) increased with rising VPD, but no effect of T was observed. T but not VPD was found to affect

stomatal sensitivity (m), where m was higher at 30°C than at 25°C. No impact of T or VPD was seen on ψ_{TLP} and g_s, although a decreasing trend with higher VPD was visible for the latter.

Q. pubescens: dPLA increased with rising VPD in *Q. pubescens* and was lower at 30°C than 25°C (Fig. A1.4, Table S2). No treatment effects were found for PLC. Higher VPD caused an increase in E and a reduction in $\psi_{leaf,md}$, and ψ_{TLP}. An interaction between T and VPD affected ψ_{TLP}, where ψ_{TLP} decreased with higher VPD only in the 30°C chambers (Fig. A1.5, Table SA1.3). m was higher and $\psi_{leaf,pd}$ was lower at 30°C than at 25°C (Figs. A1.4 & A1.5). No VPD or T effects were found for g_s, or g_{min} (Fig. A1.5).

Q. ilex: VPD did not affect either dPLA or PLC (Fig. A1.4, Table SA1.2), nor E, m, g_s, or g_{min} (Fig. A1.5, Table SA1.3). g_{min} and $\psi_{leaf,pd}$ were slightly lower in the 30°C than the 25°C chambers. As for *Q. pubescens*, ψ_{TLP} decreased with increasing VPD but only in the 30°C chambers (Fig. A1.5, Table SA1.3).

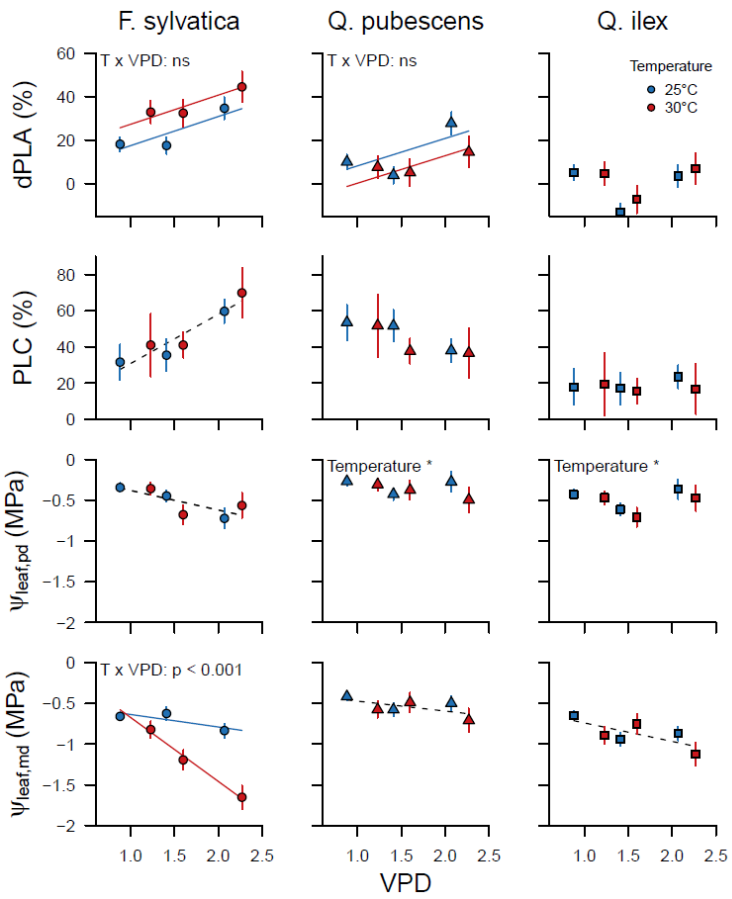

Figure A1.4: Percentage loss of conductive area, calculated as the change in PLA from the start of the experiment (dPLA, %total 2dembolized - %embolized at campaign 1), percentage loss of conductivity (PLC) and predawn and midday leaf water potential ($\psi_{leaf,pd}$ & $\psi_{leaf,md}$) in *Fagus sylvatica, Quercus pubescens* and *Quercus ilex* in the two temperature and three VPD treatments. Data are shown in relation to the average VPD in the chambers during the treatment period. Symbols indicate the mean ± SE of the three measurement campaigns (n = 18), except for PLC which was measured once at the end of the experiment (n = 6). Dashed lines indicate significant VPD effects without temperature effects. Colored lines – blue for 25°C and red for 30°C – indicate an additive (T x VPD: ns) or interacting (T x VPD: $p < 0.05$) temperature effect in addition to VPD.

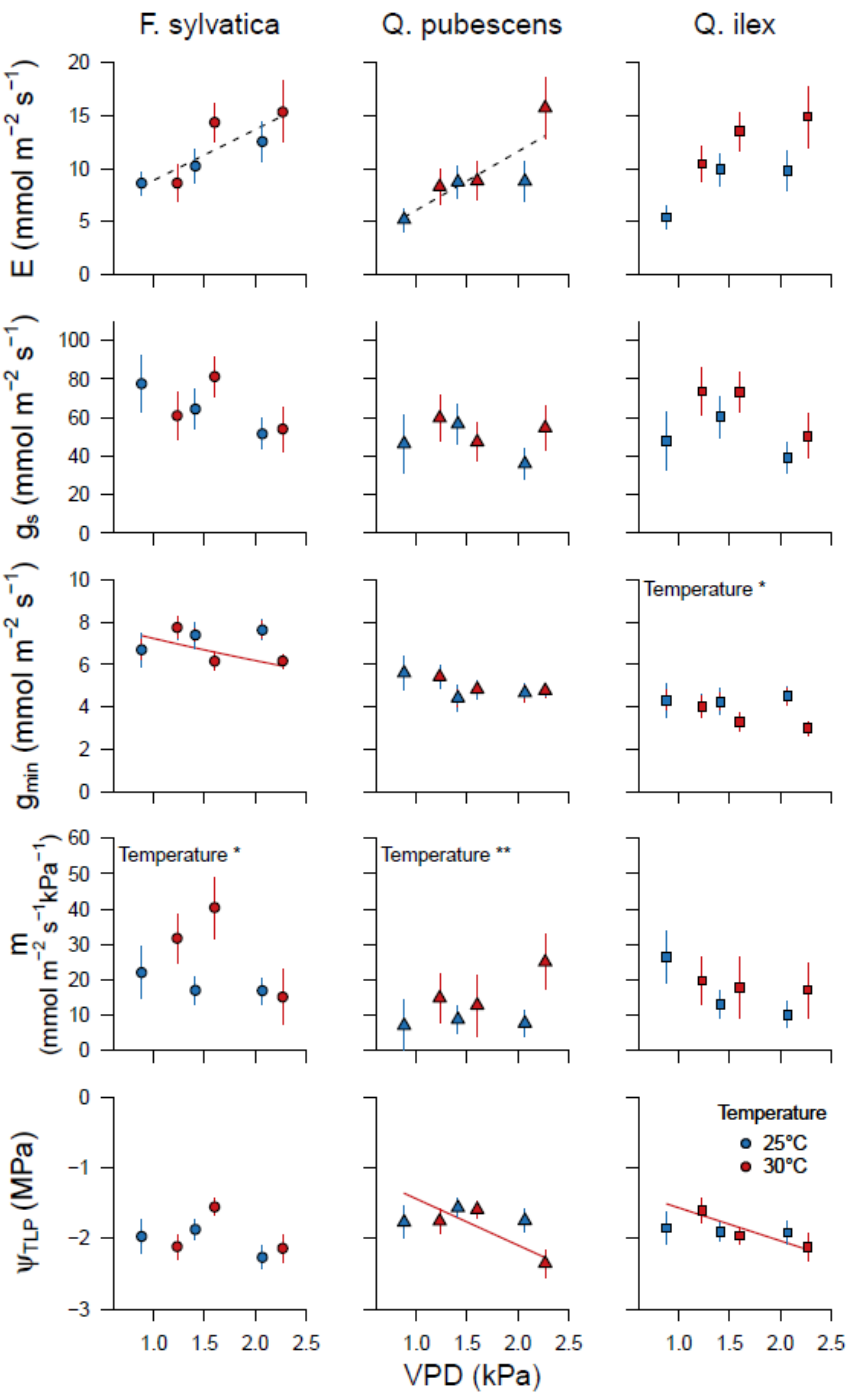

Figure A1.5: Transpiration (E), stomatal conductance (g_s), minimum leaf conductance (g_{min}), sensitivity of g_s to VPD (m) and turgor loss point (ψ_{TLP}) in *Fagus sylvatica, Quercus pubescens* and *Quercus Ilex* in the two temperature and three VPD treatments. Data are shown in relation to the average VPD in the chambers during the treatment period. Symbols indicate the mean ± SE of three measurement campaigns (n = 18). Dashed lines indicate significant VPD effects without temperature effects. Colored lines – blue for 25°C and red for 30°C – indicate the VPD effects in the separate temperature treatments in case of a T x VPD interaction. In case of absence of a VPD effect, temperature effects are indicated with asterisks (*: $p < 0.05$; **: $p < 0.01$; ***: $p < 0.001$).

A1.3.3 Correlation between PLA and leaf traits

Across all species, PLA was positively correlated with g_{min}, K_{max}, and sugar concentrations in the leaves, indicating that higher water transport rates, evaporative water loss, and osmotic potential were related to higher embolism rates (Fig. A1.6). However, the correlations between PLA and K_{max} or sugar concentrations were only found in the 30°C treatments, suggesting that enhanced water transport (potentially leading to higher E) and osmotic potential (potentially delaying stomatal closure) only drive increased PLA when the temperature is high. In addition, more negative $\psi_{leaf,md}$ were correlated to higher PLA, but only in the 30°C chambers, indicating that higher tension within the conductive leaf tissues (because of sustained stomatal opening) translated to higher levels of stem xylem embolism (Fig. A1.6). No correlation was found between PLA and g_s, m and ψ_{TLP}

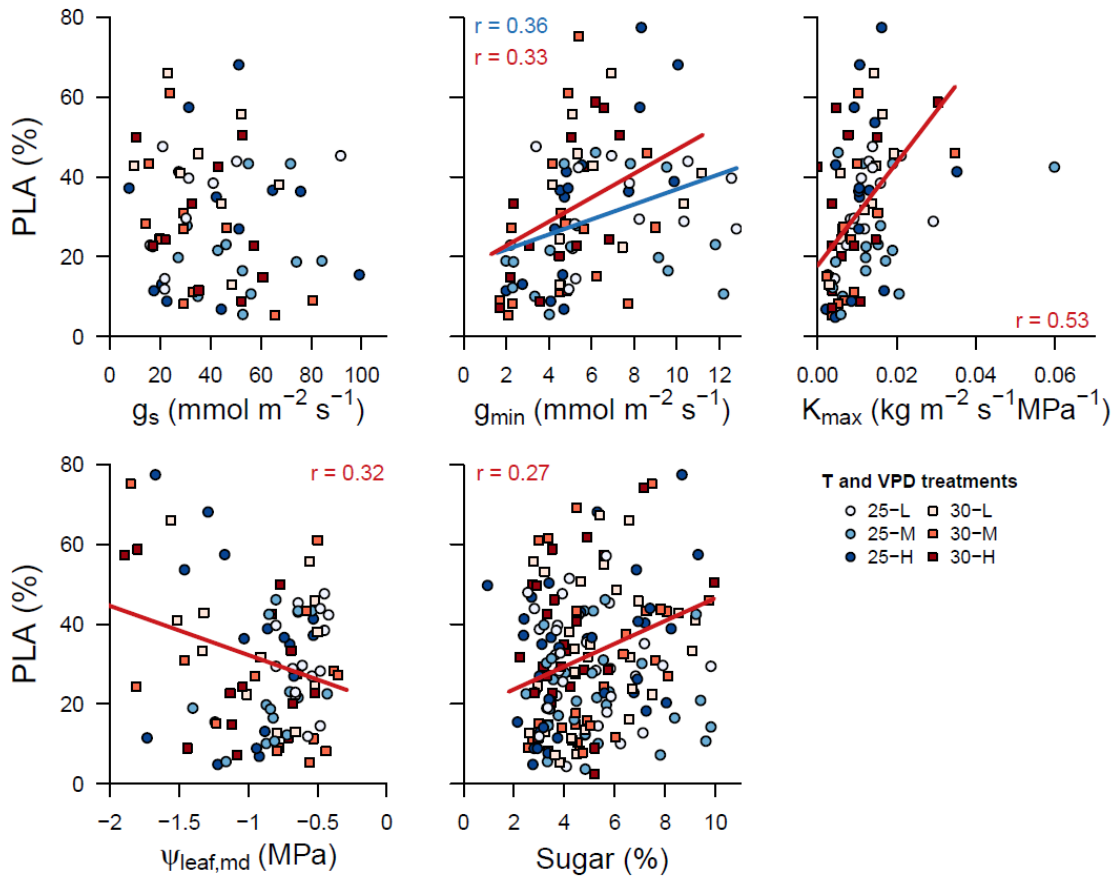

Figure A1.6: Correlation analysis of PLA with stomatal conductance (g_s), minimum leaf conductance (g_{min}), maximum hydraulic conductance of the stem (K_{max}), water potential of the leaf at midday ($\psi_{leaf,md}$) and sugar concentrations in the leaves. Colored lines indicate significant correlations within the corresponding temperature treatment (blue for 25°C and red for 30°C). Analyses were done with all species pooled.

A1.4 Discussion

A1.4.1 Effects of increasing VPD and temperature on the plant hydraulic system in the absence of soil drought

For the first time, we disentangled the effects of temperature (T), vapor pressure deficit (VPD), and their interactions in the absence of soil drought on plant hydraulic traits. Doing so is rare due to the tight relationship between T and VPD in nature. We show that rising T and VPD can cause major hydraulic dysfunctions in trees without soil drought. This was demonstrated by the significant loss of xylem conductive area and conductivity (PLA and PLC, respectively) in *F. sylvatica* and *Q. pubescens* and the increasingly negative leaf water potential ($\psi_{leaf,md}$) in all species with increasing VPD and T (Fig. A1.4). Considering that this study covered only one growing season and that VPD and T levels were moderate compared to the extreme conditions that occur in nature (e.g., the 2018 hot drought in Europe) (Fu et al. 2020; Senf & Seidl 2021), these results highlight the severe threat that chronic VPD and T rise pose on mesic trees, even without any changes in precipitation. Given the high reliability of T predictions in climate models, compared to the uncertainties associated with precipitation (IPCC 2021), these results are particularly relevant for modeling forest ecosystem functioning. While understanding how VPD and T affect plant function is fundamental, it is important to note that our experimental design limits our ability to extend these results to real-world implications. In the field, elevated VPD for several weeks would most likely lead to reduced soil moisture.

We expected to see an increasing gradient in PLA from xeric towards mesic species in response to rising T and VPD, due to differing hydraulic strategies and adaptations (Meyer, Buras, Rammig & Zang 2020), with more extensive T and VPD effects on mesic *F. sylvatica* than the rather xeric *Q. pubescens* and *Q. ilex*. Indeed, 30°C and high VPD (2.2 kPa) exposed *F. sylvatica* to ψ_{leaf} close to its turgor loss point (-2 MPa, Figs. A1.4 & A1.5, Table SA1.1). Combined with barely declining g_s and no change in sugar concentration, the absence of stomatal closure and osmotic adjustments increased PLA and PLC. Our results correspond to earlier findings where VPD levels as low as 1.4 kPa caused biomass and ψ_{leaf} -reduction in *F. sylvatica* (Lendzion & Leuschner 2008). Moreover, the lack of leaf-level acclimation (e.g., stomatal closure or adjustment of turgor loss point) was previously observed in *F. sylvatica* during soil drought (Backes & Leuschner 2000; Thomas 2000; Schipka, Heimann & Leuschner 2005; Pflug et al. 2018). Our observations that transpiration (E) continues even at high levels of embolism (Fig. A1.5) were confirmed in adult *F. sylvatica* trees in Switzerland (Walthert et al. 2021). In this study, the authors further suggested that *F. sylvatica* does not prevent water loss and embolism by leaf physiological acclimation or shedding but sheds its leaves only after embolism has occurred (Walthert et al. 2021). Recently, Zhu et al. (2022) showed how *F. sylvatica* leaf traits were driven by previous years' VPD over a record of 25 years, suggesting a strategy of leaf shedding and regrowth rather than acclimation during the current year. Overall, our work indicates that the strategy of *F. sylvatica* results in a high risk for hydraulic failure under moderate atmospheric stress (Burkhardt & Pariyar 2016). Together

with the slow recovery capability of this species after stress exposure (Hacke & Sauter 1996), these findings highlight its high sensitivity to projected climate (Dittmar, Zech & Elling 2003; Geßler, Keitel, Nahm & Rennenberg 2004).

For *Q. pubescens*, PLA increased with rising VPD, although it was generally lower than in *F. sylvatica*. $\psi_{leaf,md}$ did not reach values lower than -1 MPa, indicating a reduced T and VPD impact on the hydraulic system compared to *F. sylvatica*. In contrast to *F. sylvatica*, where no physiological adjustment to rising VPD and T was found, *Q. pubescens* lowered its ψ_{TLP} to withstand more negative leaf water potentials and sustain high g_s and E under rising T and VPD. These results indicate a more conservative water use strategy than *F. sylvatica*. *Q. pubescens* is one of the most widespread species in southern Europe and is known for its high thermal tolerance and drought resistance (Wellstein & Spada 2015). Previous studies showed that this species is well protected against heat-induced perturbations (Haldimann & Feller 2004). Yet, our work suggests that rising T and VPD levels, even moderate ones that this species is frequently exposed to in nature, could, to some extent, negatively impact the efficiency of the hydraulic system. Here we wanted to expose different tree species to comparable T and VPD levels to assess species sensitivities. Still, to better understand VPD and T effects in real-world conditions, future work should focus on extreme conditions that southern tree populations are more likely to experience.

Variation between the two xeric *Quercus* species was expected due to their contrasting leaf habit (deciduous vs. evergreen) and xylem conduit size (ring-porous vs. diffuse-porous) (Tognetti, Longobucco & Raschi 1998b). PLA and PLC of *Q. ilex* were, in contrast to *Q. pubescens*, not affected by VPD and T, confirming the low sensitivity of this species to VPD and T, partially due to its smaller, diffuse-porous vessels. This Mediterranean species is highly adapted to dry environments (Barbero, Loisel & Quézel 1992), and the T and VPD levels it was exposed to are likely far from its thermal and hydraulic limits (Fig. SA1.1, Table SA1.1). Moreover, with its tough, evergreen leaves, it reaches photosynthetic efficiency both in cool winter T and dry summers, demonstrating adaptation of the species to a range of extreme conditions far from our experiment (García-Plazaola, Artetxe & Becerril 1999). Its physiological plasticity was shown by reducing g_{min} and ψ_{TLP} in response to increasing T and VPD, respectively, even if these had no impact on PLA. The strong response to these relatively minor changes confirms the rather drought-avoiding behavior of the species (Gullo & Salleo 1990).

A1.4.2 <u>Mechanisms driving PLA</u>

We expected significant leaf-level adjustments in response to VPD and T and a correlation between the leaf-level responses and PLA. These relationships would help identify underlying drivers of hydraulic conductivity changes. Increasing VPD led to higher leaf-level transpiration (E, Fig. A1.5). Still, against our expectations, stomatal conductance and the stomatal sensitivity to VPD (m) showed the most negligible response to T and VPD, neither were they, nor E correlated with PLA (Fig. A1.6). A reason for the absence of stomatal response (g_s and m) to VPD and T in all

species might be a combination of the choice of species and the level of evaporative demand in the climate chambers. In the case of *F. sylvatica*, a moderate increase in VPD in the absence of soil drought didn't lead to stomatal closure but enhanced E, thereby creating tensions within the xylem that sustained embolism formation. The strategies discussed for *F. sylvatica* point to a risk-taking strategy where leaf shedding due to stress would be more likely than stomatal closure to prevent embolisms (Walthert et al. 2021). In contrast, *Q. pubescens* and *Q. ilex* kept their stomates open at the VPD levels in our chambers, but ψ_{leaf} was not sufficiently low to induce embolism. These findings shed new insights into the sequence of hydraulic shutdown in plants. The sequence of stomatal closure, turgor loss, and loss of xylem conductivity have been studied thoroughly in relation to soil drought, where the ψ_{leaf} is a leading indicator for the occurrence of leaf and wood hydraulic pathway failures (Bartlett, Klein, Jansen, Choat & Sack 2016). These findings suggest that 50% PLC approximately coincides with the point where g_s decreases by 95% (ψ_{gs95}), indicating a strong correlation between g_s and PLC. In our study, we could not confirm the strong correlation between hydraulic conductance and g_s, suggesting different pathways in response to atmospheric drought compared to soil drought.

Minimum leaf conductance (g_{min}) was positively correlated with PLA across all species (Fig. A1.6), indicating that plants or species with higher evaporative water loss would have a higher risk for embolisms under rising VPD and T. Interestingly, with increasing T, this correlation was even steeper. g_{min} has long been considered an insignificant factor in crop drought resistance (Kerstiens 1996). However, recent studies provide evidence that g_{min} may be the last hurdle before dehydration, thereby playing a much more important role than previously thought (Duursma et al. 2019). Here we show that g_{min} might be responsible for increased cavitation risk under high VPD, T, and non-limiting soil moisture conditions. The PLA effect of g_{min} might have been exacerbated by the relatively high nighttime VPD levels in our experiment (Fig. SA1.2), compared to natural conditions where relative humidity often approaches 100% during the night. The relatively high VPD and residual water loss from the leaves caused lowered predawn water potentials in *F. sylvatica* even though the soil was fully hydrated (Fig. A1.4). In *F. sylvatica* and *Q. pubescens*, g_{min} rates were approximately 10% of the g_s values (Fig. A1.5), indicating a significant water loss at night or when stomata close. The capability to adjust g_{min} in response to a changing environment could be advantageous for protecting valuable xylem vessels. g_{min} reduction was indeed observed in *F. sylvatica* and *Q. ilex* in response to increasing T and VPD, or T only, respectively (Fig. A1.5), suggesting lower residual water loss in warmer and drier conditions. These results correspond with other studies that have shown a decrease in g_{min} in response to higher evaporative demand (Fanourakis, Heuvelink & Carvalho 2013). It is unknown whether g_{min} changes are caused by the altered chemical composition of the cuticle, increased cuticle deposition, or changing stomatal anatomy in the longer term (Duursma et al. 2019). The relationship between g_{min} and T turns out to be even more complex: rapid increases of g_{min} were observed in response to increasing T (Schuster et al. 2016; Drake et al. 2018), but a negative relationship was found between thermal

tolerance and g_{min} (Schuster 2016), indicating that acclimation to increasing T leads to lower g_{min}. However, g_{min} adjustments in *F. sylvatica* were insufficient in our study to prevent plant dehydration and increase PLA under moderately rising VPD.

Higher PLA was also associated with higher maximum stem hydraulic conductance (K_{max}) across species, supporting previous work that reported increased risk for embolisms with higher water transport capacity (Tognetti et al. 1998b). There was a gradient in K_{max} between *F. sylvatica*, *Q. pubescens*, and *Q. ilex* (0.014, 0.013, 0.007 kg m s-1 MPa-1 resp.), in line with the degree of PLA over those three species (Table SA1, Fig. SA1.6). These results correspond to the safety-efficiency trade-off (Grossiord, Ulrich & Vilagrosa 2020b), whereby high K_{max} provides fast and efficient water transport but with an increased risk of embolism even in the absence of soil moisture stress. The strongest correlation between PLA and K_{max} in the 30°C chambers could be explained by the lower water viscosity at warmer T, as higher water transport rates could lead to faster dehydration and increased PLA (Cochard et al. 2000b).

Interestingly, leaf sugar concentration was also positively correlated with PLA. VPD and T effects were only found on sugar concentrations of *Q. pubescens* (Fig. SA1.6). Increasing T resulted in higher leaf sugar concentrations, probably due to rising assimilation rates as T optima for temperate European *Quercus* species can reach up to ~30-35°C (Daas, Montpied, Hanchi & Dreyer 2008). In contrast, higher VPD resulted in a minor but significant reduction of sugar concentration in the leaves of *Q. pubescens*, thereby reducing the osmotic potential. Trees tend to accumulate sugars in leaves and roots, lower the turgor loss point, and increase the water holding capacity in response to soil drought (Schönbeck et al. 2018). Although for *Quercus* species, an adjustment of ψ_{TLP} was observed, the reduced sugar concentrations suggest that other chemical compounds might be responsible for the reduction in ψ_{TLP}.

A1.4.3 <u>The individual role of T and VPD on plant hydraulics</u>

The aggravating effect of T in interaction with VPD, mainly in *F. sylvatica*, suggests that T and VPD play independent roles in affecting plant hydraulics. However, VPD seems to be the stronger driver of plant hydraulics. PLA, PLC, ψ_{leaf}, E, g_{min}, and ψ_{TLP} were all affected by VPD in one or more species. On the other hand, T appears to aggravate VPD effects (for ψ_{leaf}, g_{min}, ψ_{TLP}) while only acting independently towards PLA and m (Figs. A1.4 & A1.5). Earlier studies confirm that higher T can aggravate the adverse effects of increasing VPD (Barron-Gafford, Grieve & Murthy 2007), as physiological controls for water transport become less effective at higher T (Sermons, Seversike, Sinclair, Fiscus & Rufty 2012). The relationship between T and plant hydraulics is complex and partly indirect: T increases E (Urban et al. 2017), thereby providing leaf cooling in warmer climates. However, against expectation, we did not find an individual role for T in affecting E (Fig. A1.5). This finding indicates that 30°C was insufficient to induce active leaf cooling.

A1.5 Conclusion

For the first time, we show that rising VPD and T can lead to stem conductivity losses even when soil water is not limiting. Although VPD and soil water are often correlated on a monthly to seasonal time scale, our results show the possible outcomes in the case of a heatwave occurring after or during a period of sustained precipitation. Disentangling the effects of VPD and T on plant hydraulics is of the utmost importance, as future T scenarios are well developed. Still, much more uncertainty exists on the air relative humidity. Therefore, predicting the effects of rising atmospheric evaporative demand on plants is challenging. Our findings highlight that VPD and T affect different hydraulic functions, hence having differential consequences that are species-dependent. A prolonged but moderate increase in VPD and, to a certain extent, T led to hydraulic dysfunctions for *F. sylvatica* and *Q. pubescens* because of limited stomatal closure, higher transpiration, and more negative leaf water potentials. Whether these mechanisms are universal across a broad range of species remains to be tested as the relatively mild conditions used in this experiment were insufficient to induce significant xylem tensions for the xeric *Q. ilex* species. Although rising CO_2 levels are thought to possibly compensate for the adverse rising VPD effects by increasing the water use efficiency (Eamus 1991), uncertainties are significant, and further investigation into the interaction between VPD and CO_2 is needed. Nevertheless, our work emphasizes the importance of recognizing VPD and T as dominant drivers of plant functioning, both independently from each other and in interaction, to anticipate future impacts on ecosystems.

A1.6 Acknowledgements

LS, CG, PS, and MML were supported by the Swiss National Science Foundation (P500PB_203127, PZ00P3_174068, and PZ00P2_179978). The Sandoz Family Foundation also supported CG. We thank Prof. Nina Buchmann and Hans-Jürg Lendi for their support and use of the climate chambers. We are thankful to Gary Perrenoud for his help with the µCT measurements.

A1.7 References

Adams H.D., Guardiola-Claramonte M., Barron-Gafford G.A., Villegas J.C., Breshears D.D., Zou C.B., … Huxman T.E. (2009) Temperature sensitivity of drought-induced tree mortality portends increased regional die-off under global-change-type drought. Proceedings of the National Academy of Sciences 106, 7063–7066.

Allen C.D., Breshears D.D. & McDowell N.G. (2015) On underestimation of global vulnerability to tree mortality and forest die-off from hotter drought in the Anthropocene. Ecosphere 6.

Anderegg W.R.L. & Meinzer F.C. (2015) Wood anatomy and plant hydraulics in a changing climate. In Functional and Ecological Xylem Anatomy. (ed U. Hacke), pp. 235–253. Springer International Publishing, Cham.

Backes K. & Leuschner C. (2000) Leaf water relations of competitive Fagus sylvatica and Quercus petraea trees during 4 years differing in soil drought. Canadian Journal of Forest Research 30, 335–346.

Barbero M., Loisel R. & Quézel P. (1992) Biogeography, ecology and history of Mediterranean Quercus ilex ecosystems. In Quercus ilex L. ecosystems: function, dynamics and management. (eds F. Romane & J. Terradas), pp. 19–34. Springer Netherlands, Dordrecht.

Barron-Gafford G.A., Grieve K.A. & Murthy R. (2007) Leaf- and stand-level responses of a forested mesocosm to independent manipulations of temperature and vapor pressure deficit. New Phytologist 174, 614–625.

Bartlett M.K., Klein T., Jansen S., Choat B. & Sack L. (2016) The correlations and sequence of plant stomatal, hydraulic, and wilting responses to drought. Proceedings of the National Academy of Sciences 113, 13098–13103.

Bengtson C., Larsson S. & Liljenberg C. (1978) Effects of water stress on cuticular transpiration rate and amount and composition of epicuticular wax in seedlings of six oat varieties. Physiologia Plantarum 44, 319–324.

Berry J. & Bjorkman O. (1980) Photosynthetic response and adaptation to temperature in higher plants. Annual Review of Plant Physiology 31, 491–543.

Buckley T.N. (2005) The control of stomata by water balance. New Phytologist 168, 275–292.

Burkhardt J. & Pariyar S. (2016) How does the VPD response of isohydric and anisohydric plants depend on leaf surface particles? Plant Biology 18, 91–100.

Cardoso A.A., Brodribb T.J., Kane C.N., DaMatta F.M. & McAdam S.A.M. (2020) Osmotic adjustment and hormonal regulation of stomatal responses to vapour pressure deficit in sunflower. AoB PLANTS 12.

Čater M. & Kobler A. (2017) Light response of Fagus sylvatica L. and Abies alba Mill. in different categories of forest edge – Vertical abundance in two silvicultural systems. Forest Ecology and Management 391, 417–426.

Ciais P., Reichstein M., Viovy N., Granier A., Ogée J., Allard V., … Valentini R. (2005) Europe-wide reduction in primary productivity caused by the heat and drought in 2003. Nature 437, 529–533.

Cochard H. (2019) A new mechanism for tree mortality due to drought and heatwaves. bioRxiv, 531632.

Cochard H., Bodet C., Améglio T. & Cruiziat P. (2000a) Cryo-scanning electron microscopy observations of vessel content during transpiration in walnut petioles. Facts or artifacts? Plant Physiology 124, 1191–1202.

Cochard H., Martin R., Gross P. & Bogeat-Triboulot M.B. (2000b) Temperature effects on hydraulic conductance and water relations of Quercus robur L. Journal of Experimental Botany 51, 1255–1259.

Daas C., Montpied P., Hanchi B. & Dreyer E. (2008) Responses of photosynthesis to high temperatures in oak saplings assessed by chlorophyll-a fluorescence: inter-specific diversity and temperature-induced plasticity. Annals of Forest Science 65, 305.

Dai A. (2006) Recent climatology, variability, and trends in global surface humidity. Journal of Climate 19, 3589–3606.

Dittmar C., Zech W. & Elling W. (2003) Growth variations of Common beech (Fagus sylvatica L.) under different climatic and environmental conditions in Europe—a dendroecological study. Forest Ecology and Management 173, 63–78.

Drake J.E., Tjoelker M.G., Vårhammar A., Medlyn B.E., Reich P.B., Leigh A., … Barton C.V.M. (2018) Trees tolerate an extreme heatwave via sustained transpirational cooling and increased leaf thermal tolerance. Global Change Biology 24, 2390–2402.

Duursma R.A., Blackman C.J., Lopéz R., Martin-StPaul N.K., Cochard H., Medlyn B.E., … Medlyn B.E. (2019) On the minimum leaf conductance: its role in models of plant water use, and ecological and environmental controls. New Phytologist 221, 693–705.

Eamus D. (1991) The interaction of rising CO2 and temperatures with water use efficiency. Plant, Cell & Environment 14, 843–852.

Eamus D., Boulain N., Cleverly J. & Breshears D.D. (2013) Global change-type drought-induced tree mortality: vapor pressure deficit is more important than temperature per se in causing decline in tree health. Ecology and Evolution 3, 2711–2729.

Fanourakis D., Heuvelink E. & Carvalho S.M.P. (2013) A comprehensive analysis of the physiological and anatomical components involved in higher water loss rates after leaf development at high humidity. Journal of Plant Physiology 170, 890–898.

Fontes C.G., Dawson T.E., Jardine K., McDowell N., Gimenez B.O., Anderegg L., … Chambers J.Q. (2018) Dry and hot: the hydraulic consequences of a climate change-type drought for Amazonian trees. Philosophical Transactions of the Royal Society B: Biological Sciences 373, 20180209.

Fu Z., Ciais P., Bastos A., Stoy P.C., Yang H., Green J.K., … Koebsch F. (2020) Sensitivity of gross primary productivity to climatic drivers during the summer drought of 2018 in Europe. Philosophical Transactions of the Royal Society B: Biological Sciences 375, 20190747.

García-Plazaola J.I., Artetxe U. & Becerril J.M. (1999) Diurnal changes in antioxidant and carotenoid composition in the Mediterranean schlerophyll tree Quercus ilex (L) during winter. Plant Science 143, 125–133.

Gardingen P.R. VAN & Grace J. (1992) Vapour pressure deficit response of cuticular conductance in intact leaves of Fagus sylvatica L. Journal of Experimental Botany 43, 1293–1299.

Geßler A., Keitel C., Nahm M. & Rennenberg H. (2004) Water shortage affects the water and nitrogen balance in Central European beech forests. Plant Biol (Stuttg) 6, 289–298.

Gimeno T.E., Pías B., Lemos-Filho J.P. & Valladares F. (2009) Plasticity and stress tolerance override local adaptation in the responses of Mediterranean holm oak seedlings to drought and cold. Tree Physiology 29, 87–98.

Grossiord C., Buckley T.N., Cernusak L.A., Novick K.A., Poulter B., Siegwolf R.T.W., … McDowell N.G. (2020a) Plant responses to rising vapor pressure deficit. New Phytologist 226, 1550–1566.

Grossiord C., Gessler A., Reed S.C., Borrego I., Collins A.D., Dickman L.T., … McDowell N.G. (2018) Reductions in tree performance during hotter droughts are mitigated by shifts in nitrogen cycling. Plant, Cell & Environment 41, 2627–2637.

Grossiord C., Ulrich D.E.M. & Vilagrosa A. (2020b) Controls of the hydraulic safety–efficiency trade-off. Tree Physiology 40, 573–576.

Gullo M.A. Lo & Salleo S. (1990) Wood anatomy of some trees with diffuse- and ring-porous wood: Some functional and ecological interpretations. Giornale botanico italiano 124, 601–613.

Hacke U. & Sauter J.J. (1996) Xylem dysfunction during winter and recovery of hydraulic conductivity in diffuse-porous and ring-porous trees. Oecologia 105, 435–439.

Haldimann P. & Feller U. (2004) Inhibition of photosynthesis by high temperature in oak (Quercus pubescens L.) leaves grown under natural conditions closely correlates with a reversible heat-dependent reduction of the activation state of ribulose-1,5-bisphosphate carboxylase/oxyg. Plant, Cell & Environment 27, 1169–1183.

Hoch G., Popp M. & Körner C. (2002) Altitudinal increase of mobile carbon pools in Pinus cembra suggests sink limitation of growth at the Swiss treeline. Oikos 3, 361–374.

Hochberg U., Windt C.W., Ponomarenko A., Zhang Y.J., Gersony J., Rockwell F.E. & Holbrook N.M. (2017) Stomatal Closure, Basal Leaf Embolism, and Shedding Protect the Hydraulic Integrity of Grape Stems. Plant Physiology 174, 764–775.

IPCC (2021) Climate Change 2021: The Physical Science Basis. Contribution of Working Group I to the Sixth Assessment Report of the Intergovernmental Panel on Climate Change. (eds V. Masson-Delmotte, P. Zhai, A. Pirani, S.L. Connors, C. Péan, S. Berger, N. Caud, Y. Ch. Cambridge, UK and New York, NY, USA: Cambridge University Press.

Jarvis P.G. & McNaughton K.G. (1986) Stomatal control of transpiration: scaling up from leaf to region. Advances in Ecological Research 15, 1–49.

Kerstiens G. (1996) Cuticular water permeability and its physiological significance. Journal of Experimental Botany 47, 1813–1832.

Knight C.A. & Ackerly D.D. (2002) An ecological and evolutionary analysis of photosynthetic thermotolerance using the temperature-dependent increase in fluorescence. Oecologia 130, 505–514.

Koide R.T., Robichaux R.H., Morse S.R. & Smith C.M. (2000) Plant water status, hydraulic resistance and capacitance. In Plant Physiological Ecology: Field Methods and Instrumentation. pp. 161–183. Springer Netherlands, Dordrecht.

Lendzion J. & Leuschner C. (2008) Growth of European beech (Fagus sylvatica L.) saplings is limited by elevated atmospheric vapour pressure deficits. Forest Ecology and Management 256, 648–655.

Lens F., Sperry J.S., Christman M.A., Choat B., Rabaey D. & Jansen S. (2011) Testing hypotheses that link wood anatomy to cavitation resistance and hydraulic conductivity in the genus Acer. The New phytologist 190, 709–723.

Liu L., Gudmundsson L., Hauser M., Qin D., Li S. & Seneviratne S.I. (2020) Soil moisture dominates dryness stress on ecosystem production globally. Nature Communications 11, 4892.

Martínez-Vilalta J., Poyatos R., Aguadé D., Retana J. & Mencuccini M. (2014) A new look at water transport regulation in plants. New Phytologist 204, 105–115.

McAdam S.A.M. & Brodribb T.J. (2016) Linking turgor with ABA biosynthesis: Implications for stomatal responses to vapor pressure deficit across land plants. Plant Physiology 171, 2008–2016.

Meyer B.F., Buras A., Rammig A. & Zang C.S. (2020) Higher susceptibility of beech to drought in comparison to oak. Dendrochronologia 64, 125780.

Monteith J.L. (1995) A reinterpretation of stomatal responses to humidity. Plant, Cell and Environment 18, 357–364.

Monteith J.L. & Unsworth M.H. (2013) Principles of Environmental Physics. Elsevier.

Nolf M., Lopez R., Peters J.M.R., Flavel R.J., Koloadin L.S., Young I.M. & Choat B. (2017) Visualization of xylem embolism by X-ray microtomography: a direct test against hydraulic measurements. New Phytologist 214, 890–898.

Novick K.A., Ficklin D.L., Stoy P.C., Williams C.A., Bohrer G., Oishi A.C., … Phillips R.P. (2016) The increasing importance of atmospheric demand for ecosystem water and carbon fluxes. Nature Climate Change 6, 1023–1027.

Olson M.E., Anfodillo T., Rosell J.A. & Martínez-Méndez N. (2020) Across climates and species, higher vapour pressure deficit is associated with wider vessels for plants of the same height. Plant, Cell & Environment 43, 3068–3080.

Oren R., Sperry J.S., Katul G.G., Pataki D.E., Ewers B.E., Phillips N. & Schäfer K.V.R. (1999) Survey and synthesis of intra- and interspecific variation in stomatal sensitivity to vapour pressure deficit. Plant, Cell & Environment 22, 1515–1526.

Pearcy R.W., E.-D S. & Zimmermann R. (2000) Measurement of transpiration and leaf conductance. In Plant Physiological Ecology: Field Methods and Instrumentation. (eds R.W. Pearcy, J.R. Ehleringer, H.A. Mooney & P.. Rundel), pp. 137–160. Kluwer Academic, Dordrecht, The Netherlands.

Pena-Rojas K., Aranda X. & Fleck I. (2004) Stomatal limitation to CO2 assimilation and down-regulation of photosynthesis in Quercus ilex resprouts in response to slowly imposed drought. Tree Physiology 24, 813–822.

Petersson L.K., Löf M., Jensen A.M., Chastain D.R. & Gardiner E.S. (2020) Sprouts of shoot-clipped oak (Quercus alba and Q. robur) germinants show morphological and photosynthetic acclimation to contrasting light environments. New Forests 51, 817–834.

Pflug E.E., Buchmann N., Siegwolf R.T.W., Schaub M., Rigling A. & Arend M. (2018) Resilient leaf physiological response of European beech (Fagus sylvatica L.) to summer drought and drought release. Frontiers in Plant Science 9, 1–11.

Quentin A.G., Pinkard E.A., Ryan M.G., Tissue D.T., Baggett L.S., Adams H.D., … Woodruff D.R. (2015) Non-structural carbohydrates in woody plants compared among laboratories. Tree Physiology 35, 1146–1165.

Rehschuh R., Rehschuh S., Gast A., Jakab A.-L., Lehmann M.M., Saurer M., … Ruehr N.K. (2021) Tree allocation dynamics beyond heat and hot drought stress reveal changes in carbon storage, belowground translocation and growth. New Phytologist 233, 687–704.

Schipka F., Heimann J. & Leuschner C. (2005) Regional variation in canopy transpiration of Central European beech forests. Oecologia 143, 260–270.

Schleppi P. (2021) Pixstat. https://www.schleppi.ch/pixstat/.

Schönbeck L., Gessler A., Hoch G., McDowell N.G., Rigling A., Schaub M. & Li M.H. (2018) Homeostatic levels of nonstructural carbohydrates after 13 yr of drought and irrigation in Pinus sylvestris. New Phytologist 219, 1314–1324.

Schuster A.-C. (2016) Chemical and functional analyses of the plant cuticle as leaf transpiration barrier.

Schuster A.-C., Burghardt M., Alfarhan A., Bueno A., Hedrich R., Leide J., … Riederer M. (2016) Effectiveness of cuticular transpiration barriers in a desert plant at controlling water loss at high temperatures. AoB PLANTS 8.

Schuster A.-C., Burghardt M. & Riederer M. (2017) The ecophysiology of leaf cuticular transpiration: are cuticular water permeabilities adapted to ecological conditions? Journal of Experimental Botany 68, 5271–5279.

Seemann J.R., Berry J.A. & Downton W.J.S. (1984) Photosynthetic response and adaptation to high temperature in desert plants 1: A comparison of gas exchange and fluorescence methods for studies of thermal tolerance. Plant Physiology 75, 364–368.

Senf C. & Seidl R. (2021) Persistent impacts of the 2018 drought on forest disturbance regimes in Europe. Biogeosciences 18, 5223–5230.

Sermons S.M., Seversike T.M., Sinclair T.R., Fiscus E.L. & Rufty T.W. (2012) Temperature influences the ability of tall fescue to control transpiration in response to atmospheric vapour pressure deficit. Functional Plant Biology 39, 979–986.

Sperry J.S., Donnelly J.R. & Tyree M.T. (1988) A method for measuring hydraulic conductivity and embolism in xylem. Plant, Cell and Environment 11, 35–40.

Staudt M., Joffre R. & Rambal S. (2003) How growth conditions affect the capacity of Quercus ilex leaves to emit monoterpenes. New Phytologist 158, 61–73.

Tardieu F. & Simonneau T. (1998) Variability among species of stomatal control under fluctuating soil water status and evaporative demand: modelling isohydric and anisohydric behaviours. Journal of Experimental Botany 49, 419–432.

Thomas F.M. (2000) Growth and water relations of four deciduous tree species (Fagus sylvatica L., Quercus petraea [MATT.] LIEBL., Q-pubescens WILLD., Sorbus aria [L.] CR.) occurring at Central-European tree-line sites on shallow calcareous soils: physiological reactions of . Flora 195, 104–115.

Tixier A., Herbette S., Jansen S., Capron M., Tordjeman P., Cochard H. & Badel E. (2014) Modelling the mechanical behaviour of pit membranes in bordered pits with respect to cavitation resistance in angiosperms. Annals of botany 114, 325–334.

Tognetti R., Longobucco A., Miglietta F. & Raschi A. (1998a) Transpiration and stomatal behaviour of Quercus ilex plants during the summer in a Mediterranean carbon dioxide spring. Plant, Cell and Environment 21, 613–622.

Tognetti R., Longobucco A. & Raschi A. (1998b) Vulnerability of xylem to embolism in relation to plant Hhdraulic resistance in Quercus pubescens and Quercus ilex co-occurring in a Mediterranean coppice stand in Central Italy. The New Phytologist 139, 437–447.

Trotsiuk V., Babst F., Grossiord C., Gessler A., Forrester D.I., Buchmann N., … Eugster W. (2021) Tree growth in Switzerland is increasingly constrained by rising evaporative demand. Journal of Ecology 109, 2981–2990.

Urban J., Ingwers M.W., McGuire M.A. & Teskey R.O. (2017) Increase in leaf temperature opens stomata and decouples net photosynthesis from stomatal conductance in Pinus taeda and Populus deltoides x nigra. Journal of Experimental Botany 68, 1757–1767.

Walthert L., Ganthaler A., Mayr S., Saurer M., Waldner P., Walser M., … von Arx G. (2021) From the comfort zone to crown dieback: Sequence of physiological stress thresholds in mature European beech trees across progressive drought. Science of The Total Environment 753, 141792.

Wellstein C. & Spada F. (2015) The Status of Quercus pubescens Willd. in Europe. In Warm-Temperate Deciduous Forests around the Northern Hemisphere. (eds E.O. Box & K. Fujiwara), pp. 153–163. Springer International Publishing, Cham.

Wong S.C. (1990) Elevated atmospheric partial pressure of CO2 and plant growth - II. Non-structural carbohydrate content in cotton plants and its effect on growth parameters. Photosynthesis Research 23, 171–180.

Yang Y., Zhang Q., Huang G., Peng S. & Li Y. (2020) Temperature responses of photosynthesis and leaf hydraulic conductance in rice and wheat. Plant, Cell & Environment 43, pce.13743.

Zhu J., Thimonier A., Etzold S., Meusburger K., Waldner P., Schmitt M., … Lehmann M.M. (2022) Variation in leaf morphological traits of European beech and Norway spruce over two decades in Switzerland. Frontiers in Forests and Global Change 4.

A1.8 Supporting information

A1.8.1 Supporting figures

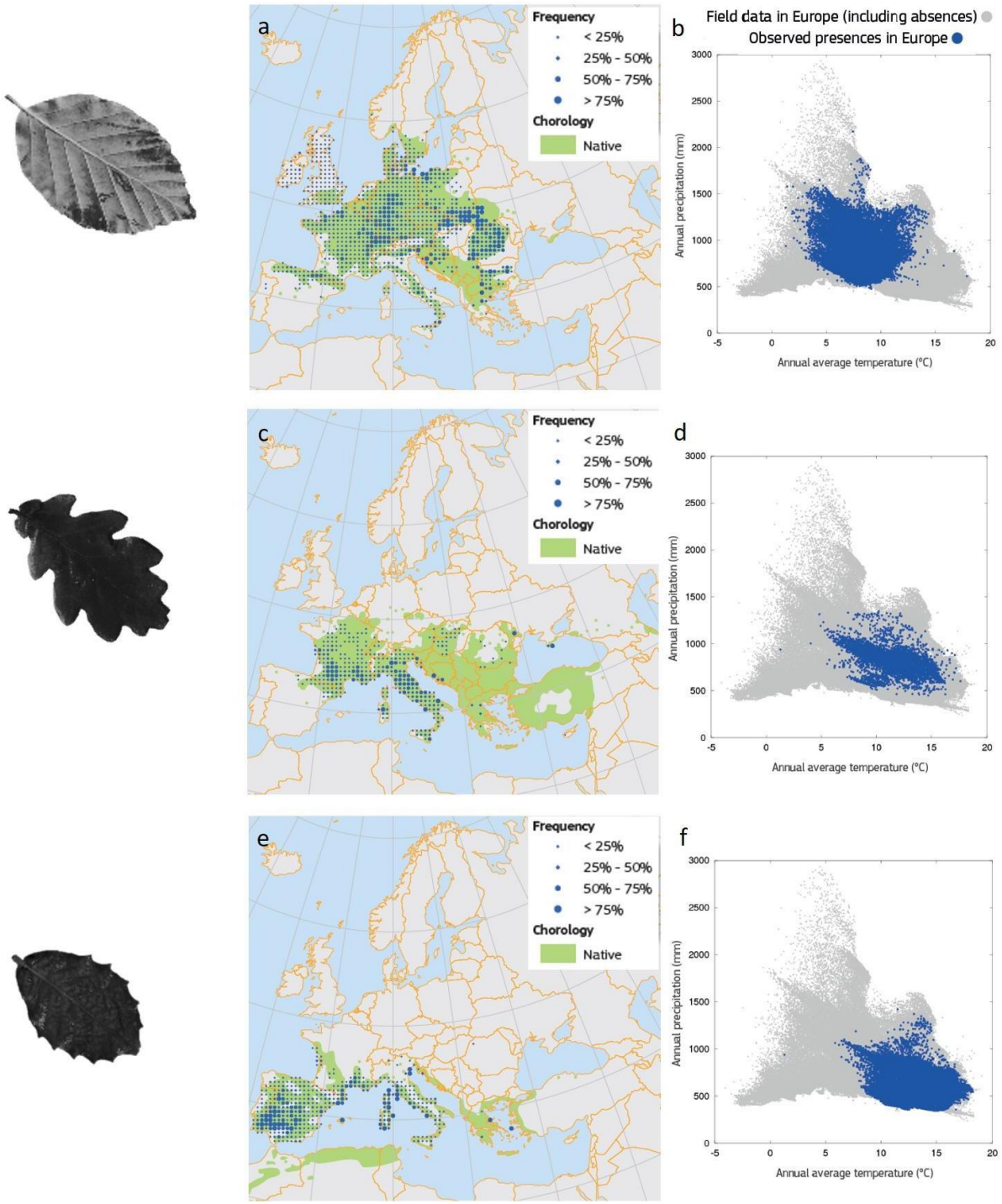

Figure SA1.1: Distribution throughout Europe and the climatic envelopes of *Fagus sylvatica* L. (a, b), *Quercus pubescens* Wildd (c, d), and *Quercus ilex* L. (e, f) (Distribution maps from EUFORGEN, euforgen.org).

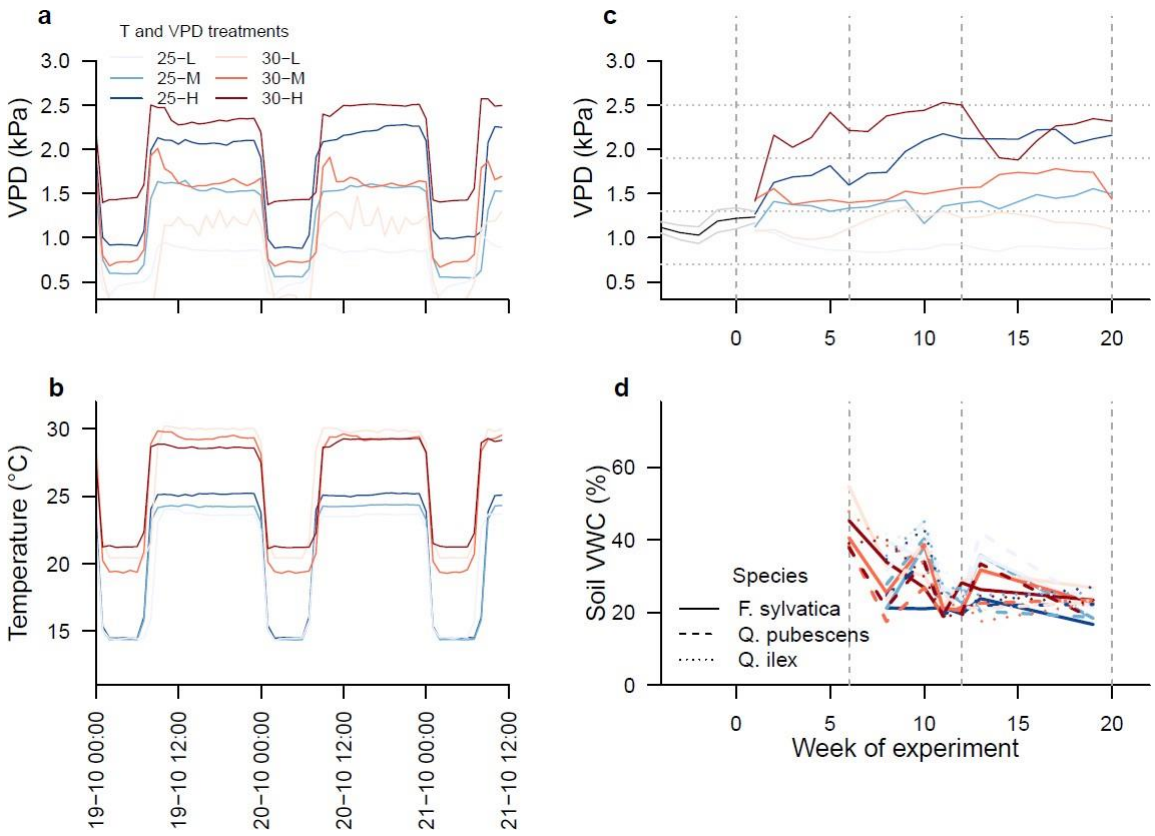

Figure SA1.2: a & b) Example of diurnal patterns over the course of 3 days of VPD (a) and temperature (b) in the six climate chambers; **c)** Weekly means of daytime VPD throughout the experiment. The black line indicates the average VPD in all six chambers during the acclimation period, with the standard error indicated by the grey lines.; **d)** Soil volumetric water content, measured using a TDR 100 Soil Moisture Probe. Line types indicate the three species. In all panels, colors indicate the different T and VPD treatments in the six climate chambers.

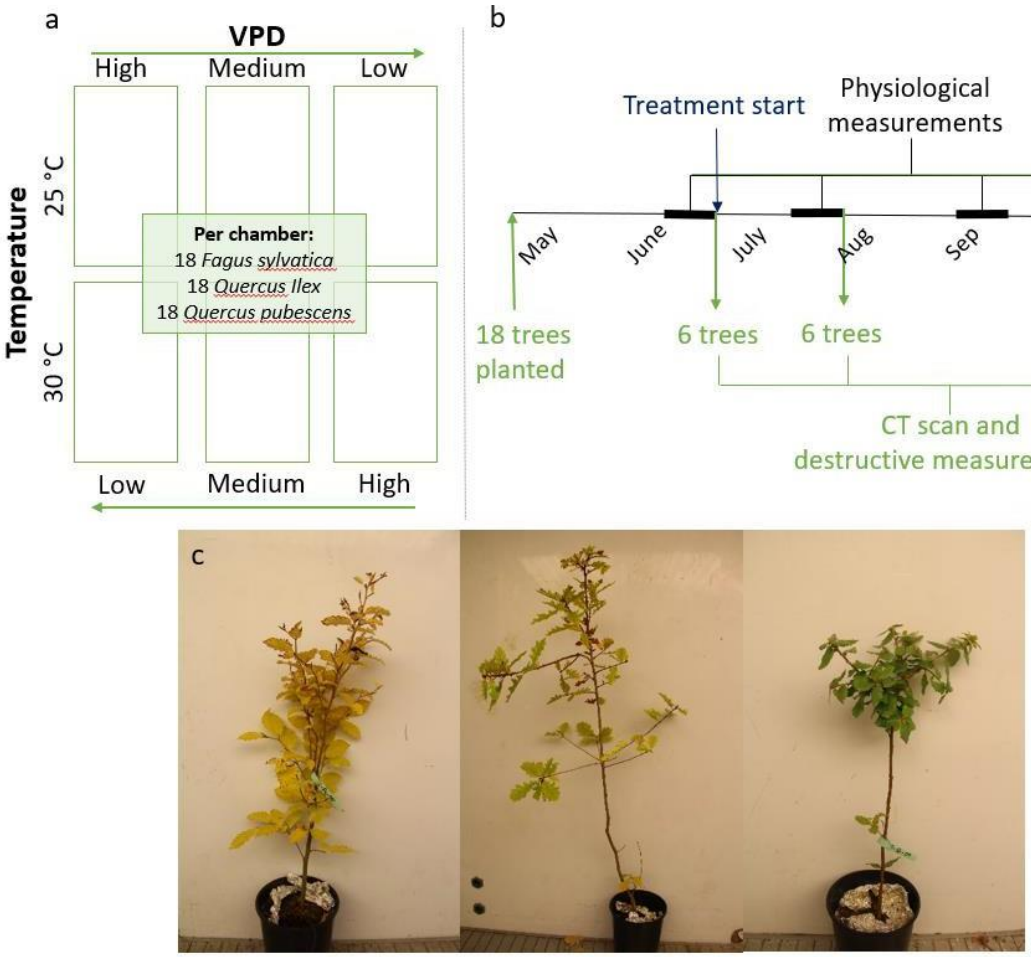

Figure SA1.3: Schematic overview of the experimental setup. a) Climate settings of the six climate chambers, with three chambers set to daytime temperatures of 25°C and three chambers to 30°C. Within each temperature level, chambers were set to low (0.7-1.3 kPa), medium (1.3-1.9 kPa) or high (1.9-2.5 kPa) VPD. b) Timeline of the experiment. All trees were left for acclimation over five weeks at the start of the experiment. The week before the treatments started, physiological measurements were carried out, and six trees per species were harvested and scanned using µCT (campaign 1). After 5, 10, and 15 weeks of treatment, similar physiological measurements were carried out (campaigns 2- 4). After 5 and 15 weeks, another six individuals per species were harvested and scanned using µCT.c) Pictures of an individual of each species *F. sylvatica* (l), *Q. pubescens* (m), and *Q. ilex* (r) before the final harvest.

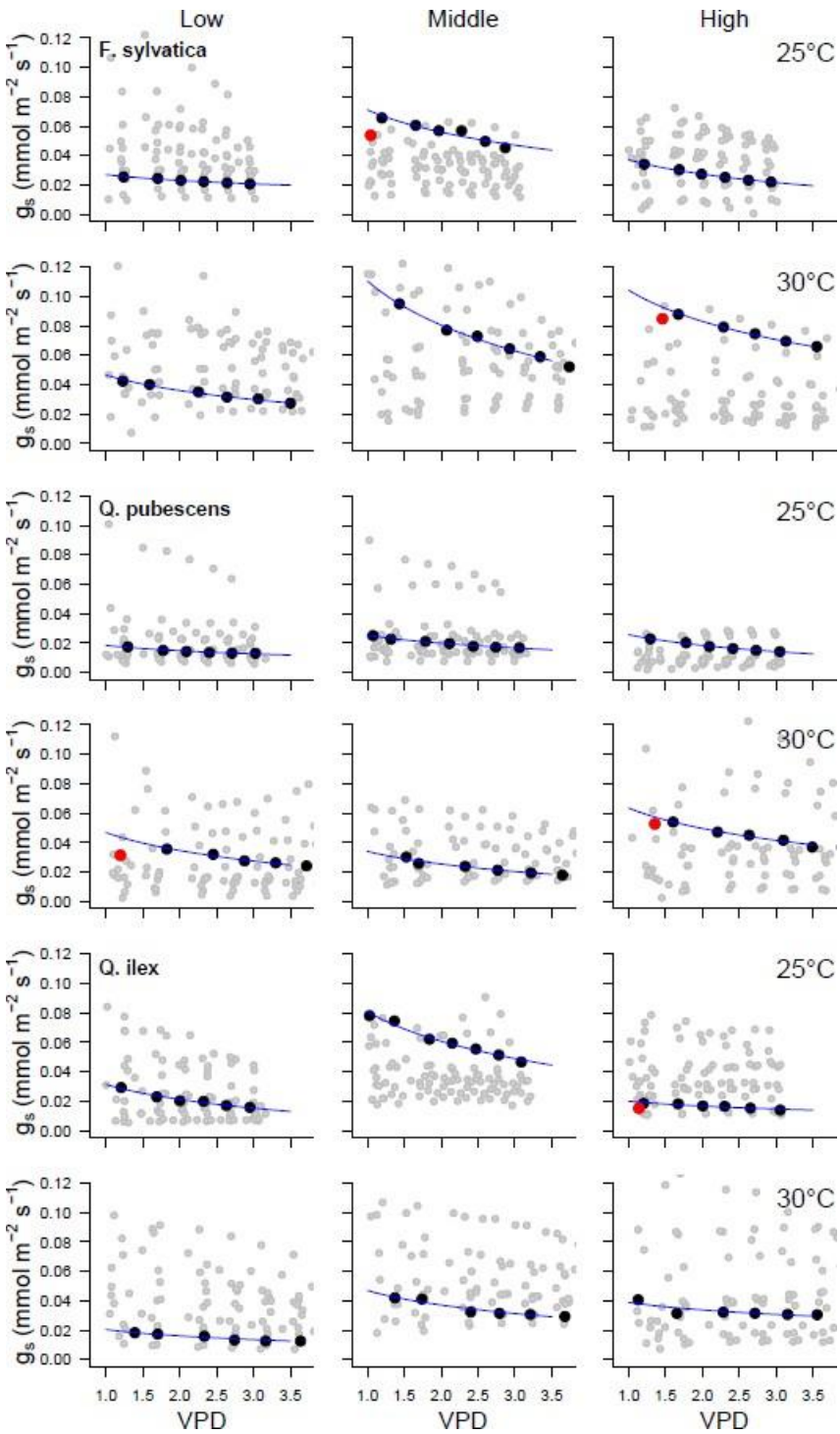

Figure SA1.4: G_S *vs.* VPD curves for each species during all measurement campaigns in the six climate chambers: Low, middle, and high VPD at 25°C and 30°C. Blue lines indicate the fitted model of one curve (black dots) to highlight the method used (see Methods S1). Model fitting started at the VPD level where g_S was the highest, in some cases thereby eliminating the first point of a curve, indicated here by red dots.

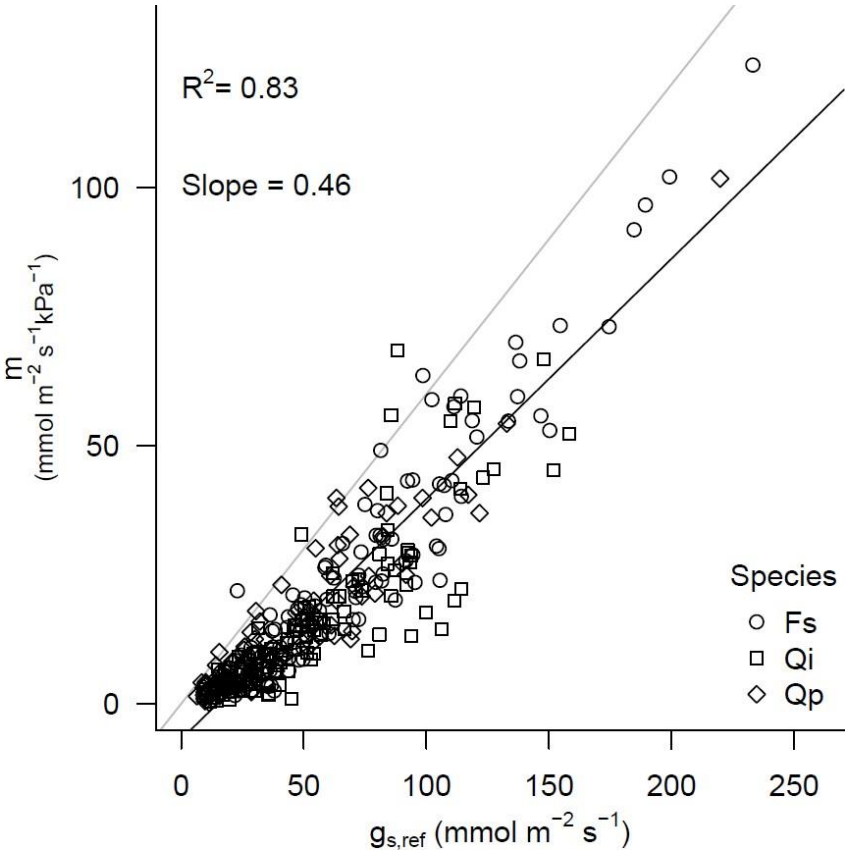

Figure SA1.5: Stomatal sensitivity (*m*, the slope of the logarithmic curve of g_S to VPD, see Fig. S5) as a function of the reference stomatal conductance ($g_{S,ref}$). The universal ratio of 0.6 suggested by Oren et al. (1999) is indicated by a grey line. The black line indicates the ratio measured in this study (slope = 0.46, R^2 = 0.83).

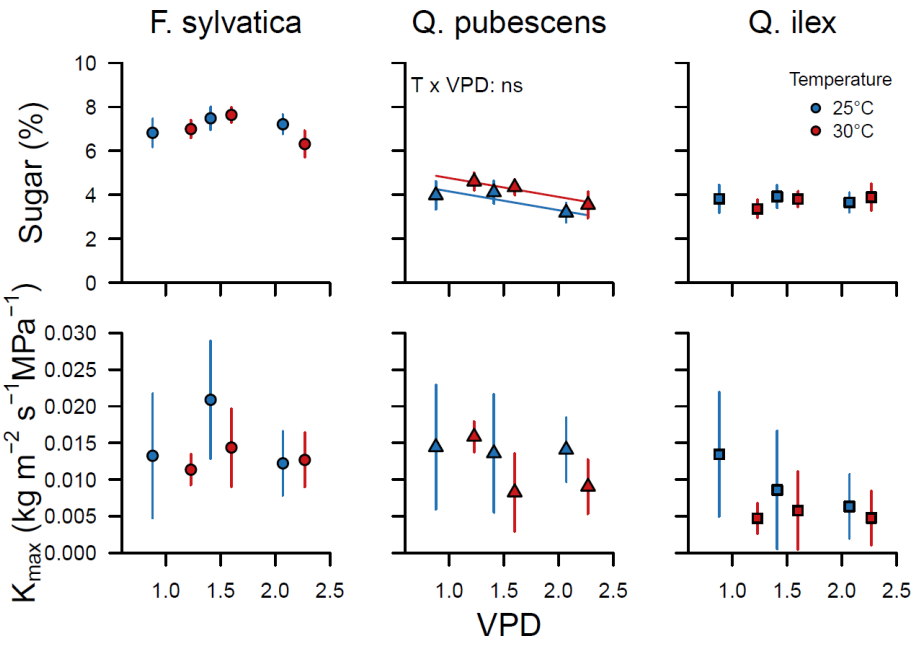

Figure SA1.6. Sugar concentration in the leaves and maximum xylem hydraulic conductance (K_{max}) in *Fagus sylvatica, Quercus pubescens,* and *Quercus ilex* in the two temperature and three VPD treatments. Data are shown in relation to the average VPD in the chambers during the treatment period. Symbols indicate the mean ± SE of three measurement campaigns (n = 18). Colored lines – blue for 25°C and red for 30°C – indicate the VPD effects in the different temperature treatments in case of a T and VPD effect or interaction.

A1.8.2 Supporting tables and notes

Methods SA1.1

First, apparent outliers of g_s were cleaned with visual inspection and by removing g_s values below 0 and above 1.5 mol m^{-2} s^{-1} (Ely *et al.*, 2021). Different fitting curves were tested to calculate the sensitivity of g_s to VPD. The Oren model (Oren *et al.*, 1999) was used in the first instance, assuming a logarithmic decrease in g_s with increasing VPD, but many response curves seemed to follow different patterns. For example, we sometimes observed an initial increase of g_s with increasing VPD followed by a logarithmic decrease. Accordingly, polynomial (2nd and 3rd degree), logarithmic curves, and a logarithmic curve starting from the maximum measured g_s, independent of the VPD where it was measured, were tried, and the goodness of fit was compared. Fitting the logarithm from the maximum g_s resulted in the best fit that was comparable between all species, treatments, and campaigns.

Table SA1.1: Average values of stomatal closure (P_{close}), minimum and maximum values of turgor loss point (ψ_{TLP}) and P50 found in the literature for the three studied species. K_{max} values come from direct measurements in this study.

Species	P_{close}	ψ_{TLP} (MPa)	P50 (stem, MPa)	K_{max} (kg m^{-2} s^{-1} MPa^{-1})	Reference
F. sylvatica	-2.50	-2.04 – -2.50	-3.15	0.014	(Aranda *et al.*, 2001; Choat *et al.*, 2012)
Q. pubescens	-2.75	-2.24 – -2.80	-3.3 – -4.81	0.013	(Choat *et al.*, 2012; Nardini *et al.*, 2012)
Q. ilex	-3.18	-2.84 – -3.15	-3.3 – -6.9	0.007	(Nardini *et al.*, 2012; Martin-StPaul *et al.*, 2014)

Table SA1.2: Results from the ANOVA analysis for midday water potential (ψ_{md}, MPa), loss of conductive area (PLA, %), and conductivity (PLC, %). The interaction is shown when significant ($p<0.05$). Otherwise, only the results from the additive model are shown. Bold numbers indicate significant treatment effects.

		Ψ_{md}		*PLC*		*PLA*	
F. sylvatica	**df**	**F**	**p**	**F**	**p**	**F**	**p**
Temperature	**1**	**4.27**	**0.041**	4.07	0.053	**10.12**	**0.002**
VPD	**2**	**29.28**	**<0.001**	**21.29**	**<0.001**	**10.39**	**0.002**
Temp*VPD	**2**	**13.25**	**<0.001**				
Q. pubescens							
Temperature	**1**	**7.57**	**0.007**	2.47	0.128	**6.82**	**0.011**
VPD	**2**	**3.95**	**0.022**	**5.76**	**0.024**	**4.05**	**0.049**
Temp*VPD	**2**	**6.86**	**0.001**				
Q. ilex							
Temperature	**1**	0.60	0.443	0.40	0.534	0.17	0.685
VPD	**2**	**9.03**	**0.005**	0.16	0.690	1.27	0.265
Temp*VPD	**2**						

Table SA1.3: Results from the ANOVA analysis for leaf water evaporation (E, mmol m^{-2} s^{-1}), stomatal conductance (g_S, mmol m^{-2} s^{-1}), stomatal sensitivity to VPD (*m,* mmol m^{-2} s^{-1} kPa^{-1}), minimum conductance (g_{min}, mmol m^{-2} s^{-1}), and turgor loss point (ψ_{TLP}, MPa). The interaction is shown when significant ($p<0.05$). Otherwise, only the results from the additive model are shown. Bold numbers indicate significant treatment effects.

		E		g_s		*m*		g_{min}		Ψ_{TLP}		*Sugar*	
F. sylvatica	**df**	**F**	**p**	**F**	**p**	**F**	**p**	**F**	**p**	**F**	**p**	**F**	**p**
T	**1**	0.78	0.387	0.24	0.632	**5.08**	**0.033**	3.87	0.058	0.45	0.451	0.31	0.580
VPD	**2**	**8.05**	**0.008**	3.97	0.058	0.89	0.354	0.09	0.925	1.34	0.255	0.16	0.686
T*VPD	**2**							**5.25**	**0.029**				
Q. pubescens													
T	**1**	2.08	**0.005**	1.37	0.251	**8.31**	**0.005**	0.40	0.529	**5.34**	**0.023**	**5.66**	**0.020**
VPD	**2**	9.11	0.161	0.18	0.677	0.22	0.638	1.68	0.204	**7.36**	**0.008**	**7.09**	**0.010**
T*VPD	**2**									**7.75**	**0.006**		
Q. ilex													
T	**1**	4.04	0.055	2.83	0.105	0.72	0.407	**6.28**	**0.017**	**7.44**	**0.010**	0.33	0.566
VPD	**2**	3.81	0.061	0.84	0.369	1.27	0.271	0.74	0.396	**10.41**	**0.003**	0.12	0.727
T*VPD	**2**									**6.85**	**0.013**		

Appendix 2

Warming may extend tree growing seasons but does not always compensate for reduced carbon uptake during dry periods

Charlotte Grossiord[1,2*], Christoph Bachofen[1,2], Jonas Gisler[3], Eugénie Mas[1,2], Yann Vitasse[3], Margaux Didion-Gency[3]

[1]Plant Ecology Research Laboratory PERL, School of Architecture, Civil and Environmental Engineering, EPFL, CH-1015 Lausanne, Switzerland

[2]Community Ecology Unit, Swiss Federal Institute for Forest, Snow and Landscape WSL, CH-1015 Lausanne, Switzerland.

[3]Forest Dynamics Unit, Swiss Federal Institute for Forest, Snow and Landscape WSL, CH-8903 Birmensdorf, Switzerland

This appendix has been published in the peer-reviewed journal "*New Phytologist*"

Grossiord, C., Bachofen, C., Gisler, J., Mas, E., Vitasse, Y., & Didion-Gency, M. (2022). Warming may extend tree growing seasons and compensate for reduced carbon uptake during dry periods. *Journal of Ecology*, *110*(7), 1575-1589. https://doi.org/10.1111/1365-2745.13892

Abstract

1. Warming and drought alter plant phenology, photosynthesis and growth with important consequences for the global carbon cycle and the earth's climate. Yet, few studies have attempted to tease apart their effects on tree phenology, particularly leaf senescence, and on source and sink activity.

2. We experimentally assessed the single and combined effects of warming and reduced soil moisture on the phenology (leaf-out and senescence date, growing season length) and aboveground sink (height and diameter growth, leaf area and Huber values) and source activity (net photosynthesis, photosynthetic efficiency, chlorophyll concentration and total carbon (C) uptake) of two tree species with distinct strategies to deal with drought: European beech and pubescent oak.

3. Warming advanced leaf-out, irrespective of soil moisture levels, particularly in oak and to a lower extent in beech, leading to a prolonged growing season in oak but not beech. No impacts of warming on senescence timing were found for both species. Reduced moisture had little impact on the phenology of both species. Warming-induced advances in phenology and higher photosynthetic efficiency increased the annual C uptake for oak and compensated for the reduced photosynthetic activity in the presence of reduced moisture. Conversely, for beech, source activity, including yearly C uptake, was lower in all treatments than the control, indicating no compensation of the C budget by phenological shifts.

4. ***Synthesis.*** Our results demonstrate that a warming-driven earlier activity and higher photosynthetic efficiency compensates for reduced photosynthesis during hot and dry periods, but only for pubescent oak, which is a rather drought tolerant species. Current predictions of warming-induced mitigation effects through extended C uptake seem incorrect for beech.

Keywords: *Fagus sylvatica* L., growth, *Quercus pubescens* Willd., photosynthesis, Vc_{max}, J_{max}, senescence, SPAC model, warming.

A2.1 Introduction

Reduced precipitation and rising temperature are among the most critical environmental stresses for vegetation because of their impacts on plant sink and source activity (i.e., growth and photosynthesis, respectively) and phenology. For instance, warmer climate and hotter droughts have led to important phenological shifts (e.g., Piao et al., 2019; Geng et al., 2020), a widespread reduction in plant carbon assimilation (e.g., Santos et al., 2018; Rödenbeck et al., 2020) and forest productivity (e.g., Ciais et al., 2005; Fu et al., 2020). Yet, although high temperature and reduced precipitation tend to co-occur in nature and few studies have attempted to tease apart their effects, they are thought to have very different impacts on tree' phenology (Fatichi et al., 2014).

In broadleaved trees, the timing of leaf-out and senescence are important phenological events that arbitrate the length of the growing season, the duration of sink/source activity and consequently affect the global carbon (C) cycle (Richardson et al., 2013; Keenan et al., 2014). It is widely recognized that global warming has generally advanced the leaf-out of temperate trees (Piao et al., 2019). However, temperature impacts on leaf senescence timing, and thus on the growing season length, are less consistent (e.g., Estiarte & Peñuelas, 2015; Xie et al., 2018; Chen et al., 2020) and may depend on moisture availability (Xie et al., 2015). For instance, while drought can lead to premature leaf fall in deciduous species (Bigler & Vitasse, 2021; Dallstream & Piper, 2021), for some species such as *F. sylvatica*, soil moisture stress can be compensated by delayed senescence and higher photosynthesis later in the season (Leuschner, 2020). High temperature and drought may also cause embolism in the vascular system, leading to the desiccation of branches and earlier leaf fall (e.g., Cochard et al., 2020; Schuldt et al., 2020). Contrary to leaf-out timing, the exact underlying processes driving senescence remain unclear, but temperature and drought impacts on autumn phenology have been linked to sink/source activity. For instance, a recent study showed that increasing photosynthetic productivity in spring and early summer due to warming drives earlier autumn leaf senescence (Zani et al., 2020, but see Norby, 2021). Indeed, during periods of limited growth demand, photosynthesis can be downregulated by an excess of accumulated carbohydrates (Paul & Foyer, 2001), which can induce degradation of chlorophyll and photosystems and lead to the acceleration of leaf senescence (e.g., Juvany et al., 2013). However, it is unclear whether high carbon supply during periods of low growth demand accelerates the initiation of senescence, the velocity of the senescence process, or both. Hence, the link between warming- and drought-induced changes in C assimilation, growth, and phenological events remains to be tested experimentally to understand better how global warming will alter carbon sequestration.

Source activity is known to reach a maximum efficiency within a given temperature range and declines after that. For instance, photosynthetic electron transport of *F. sylvatica* peaks at around 34ºC (Dreyer et al., 2001; Leuschner, 2020), and net C uptake reaches a temperature optimum at 15–28ºC (Schulze, 1970). However, above a given threshold (>40 ºC), hot spells may

impact the integrity of the photosynthetic apparatus (Qu et al., 2013). Contrary to temperature, soil moisture stress is commonly thought to impair source activity because of CO_2 diffusion limitation through the stomata (Chaves et al., 2009). Water stress results in decreasing leaf water content and leaf water potential, leading to stomatal closure and a reduction of intercellular CO_2 concentrations (Flexas et al., 2004). Furthermore, temperature and soil moisture impacts are not entirely independent: reduced stomatal conductance during drought leads to lower leaf evaporative cooling (e.g., Muller et al., 2021), thereby enhancing thermal stress and restricting carbon C uptake. Contrary to photosynthetic properties, far less is known on temperature impacts on sink activity. We can expect cell expansion and tissue growth to cease before C uptake decreases when temperatures rise, resulting in an increase in non-structural carbohydrates (NSC) concentration with higher temperatures. However, higher maintenance respiration under warming (Teskey et al., 2015) might reduce NSC reserves under these conditions. Similarly, drought inhibits sink activity at less negative water potentials than photosynthesis (Tardieu et al., 2011). Plants would thus first stop growth before photosynthesis and accumulate NSC (Körner, 2003; Woodruff & Meinzer, 2011; Weber et al., 2019). The differential sensibility of the sink and source activity to warming and moisture stress could lead to an imbalance between C supply and C demand, which should influence NSC dynamics and could feedback to plant phenology (Estiarte & Peñuelas, 2015).

Moreover, temperature and drought impacts on phenology, and sink/source responses will likely differ between co-existing species. Some species tend to close their stomata at more positive water potentials than others (Tardieu & Simonneau, 1998), leading to lower photosynthesis, reduced growth, and NSC storage during drought and/or heat stress (Dickman et al., 2015; Manrique-Alba et al., 2018). Furthermore, the temperature optimum for photosynthesis is highly variable between species because of adaptation to their climate of origin (Fryer & Ledig, 1972; Berry & Bjorkman, 1980) and rapid acclimation to changes in temperature (Gunderson et al., 2010; Kumarathunge et al., 2019). For instance, many studies have shown that the photosynthetic thermal optima can shift by 0.3-0.5°C per degree change in daytime temperature (e.g., Way & Yamori 2014; Gunderson et al., 2010). Plants can also acclimate to soil moisture to optimize their C uptake efficiency under more restrictive moisture conditions. These processes involve cellular adjustments to maintain leaf turgor to whole-plant allometry adjustments to reduce water loss (reviewed in Bréda et al., 2006; Niinemets, 2010). In addition to addressing species differences, we further need to explore heat and drought impacts independently and combined under controlled conditions (e.g., Grossiord et al., 2016, 2017). Such experiments have shown that high temperature and soil moisture limitation reduce photosynthesis and growth in semi-arid systems, thereby reducing foliar NSC concentrations and delaying leaf out timing in the following spring (Adams et al., 2015). Whether a similar response can be expected in temperate systems is unclear as no study has experimentally investigated the relative and combined impacts of warming and drought on the phenology of temperate trees, including their link to sink/source activities.

We used an open-top chamber facility where European beech (*Fagus sylvatica L.*) and pubescent oak (*Quercus pubescens Willd*.) seedlings were exposed for multiple years to warming and soil moisture reduction acting alone or together. Beech and oak present essential differences in their strategy to deal with drought, with oak being more tolerant to low moisture and heat (e.g., Robson et al., 2009; Nardini et al., 2012; Barigah et al., 2013; Urli et al., 2013). Our objectives are to (1) determine how individual and combined effects of warming and soil moisture reduction influence phenology and aboveground sink in two temperate trees with contrasting strategies to deal with drought, and (2) assess the relationship between source activity, sink activity, and autumn phenology under warming and soil moisture reduction. We expect warming to advance leaf-out timing, accelerate leaf development time, and delay and/or slow down leaf senescence, resulting in longer growing seasons. On the contrary, we expect soil moisture reduction to slow down leaf development in spring and advance and accelerate senescence, resulting in a shorter growing season than in ambient conditions. These responses should be stronger in oak, which is under lower photoperiodic control than beech and has lower chilling requirement to break winter dormancy (Baumgarten et al., 2021). Warming may increase the photosynthetic capacity (i.e., net photosynthesis, rubisco carboxylation, electron transport rate, chlorophyll concentration) in these temperate trees, which could lead to higher C uptake and growth, particularly for the Mediterranean pubescent oak, while soil moisture reduction should decrease these same functions but more severely in European beech (González de Andrés et al., 2021). We further expect changes in autumn phenology, and thus growing season length, to be linked to shifts in the sink/source activity with earlier and accelerated senescence under high carbon assimilation but low growth demand, independently of the species. Finally, we expect the combination of warming and soil moisture reduction to exacerbate the responses observed under moisture reduction-only conditions because of enhanced moisture stress (Adams et al., 2015), particularly for the more vulnerable beech trees (González de Andrés et al., 2021).

A2.2 Material and methods

A2.2.1 Site description

The study was conducted at the model ecosystem facility of the Swiss Federal Research Institute WSL (47°21'48" N, 8°27'23" E, 545 m a.s.l). The facility comprises 16 hexagonal glass-walled open-top chambers (3 m height, 6 m2 each, Fig. SA2.1). The roofs were kept closed during the entire experiment to exclude natural precipitation. The lower parts of each chamber are divided into two lysimeters (1.5 m deep, 2.5 m2 each) that are each divided into 4 compartments using PVC shields leading to eight compartments per chamber. The compartments are filled with a 1 m-deep layer of gravel for fast drainage, covered with a fleece layer that is impermeable for roots (to restrict root growth below the soil layers) but permeable for water, and topped by a 50 cm layer of sandy soil (pH = 6.3). This artificial soil with high sand content was selected to ensure good drainage (Ökohum Gmbh, Herbertingen, Germany). Long-term mean annual and mean summer (June, July, August) air temperature are 9.5 and 17.7°C, respectively and the average yearly and summer precipitation are 1124 and 377 mm (MeteoSwiss, Station Zurich-Fluntern).

In winter 2018, compartments within each chamber were planted with one two-year-old individual of common beech and pubescent oak to avoid effects related to competition. In addition, some compartments were planted with monocultures (four trees from the same species) and mixtures (two trees from each species) of the two species but they were not considered in this study. Tree saplings (70.8 cm height ± 12.0 cm and 71.8 cm ± 15.0 cm for beech and oak, respectively) were purchased from a local nursery and originate from canton Aargau, northern Switzerland (for beech) and canton Valais, southern Switzerland (for oak). Fertilizations were conducted yearly in spring using granules (Unikorn I, Hauert, Switzerland). In the open-top chambers, the trees were subjected to a fully crossed combination of soil moisture and an air temperature treatment since April 2019 (i.e., after leaf emergence). This resulted in four treatment combinations: 1) control, where trees were exposed to ambient air temperature, and soil moisture was maintained at field capacity (corresponding to approx. 10% relative volumetric water content in these sandy soils); 2) warming, where the air temperature inside the chambers was maintained at 5.0°C (±0.4°C) above the temperature of the control using heating units; 3) moisture reduction, where irrigation was reduced by 70% leading to a reduction in soil moisture of 51.5.0% ± 11.8% relative to the control; and 4) warming + moisture reduction, where both treatments were applied simultaneously (i.e., +4.8°C ±0.4°C and irrigation reduction of 70% leading to a soil moisture of –47.8% ± 12.4%, Fig. S2). The trees were irrigated every second day using an automatic irrigation system between April and November 2019. The amount of water added to each treatment was adapted throughout the year to maintain field capacity in the control and the treatment differences (Fig. SA2.2). The irrigation system was removed from December 2019 to March 2020 to prevent frost damage to the pipes, and watering was done manually bi-monthly to maintain differences

between treatments during the winter. An increase in air temperature of 5°C and a decrease of approx. 70% in irrigation was selected at our facility to match values observed during extreme hot droughts in this region, such as the one that occurred during summer 2018 (Peters et al., 2020; Schuldt et al., 2020). In 2020, the treatments resulted in a mean annual temperature of 11.6°C, 11.8°C, 16.5°C and 16.3°C in the control, moisture reduction, warming and warming + moisture reduction treatments, respectively. During the summer 2020, the maximum daytime temperature in the chambers reached 37.0°C, 37.6°C, 43.8°C and 44.4°C in the control, moisture reduction, warming and warming + moisture reduction treatments, respectively. Each climatic treatment was replicated four times (n=4 chambers per climatic treatment) with six replications per species and climatic treatment (n=48 trees in total, i.e., 24 trees per species). Air temperature and relative humidity (ATMOS 14, Meter Group Inc, USA) were measured under a white radiation shield inside all chambers at two heights (0.5 and 2 m above ground) and used to control the heating units. Soil water content and temperature were measured automatically (5TM, Decagon Devices, USA) every minute at 25 cm depth in all chambers (one probe per compartment).

A2.2.2 Phenology and growth

In March 2020 (during the second growing season, i.e., approx. 11 months after the beginning of the treatments), one observer monitored bud development three times per week until early June using a categorical scale from ‘0’ (no bud activity) to ‘4’ (leaves out and flat) (Vitasse et al., 2013). At stage 1, buds were swollen, elongating, and became green; at stage 2, buds were open, and leaves were partially visible; at stage 3, leaves had fully emerged from the buds but were still folded, crinkled, or pendant, depending on the species; at stage 4, at least one leaf was fully unfolded. We considered the bulk of the foliage for each tree and assessed the proportion of the buds having reached the most advanced phenological stage, allowing for a tree-level estimate of leaf unfolding. In addition, each phenological score from ‘1’ to ‘4’ was reached by a given tree when at least one bud was at the corresponding stage. We present here only the results of stage 4 (i.e., leaf-out date) and the development time (i.e., the number of days needed to pass from stage 1 to 4) for the analyses. Starting in September, we monitored leaf senescence by estimating the percentage of colored and dropped leaves of each tree. We then calculated the date when 50% of the leaves were either colored or had fallen using linear interpolations between two monitoring dates when necessary. The velocity of the senescence process was estimated as the number of days between the stage of 10% and 80% of either colored and dropped leaves. Every individual tree's growing season length was calculated as the number of days between leaf-out (i.e., stage 4) and leaf senescence date.

At 10 cm above the ground (i.e., below the first branches), tree diameter was measured twice in 2020 using an electronic digital caliper: in spring before leaf-out and autumn after leaf fall. At the same time, tree height was measured on all trees. The difference between the spring and

autumn growth measurements was used to calculate yearly height and diameter increment per tree. As no destructive measurements could be carried out in this ongoing experiment to estimate whole-tree biomass, we cut a 15-cm long branch in September 2020 to estimate the mean branch leaf area (cm^2) and Huber value (i.e., ratio of sapwood area over leaf area, cm^2 m^{-2}) from each tree.

A2.2.3 Leaf-level photosynthetic capacity, non-structural carbohydrates, leaf water potential and percentage loss of conductivity

We measured leaf-level light-saturated photosynthesis (A_{sat}, µmol m^{-2} s^{-1}), stomatal conductance (g_s, mmol m^{-2} s^{-1}), maximum rate of rubisco carboxylation (V_{cmax}, µmol m^{-2} s^{-1}), and electron transport rate (J_{max}, µmol m^{-2} s^{-1}) on one leaf from the highest part of the crown of all 48 trees three times per year in 2020 (i.e., after the trees had been exposed to a full year of treatment manipulation). Chlorophyll concentration (µmol m^{-2}) was measured on the same leaves with a chlorophyll content meter (MC-100, Apogee Instruments, Inc., USA). Measurements took place during three campaigns: once the leaves were fully mature (June), in the middle of the growing season (July/August), and before the first sign of leaf senescence (early September). Gas exchange measurements were conducted using A/Ci (i.e., intercellular CO_2 concentration) curves between 9 am and 5 pm (local time) using two LI-6800 infrared gas exchange analyzer systems (LICOR Biosciences, Lincoln, USA). We used the Auto program “CO2_response” with relative humidity set to 50% to match average daily environmental conditions inside the chambers. Based on light response curves conducted on our trees (Fig. SA2.3), we used a photosynthetic photon flux density (PPFD) of 1500 µmol m^{-2} s^{-1} to ensure saturating light conditions. The air temperature inside the cuvette was fixed to 20, 25, or 30°C to fit the mean midday air temperature during the measurements (i.e., 20°C in June and September and 25°C in July) with +5°C for the warming and hot drought treatments. The A/Ci response curves were measured by stepping down CO_2 inside the cuvette from 400 ppm to 300, 200, 100, 50, 0 ppm and then returned to 400 ppm. The CO_2 concentration was then stepped up to saturation from 400 ppm to 600, 800, 1000, 1200, 1500, and 2000 ppm. When the leaves did not fully cover the LI-6800 cuvette, the projected leaf area of the measured foliage was determined to correct Asat using a flatbed scanner (EPSON Perfection V800 Photo, EPSON, Amsterdam) and the Silver Fast 8 software (Laser soft imagine AG, Germany).

A_{sat} (A at 400 ppm), g_s, V_{cmax}, and J_{max} were extracted from the A/Ci curves using the Farquhar, von Caemmerer & Berry model computed in the “plantecophys” R-package (Duursma, 2015). Several criteria were used to manually clean the A/Ci curves before fitting, following the recommendations by Gu et al., (2010). To ensure a saturating plateau, all curves that did not reach a Ci of 600 ppm and did not have a minimum of 7 measurement points (because of outlier exclusion) were excluded. Using the default method in the “plantecophys” R-package, the model used a temperature correction to fit all curves to 25°C (see Duursma, 2015 for more details on the modelling procedure). After cleaning the data, 133 out of 144 A/Ci curves were further considered

in the analyses. On the same day as gas exchange measurements, one leaf per tree was collected at midday (between 11:30 am and 1:30 pm). The leaf was microwaved at 600W for 90s and oven-dried for at least 48h at 65°C. The leaves were ground to a fine powder and analyzed for non-structural carbohydrates (NSC) content following the protocol by Hoch et al., (2002). See Hoch et al., (2002) and Schönbeck et al., (2020) for more details on the NSC extraction steps. NSC concentrations are expressed on a percent dry matter basis. During each campaign, we sampled one leaf per tree before sunrise and measured leaf water potential (MPa) with a Scholander-type pressure chamber (PMS Instruments, Albany, OR, USA).

One 10-15 cm-long stem per tree was cut underwater in the field between 07:00 and 10:00 am during the last campaign. Branches were transported to the laboratory and kept with their cut ends immersed in water and with foliage enclosed in a plastic bag. After at least 30 min of immersion, the stem was cut again in its current-year part and connected to a hydraulic apparatus (Xyl'Em Plus – Xylem Embolism Meter; Bronkhorst, Montigny-les-Cormeilles, France) and perfused with deionized filtered water with 10 mM KCl and 1mM CaCl2 that had been previously degassed. After measuring the initial hydraulic conductivity at low pressure, the segment was flushed at 1.5 bar for 1 min to measure its maximal conductivity. A second flush at 1.5 bar for 30 s was conducted to confirm the maximal conductivity value. The initial hydraulic conductivity and the value measured after embolism removal were used to estimate the percentage loss of conductivity (PLC).

A2.2.4 SPAC modeling of leaf-level photosynthesis

We simulated leaf-level net photosynthesis with a mechanistic soil-plant-atmosphere continuum (SPAC) model proposed by García-Tejera et al., (2017), which allows calculating photosynthetic CO_2 uptake based on plant physiological parameters and environmental drivers. The model uses an iterative optimization process to determine the equilibrium between the photosynthetic demand (A) for Ci and the supply of extracellular CO_2 (Ca) through stomatal conductance (g_S). First, the potential A under a given photosynthetic photon flux density (PPFD), Vcmax and Jmax determines the required g_S for sufficient CO_2 supply (i.e., CO_2 supply that is not limiting A by keeping Ci at the concentration of Ca). Second, gs determines the transpirational water loss (E), which is used to calculate the leaf water potential (Ψ_{leaf}) as a function of T, soil water potential (Ψ_{soil}), and the soil, root, and xylem hydraulic resistances. Finally, Ψ_{leaf} is used to calculate the hydraulic restriction on g_S, limiting A due to a restricted supply of intercellular CO_2. The iteration procedure starts again until the demand and supply for CO_2 converge (difference of less than 0.1%). The initial gs is based on Farquhar's equation for biochemical photosynthesis (Farquhar, Caemmerer, & Berry, 1980) and reformulated according to García-Tejera et al., (2017) as:

$$g_{S_{max}} = \frac{B(C_i-\Gamma)-R_d(VC_i+D)}{(EC_i+D)(C_i-C_a)} \qquad \text{eqn.1}$$

with B representing the V_{cmax} or J_{max} limited rates of CO_2 uptake, Γ the CO_2 compensation point of photosynthesis, and D is a combination of Michaelis-Menten coefficients for carboxylation and oxygenation rates (K_C, K_O), or the light compensation point of photosynthesis. *V* is a constant parameter. D is derived from K_C, K_O and the O_2 partial pressure (O_i) as:

$$D = K_C\,(1 + \frac{O_i}{K_O}) \qquad \text{eqn. 2}$$

The actual gS is then calculated with Ψleaf using the equations of Tuzet et al., (2003):

$$g_S = g_0 + \frac{m\,A}{C_i - \Gamma}\,f_{\psi leaf} \qquad \text{eqn. 3}$$

and

$$f_{\psi leaf} = \frac{1 + e^{[S_f\,\Psi_f]}}{1 + e^{[S_f\,(\Psi_f - \Psi_{leaf})]}} \qquad \text{eqn. 4}$$

with g_0 as g_S when A_{net} equals 0, m an empirical proportionality factor between A and g_S, and $f_{\psi leaf}$ a factor for reducing g_S as a function of Ψ_{leaf}. S_f is the stomatal sensitivity to Ψ_{leaf} and Ψ_f the leaf turgor loss point (measured using pressure-volume curves). C_i and g_S are then used to obtain A with:

$$A = g_S(C_a - C_i) \qquad \text{eqn. 5}$$

We used the SPAC model to simulate A based on soil water content, air temperature and humidity measured at 10-minute intervals in the chambers, and PPFD recorded at a nearby long-term forest monitoring site. As the chamber structures intercept part of the incoming radiation, we additionally recorded PPFD with quantum sensors (Apogee Instruments Inc., USA) in 8 of the 16 chambers during one week in June 2021. We calculated the fraction of transmitted light (43%) from these measurements, which we used to correct the radiation measured at the nearby forest monitoring site. Model parameters were measured if possible at the study site (tree hydraulic traits), taken from literature, or calibrated (Table SA2.1). We calibrated the model parameters using a Bayesian approach, which allows the inference of parameters from observations via the likelihood (Hartig et al., 2012). We used instantaneous and hourly A and g_S measurements of beech and oak saplings taken during three campaigns in June, July, and September 2020 from sunrise to sunset. As prior knowledge for each parameter, we used values inferred from literature (García-Tejera et al., 2017) and calculated a truncated normal distribution. For the calibration, we used a joint Gaussian likelihood based on A and g_S measurements. As A and g_S are expected to be autocorrelated during the diurnal measurements, we used an autoregressive (AR1) likelihood using the function likelihoodAR1 from the R package BayesianTools (Hartig et al., 2018). The parameters of the two likelihood components (σ2 and the AR1 term) were included in the calibration. We obtained the posterior distributions of the parameters used by the SPAC model with a differential evolution (DEzs) Markov chain Monte Carlo (MCMC) sampler (Ter Braak & Vrugt, 2008) using the R package BayesianTools (Hartig et al., 2018). 10'000 iterations of three independent chains were

run, and convergence after burn-in (50% of the chain) was confirmed with the Gelman-Rubin diagnostic (Gelman & Rubin, 1992). The chain was considered to have converged if the potential scale reduction factor (psrf) was below 1.1. We then used the maximum a-posteriori values as parameters for the SPAC model. The model calibration was evaluated by simulating A for the conditions during three diurnal campaigns in June, July, and September 2020, and calculating the root mean squared error (RMSE) and percentage of bias for the simulated compared to measured A (Figs. SA2.4 & SA2.5). We calculated the yearly assimilated leaf-level carbon A_{tot} (gC) of beech and oak trees in all chambers as the cumulative A multiplied with the molar weight of CO_2 from leaf flushing date to leaf senescence date.

A2.2.5 Data analysis

The response of the measured variables (leaf-out date, leaf development time, senescence date, senescence development time, growing season length, height increment, diameter increment, leaf area, Huber value, A_{sat}, g_s, V_{cmax}, J_{max}, chlorophyll content, A_{tot}) to the treatment combinations were determined for each species through linear mixed-effects models. The temperature (control temperature/warming) and soil moisture treatment (control irrigation/moisture reduction) and their interactions were fixed effects, and the individual chamber was considered a random effect. The measurement campaign was included as a fixed effect for measurements repeated during multiple campaigns (i.e., A_{sat}, g_s, V_{cmax}, J_{max}, chlorophyll content). Post-hoc analysis was performed with Tukey's HSD test, with FDR correction for multiple testing. Linear regressions were used to test the relationship between senescence date, growing season length, source (A_{tot}), and sink activity (height and diameter growth increment). All analyses were performed using the software R Studio (3.5.1, R Development Core Team 2018).

A2.3 Results

A2.3.1 Phenology and growth

In both species, warming advanced leaf-out (Table A2.1), which occurred on average 4.5 or 15 days earlier than ambient conditions, for beech and oak, respectively (Fig. A2.1). Moisture reduction did not affect leaf-out timing in beech but advanced leaf-out in oak by 4.9 days. Warming combined with moisture reduction advanced leaf-out by more than 5 days for beech and 12 days for oak (Table A2.1 & Fig. A2.1, significant warming x moisture reduction interaction). In spring, oak leaf development time (i.e., number of days between stages 1 and 4) was significantly prolonged by 3.5 days in response to warming (Table A2.1). No significant impact of the other treatments was found for beech and oak leaf development time (Table A2.1). No significant effect of the treatments on the senescence date was found for either species (Fig. A2.1 & Table A2.1). However, leaf senescence occurred over a more extended period under warmed conditions for oak (20 days longer), while no other effects of the treatments were found for both species (Fig. A2.1 & Table A2.1). For oak, the growing season length was significantly prolonged by warming (by 27.3 days), while no changes were observed for beech in response to the treatments (Fig. A2.1 & Table A2.1). No impact of the treatments or their interaction was found on diameter and height increment, leaf area and Huber values for either species (Fig. SA2.6 & Table A2.1).

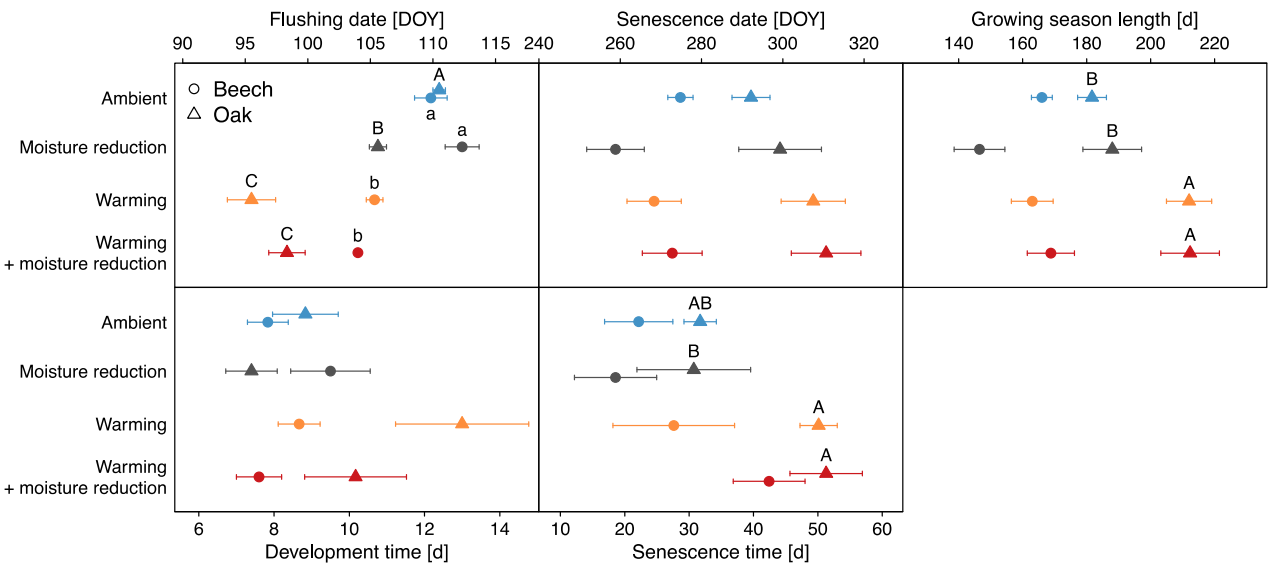

Figure A2.1: Mean leaf flushing date, senescence date, growing season length, leaf development time, and senescence development time (mean ± s.e.; n = 5–6 trees per treatment and species) for European beech (circles) and pubescent oak (triangles) grown under control, warming, moisture reduction and warming + moisture reduction conditions. Significant differences between treatments for each species are indicated with capital (pubescent oak) and small (European beech) letters (Tukey's HSD post-hoc test, alpha = 0.05).

Table A2.1: Linear mixed model results (*F*- and *P*-value) of the effect of warming (W) and moisture reduction (MR) and their interactive effect (W × MR) on the leaf-out date, leaf development time, senescence date, senescence development time, growing season length, diameter and height increment, leaf area, Huber value and the yearly assimilated carbon in beech and oak. Significant effects are highlighted in bold.

Explained variables	Species	Treatment		
		W	MR	W × MR
Leaf-out	Beech	**27.02 (< 0.001)**	0.34 (0.572)	2.78 (0.129)
	Oak	**54.55 (< 0.001)**	0.85 (0.519)	**5.78 (0.033)**
Leaf development	Beech	0.41 (0.528)	0.07 (0.789)	3.61 (0.073)
	Oak	**5.48 (0.041)**	1.92 (0.194)	0.01 (0.990)
Senescence	Beech	0.31 (0.579)	0.82 (0.375)	2.51 (0.131)
	Oak	2.67 (0.118)	0.34 (0.561)	0.04 (0.827)
Senescence development	Beech	2.07 (0.166)	0.49 (0.488)	2.56 (0.126)
	Oak	**10.19 (0.005)**	0.53 (0.472)	0.57 (0.459)
Growing season length	Beech	2.03 (0.171)	1.23 (0.281)	3.69 (0.070)
	Oak	**12.11 (0.003)**	0.13 (0.713)	0.14 (0.706)
DBH increment	Beech	0.17 (0.686)	2.43 (0.145)	3.39 (0.090)
	Oak	0.39 (0.541)	0.01 (0.917)	1.64 (0.225)
Height increment	Beech	0.30 (0.589)	0.33 (0.571)	0.01 (0.897)
	Oak	1.08 (0.319)	0.55 (0.472)	0.10 (0.753)
Leaf area	Beech	0.19 (0.667)	0.685 (0.370)	0.76 (0.696)
	Oak	0.24 (0.625)	0.23 (0.631)	0.24 (0.626)
Huber value	Beech	0.31 (0.587)	0.14 (0.710)	0.02 (0.870)
	Oak	1.49 (0.236)	0.20 (0.652)	1.09 (0.308)
Yearly assimilated carbon	Beech	**29.63 (< 0.001)**	**63.04 (< 0.001)**	0.01 (0.915)
	Oak	**70.40 (< 0.001)**	**85.27 (< 0.001)**	**16.41 (0.002)**

A2.3.2 Leaf-level photosynthetic capacity, NSC, leaf water potential and PLC

While moisture reduction significantly reduced A_{sat} and g_s compared to ambient conditions, warming had no impact on A_{sat} and g_s in either species (Fig. A2.2 & Table SA2.2). Treatment impacts on A_{sat} and g_s did not vary seasonally (i.e., no interaction between treatments and campaigns). A_{sat} and g_s did not differ between campaigns for oak but were significantly reduced during the last campaign compared to previous ones for beech (Fig. A2.2). V_{cmax} was significantly reduced by moisture reduction for oak, whereas warming increased V_{cmax} in both species. Similarly, J_{max} was significantly reduced by moisture reduction for oak, but neither warming nor moisture reduction affected J_{max} for beech (Fig. A2.2 & Table SA2.2). Warming had no impact on oak J_{max}. V_{cmax} and J_{max} varied during the season for both species, but the treatment effects were not affected by seasonality (Table SA2.2). Chlorophyll content varied between campaigns for beech but was

not impacted by moisture reduction and warming for both species (Fig. A2.2 & Table SA2.2). For oak, we observed higher total NSC and starch concentration in September 2020 in the warming treatment compared to the control, while for beech no effect was found (Fig. SA2.7). No effect of the treatments was found for PLC for both species (Fig. SA2.7 & SA2.8). Predawn leaf water potential was reduced by warming for both species (only in the single warming treatment for beech), and by drought for oak with lower values in the warming and moisture reduction treatments acting alone and together compared to ambient conditions (Fig. SA2.9).

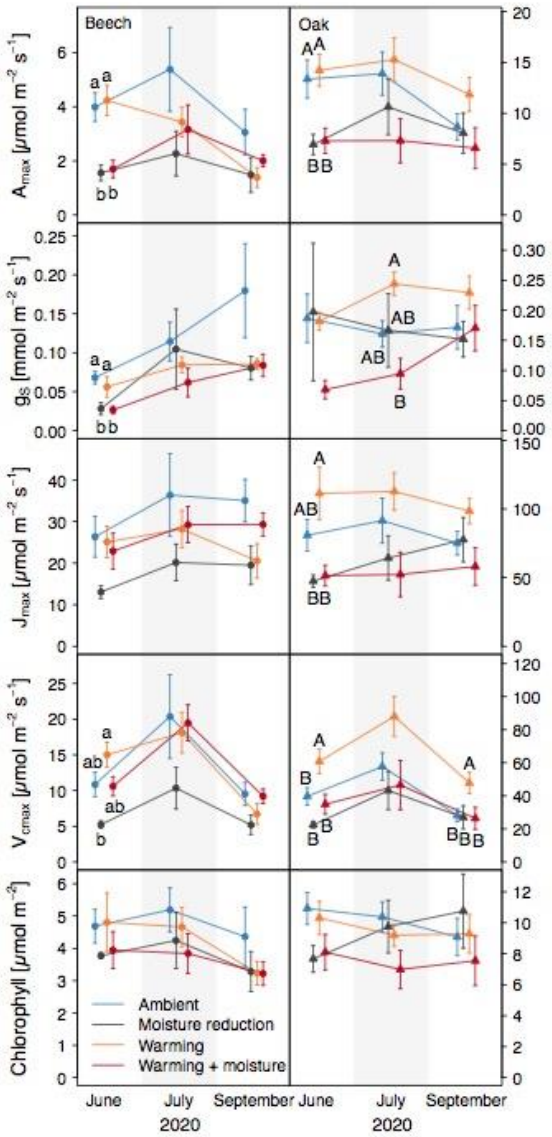

Figure A2.2: Light-saturated photosynthesis (A_{sat}), stomatal conductance (g_S), maximum electron transport rate (J_{max}), maximum rate of rubisco carboxylation (V_{cmax}) and leaf chlorophyll content (mean ± s.e.; n = 5–6 trees per treatment, species and measurement campaign) for European beech (circles) and pubescent oak (triangles) growing under control, warming, moisture reduction and warming + moisture reduction conditions. Measurements took place in June, July, and September 2020. Significant differences between treatments for a given campaign and species are indicated with capital (pubescent oak) and small (European beech) letters (Tukey's HSD post-hoc test, alpha = 0.05).

A2.3.3 Modelled leaf-level carbon uptake during the growing season

The SPAC model captured diurnal and seasonal changes, as well as treatment effects and species differences of A (Figs. SA2.4 & SA2.5). Total root-mean square deviation of the simulated A was 2.35 and the bias was -13%, indicating that the model generally underestimated photosynthesis. This was mostly due to an underestimation of assimilation peaks of oak trees in the ambient and warmed treatment (Fig. SA2.4).

In oak, while warming led on average to a 14.5% increase in A_{tot}, soil moisture reduction reduced total leaf-level C uptake by 12.4% (Table A2.1). The negative moisture reduction effect was to a certain degree mitigated by warming (significant warming x moisture reduction interaction, Fig. A2.3). Consequently, the warmed oak trees had the highest C uptake (1760 gC m^{-2} y^{-1}), whereas the ones exposed to moisture reduction had the lowest A_{tot} (1359 gC m^{-2} y^{-1}). In beech, A_{tot} was on average 12.5% and 16.4% lower in response to warming and soil moisture reduction, respectively (Fig. A2.3 & Table A2.1). The warming and moisture reduction effects were additive, so that the highest C uptake was found in beech seedlings from the ambient treatment (637 gC m^{-2} y^{-1}), whereas the lowest C uptake was in the warming + moisture reduction treatment (467 gC m^{-2} y^{-1}, i.e., 26.5% less).

In both species, warming (alone and in combination with moisture reduction) advanced leaf out, which contributed considerably to their surplus of A_{tot} compared to trees in ambient condition: warmed beech and oak gained 3.8% and 8.4%, respectively, of their annual C during the period before ambient tree activity started. Similarly, beech and oak in the warming + moisture reduction treatment gained 4.4% and 7.9% of their yearly C before ambient trees flushed. Moisture reduction, in contrast, increased the annual C uptake by only 0.4% and 3.3% for beech and oak, respectively. In both species, warming and moisture reduction slightly delayed senescence compared to ambient trees (but not significantly), which contributed to 0.6% and 3.5% of their annual C uptake in warmed beech and oak, 0.8% and 1.4% in the moisture reduction treatment, and 1.7% and 4.1% in the warming + moisture reduction treatment. During the period where all trees were simultaneously active, beech assimilated 19.6%, 18.5%, 31.1% less carbon in the moisture reduction, warming, and warming + moisture reduction treatment, respectively, compared to ambient conditions. In contrast, oak only reduced their assimilation by 9.8% and 11.8% in the moisture reduction and warming + moisture reduction treatment, respectively, and increased their C uptake by 7.9% in the warming treatment compared to ambient conditions.

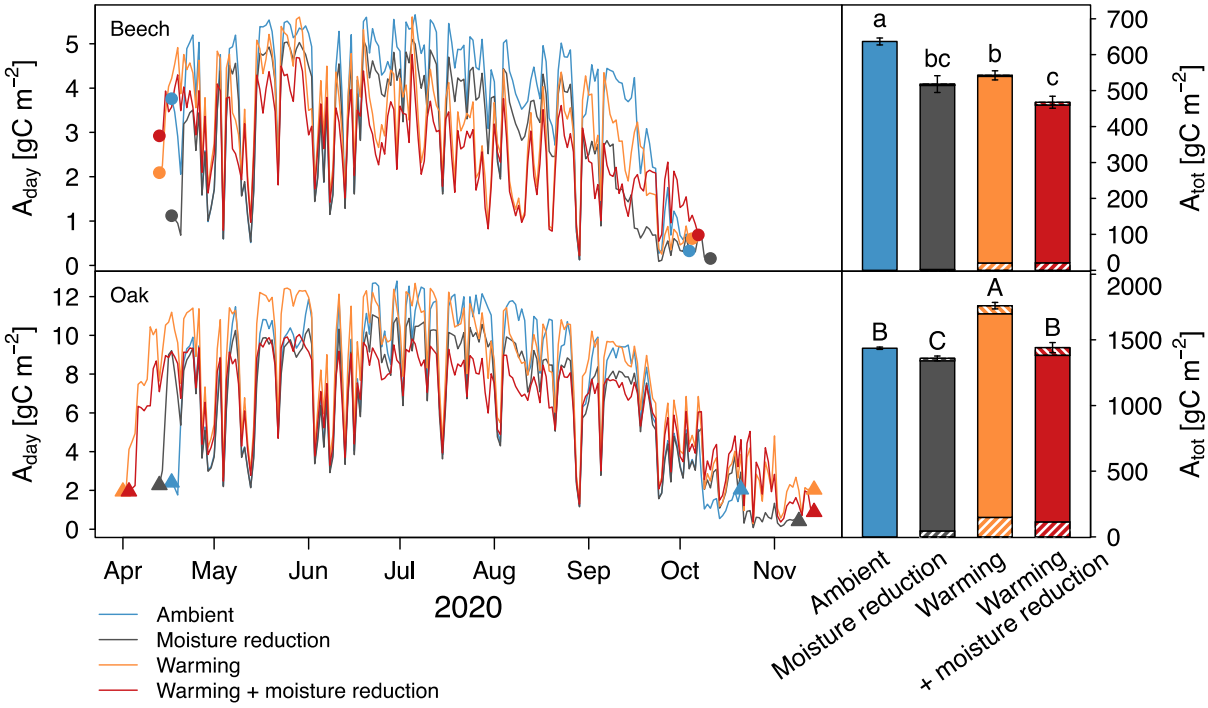

Figure A2.3: Mean simulated daily carbon uptake (A_{day}, n = 4 chambers per treatment and species) of European beech and pubescent oak growing under control, warming, moisture reduction and warming + moisture reduction conditions during the growing season of 2020 and their respective annual carbon uptake (A_{tot}). The surplus of carbon uptake in warming, moisture reduction and warming + moisture reduction treatments before the leaf-out and after senescence of ambient trees are shown with right and left dash, respectively. Significant differences between treatments are indicated with capital (pubescent oak) and small (European beech) letters (Tukey's HSD post-hoc test, alpha = 0.05).

A2.3.4 Relationship between autumn phenology and sink/source activity

In both species, delayed senescence and a longer growing season were related to a higher A_{tot} (Fig. A2.4). However, none of the phenological measurements were correlated with sink activity (i.e., height and DBH increment).

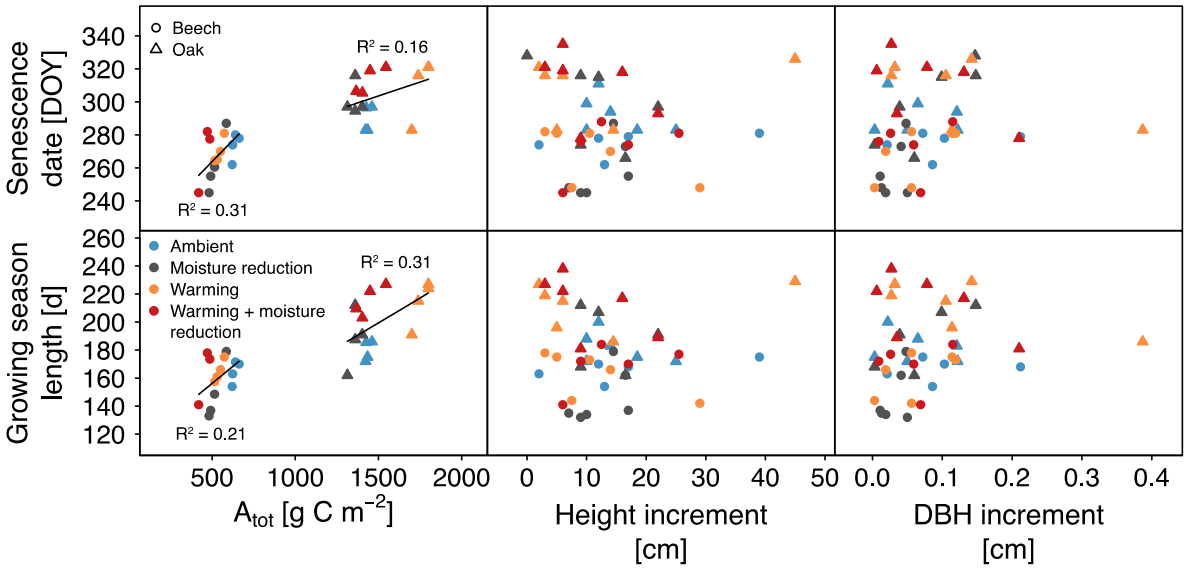

Figure A2.4: Phenology of European beech and pubescent oak growing under control, warming, moisture reduction and warming + moisture reduction conditions in relation to the source (modeled annual carbon uptake, A_{tot}) and the sink (increments of height and diameter at breast height, DHB). Significant linear relationships of each species (alpha = 0.05) are indicated with regression lines.

A2.4 Discussion

A2.4.1 Warming and moisture reduction effects on spring and autumn phenology

Our results support previous studies showing that global warming induces earlier tree activity (e.g., Vitasse et al., 2018; Piao et al., 2019; Beil et al. 2021). In addition, our results demonstrate that temperature impacts on spring phenology are independent of soil moisture in temperate trees as an advanced leaf unfolding occurred even when warming was combined to a substantial irrigation reduction (i.e., warming + soil moisture reduction treatment; Fig. A2.1). These impacts were observed only one year after the treatment started, demonstrating the importance of winter and spring temperature for spring phenology and explaining the high year-to-year variability of this phenological event (Meier et al., 2021). However, the magnitude of the phenological shift induced by warming differ widely between the two species with an advance of 15 days for oak and only 4.5 days for beech, a difference that remains similar when soil moisture reduction co-occurs with warming (Fig. A2.1). These differences, which are consistent with previous work (e.g., Vitasse et al., 2009), may be driven by a higher control of the photoperiod in beech trees compared to oak (Baumgarten et al., 2021). Our findings contradict, however, some work showing an earlier leaf-out in diffuse-porous species compared to ring-porous ones (e.g., Wang et al., 1995), which has been attributed to greater embolism in trees with larger vessels by the end of winter thereby impairing the supply of water to emerging leaves. As little loss of stem hydraulic conductivity was observed in our study (Fig. SA2.8) and leaf water potentials did not go beyond typical P_{50} (i.e., xylem pressure inducing a 50% loss of conductivity) values for those species (Fig. SA2.9) it is not surprising that treatment-induced phenological shifts were not associated to xylem vulnerabilities. Overall, our findings suggest that pubescent oak could benefit more than European beech from climate warming since it may become more competitive for resources such as water, nutrients, and light earlier in the growing season, particularly in stands where the two species co-occur. However, this response could also expose trees to other climate-associated stressors such as frost and herbivory damages (Vitasse et al., 2014; Chamberlain & Wolkovich, 2021).

Our results differ strikingly from previous work in semi-arid systems where similar warming of 5°C delayed the start of the growing season (Adams et al., 2015). The contrast between the two studies highlights the context-dependency of temperature impacts and suggests an essential role of the background climate. Indeed, as our results tend to show, temperate ecosystems, which are not yet limited by extreme drought and heat, are more likely to take advantage of warming-induced phenological shifts (Moritz & Agudo, 2013). Adams et al., (2015) further showed that soil moisture reduction exacerbates high temperature impact in semi-arid conditions, which contradicts our observations. Contrary to the strong effects found on source activity (Fig. A2.2), we observed no impact of soil moisture reduction on spring phenology for European beech, suggesting that temperature was solely responsible for shifts in leaf-out timing. Yet, opposite to our expectations,

an earlier leaf-out occurred for pubescent oak in response to soil moisture reduction, even if only by 4.9 days. Few studies have investigated moisture impacts on spring phenology in temperate regions. Using a similar experimental design, Kuster et al., (2014) also observed an earlier moisture-induced leaf-out in three oak species, including pubescent oak. However, the underlying mechanisms driving this response remains unknown. In Mediterranean ecosystems, Peñuelas et al., (2004) showed that precipitation correlates well with the timing of leaf development. Nevertheless, even in this dry ecosystem, the effects of moisture on leaf out date were still weaker than those associated with temperature (Peñuelas et al., 2002).

Despite our expectations and contrary to previous work (Arend et al., 2015), warming and soil moisture reduction had no impact on beech autumn phenology, but they prolonged the period of senescence in oak. Consequently, a longer growing season was observed for oak but not for beech, where temperature impacts on spring phenology were not as strong. This result suggests that different underlying processes are driving leaf-out and senescence timing. The initiation of senescence may be more controlled by the photoperiod (Keskitalo et al., 2005) even if, as shown in our study (Fig. A2.1), the duration of the senescence process can be extended with warming in more plastic species such as pubescent oak.

A2.4.2 Warming and soil moisture reduction effects on sink and source activity

Warming led to higher total modelled leaf-level C uptake in oak trees, mainly due to an extended growing season and earlier source activity. Warming further enhanced oak V_{cmax} throughout the growing season, resulting in higher modelled C uptake when all trees were active. We found no changes in chlorophyll content, which indicates that warming-exposed trees increased the amount and activity of the Rubisco enzyme but not necessarily the harvesting of the light energy (i.e., leaf absorbance), which is largely determined by the chlorophyll pigment concentration (Collatz et al., 1991). Hence, both a warming-extended growing season and increased C assimilation through warming-enhanced photosynthetic efficiency (i.e., enhanced amount of CO_2 catalyzed by Rubisco) led to a higher annual C uptake in warmed pubescent oaks. These findings are in agreement with previous work on pubescent oak from open-top chamber experiments where elevated temperature led to higher net photosynthesis (Arend et al., 2013). As we could not obtain whole-tree leaf area estimates it is difficult to predict temperature impacts at the whole-tree scale. Moreover, care should be taken with modelled results as they are not as reliable as empirical data, particularly during periods of high photosynthesis (Fig. SA2.5). Yet, no changes in leaf size and Huber values were observed, suggesting that our leaf-level findings could be representative of whole-tree C uptake strategy. We also observed substantial reductions in CO_2 uptake, stomatal conductance, V_{cmax}, and J_{max} in response to reduced soil moisture, supporting many previous studies (e.g., Xu & Baldocchi, 2003; Vaz et al., 2010; Arend et al., 2013). Consequently, oaks exposed to irrigation reduction had 12% less C uptake during the period when ambient trees were

also active. This reduction was entirely compensated in trees exposed to combined warming and irrigation reduction because of the extended growing season (Fig. A2.3). These findings are crucial as they suggest that advanced spring phenology and a longer growing season driven by higher temperature compensate for a drought-induced reduction in C uptake in pubescent oak (Ciais et al., 2005). C compensation under warming increased the amount of stored NSC concentrations, especially starch levels (Fig. SA2.7), which could play a significant role in the long-term for pubescent oak vulnerability to and recovery from climate extremes (Piper & Paula, 2020). Our study is the first to show this delicate balance existing between C-fixation limitations under limited soil moisture, increased photosynthetic efficiency and growing season length with warming, potentially allowing some species to persist under rising temperature by shifting their C uptake to the edge of the growing season. If these results can be validated for numerous species and if we could determine how it translates into annual carbon fixation, such compensation could substantially affect the strength of the carbon-climate feedback.

For European beech trees, an earlier photosynthetic activity was insufficient to compensate for the substantial reduction in modelled C uptake due to warming and limited soil moisture (Fig. A2.3). As strong reduction in stomatal conductance together with no changes in J_{max}, V_{cmax} and chlorophyll content was observed, these results indicate that stomatal closure and thus reduced intercellular CO_2 concentrations must be driving climate impacts on beech C uptake (Flexas et al., 2004). Large reductions of up to 44% in net photosynthesis and in the allocation of C resources belowground were also previously found for beech in response to warming and soil drought in such manipulative experiments (Hagedorn et al., 2016). Taken together, these findings suggest that, in the coming years, European beech may have to rely more often on an early-season C uptake when the air temperature is still low. Our results thus also contradict predictions of a longer growing season with global warming and climate mitigation effects through extended C uptake for temperate species such as European beech. Still, this finding corroborates many studies reporting that beech trees will likely experience population decline with future warming (Hanewinkel et al., 2013; Leuschner, 2020), likely because of the absence of warming-induced compensation through phenological adjustments. Moreover, as a species known for its low sensitivity to temperature compared to photoperiod limitation and chilling requirement (Vitasse & Basler, 2013), European beech may not have strong potential to adapt to global warming via phenological shifts. Nevertheless, care must be taken when interpreting these findings as beech showed low assimilation rates (Fig. A2.2) compared to previous work using the same experimental settings (Pflug et al., 2018). Low photosynthesis could be associated to high stress levels already under control conditions, which could explain the absence of C compensation found for this species (Fig. A2.3).

The absence of warming and soil moisture reduction impacts on sink activity (i.e., growth increment in height and DBH) is surprising but coherent with the absence of changes in leaf area, huber values and non-structural carbohydrates (Fig. SA2.7). Even if a large variability between

trees restricts our interpretation and raises uncertainties about sink activity results (Fig. SA2.6), these findings could suggest no imbalance or strong compensation between the sink and source activity. Previous studies have found reductions, increases, and no changes in productivity in response to warming and soil moisture limitation (e.g., Taeger et al., 2015; Liu et al., 2017; Manrique-Alba et al., 2018; Vanhellemont et al., 2019). For instance, using a similar experimental design, Arend et al., (2011) found that soil moisture stress decreased aboveground growth in pubescent oak by approx. 45% while warming enhanced it by 14%. Similarly, several studies reported that beech growth was severely reduced by higher vapor pressure deficit and soil moisture stress using open-top chamber experiments (e.g., Lendzion & Leuschner, 2008; Liu et al., 2017). The divergent findings could be attributed to local environmental factors, measuring approaches, or contrasting drought and warming levels. For instance, Arend et al., (2011) used different provenances and increased daytime air temperatures by approx. 2 °C while soil moisture was reduced by 50% in the warmed and moisture reduction treatments, respectively, compared to the control. Moreover, an essential part of the sink activity is taking place belowground, particularly in the earlier life stages and under temperature and soil moisture stress (Hertel et al., 2013). A higher allocation of assimilates belowground has been demonstrated in many species, including European beech (Hagedorn et al., 2016). However, as the actual contribution of the belowground sink activity is poorly known, future work should include a whole-tree sink and source activity perspective, as well as temperature and soil moisture gradients, to shed more light on the mechanisms driving phenological shifts. Further assessments across years would also be needed to confirm our observations and provide additional insight into sink/source feedbacks, mainly as warming effects in manipulative experiments can sometimes dissipate with time (Wolkovich et al., 2012).

A2.4.3 Effect of sink and source activity on autumn phenology

We hypothesized that changes in the source (i.e., net photosynthesis and total C uptake) and sink activity (i.e., height and diameter increment) would be associated with shifts in leaf senescence and growing season length. Our findings show that higher C uptake was consistently related to delayed leaf senescence and longer growing seasons, independently of the treatment, as highlighted by the positive relationships observed between variables (Fig. A2.4). Leaf senescence responses to warming and soil moisture changes are complex because they are determined by the interaction of many internal and external factors, among them hormones, sugar concentration, temperature, photoperiod, and water availability. In this context, while the cross-correlation of all these factors limits interpretation from long-term observations, manipulative experiments allow us to decipher more precisely the underlying processes, and our study tends to show that leaf senescence occurs later in plants that have assimilated more C. Yet, we urge caution in interpreting the significant relationships between senescence, growing season length, and A_{tot} observed here as the exact link between the two may be associated with other processes not accounted for. Recent work has associated senescence to source and sink activity whereby

elevated CO_2 and temperature stimulated photosynthesis earlier in the growing season, creating a sink limitation that subsequently causes earlier senescence (Zani et al., 2020). These findings are contradicting evidence provided by free-air CO_2 enrichment (FACE) experiments where, similarly as in our work, a warmer (and/or a CO_2-richer) environment lead to advanced and enhanced sink/source activity in temperate trees but no change or even delayed senescence depending on the species and duration of the manipulation (Norby, 2021). These inconsistencies may be related to the timing of warming and soil moisture limitation. If warming occurs early in the growing season, it should stimulate photosynthesis when growth demand is high and prolong senescence. However, warming could accelerate autumn phenology if it occurs towards the end of the growing season when growth demand is low (Beil et al., 2021). As our treatments were applied all along the growing season, the two effects may have been triggered and compensated for each other. More work on the importance of the soil moisture and warming timing would be needed to understand better the drivers of leaf senescence and their interactive effects. Overall, senescence drivers have not been well studied, and our results highlight the need to further evaluate these drivers in numerous species and across broad gradients of temperature and soil moisture.

A2.5 Acknowledgments

CG and MD were supported by the Swiss National Science Foundation SNF (PZ00P3_174068). YV was supported by the Swiss National Science Foundation SNF (315230_192712). The Sandoz Family Foundation supported CG, CB, and EM. We thank Marcus Schaub for his support with the experimental site. CG planned and designed the research. CG, JG, EM, and MDG conducted fieldwork. CG and CB analyzed the data. CG, CB, JG, EM, YV and MDG wrote the manuscript. The data that support the findings will be made openly available in a public repository (Zenodo or Dryade) upon acceptance of the manuscript.

A2.6 References

Adams HD, Collins AD, Briggs SP, Vennetier M, Dickman LT, Sevanto SA, Garcia-Forner N, Powers HH, Mcdowell NG. 2015. Experimental drought and heat can delay phenological development and reduce foliar and shoot growth in semiarid trees. Global Change Biology 21: 4210–4220.

Arend M, Brem A, Kuster TM, Günthardt-Goerg MS. 2013. Seasonal photosynthetic responses of European oaks to drought and elevated daytime temperature. Plant Biology 15: 169–176.

Arend M, Kuster T, Günthardt-Goerg MS, Dobbertin M. 2011. Provenance-specific growth responses to drought and air warming in three European oak species (Quercus robur, Q. petraea and Q. pubescens). Tree Physiology 31: 287–297.

Barigah TS, Charrier O, Douris M, Bonhomme M, Herbette S, Améglio T, Fichot R, Brignolas F, Cochard H. 2013. Water stress-induced xylem hydraulic failure is a causal factor of tree mortality in beech and poplar. Annals of Botany 112: 1431–1437.

Baumgarten F, Zohner CM, Gessler A, Vitasse Y. 2021. Chilled to be forced: the best dose to wake up buds from winter dormancy. New Phytologist 230: 1366–1377.

Berry J, Bjorkman O. 1980. Photosynthetic Response and Adaptation to Temperature in Higher Plants. Annual Review of Plant Physiology 31: 491–543.

Bigler C, Vitasse Y. 2021. Agricultural and Forest Meteorology Premature leaf discoloration of European deciduous trees is caused by drought and heat in late spring and cold spells in early fall. 307.

Ter Braak CJF, Vrugt JA. 2008. Differential Evolution Markov Chain with snooker updater and fewer chains. Statistics and Computing 18: 435–446.

Bréda N, Huc R, Granier A, Dreyer E. 2006. Temperate forest trees and stands under severe drought: A review of ecophysiological responses, adaptation processes and long-term consequences. Annals of Forest Science 63: 625–644.

Chamberlain CJ, Wolkovich EM. 2021. Late spring freezes coupled with warming winters alter temperate tree phenology and growth. New Phytologist 231: 987–995.

Chaves MM, Flexas J, Pinheiro C. 2009. Photosynthesis under drought and salt stress: Regulation mechanisms from whole plant to cell. Annals of Botany 103: 551–560.

Chen X, Wang W, Chen J, Zhu X, Shen M, Gan L, Cao X. 2020. Does any phenological event defined by remote sensing deserve particular attention? An examination of spring phenology of winter wheat in Northern China. Ecological Indicators 116: 1–8.

Ciais P, Reichstein M, Viovy N, Granier A, Ogée J, Allard V, Aubinet M, Buchmann N, Bernhofer C, Carrara A, et al. 2005. Europe-wide reduction in primary productivity caused by the heat and drought in 2003. Nature 437: 529–533.

Cochard H, Pimont F, Ruffault J, Martin-StPaul N. 2020. SurEau.c: A mechanistic model of plant water relations under extreme drought. bioRxiv.

Collatz GJ, Ball JT, Grivet C, Berry JA. 1991. Physiological and environmental regulation of stomatal conductance, photosynthesis and transpiration: a model that includes a laminar boundary layer. Agricultural and Forest Meteorology 54: 107–136.

Dallstream C, Piper FI. 2021. Drought promotes early leaf abscission regardless of leaf habit but increases litter phosphorus losses only in evergreens. Australian Journal of Botany 69: 121–130.

Dickman LT, Mcdowell NG, Sevanto S, Pangle RE, Pockman WT. 2015. Carbohydrate dynamics and mortality in a piñon-juniper woodland under three future precipitation scenarios. Plant, Cell and Environment 38: 729–739.

Dreyer E, Le Roux X, Montpied P, Daudet FA, Masson F. 2001. Temperature response of leaf photosynthetic capacity in seedlings from seven temperate tree species. Tree Physiology 21: 223–232.

Duursma RA. 2015. Plantecophys - An R package for analysing and modelling leaf gas exchange data. PLoS ONE 10: 1–13.

Estiarte M, Peñuelas J. 2015. Alteration of the phenology of leaf senescence and fall in winter deciduous species by climate change: Efects on nutrient proficiency. Global Change Biology 21: 1005–1017.

Fatichi S, Leuzinger S, Körner C. 2014. Moving beyond photosynthesis: From carbon source to sink-driven vegetation modeling. New Phytologist 201: 1086–1095.

Flexas J, Bota J, Loreto F, Cornic G, Sharkey TD. 2004. Diffusive and metabolic limitations to photosynthesis under drought and salinity in C3 plants. Plant Biology 6: 269–279.

Fryer JH, Ledig FT. 1972. Microevolution of the photosynthetic temperature optimum in relation to the elevational complex gradient. Canadian Journal of Botany 50: 1231–1235.

Fu Z, Ciais P, Bastos A, Stoy PC, Yang H, Green JK, Wang B, Yu K, Huang Y, Knohl A, et al. 2020. Sensitivity of gross primary productivity to climatic drivers during the summer drought of 2018 in Europe: Sensitivity of GPP to climate drivers. Philosophical Transactions of the Royal Society B: Biological Sciences 375.

García-Tejera O, López-Bernal Á, Testi L, Villalobos FJ. 2017. A soil-plant-atmosphere continuum (SPAC) model for simulating tree transpiration with a soil multi-compartment solution. Plant and Soil 412: 215–233.

Geng X, Fu YH, Hao F, Zhou X, Zhang X, Yin G, Vitasse Y, Piao S, Niu K, De Boeck HJ, et al. 2020. Climate warming increases spring phenological differences among temperate trees. Global Change Biology 26: 5979–5987.

González de Andrés E, Rosas T, Camarero JJ, Martínez-Vilalta J. 2021. The intraspecific variation of functional traits modulates drought resilience of European beech and pubescent oak. Journal of Ecology 109: 3652–3669.

Grossiord C, Sevanto S, Adams HD, Collins AD, Dickman LT, McBranch N, Michaletz ST, Stockton EA, Vigil M, McDowell NG, et al. 2016. Precipitation, not air temperature, drives functional responses of trees in semi-arid ecosystems. Journal of Ecology.

Grossiord C, Sevanto S, Borrego I, Chan AM, Collins AD, Dickman LT, Hudson PJ, McBranch N, Michaletz ST, Pockman WT, et al. 2017. Tree water dynamics in a drying and warming world. Plant, Cell & Environment.

Gu L, Pallardy SG, Tu K, Law BE, Wullschleger SD. 2010. Reliable estimation of biochemical parameters from C3 leaf photosynthesis-intercellular carbon dioxide response curves. Plant, Cell and Environment 33: 1852–1874.

Gunderson CA, O'hara KH, Campion CM, Walker A V., Edwards NT. 2010. Thermal plasticity of photosynthesis: The role of acclimation in forest responses to a warming climate. Global Change Biology 16: 2272–2286.

Hagedorn F, Joseph J, Peter M, Luster J, Pritsch K, Geppert U, Kerner R, Molinier V, Egli S, Schaub M, et al. 2016. Recovery of trees from drought depends on belowground sink control. Nature Plants 2.

Hanewinkel M, Cullmann DA, Schelhaas MJ, Nabuurs GJ, Zimmermann NE. 2013. Climate change may cause severe loss in the economic value of European forest land. Nature Climate Change 3: 203–207.

Hartig F, Dyke J, Hickler T, Higgins SI, O'Hara RB, Scheiter S, Huth A. 2012. Connecting dynamic vegetation models to data - an inverse perspective. Journal of Biogeography 39: 2240–2252.

Hartig F, Minunno F, Paul S, Cameron D, Ott T. 2018. BayesianTools: General-Purpose MCMC and SMC Samplers and Tools for Bayesian Statistics. R package version.

Hertel D, Strecker T, Müller-Haubold H, Leuschner C. 2013. Fine root biomass and dynamics in beech forests across a precipitation gradient - Is optimal resource partitioning theory applicable to water-limited mature trees? Journal of Ecology 101: 1183–1200.

Hoch G, Popp M, Körner C. 2002. Altitudinal increase of mobile carbon pools in Pinus cembra suggests sink limitation of growth at the Swiss treeline. Oikos 98: 361–374.

Juvany M, Müller M, Munné-Bosch S. 2013. Photo-oxidative stress in emerging and senescing leaves: A mirror image. Journal of Experimental Botany 64: 3087–3098.

Kattge J, Knorr W. 2007. Temperature acclimation in a biochemical model of photosynthesis: A reanalysis of data from 36 species. Plant, Cell and Environment 30: 1176–1190.

Keenan TF, Gray J, Friedl MA, Toomey M, Bohrer G, Hollinger DY, Munger JW, O'Keefe J, Schmid HP, Wing IS, et al. 2014. Net carbon uptake has increased through warming-induced changes in temperate forest phenology. Nature Climate Change 4: 598–604.

Keskitalo J, Bergquist G, Gardeström P, Jansson S. 2005. A cellular timetable of autumn senescence. Plant Physiology 139: 1635–1648.

Körner C. 2003. Carbon limitation in trees. Journal of Ecology 91: 4–17.

Kumarathunge DP, Medlyn BE, Drake JE, Tjoelker MG, Aspinwall MJ, Battaglia M, Cano FJ, Carter KR, Cavaleri MA, Cernusak LA, et al. 2019. Acclimation and adaptation components of the temperature dependence of plant photosynthesis at the global scale. New Phytologist 222: 768–784.

Lendzion J, Leuschner C. 2008. Growth of European beech (Fagus sylvatica L.) saplings is limited by elevated atmospheric vapour pressure deficits. Forest Ecology and Management 256: 648–655.

Leuschner C. 2020. Perspectives in Plant Ecology , Evolution and Systematics Drought response of European beech (Fagus sylvatica L .) — A review. 47.

Liu JF, Arend M, Yang WJ, Schaub M, Ni YY, Gessler A, Jiang ZP, Rigling A, Li MH. 2017. Effects of drought on leaf carbon source and growth of European beech are modulated by soil type. Scientific Reports 7: 1–9.

Manrique-Alba À, Sevanto S, Adams HD, Collins AD, Dickman LT, Chirino E, Bellot J, McDowell NG. 2018. Stem radial growth and water storage responses to heat and drought vary between conifers with differing hydraulic strategies. Plant Cell and Environment 41: 1926–1934.

Meier M, Vitasse Y, Bugmann H, Bigler C. 2021. Phenological shifts induced by climate change amplify drought for broad-leaved trees at low elevations in Switzerland. Agricultural and Forest Meteorology 307.

Moritz C, Agudo R. 2013. The future of species under climate change: Resilience or decline? Science 341: 504–508.

Muller JD, Rotenberg E, Tatarinov F, Oz I, Yakir D. 2021. Evidence for efficient non-evaporative leaf-to-air heat dissipation in a pine forest under drought conditions.

Nardini A, Pedà G, Rocca N La. 2012. Trade-offs between leaf hydraulic capacity and drought vulnerability: Morpho-anatomical bases, carbon costs and ecological consequences. New Phytologist 196: 788–798.

Niinemets Ü. 2010. Responses of forest trees to single and multiple environmental stresses from seedlings to mature plants: Past stress history, stress interactions, tolerance and acclimation. Forest Ecology and Management 260: 1623–1639.

Niinemets Ü, Valladares F. 2006. Tolerance to shade, drought, and waterlogging of temperate northern hemisphere trees and shrubs. Ecological Monographs 76: 521–547.

Norby RJ. 2021. Comment on "increased growing-season productivity drives earlier autumn leaf senescence in temperate trees. Science 371: 1066–1071.

Paul MJ, Foyer CH. 2001. Sink regulation of photosynthesis. Journal of Experimental Botany 52: 1383–1400.

Peñuelas J, Filella I, Comas P. 2002. Changed plant and animal life cycles from 1952 to 2000 in the Mediterranean region. Global Change Biology 8: 531–544.

Peñuelas J, Filella I, Zhang X, Llorens L, Ogaya R, Lloret F, Comas P, Estiarte M, Terradas J. 2004. Complex spatiotemporal phenological shifts as a response to rainfall changes. New Phytologist 161: 837–846.

Peters JMR, Gauthey A, Lopez R, Carins-Murphy MR, Brodribb TJ, Choat B. 2020. Non-invasive imaging reveals convergence in root and stem vulnerability to cavitation across five tree species. Journal of Experimental Botany 71: 6623–6637.

Pflug EE, Buchmann N, Siegwolf RTW, Schaub M, Rigling A, Arend M. 2018. Resilient leaf physiological response of European beech (Fagus sylvatica L.) to summer drought and drought release. Frontiers in Plant Science 9: 1–11.

Piao S, Liu Q, Chen A, Janssens IA, Fu Y, Dai J, Liu L, Lian X, Shen M, Zhu X. 2019. Plant phenology and global climate change: Current progresses and challenges. Global Change Biology 25: 1922–1940.

Piper FI, Paula S. 2020. The Role of Nonstructural Carbohydrates Storage in Forest Resilience under Climate Change. Current Forestry Reports 6: 1–13.

Qu AL, Ding YF, Jiang Q, Zhu C. 2013. Molecular mechanisms of the plant heat stress response. Biochemical and Biophysical Research Communications 432: 203–207.

Richardson AD, Keenan TF, Migliavacca M, Ryu Y, Sonnentag O, Toomey M. 2013. Climate change, phenology, and phenological control of vegetation feedbacks to the climate system. Agricultural and Forest Meteorology 169: 156–173.

Robson TM, Rodrguez-Calcerrada J, Snchez-Gmez D, Aranda I. 2009. Summer drought impedes beech seedling performance more in a sub-Mediterranean forest understory than in small gaps. Tree Physiology 29: 249–259.

Rödenbeck C, Zaehle S, Keeling R, Heimann M. 2020. The European carbon cycle response to heat and drought as seen from atmospheric CO 2 data for 1999-2018: Carbon cycle response in summer. Philosophical Transactions of the Royal Society B: Biological Sciences 375.

Santos VAHF dos, Ferreira MJ, Rodrigues JVFC, Garcia MN, Ceron JVB, Nelson BW, Saleska SR. 2018. Causes of reduced leaf-level photosynthesis during strong El Niño drought in a Central Amazon forest. Global Change Biology 24: 4266–4279.

Schönbeck L, Gessler A, Schaub M, Rigling A, Hoch G, Kahmen A, Li MH. 2020. Soil nutrients and lowered source:sink ratio mitigate effects of mild but not of extreme drought in trees. Environmental and Experimental Botany 169.

Schuldt B, Buras A, Arend M, Vitasse Y, Beierkuhnlein C, Damm A, Gharun M, Grams TEE, Hauck M, Hajek P, et al. 2020. A first assessment of the impact of the extreme 2018 summer drought on Central European forests. Basic and Applied Ecology 45: 86–103.

Taeger S, Sparks TH, Menzel A. 2015. Effects of temperature and drought manipulations on seedlings of Scots pine provenances. Plant Biology 17: 361–372.

Tardieu F, Granier C, Muller B. 2011. Water deficit and growth. Co-ordinating processes without an orchestrator? Current Opinion in Plant Biology 14: 283–289.

Tardieu F, Simonneau T. 1998. Variability among species of stomatal control under fluctuating soil water status and evaporative demand: modelling isohydric and anisohydric behaviours. Journal of Experimental Botany 49: 419–432.

Teskey R, Wertin T, Bauweraerts I, Ameye M, McGuire MA, Steppe K. 2015. Responses of tree species to heat waves and extreme heat events. Plant Cell and Environment 38: 1699–1712.

Tuzet A, Perrier A, Leuning R. 2003. A coupled model of stomatal conductance and photosynthesis for winter wheat. Plant, Cell & Environment 26: 1097–1116.

Urli M, Porté AJ, Cochard H, Guengant Y, Burlett R, Delzon S. 2013. Xylem embolism threshold for catastrophic hydraulic failure in angiosperm trees. Tree Physiology 33: 672–683.

Vanhellemont M, Sousa-Silva R, Maes SL, Van den Bulcke J, Hertzog L, De Groote SRE, Van Acker J, Bonte D, Martel A, Lens L, et al. 2019. Distinct growth responses to drought for oak and beech in temperate mixed forests. Science of the Total Environment 650: 3017–3026.

Vaz M, Pereira JS, Gazarini LC, David TS, David JS, Rodrigues A, Maroco J, Chaves MM. 2010. Drought-induced photosynthetic inhibition and autumn recovery in two Mediterranean oak species (Quercus ilex and Quercus suber). Tree Physiology 30: 946–956.

Vitasse Y, Basler D. 2013. What role for photoperiod in the bud burst phenology of European beech. European Journal of Forest Research 132: 1–8.

Vitasse Y, Delzon S, Dufrêne E, Pontailler JY, Louvet JM, Kremer A, Michalet R. 2009. Leaf phenology sensitivity to temperature in European trees: Do within-species populations exhibit similar responses? Agricultural and Forest Meteorology 149: 735–744.

Vitasse Y, Hoch G, Randin CF, Lenz A, Kollas C, Scheepens JF, Körner C. 2013. Elevational adaptation and plasticity in seedling phenology of temperate deciduous tree species. Oecologia 171: 663–678.

Vitasse Y, Lenz A, Körner C. 2014. The interaction between freezing tolerance and phenology in temperate deciduous trees. Frontiers in Plant Science 5: 1–12.

Vitasse Y, Signarbieux C, Fu YH. 2018. Global warming leads to more uniform spring phenology across elevations. Proceedings of the National Academy of Sciences of the United States of America 115: 1004–1008.

Weber R, Gessler A, Hoch G. 2019. High carbon storage in carbon-limited trees. New Phytologist 222: 171–182.

Wolkovich EM, Cook BI, Allen JM, Crimmins TM, Betancourt JL, Travers SE, Pau S, Regetz J, Davies TJ, Kraft NJB, et al. 2012. Warming experiments underpredict plant phenological responses to climate change. Nature 485: 494–497.

Woodruff DR, Meinzer FC. 2011. Water stress, shoot growth and storage of non-structural carbohydrates along a tree height gradient in a tall conifer. Plant, Cell and Environment 34: 1920–1930.

Xie Y, Wang X, Silander JA. 2015. Deciduous forest responses to temperature, precipitation, and drought imply complex climate change impacts. Proceedings of the National Academy of Sciences of the United States of America 112: 13585–13590.

Xie Y, Wang X, Wilson AM, Silander JA. 2018. Predicting autumn phenology: How deciduous tree species respond to weather stressors. Agricultural and Forest Meteorology 250–251: 127–137.

Xu L, Baldocchi DD. 2003. Seasonal trends in photosynthetic parameters and stomatal conductance of blue oak (Quercus douglasii) under prolonged summer drought and high temperature. Tree Physiology 23: 865–877.

A2.7 Supporting information

A2.7.1 Supporting figures

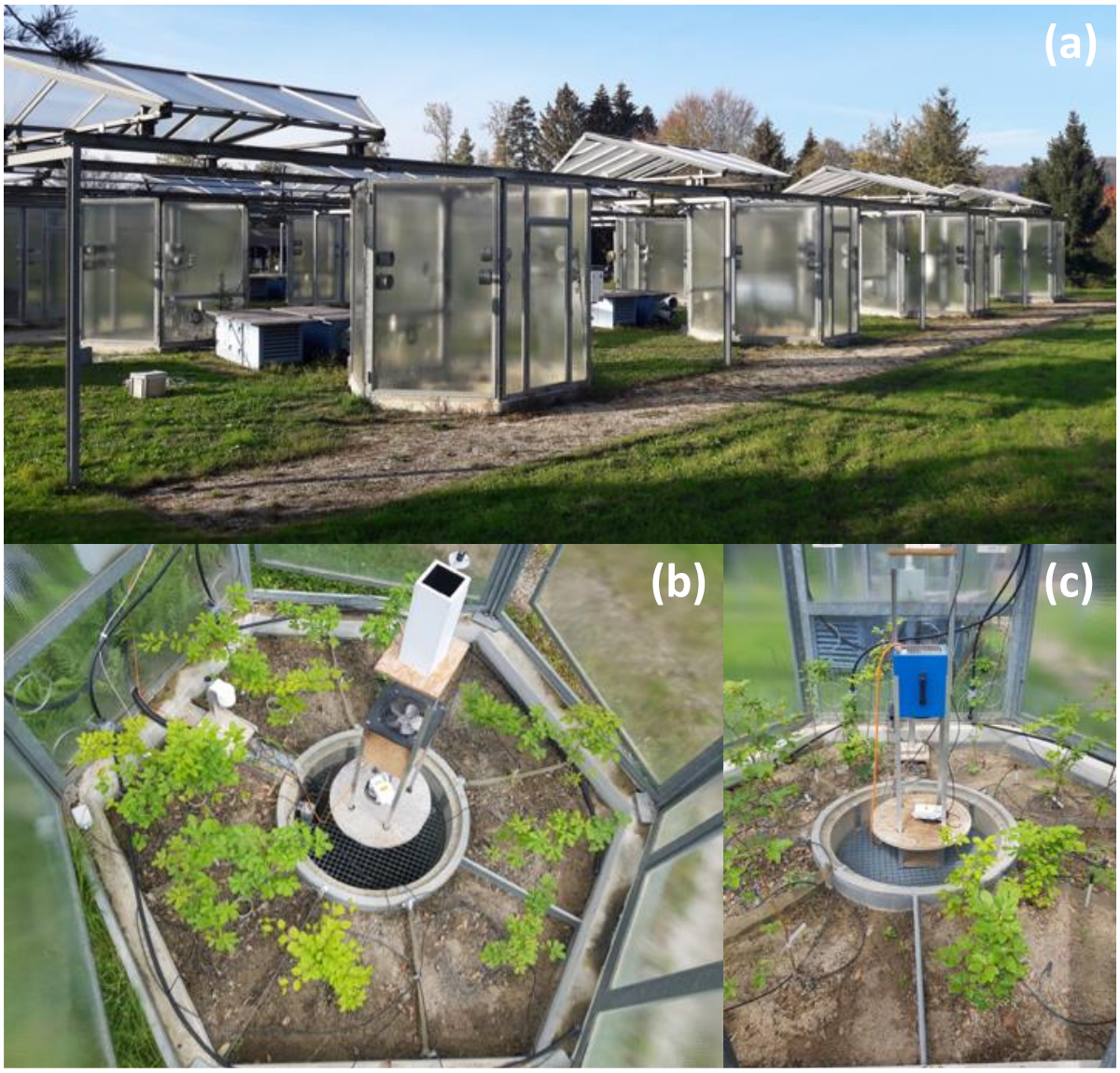

Figure SA2.1: Pictures showing the experimental design implemented at the facility. Sixteen open-top chambers are assigned to four treatments (a) (n=4 chambers per treatment): control (no heating and irrigation restriction not applied), warming (+5 °C above the air temperature inside the control chambers), moisture reduction (irrigation reduced by approx. 70%), and warming + moisture reduction (both treatments applied simultaneously). A simple fan (b) (for maintaining similar air circulation in non-warmed chambers) or a heating unit blowing hot air (c) (for warmed chambers) is located at the center of each chamber.

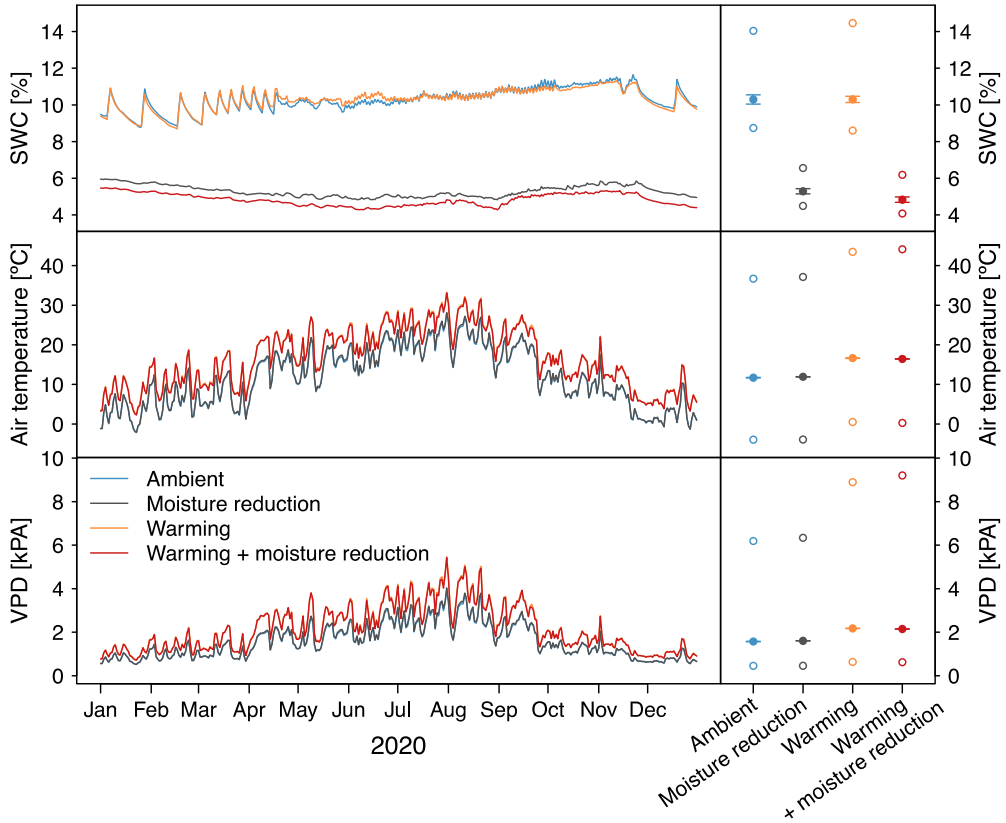

Figure SA2.2: Daily and annual mean soil water content (SWC), air temperature, and vapor pressure deficit (VPD) measured in the open-top chambers in each treatment. Filled symbols show the annual means ± s.e. (n = 4 chambers per treatment), open symbols show the hourly minima and maxima.

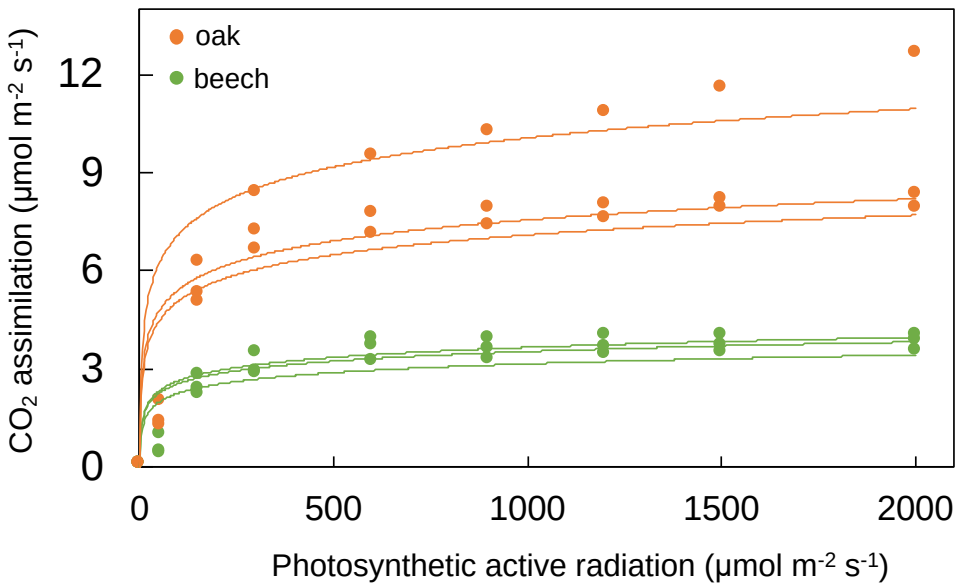

Figure SA2.3: Photosynthetic light-response curves in the control treatment measured in June 2019 on three trees per species.

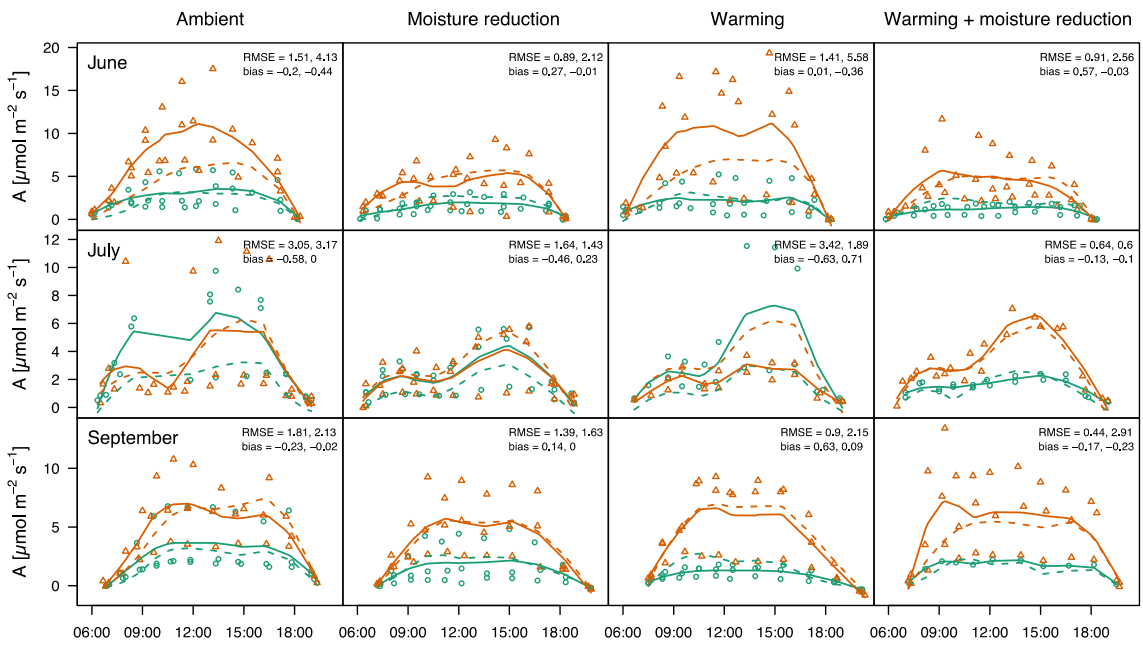

Figure SA2.4: Photosynthesis (A) measured from sunrise to sunset on beech (green) and oak (orange) seedlings growing under ambient, moisture reduction, warming and warming + moisture reduction conditions and measured in June, July and September 2020. Locally weighed regression lines are added for the measured A (solid lines) and for A simulated with the SPAC model (dashed lines). The root mean squared error (RMSE) and bias are shown for each treatment and measurement campaign for beech and oak, respectively.

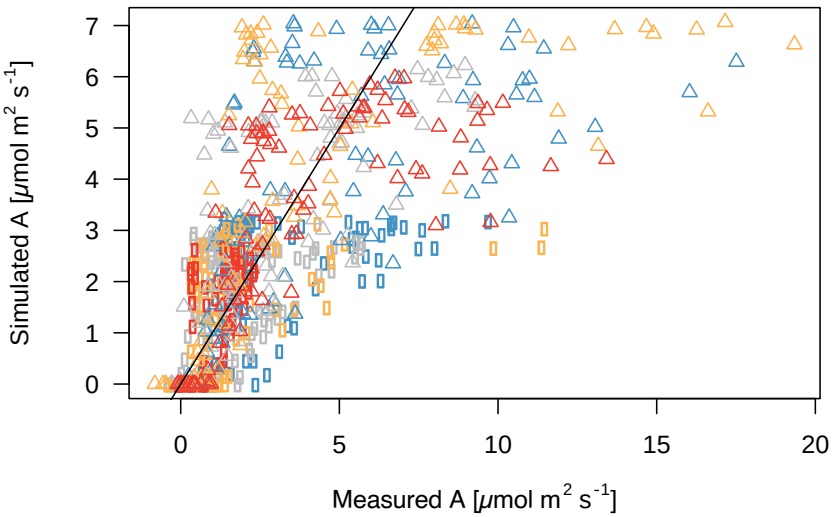

Figure SA2.5: Simulated photosynthesis (A) compared to values measured from sunrise to sunset on beech (circles) and oak (triangles) seedlings growing under control (blue), moisture reduction (grey), warming (orange) and warming + moisture reduction (red) conditions and measured in June, July and September 2020. The solid line depicts the 1:1 ratio and shows that simulated A was underestimated mostly for oak seedlings grown in control and warmed conditions.

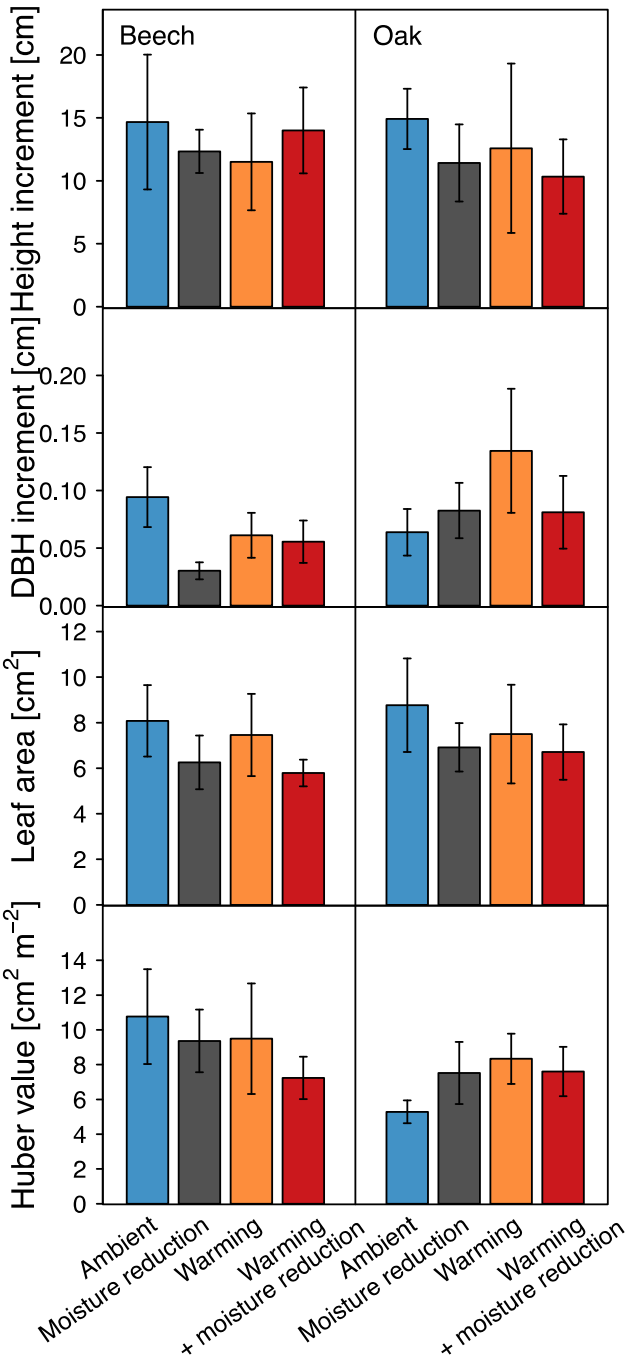

Figure SA2.6: Seedling height and diameter at breast height (DBH) increments between May and September 2020, single leaf area and Huber value for beech and oak growing under control, warming, moisture reduction and warming + moisture reduction conditions (mean ± s.e.; n = 5–6 trees per treatment and species). No significant differences between treatments were found.

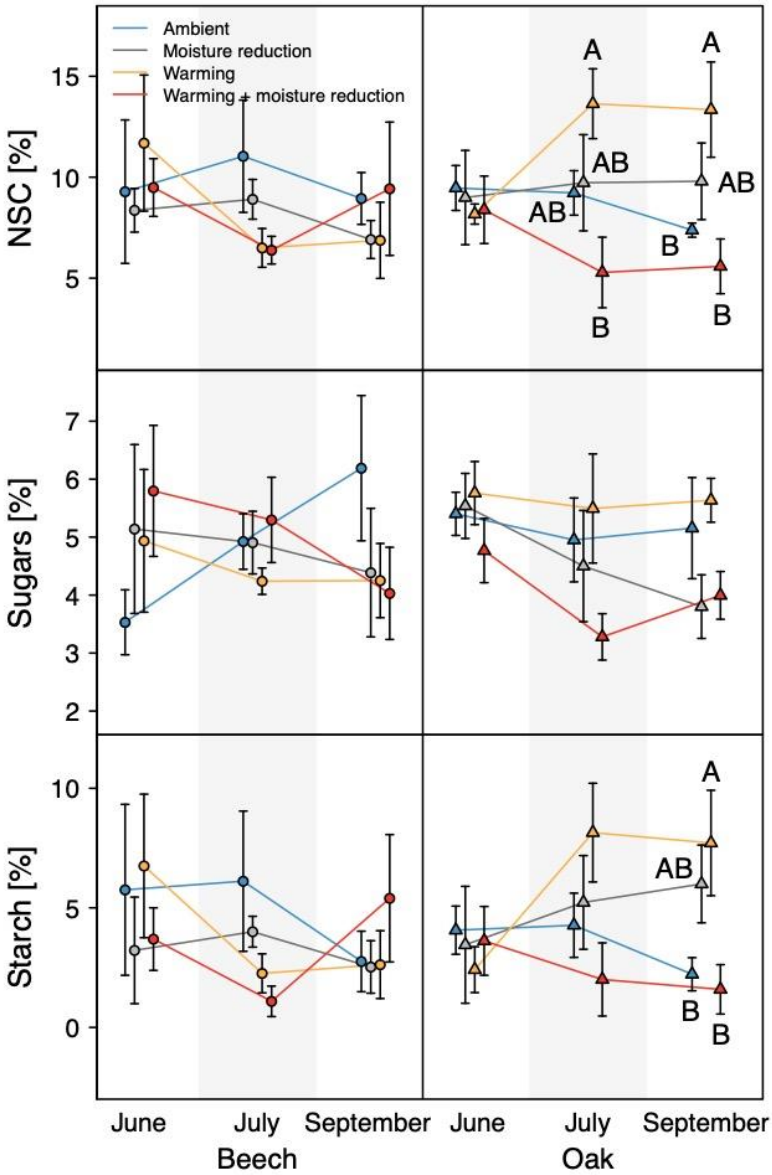

Figure SA2.7: Total leaf non-structural carbohydrate (NSC) concentration, starch (St) concentration, and sugar (Sg) concentration (mean ± s.e.; n = 6 trees per treatment and species) for beech (circles) and oak (triangles) growing under control (blue), moisture reduction (grey), warming (orange) and warming + moisture reduction (red) conditions and measured in June, July and September 2020. Significant differences between treatments for a given campaign are indicated with letters (Tukey's HSD post-hoc test, alpha = 0.05).

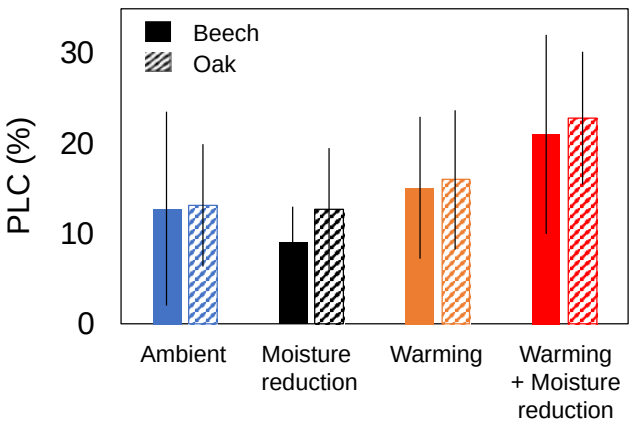

Figure SA2.8: Mean percentage loss of conductivity (PLC, %) for beech and oak growing under control (blue), moisture reduction (black), warming (orange) and warming + moisture reduction (red) conditions and measured in September 2020. No significant differences between species and treatments were found.

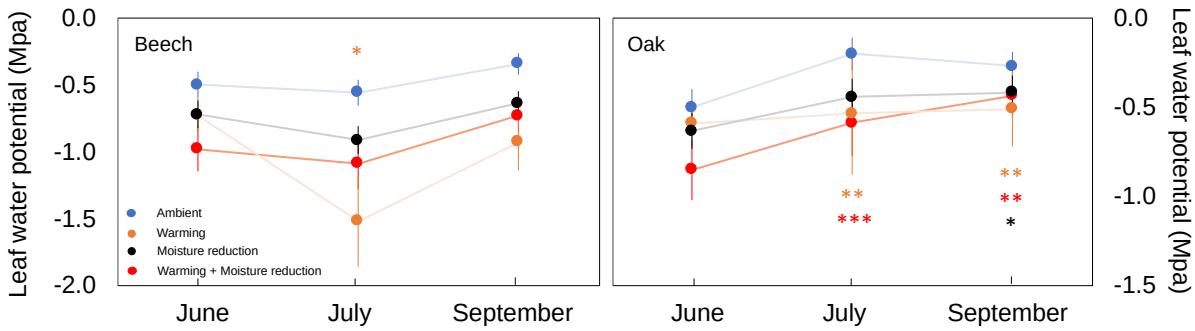

Figure SA2.9: Mean predawn leaf water potential (MPa) for beech and oak growing under control (blue), moisture reduction (black), warming (orange) and warming + moisture reduction (red) conditions and measured in June, July and September 2020. Significant differences between treatments and ambient conditions for a given campaign are indicated with stars (*P< 0.05, **P<0.01, ***P<0.001).

A2.7.2 Supporting tables

Table SA2.1: Model parameters that were either measured in our field experiment, extracted from the literature, or calibrated as indicated.

Acronym	Parameter	Units	Parameter value	Source
V_{cmax}	carboxylation capacity	µmol m^{-2} s^{-1}	31.5 (beech); 57.7 (oak)	calibrated
J_{max}	electron transport capacity	µmol m^{-2} s^{-1}	49.8 (beech); 66.7 (oak)	calibrated
$T_{max(Jmax)}$	temperature maximum of J_{max}	ºC	57.05 for both species	Williams et al., 1996
$T_{max(Vcmax)}$	temperature maximum of V_{cmax}	ºC	65.03 for both species	Williams et al., 1996
$T_{opt(Jmax)}$	temperature optimum of J_{max}	ºC	32 (beech); 34 (oak)	Medlyn et al., 2002
$T_{opt(Vcmax)}$	temperature optimum of V_{cmax}	ºC	36 (beech); 39 (oak)	Medlyn et al., 2002
Ψ_f	leaf turgor loss point	kPa	-354 (beech); -346 (oak)	measured
g_0	minimum leaf conductance	mmol m^{-2} s^{-1}	0.010 (beech); 0.0078 (oak)	measured
S_f	stomatal sensitivity to Ψ_{leaf}		0.0086 (beech); 0.0089 (oak)	calibrated
m	proportionality factor between g_S and A		1.195 (beech); 1.001 (oak)	calibrated
R_{soil}	soil resistance to water flow		10'000	Garcia-Tejera et al., 2017
R_{root}	root resistance to water flow		10'000	Garcia-Tejera et al., 2017
R_{xylem}	xylem resistance to water flow		0.1	Garcia-Tejera et al., 2017

Table SA2.2: Linear mixed model results (*F*- and *P*-value) of the effect of warming (W), moisture reduction (MR), campaign (C), and their interactive effects on maximum photosynthesis (A_{max}), stomatal conductance (g_s), rubisco carboxylation (V_{cmax}), electron transport rate (J_{max}), and chlorophyll concentration ([Chl]). Significant effects are highlighted in bold.

Explained variables	Species	Treatment						
		W	MR	C	W x MR	W x C	MR x C	W x MR x C
A_{max}	Beech	0.01 (0.979)	**6.35 (0.028)**	**5.45 (0.008)**	1.49 (0.247)	0.08 (0.914)	2.08 (0.137)	2.62 (0.084)
	Oak	0.08 (0.766)	**21.03 (< 0.001)**	2.10 (0.131)	2.27 (0.137)	0.26 (0.769)	0.10 (0.898)	0.51 (0.598)
g_s	Beech	1.05 (0.329)	**10.30 (0.009)**	**13.50 (< 0.001)**	0.71 (0.416)	0.13 (0.874)	1.01 (0.369)	0.46 (0.629)
	Oak	0.01 (0.996)	**14.60 (0.003)**	1.67 (0.196)	3.96 (0.051)	0.71 (0.494)	1.00 (0.373)	0.32 (0.776)
V_{cmax}	Beech	**5.43 (0.040)**	2.50 (0.142)	**28.27 (< 0.001)**	2.63 (0.133)	2.55 (0.091)	1.78 (0.180)	1.78 (0.181)
	Oak	3.90 (0.076)	**16.29 (0.002)**	**7.33 (0.002)**	1.87 (0.200)	0.31 (0.729)	0.09 (0.907)	0.48 (0.622)
J_{max}	Beech	1.36 (0.268)	1.47 (0.250)	**4.25 (0.021)**	2.96 (0.113)	1.67 (0.201)	0.91 (0.410)	1.06 (0.356)
	Oak	0.04 (0.834)	**21.23 (< 0.001)**	0.08 (0.917)	3.98 (0.051)	0.37 (0.693)	0.58 (0.562)	0.29 (0.743)
[Chl]	Beech	0.04 (0.843)	1.65 (0.227)	**5.09 (0.010)**	0.01 (0.921)	0.45 (0.637)	0.14 (0.869)	0.37 (0.691)
	Oak	1.81 (0.217)	5.07 (0.056)	0.17 (0.840)	0.51 (0.496)	0.41 (0.663)	0.47 (0.624)	0.48 (0.620)

References

Hoch, G., Popp, M. and Körner, C., 2002. Altitudinal increase of mobile carbon pools in Pinus cembra suggests sink limitation of growth at the Swiss treeline. Oikos, 98(3), pp.361-374.

Medlyn, B.E., Dreyer, E., Ellsworth, D., Forstreuter, M., Harley, P.C., Kirschbaum, M.U.F., Le Roux, X., Montpied, P., Strassemeyer, J., Walcroft, A. and Wang, K., 2002. Temperature response of parameters of a biochemically based model of photosynthesis. II. A review of experimental data. Plant, Cell & Environment, 25:1167-1179.

Schönbeck, L., Gessler, A., Hoch, G., McDowell, N.G., Rigling, A., Schaub, M. and Li, M.H., 2018. Homeostatic levels of nonstructural carbohydrates after 13 yr of drought and irrigation in Pinus sylvestris. New Phytologist, 219(4), pp.1314-1324.

Williams, M., E.B. Rastetter, D.N. Fernades et al. 1996. Modelling the soil-plant-atmosphere continuum in a Quercus–Acer stand at Harvard Forest: the regulation of stomatal conductance by light, nitrogen and soil/plant hydraulic properties. Plant, Cell & Environment, 19: 911–927.

Appendix 3

Absence of canopy temperature variation despite stomatal adjustment in *Pinus sylvestris* under multidecadal soil moisture manipulation

Alice Gauthey[1,2], Christoph Bachofen[1,2], Janisse Deluigi[1,2], Margaux Didion-Gency[3], Petra D'Odorico[4], Jonas Gisler[3], Eugénie Mas[1,2], Marcus Schaub[3], Philipp Schuler[3], Christopher Still[5], Alex Tunas[1,2], Charlotte Grossiord[1,2]

[1] Plant Ecology Research Laboratory PERL, School of Architecture, Civil and Environmental Engineering, EPFL, CH-1015 Lausanne Switzerland

[2] Community Ecology Unit, Swiss Federal Institute for Forest, Snow and Landscape research WSL, CH- 8903, Birmensdorf, Switzerland

[3] Forest Dynamics Unit, Swiss Federal Institute for Forest, Snow and Landscape WSL, CH-8903 Birmensdorf, Switzerland.

[4] Land Change Science Unit, Swiss Federal Institute for Forest, Snow and Landscape WSL, CH-8903 Birmensdorf, Switzerland.

[5] Forest Ecosystems and Society, Oregon State University, Corvallis, OR 97331, USA

This appendix has been published in the peer-reviewed journal "*New Phytologist*"

Gauthey, A., Bachofen, C., Deluigi, J., Didion-Gency, M., Gisler, J., Mas, E., Schaub, M., Schuler, P., Still, C. J., Tunas, A., & Grossiord, C. (2023). Absence of canopy temperature variation despite stomatal adjustment in Pinus sylvestris under multidecadal soil moisture manipulation. *New Phytologist*, *240*(1), 127-137. https://doi.org/10.1111/nph.19136

Abstract

- Global warming and droughts push forests closer to their thermal limits, altering tree carbon uptake and growth. To prevent critical overheating, trees can adjust their thermotolerance (T_{crit}), temperature and photosynthetic optima (T_{opt} and A_{opt}) and canopy temperature (T_{can}) to stay below damaging thresholds. However, we lack understanding of how soil droughts affect photosynthetic thermal plasticity and T_{can} regulation.
- In this study, we measured the effect of soil moisture on the seasonal and diurnal dynamics of net photosynthesis (A), stomatal conductance (g_s), and T_{can}, as well as the thermal plasticity of photosynthesis ($T_{crit,}$ $T_{opt,}$ and A_{opt}), over the course of one year using a long-term irrigation experiment in a drought-prone *Pinus sylvestris* forest in Switzerland.
- Irrigation resulted in higher needle-level A, g_s, $T_{opt,}$ and A_{opt} compared to naturally drought-exposed trees. No daily or seasonal differences in T_{can} were observed between treatments. Trees operated below their thermal thresholds (T_{crit}), independently of soil moisture content.
- Despite strong T_{can} and T_{air} coupling, we provide evidence that drought reduces trees' temperature optimum due to a substantial reduction of g_s during warm and dry periods of the year. These findings provide important insights regarding the effects of soil drought on the thermal tolerance of *Pinus Sylvestris*.

Keywords: drought, irrigation, photosynthesis, *Pinus sylvestris*, plasticity, temperature response, thermoregulation

A3.1 Introduction

Heatwaves and droughts are expected to increase in magnitude, frequency, and duration throughout the 21st century (Pachauri et al., 2015). Heat drives higher vapour pressure deficit (VPD), which increases the effects of soil drought, leading to reduced photosynthesis and altered global carbon cycling (Grossiord et al., 2020). While leaves can operate within a broad range of air temperatures (T_{air}), they must stay under a species-specific temperature threshold to sustain their function. With increasing heatwaves and droughts, temperatures exceeding these thresholds might become common and negatively impact photosynthesis, carbon gain, and the growth of forests (O'sullivan et al., 2017).

While species from hotter and drier climates can typically withstand higher temperatures than those from mesic environments (Zhu et al., 2018), individuals may acclimate to global warming and reduced precipitation by increasing their heat tolerance. Thermotolerance is an important parameter for measuring thermal safety margins in plants. Thermotolerance is often assessed by measuring the critical temperature that induced a steep rise in chlorophyll fluorescence (Tcrit, Schreiber & Berry, 1977; Kitudom et al., 2022) or the temperature causing a 50% reduction of the maximum quantum yield of the photosystem II (PSII) (T_{50}, Marias et al., 2017). The two parameters indicate different damage levels to the PSII associated with high temperature, and, as such, they are both essential for understanding plant heat-tolerance mechanisms (Marias et al., 2017). Previous work has shown a broad variability in thermotolerance with T_{50} in conifers typically exceeding the maximum air and leaf temperatures experienced during heat stress (T_{air} and leaf>40°C, e.g., Kunert et al., 2021). Interspecific variation in thermotolerance seems to be driven by extreme leaf temperatures experienced by species, with species experiencing higher leaf temperatures typically having stronger heat tolerances (Perez & Feeley, 2020). Moreover, trees can adjust their thermal thresholds to drier and warmer conditions (Knight & Ackerly, 2002). For instance, Marchin et al., (2022) found an increase in T_{crit} of +1.3°C across a broad range of evergreen species exposed to an artificial hot drought in a greenhouse experiment. Similarly, higher T_{50} was found in water-stressed desert species than well-watered ones (Cook et al., 2021) and plants exposed to a heatwave (Drake et al., 2018). Shifts in thermotolerance could result from an accumulation of heat shock proteins, osmolytes, and secondary metabolites (Wahid et al., 2007) and depend on the species acclimation potential (Zhu et al., 2018). Yet, whether significant shifts in thermotolerance in response to drier conditions take place in long-lived foliage of coniferous trees remains unclear.

In addition to thermotolerance acclimation, adjustment of the optimum photosynthetic temperature (T_{opt}) may allow plants to reach maximum CO_2 uptake (A_{opt}) under higher leaf temperatures. Adjustments of T_{opt} are mostly dependent on biochemical processes such as carboxylation capacity (V_{cmax}), electron transport capacity (J_{max}), and leaf respiration, as well as adjustments in stomatal conductance (g_s) (Hikosaka et al., 2006; Smith & Dukes, 2017). Plants

exposed to hot or dry conditions can quickly adjust their Topt (within a few days), indicating that photosynthetic acclimation to temperature is a dynamic mechanism that will play an increasingly important role in forest trajectories under global warming (Yamori et al., 2014; Sperlich et al., 2019; Kumarathunge et al., 2020). For example, during drought, it was shown that T_{opt} decreases (in seedlings of Eucalyptus tereticornis, Kumarathunge et al., 2020; in wheat, Fang et al., 2023) because of stomatal closure. In warming experiments, Topt has been shown to increase by 0.4°C per 1°C of warming in a broad range of boreal and temperate species (Sendall et al., 2015) or by more than 1°C per 1°C of warming in tropical species (Wittemann et al., 2022). Globally, it was found that T_{opt} increases on average by 0.34°c per 1°C of warming in a broad scope of evergreen species ranging from boreal to tropical biomes (Crous et al., 2022). During droughts, trees can also shift their timing of optimum photosynthesis (A_{opt}) to spring and autumn because of tighter stomatal control to avoid summertime periods of extreme soil moisture shortage and high VPD, as was found in evergreen *Juniperus thurifera* L. (Gimeno et al., 2012). However, photosynthetic plasticity under drought is not always observed (Limousin et al., 2010; Gagne et al., 2020), and A_{opt} is usually optimised under maximum daytime temperatures (Slot & Winter, 2017; Tan et al., 2017). Yet, as most of the work investigating acclimation of thermotolerance and thermal plasticity was undertaken in controlled conditions on young plants exposed to short-term temperature or soil moisture variations, it is difficult to translate these findings to in-situ conditions in mature forests. To date, few studies have investigated how long-term changes in soil moisture alter the photosynthetic optima and thermotolerance in natural forests (Sastry et al., 2018; Docherty et al., 2023).

Acclimation strategies such as increased T_{crit}, T_{50}, and T_{opt} should be directly associated with higher temperature ranges experienced by tree canopies during droughts (Gunderson et al., 2010). Regulation of leaf temperature (T_{leaf}) is an important mechanism to control plant physiology such as respiration, transpiration, and photosynthesis, but also biochemical processes such as enzymatic inactivation or chlorophyll degradation (Ribeiro et al., 2004; Wahid et al., 2007; Teskey et al., 2015; Still et al., 2021; Tarvainen et al., 2022). T_{leaf} depends directly on leaf traits, canopy structure, and the local environmental conditions that determine the leaf energy balance (Balota et al., 2008; Blonder & Michaletz, 2018). The absorbed energy from short and longwave radiation (i.e., net radiation) is partially offset by latent (LE) heat flux (evapotranspiration) and sensible (H) heat flux, which is positively related to air turbulence (Still et al., 2021). Tleaf is therefore affected by several leaf traits such as leaf size, thickness, roughness, structure, and angle, which all influence the interception of radiation and latent and sensible heat fluxes (Monteith & Unsworth, 2013; Wright et al., 2017). For instance, larger leaf area and width are related to higher leaf temperature and extended temperature range during hot periods (Leigh et al., 2017), while thicker leaves can considerably reduce damage from high temperatures (Leigh et al., 2012).

Under water-limited conditions, leaf cooling through evapotranspiration is reduced due to stomatal closure to prevent excessive water loss. This reduction of latent heat fluxes can cause

large deviations of T_{leaf} above T_{air} (Fauset et al., 2018; Cook et al., 2021), bringing leaves closer to their thermal thresholds (Marchin et al., 2022). Alternatively, heat can be dissipated through sensible heat fluxes via air turbulence, which can be the main heat dissipation pathway when latent heat fluxes are reduced or suppressed under dry conditions and high VPD (Muller et al., 2021). This 'canopy convector effect' happens particularly efficiently in dry conifer forests with low tree density and open canopies, where the coupling between the canopy and atmosphere is high, and the aerodynamic resistance is low (Rotenberg & Yakir, 2010). Most work investigating drought impacts on leaf temperature regulation has been conducted on broadleaf species in experimental conditions and has shown that drought-exposed potted trees can heat up to +4°C compared to well-watered plants (Buddenbaum et al., 2015; Peguero-Pina et al., 2020; Marchin et al., 2022). In coniferous forests, needle-like leaves are much thinner and smaller than broadleaved ones, resulting in a higher air-to-leaf heat transfer due to a close coupling of canopy temperature (T_{can}) and T_{air} (Still et al., 2022). For instance, in a very dry pine forest, Muller et al., (2021) found little variation in T_{can} between drought-exposed vs. irrigated trees despite a 10-fold higher transpiration rate of the latter. These findings suggest that moisture-limited coniferous forests are less likely to experience large leaf temperature variations during severe droughts because of the predominant role of non-evaporative cooling in such sparse canopies. However, whether these observations can be transferred to more humid regions with forests that have higher needle areas remains to be tested. Further, whether a more limited T_{can} variability also translates into lower photosynthetic thermal acclimation remains unknown. Very little work has investigated how long-term soil moisture changes affect the diurnal and seasonal dynamics of photosynthesis and its thermal plasticity in relation to T_{can} in natural ecosystems. Nevertheless, understanding the interactions between heat stress and water limitation is essential to accurately parameterize climate-vegetation models and predict the effects of global warming on vegetation dynamics (Kunert et al., 2022).

In this study, we investigated how long-term plasticity to contrasting soil moisture affects the diurnal and seasonal patterns of net photosynthesis (A), stomatal conductance (g_s), transpiration (E), the thermal tolerance of photosynthesis (T_{opt}, A_{opt}, T_{crit}, and T_{50}), and canopy temperature (T_{can}). The work was conducted in a Scots pine forest in a drought-prone region, where part of the forest has been irrigated since 2003. Despite results from Muller et al. (2021), we expected to see higher T_{can} in trees growing under seasonally water-limited conditions (i.e., control, non-irrigated trees) because of reduced latent heat flux compared to trees growing in higher soil moisture (i.e., irrigated trees), especially during the warmest and driest period of the day (i.e., after midday) and the year (in mid-summer). Moreover, increasing T_{can} in control trees should lead to higher T_{opt}, T_{50}, and T_{crit} compared to irrigated trees, potentially resulting in less severe downregulation of photosynthesis during the warmest period of the year. We also expected to see a strong response of gas exchange to water availability, with irrigated trees having higher A, g_s, and E than control trees throughout the day in mid-summer when soil moisture significantly drops in non-irrigated conditions.

A3.2 Materials and methods

A3.2.1 Study site and experimental design

Our study site is a naturally regenerated 120-year-old forest (Pfynwald) situated in the Rhone valley, a dry inner-alpine region in south-western Switzerland (615 m a.s.l., 46°18'N, 7°37'E), whose forest cover is dominated by Scots pine (*Pinus sylvestris*). The average canopy height is approximately 12 m with a stand density of 730 stems ha-1 and a basal area of 27.3 m^2 ha^{-1}. This site's mean annual temperature and cumulative precipitation are 10.7°C (maximum temperature of 37.2°C in July) and 575 mm (lowest values of 34 mm in July), respectively, for the period 1995-2014 (from the closest meteorological station in Sion; Herzog et al., 2014). The terrain is flat, and the soil is composed of an alluvial fan made of limestone, marble, quartzite, and gneiss, allowing the water to penetrate the bedrock easily.

In 2003, an experimental site was set up in an area of 1.2 ha (~800 trees) divided into eight plots of 25 x 40 m each, separated by a 5 m buffer zone (Dobbertin et al., 2010). Half of the plots are watered each night (~600 mm year-1, between May and October) with sprinklers at 1 m height using a nearby channel fed by the Rhone river (irrigated treatment), while the other half is exposed to natural dry conditions (control treatment). In 2015, scaffolds were installed in 6 plots (3 controls and 3 irrigated) to reach tree crowns and enable in-situ canopy measurements.

We carried out five measurement campaigns of two days each in March, May (i.e., before the start of the irrigation), June, August (i.e., during irrigation), and October (i.e., after stopping the irrigation) of 2022. During each campaign, drone flights for acquiring thermal images of the canopy and needle-level gas exchange measurements were conducted simultaneously. For the gas exchange measurements, we selected 2 to 5 trees per plot that could be reached from the top of the scaffolds, for a total of 19 sampled trees (10 irrigated, 9 control). Gas exchange measurements and capture of thermal images (described in detail below) were taken diurnally, between sunrise and sunset at 1 h or 2 h intervals (resulting in 9 to 11 measurements per replicate each day). Measurements were performed over two consecutive days with similar temperatures, humidity, and insolation for each campaign.

A3.2.2 Environmental measurements

Air temperature, relative humidity (HydroVUE10 sensors in a RAD10 radiation shield, Campbell Scientific, Logan, UT, USA), and precipitation (rain[e]H3, Lambrecht Meteo GmbH, Germany) were recorded at 10 min intervals using sensors installed at the top of a 13 m high scaffold and jutting 1 m above the tree canopy. Some meteorological data outside the measurement periods were missing because of sensor failures. The data were filled with

observations extracted from the closest meteorological station 20 km away (Idaweb, MeteoSwiss) to complete Fig. A3.1.

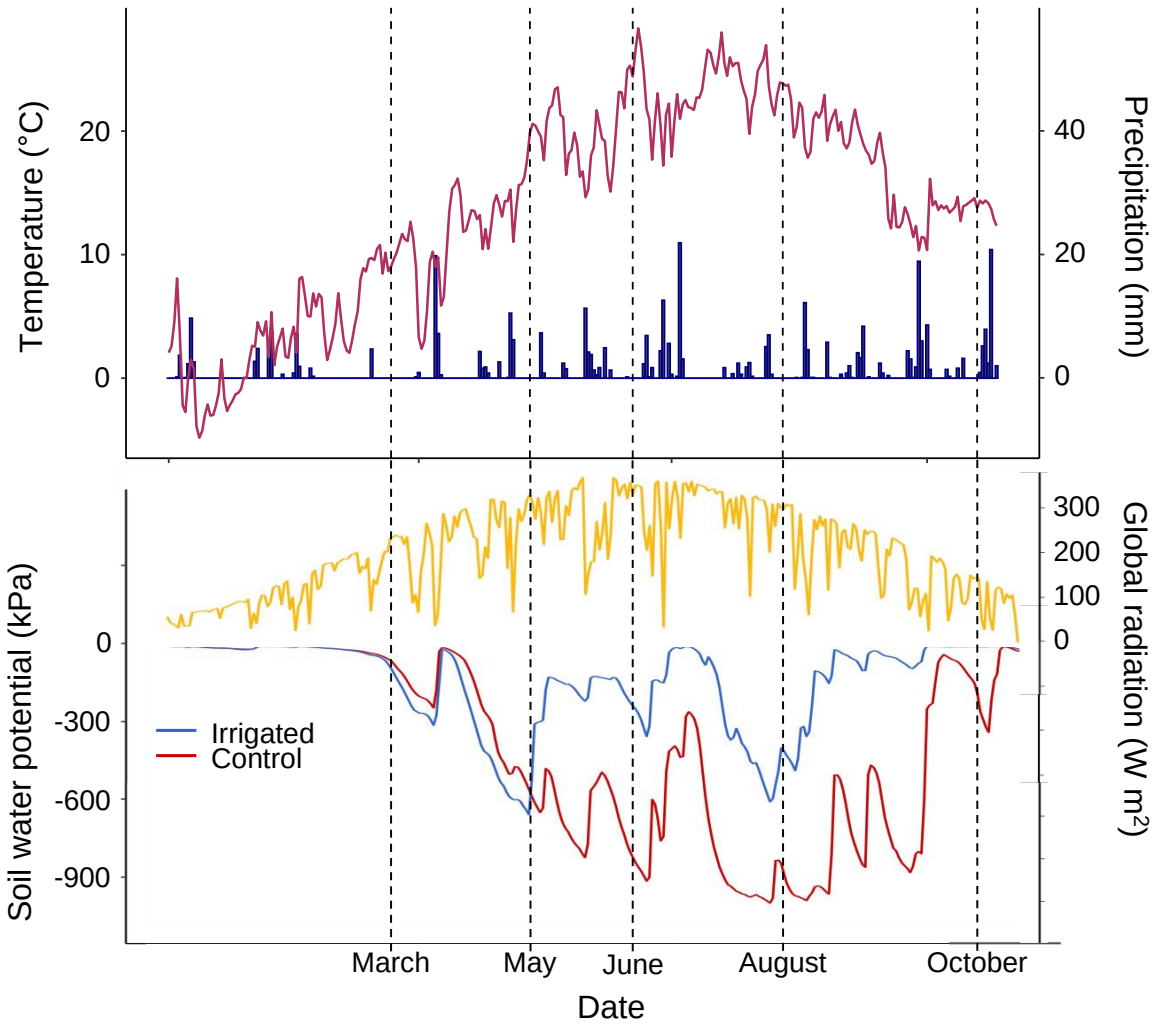

Fig. A3.1: Environmental parameters at the Pfynwald forest in 2022. Daily average air temperature (purple) and sum of precipitation (dark blue) (top panel). Mean soil water potential measured at 10 cm depth for control (red) and irrigated (blue) treatments, and daily average global radiation (yellow) (bottom panel). The dotted lines indicate the measurement campaigns.

Soil water content (SWC) and soil water potential (SWP) were recorded at 10 and 80 cm soil depth (at two locations per plot and treatment) with volumetric soil water content probes (10HS, Decagon Devices, Pullman, WA) and SWP probes (MPS-2, Decagon Devices), respectively. All plots were equipped with sensors at two locations within the plot, recording measurements at 15 min intervals.

A3.2.3 Canopy temperature

Thermal images were obtained using an uncooled infrared sensor (model DJI Zenmuse XT2) measuring between 7.5 - 13.5 µm with a 640x512 pixel resolution mounted on a DJI M210 RTK V2 drone platform (DJI Technology Co, Ltd., Shenzhen, China). During each campaign, 9 to 12 drone flights (depending on the season) were executed from 8h to 19h at 60 m aboveground with 90% side and frontal frame overlaps, resulting in a ground sampling distance (GSD) of approximately 17 cm/pixel. Drone flights took approximately 20 to 30 minutes and were conducted simultaneously with the physiological measurements (see next section). We operated drone flights under a clear sky and low wind speed to minimise variations in acquisition geometry and associated noise. Thermal radiometric images were first converted to TIFF (32-bit) using FLIR Research Studio V 2.0 software (FLIR Systems Inc., North Billerica, MA, USA) using an emissivity of 0.98.

A custom-built black painted (PNM400, Electrolube Ltd, UK) ventilated reference aluminium plate (500 x 500 x 10mm) was installed at the field site in June and allowed comparing surface temperatures extracted from drone imagery ($T_{plate\text{-}drone}$) with temperatures measured with a PT100 1/10 DIM resistance temperature sensor (GD-7124, Gräff GmbH, Germany) applied on the reference plate ($T_{plate\text{-}sensor}$).

The relationship between $T_{plate\text{-}drone}$ extracted from drone images and $T_{plate\text{-}sensor}$ measured directly by the contact sensor over a wide range of T_{air} (22-32°C) was linear: $T_{plate\text{-}sensor} = T_{plate\text{-}drone} * 1.07 + 1.07$ (R2 = 0.99) (Fig. SA3.1). This equation was applied to correct all data from the drone. In addition, we found a strong correlation between corrected T_{can} from the drone and T_{can} from one fixed IR point sensor (emissivity of 0.94, at 5 meters with a narrow field, IR120 radiometer, Campbell Scientific, Logan, UT, USA) installed on site prior to our study (R2=0.8) (Fig. SA3.1).

Images were georeferenced, geometrically calibrated, and assembled into ortho-mosaics using Agisoft PhotoScan (Agisoft LLC, St. Petersburg, Russia). In QGIS (QGIS Development Team 2022), we masked understory vegetation and bare soil temperature pixels (with the SAGA plugin), which had extreme temperature values compared to tree canopies. Individual tree canopies (mostly exposed canopy but also parts of the shaded lower canopy) were manually delineated as polygons, and the average canopy temperature for each sampled tree (n=19) was calculated using the zonal statistics plugin in QGIS (Fig. SA3.2).

A3.2.4 Diurnal course of gas exchange and temperature response curves

On each scaffold (n= 3 per treatment), we measured 2 to 5 trees (depending on tree accessibility), leading to a total of n=9 and n=10 trees in control and irrigated treatments, respectively. One to three branches from each tree were measured. Gas exchange was measured on top of the scaffolds on sun-exposed branches using portable infrared gas analysers (LI-6800,

LI-COR Inc., Lincoln, NE) equipped with a 6 cm^2 leaf cuvette on one-year-old needles. Repeated net photosynthesis (A), stomatal conductance (g_s), and transpiration (E) measurements were taken under ambient temperature and humidity (ambient VPD), measured at the local Pfynwald meteorological station and set prior to every round of measurements (lasting approx. 30 min), and ambient PAR, measured instantaneously before the measurements either with the LI-6800 or with a hand-held PAR sensor (model MQ-200X, Apogee Instruments, Logan, UT, USA). Measurements were done on the same set of needles (between 5 and 10 individual needles assembled in fascicles per branch) every 1-2 h from sunrise to sunset and after steady-state gas exchange rates had been maintained for at least 2 min. The reference CO_2 was set to 400 µmol mol^{-1}. At the end of each day, the needles were collected, and the needle area was determined using a scanner (model CanoScan LiDE 300) and the software ImageJ and it's descendant Fiji (Schindelin et al., 2012). The needle area was used to correct the recorded gas exchange values.

After each diurnal gas exchange measurement, we measured the light-saturated photosynthesis rates at different air temperatures to build temperature response curves of photosynthesis (TRC) on the same needles. TRC measurements were done during the summer months (June and August) when the irrigation was active. Specifically, we measured light-saturated photosynthesis every 1-2 h from sunrise to the peak of daily temperatures (between 12h and 15h) following the daily variation of ambient air temperatures (i.e., the air temperature inside the cuvette was set to ambient air temperature). With this method, we tracked ambient air temperature and avoided potential artefacts associated with differences between the ambient temperature experienced by the trees and the conditions in the cuvette. To avoid potential drivers that would confound the interpretation of the temperature curves, chamber VPD was set as close as possible to 1.1 kPa, CO^2 to ambient 400 µmol mol^{-1}, and saturating light to 1500 µmol m^2 s^{-1} PAR.

A3.2.5 Thermotolerance fluorescence curves

In October 2022, we collected one branch from a subset of 5 trees per treatment. We followed the protocol established by Marias et al. (2017) by collecting two needles per branch, placing them in closed plastic bags and immersing them in a covered preheated water bath for 15 min at nine temperatures ranging from 25 to 58 °C. We used different needles for each temperature and measured chlorophyll fluorescence 15 min and 24 h after exiting the bath. The 24h measurement was used to assess the long-term heat damages on thermoregulation parameters, The 15 min and 24 h measurements were similar, and thus, we only used data from the 15 min round (Fig. SA3.3). During this time, needles were stored in the dark with moist paper. Chlorophyll fluorescence was measured on these dark-adapted needles (at least 30 min in the dark) at each experimental temperature using the same portable infrared gas analysers Li-COR 6800 described previously and including a multiphase flash fluorometer. The ratio of variable to maximum fluorescence (F_v/F_m) and the steady state fluorescence (F_0) of dark-adapted leaves are considered

a good proxy for the maximum quantum efficiency of the PSII photochemistry and initial fluorescence, respectively (Genty et al., 1989) and were taken as our temperature response metric for thermotolerance. The ratio of variable to maximum fluorescence is calculated as:

$$\frac{F_v}{F_m} = \frac{F_m - F_o}{F_m} = 1 - \frac{F_o}{F_m} \qquad \text{Equation 1}$$

Where F_m is the maximum level of fluorescence. Thermotolerance curves were fitted with a third-order sigmoid function following Marias et al. (2017):

$$\frac{F_v}{F_m} = \frac{a}{1 + e^{-\frac{(x - x_0)}{b}}} \qquad \text{Equation 2}$$

Where x is the treatment temperature, and a, x_0, and b are fitting parameters. The temperature that caused a 50% reduction of F_v/F_m (T_{50}) was determined from this fitted curve. Furthermore, the tissue temperature inducing a steep rise in chlorophyll fluorescence (T_{crit}) was extracted from the thermotolerance curve as the intersection point between a regression fitted on the slow and the fast-rising part of the F_o temperature curve (Marias et al., 2017). Thermotolerance parameters were extracted from plotting F_v/F_m and F_o against bath temperatures.

A3.2.6 Leaf area index

The plot-level leaf area index (LAI) was extracted from the DIAS WEkEO platform from Copernicus (Copernicus Data and Information Access Service). A 30x30m ROI was delimited from the centre of the coordinates of each plot (n=6, 9 pixels each). Only the dates with clear sky were taken, and pixels were averaged per plot, for all dates available from 2017 to 2022 (n=118 dates).

A3.2.7 Statistical analysis

We tested the effect of irrigation on the diurnal dynamics of net photosynthesis (A), stomatal conductance (g_s), and transpiration (E) with a linear mixed-effect model (LMM, part of the lme4 package). The treatment was the fixed effect, and tree identity and hour of measurement were incorporated as random effects to account for repeated measurements on a single tree individual. The irrigation effect on the diurnal dynamic of canopy temperature (T_{can}) was also tested using an LMM with treatment as the fixed effect and plot number and hour of measurement as random effects. The leaf area index (LAI) was tested using an LMM with treatment as the fixed effect and plot number and year and day of measurement as random effects.

For the TRC, we observed no differences of A and T_{can} between June and August (as climatic conditions were similar). We, therefore, decided to pool data for these two months to improve the model performance. To estimate the optimal photosynthesis (A_{opt}, the peak of the TRC) and the optimum photosynthetic temperature (T_{opt}, temperature corresponding to A_{opt}), we fitted a nonlinear regression to the data following a second-order Gaussian function:

$$A = A_{opt} \times e^{-\frac{(T_{air}-T_{opt})^2}{2 \times c^2}} \qquad \text{Equation 3}$$

Where c is a fitting parameter.

The relationship between T_{can} and air temperature (T_{air}) was analysed across all months and for the treatments. Linear regressions were fitted and compared with the 1:1 line. Thermotolerance parameters (T_{crit} and T_{50}) were extracted from fluorescence curves for each individual measured and compared between treatments using an LMM with tree identity as a random effect. Relationships between T_{air}, T_{can}, A, incident light (Q_{in}), and treatments were analysed with regression models and ANOVA.

A3.3 Results

A3.3.1 Diurnal and seasonal variations of gas exchange

The needle-level daily net assimilation rate (A) of irrigated trees was significantly lower in May and October (p=0.02, p=0.033, respectively) and higher for the summer months (June and August, p=0.002, p=0.008, respectively) compared to the control. In contrast, there was no difference between control and irrigated trees in March (Fig. A3.2). The differences between treatments were particularly evident in the mornings of June and August when A was two times higher in irrigated than control trees (Fig. A3.2).

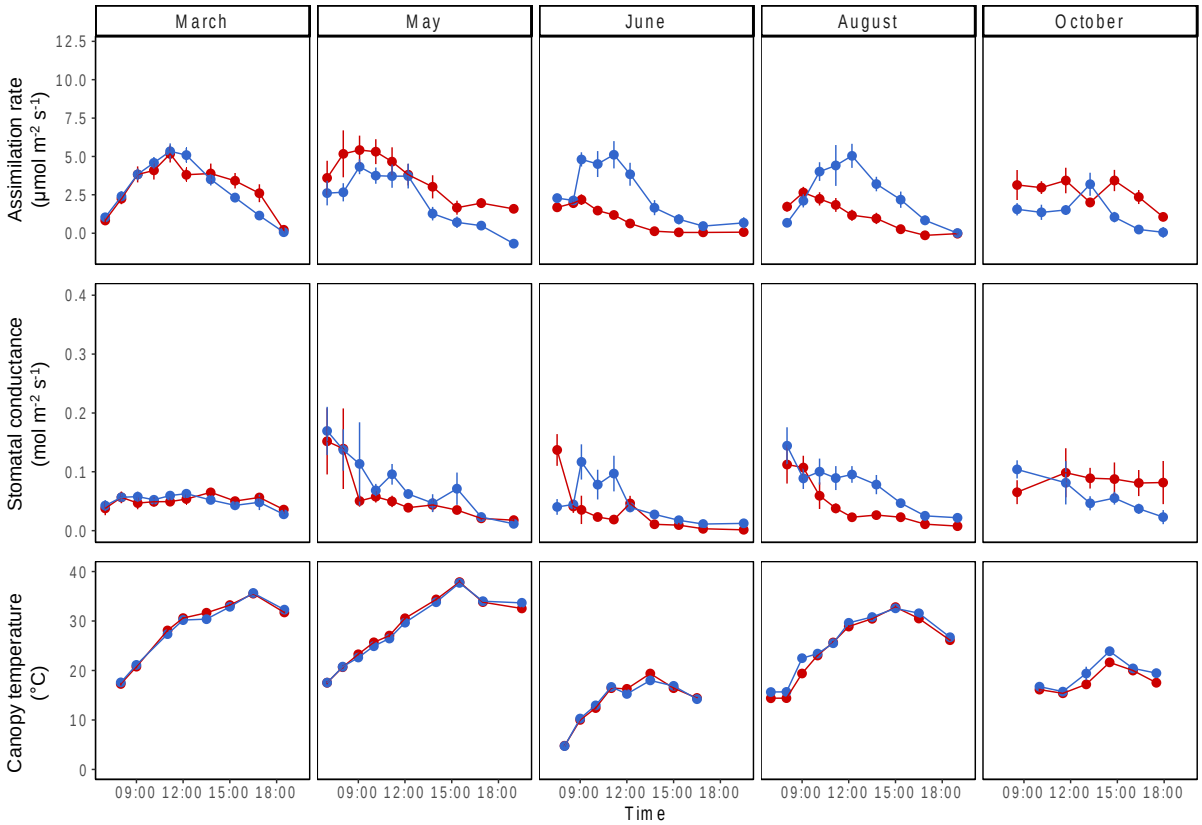

Fig. A3.2: Mean diurnal variation of net photosynthesis (top), stomatal conductance (centre) and canopy temperature (bottom) over the course of the year, in March, May, June, August and October, for control (red) and irrigated (blue) trees. N=30 (for A and g_s), N=19 (for T_{can}), error bars represent SE.

Similarly, stomatal conductance (g_s) was significantly higher in irrigated trees during the summer months (June p=0.002 and August p=0.003). During those months, just before midday, g_s was five times higher in irrigated trees than in control trees. In contrast, there were no significant differences between irrigated and control trees in March, May, or October (p>0.05).

The diurnal course of A and g_s in the two treatments did not change during the year and was the highest in the morning, between 9h and 12h. In summer, A and g_s were very low (below 2

µmol m^{-2} s^{-1} and 0.03 mol m^{-2} s^{-1}, respectively) for control trees from noon onwards. Seasonal variation of A was more accentuated in control trees than in irrigated trees, with an average maximum rate ranging from 2.2 to 5.4 µmol m^{-2} s^{-1} for control and 3.2 to 5.3 µmol m^{-2} s^{-1} for irrigated trees. In contrast, seasonal variation of g_s was more similar between control and irrigated trees, with an average maximum conductance ranging from 0.08 to 1.7 mol m^{-2} s^{-1} and from 0.08 to 1.8 mol m^{-2} s^{-1}, respectively.

Transpiration rate (E) was significantly higher in irrigated trees compared to control trees during June ($p<0.05$) and August ($p<0.001$), but there were no differences during the rest of the year (March, May, and October, $p>0.05$) (Fig. SA3.4).

A3.3.2 Canopy temperature

Daytime canopy temperature (T_{can}) did not differ between treatments throughout the year (Fig. 2; $p > 0.05$). T_{can} was higher in the summer months, with a daily average maximum of 37.8°C in June, while the lowest temperature recorded (4.8°C) was in March morning. Across all months, T_{can} had a similar diurnal pattern, which increased from the morning until it peaked in the mid to late afternoon (2 pm in March, 5 pm in August). T_{can} followed the ambient air temperature closely but exhibited lower values in the morning ($\Delta T_{leaf\text{-}air}<0$) and rapidly increased over T_{air} in the afternoon (i.e., $\Delta T_{leaf\text{-}air}>0$; Figs. A3.3 & SA3.5). The maximum $\Delta T_{leaf\text{-}air}$ recorded was +9°C in the late afternoon of June.

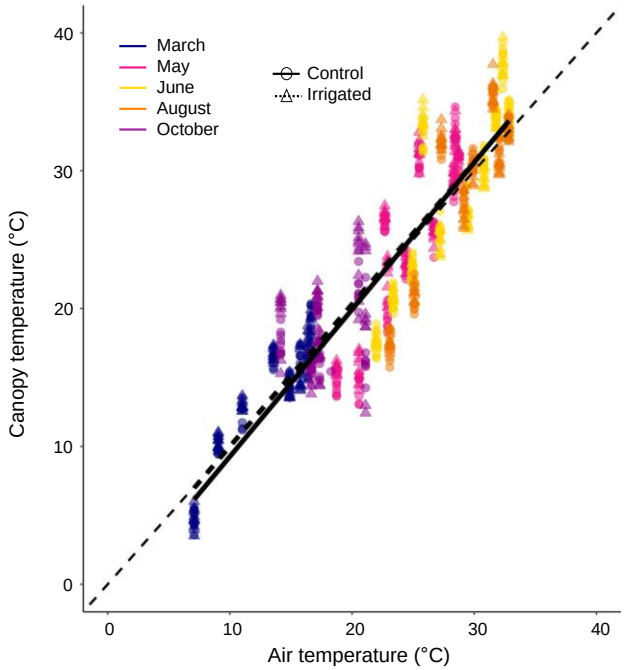

Fig. A3.3: Relationship between canopy temperature measured with the drone and infrared camera and air temperature recorded from a weather station. Colours represent months (dark blue: March, pink: May, yellow: June, orange: August, purple: October) and symbols represent treatments (circle: control, triangle: irrigated). The regression lines were fitted with a linear model. Thin dotted line is the 1:1 line. N=19 trees.

A3.3.3 Thermotolerance and photosynthetic response to temperature

Both A_{opt} (3±0.2 and 6±0.3 µmol m^{-2} s^{-1}, for control and irrigated trees, respectively) and T_{opt} (16.8± 0.9 °C and 22.3± 0.6 °C, for control and irrigated trees, respectively) were significantly higher in irrigated trees than in control trees (Fig. A3.4).

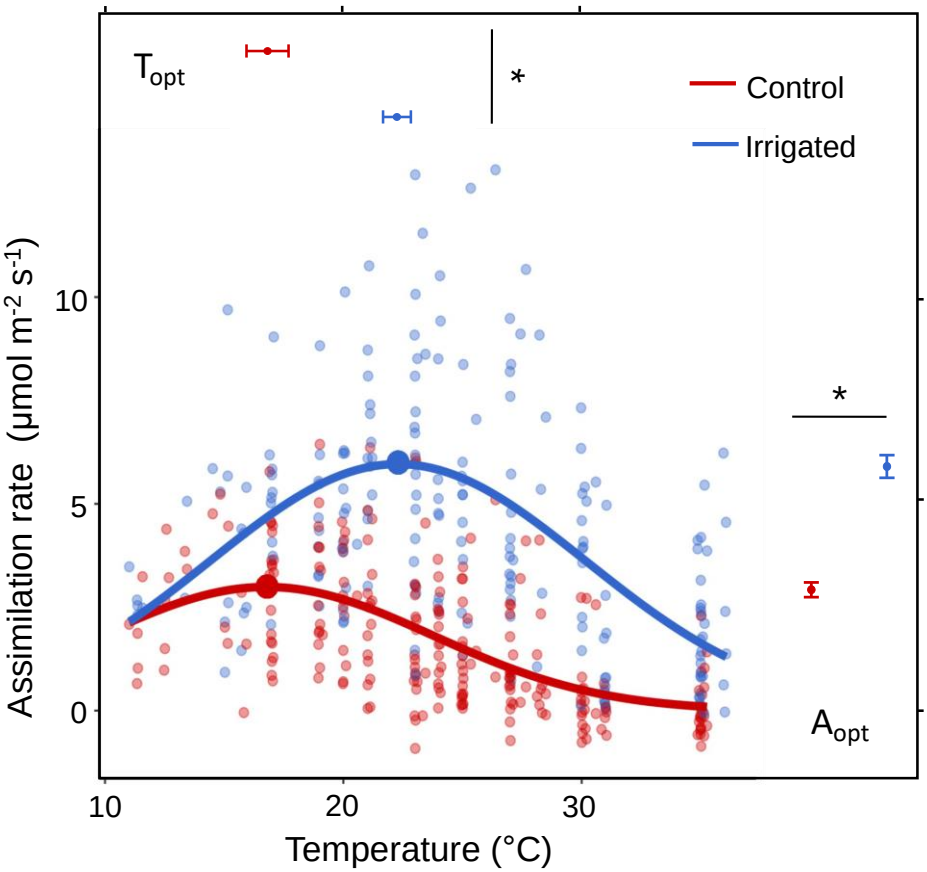

Fig. A3.4: Photosynthesis-temperature response curves for the summer months (June and August) for control (red) and irrigated (blue) trees. The inserted top and right panels show the mean differences of A_{opt} and T_{opt}, respectively, between treatments. N=30 trees, error bars represent SE.

Critical temperatures (T_{crit}) were not significantly different between treatments (mean of 45±2.4°C °C of both treatments, p=0.79; Fig. A3.5). T_{50} was also similar between treatments (mean 58.2±1.2°C of both treatments, p=1 Fig. A3.5).

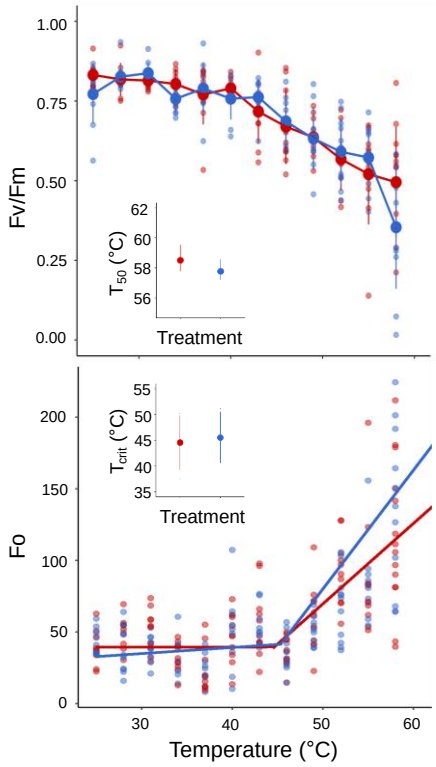

Fig. A3.5: *Thermotolerance curves measured with* Fv/Fm *and* F_o *as a function of temperature for control (red) and irrigated (blue) trees. Mean (± SE) leaf temperature that causes 50% reduction of the maximum fluorescence* (T_{50})*, and critical temperature* (T_{crit}) *are shown in the inserted panels. N=10 trees.*

A3.3.4 Morphological adjustments

The long-term plot-level leaf area index (LAI) was significantly higher in irrigated (1.8 m^2 m^{-2}) than in control (1.6 m^2 m^{-2}) trees ($p<0.05$) (Fig. A3.6). The LAI of control trees was 14% lower than irrigated trees.

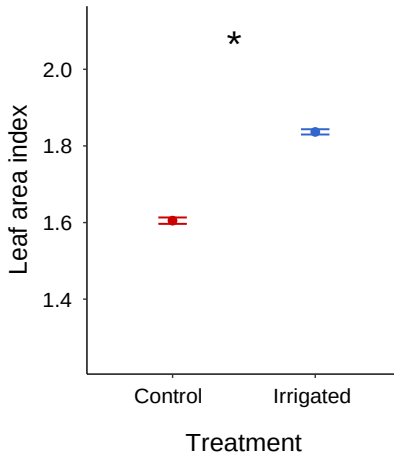

Fig. A3.6: Leaf area index for control (red) and irrigated (blue) trees. Asterisks show significant differences between treatments.

A3.4 Discussion

A3.4.1 Thermal response of photosynthesis to long-term changes in soil moisture

Despite minimal variation in canopy temperature and the limited thermal plasticity of photosynthesis between irrigated and control plots, the trees strongly adjusted their photosynthesis and stomatal conductance rates when exposed to long-term changes in soil moisture. Control trees had a 5.5 ºC lower thermal optimum (T_{opt}) and a 3 µmol m^{-2} s^{-1} lower peak photosynthesis (A_{opt}) compared to irrigated trees (Fig. A3.4), which were driven by stomatal closure during summer (Fig. A3.2). Although few studies have investigated drought impacts on photosynthetic thermal optima, our observations are similar to previous work that found reduced A_{opt} and T_{opt} in response to drought (Kumarathunge et al., 2020; Fang et al., 2023). In our study, the response of T_{opt} ($T_{opt\_irrigated}$ = 22.3°C while $T_{opt\_control}$ = 16.8°C) did not allow trees growing in drier environments to match the prevailing air temperature in the middle of the summer (maximum T_{air} of 33°C in June-August). Consequently, while the net photosynthesis (i.e., A; Fig. A3.2) was similar between treatments in March, A was severely depressed in June and August for control trees. On the other hand, A was higher in the control during non-limiting soil moisture conditions in May and October when temperatures were closer to their thermal optimum (Figs. A3.1 & A3.2). The underlying mechanism driving lower A_{opt} and T_{opt} in naturally droughted trees seems associated with stronger stomatal regulation during the summer months as g_s was significantly reduced in control trees in June and August, thereby limiting CO_2 uptake for photosynthesis, rather than shifts in photosynthetic capacity (V_{cmax} and J_{max}). Moreover, at the same study site, Schönbeck et al., (2022) found no differences in V_{cmax} and J_{max} after 16 years of irrigation, while, in accordance with our results, g_s was significantly reduced in control trees. Morphological adjustments such as smaller needles, lower stomatal density, and lower growth rate in control compared to irrigated trees have been found within a few years after the irrigation start (Dobbertin et al., 2010). This was also supported by the lower LAI found on the control plots, suggesting a sparser canopy in droughted trees (Fig. A3.6). These morphological adjustments, combined with tighter stomatal control, may allow for a more efficient control of water loss during hot and dry conditions through decreased leaf area.

Higher g_s, A_{opt}, and T_{opt} values with irrigation further suggest that trees were able to keep stomata open to maintain photosynthesis in higher temperatures and for longer periods during the day (Fig. A3.2). However, irrigated trees were also more sensitive to changes in temperature when the soil was drying. Upon irrigation stop, trees might have difficulty maintaining their A and g_s, and the release of long-term soil irrigation can reduce the sensitivity to VPD and temperature (Schönbeck et al., 2022). Indeed, we observed a strong impact of soil moisture on the seasonal and diurnal gas exchange rates. Under high VPD (e.g., in the summer), A and g_s were systematically higher in irrigated trees than in control ones, whereas water-limited trees were not sustaining high A and g_s across the whole day (Figs. A3.2 and SA3.7). Hence, the trees were

restricting gas exchange to early morning hours, when air temperatures and VPD were lower, confirming previous observations on seedlings of *P. sylvestris* (Bachofen et al., 2018). Reducing g_s and, consequently, A, is one of the first responses of plants to high VPD and drying soil. This mechanism prevents water loss through stomata and reduces the risk of cavitation inside the xylem. These findings agree with the many prior observations of reduced A and g_s during drought (e.g., Epron et al., 1992; Limousin et al., 2013; Santos et al., 2018). As expected, there was also a strong relationship between incident light (PPFD) and A (Fig. SA3.6). In our study, A of control trees peaked much earlier during the day than the irrigated trees while temperature and PPFD were still increasing (Fig. SA3.6). This suggests that, during the summer months, even though PPFD was high and capable of inducing high rates of photosynthesis, soil moisture limited A in control trees, while high VPD (>3kPa) may have constrained g_s and A in irrigated trees later in the day (Fig. SA3.7). Reduced g_s and photosynthesis due to high VPD can happen in well-irrigated plants with high temperatures impacting enzymatic activity and increasing photorespiration above a specific threshold (Zhang et al., 2021). More recently, Schönbeck et al. (2022) also showed that high VPD induced loss of xylem conductivity in well-irrigated plants, suggesting that reduced photosynthesis as a response to high VPD and temperature could prevent xylem embolism.

A3.4.2 Response of canopy temperature to long-term soil moisture changes

Soil moisture did not affect T_{can} (Fig. A3.2), and canopy temperature stayed mostly below the air temperature in the morning ($\Delta T_{can\text{-}air}<0$) and above T_{air} in the afternoon in both treatments (maximum +9°C in June). Similarly to our findings, Müller et al. (2021) also showed that $\Delta T_{can\text{-}air}$ was not dependent on soil water availability (and consequently evapotranspiration) in a pine forest subjected to long-term irrigation. Instead, they proposed that $\Delta T_{can\text{-}air}$ was regulated by leaf and canopy sensible heat flux, which is affected by needle morphology and density and the associated impacts on the heat transfer resistance. When soil moisture is low, latent heat flux is reduced by suppressed transpiration. In dry pine ecosystems, this effect leads the forest to function as a heat convector (Rotenberg & Yakir, 2010). The morphological adjustments to drought (i.e., shorter needles, lower canopy density) found in the control plots at our site (Fig. A3.6) (Dobbertin et al., 2010) may increase the surface roughness and the heat convection compared to the irrigated plots. Moreover, control plots have more exposed soil, contributing to higher plot-level temperatures due to heat radiating off the bare ground and enhancing surface irregularity. Hence, the canopy in control plots has a lower aerodynamic surface-to-air resistance, potentially generating higher values of sensible heat flux dissipation (Rotenberg & Yakir, 2010). This pattern was shown in several coniferous forests, which tended to have high surface resistance to water vapor transport, enhancing the Bowen ratio (i.e., the ratio of sensible and latent heat fluxes; Wilson et al., 2002). The partitioning between latent and sensible heat fluxes varies among forest types, with higher LE in warm and temperate wet forests and higher H in subtropical dry regions (Jung et al., 2011). While these mechanisms can be seen globally, our findings suggest that the trees growing in different

treatments within the same area could also exhibit different heating and cooling characteristics due to morphological adjustments. While irrigated trees can cool their canopy with high evapotranspiration (as shown by the higher gs and E, Figs. A3.2 & SA3.4), the similar T_{can} recorded on control plots could result from higher wind cooling and air turbulence, allowed by the shorter needles and sparser canopy. This type of non-evaporative canopy cooling in low-density and drought-prone forests could allow trees to avoid operating closer to their thermal limit compared to broadleaved ones (Muller et al., 2021).

A3.4.3 Thermotolerance response to long-term changes in soil moisture

To our knowledge, our results are one of the few to show the very high tolerance to extreme heat in *Pinus sylvestris* (T_{crit} and T_{50} of 45°C and 58.1°C, respectively, on average) and the low plasticity in thermotolerance metrics in response to soil moisture changes (Fig. A3.5). These results are slightly higher than the ones measured for the same species at a slightly colder site in Germany (T_{50} of 47.8°C, see Kunert et al., 2022). Although photosynthetic parameters (A_{opt} and T_{opt}) differed between control and irrigated trees, thermotolerance did not change between treatments, and we found no variation in A_{opt} or T_{opt} in response to temperature variation during the summer. While no previous work investigated drought impacts on thermotolerance in mature coniferous forests, the impact of drought on changes in T_{crit} and T_{50} is not in complete consensus across previous studies. The effect of long-term drought has been shown to cause a slight reduction of T_{50} while not impacting the thermal sensitivity (A_{opt}) of trees in tropical or Mediterranean forests (Gimeno et al., 2009; Grant et al., 2010; Ogaya et al., 2011; Docherty et al., 2023). In contrast, work conducted along broad temperature gradients ranging from coastal to desert environments has shown high plasticity in T_{50} driven by molecular and morphological changes such as the accumulation of heat shock proteins or the development of thicker and smaller leaves (Knight & Ackerly, 2003). The lack of shift in PSII thermotolerance in our study may stem from its absence of plasticity compared to net photosynthesis and g_s, which is quickly adjusted in response to soil moisture and VPD. In contrast to our results, Marchin et al. (2022) found that drought can increase T_{crit} by up to 2°C in tropical deciduous trees. Thermotolerance is usually higher in coniferous and evergreen than in deciduous species, as the former maintain their canopy throughout the year and possibly for several consecutive ones (Sastry & Barua, 2017). Thus, since leaves are exposed to a broader range of temperatures throughout their lifespan, they need a higher thermotolerance. Hence, a long leaf lifespan could explain why there was no difference in thermotolerance between the trees growing under irrigated and control conditions. More work would be needed to understand thermotolerance variability in coniferous species and the underlying drivers of thermotolerance plasticity, particularly in response to drought.

A3.5 Conclusion

We observed a strong downregulation of photosynthesis, stomatal conductance, and transpiration, leading to an apparent shift in photosynthetic optima (A_{opt}) and temperature optima (T_{opt}) of trees experiencing reduced soil moisture. During the hottest months, A, g_s, E, T_{opt}, and A_{opt} were higher in irrigated trees. However, there was no measurable difference in canopy temperature between treatments, supporting that shifts in photosynthetic and temperature optima were not necessarily a result of the canopies experiencing different temperatures but rather stronger stomatal regulation. Photosynthetic adjustments can be beneficial in the future as temperatures and frequency of heatwaves are predicted to increase, and trees seasonally exposed to drought may mitigate some adverse impacts by maximizing photosynthesis during colder and wetter periods. Moreover, we showed that canopy temperature was independent of soil moisture and evaporative cooling. The overall tight coupling between T_{air} and T_{can} partially allowed *Pinus sylvestris* to avoid critical temperatures (>45°C) that would otherwise degrade photosynthetic machinery, suggesting a high tolerance to the exacerbation of drought and heat stress in the future. We suggest that, while E decreased in drought-exposed trees, sensible heat fluxes stayed constant during the day, stimulating non-evaporative cooling and allowing T_{can} to remain well coupled with T_{air}. Nevertheless, large uncertainties remain regarding the impact of drought on the heat tolerance of coniferous trees and the feedback on forest carbon budget. Hence, future work should put more effort into understanding other components of the carbon balance, especially respiration responses to long-term drought (Teskey et al., 2015). Moreover, studies measuring tree thermotolerance responses to drought in situ are severely lacking but are needed to increase the accuracy of predictions in mature managed and natural forests.

A3.6 Acknowledgments

AG and CG were supported by the Sandoz Family Foundation. CG was further supported by the Swiss National Science Foundation SNSF (310030_204697). We thank Stefan Jenni, Kevin Knecht, Elias Ackermann for contributing to the data collection. The authors declared no competing interests. A.G. and C.G. conceived and designed the study; M.S. and J.G. provided and managed the Pfynwald long-term experimental platform and implemented measurement and control systems; P.D'O. and C.S. provided guidance for drone flights, measurements and analysis; A.G., C.B., A.T., M.D-G., P.S., J.D., E.M., and C.G. collected the data; A.G. analysed the data and led the writing of the manuscript; all authors critically contributed to the manuscript and gave final approval for publication. Data used in this manuscript will be available on the Dryad Digital Repository after acceptance. DOI: 10.5061/dryad.41ns1rnkj

A3.7 References

Bachofen C, Moser B, Hoch G, Ghazoul J, Wohlgemuth T. 2018. No carbon “bet hedging” in pine seedlings under prolonged summer drought and elevated CO2. Journal of Ecology 106: 31–46.

Balota M, Payne WA, Evett SR, Peters TR. 2008. Morphological and Physiological Traits Associated with Canopy Temperature Depression in Three Closely Related Wheat Lines. Crop Science 48: 1897–1910.

Birami B, Nägele T, Gattmann M, Preisler Y, Gast A, Arneth A, Ruehr NK. 2020. Hot drought reduces the effects of elevated CO2 on tree water-use efficiency and carbon metabolism. New Phytologist 226: 1607–1621.

Blonder B, Michaletz ST. 2018. A model for leaf temperature decoupling from air temperature. Agricultural and Forest Meteorology 262: 354–360.

Breshears DD, Myers OB, Meyer CW, Barnes FJ, Zou CB, Allen CD, McDowell NG, Pockman WT. 2009. Tree die-off in response to global change-type drought: mortality insights from a decade of plant water potential measurements. Frontiers in Ecology and the Environment 7: 185–189.

Buddenbaum H, Rock G, Hill J, Werner W. 2015. Measuring Stress Reactions of Beech Seedlings with PRI, Fluorescence, Temperatures and Emissivity from VNIR and Thermal Field Imaging Spectroscopy. European Journal of Remote Sensing 48: 263–282.

Cook AM, Berry N, Milner KV, Leigh A. 2021. Water availability influences thermal safety margins for leaves. Functional Ecology 35: 2179–2189.

Crous KY, Uddling J, De Kauwe MG. 2022. Temperature responses of photosynthesis and respiration in evergreen trees from boreal to tropical latitudes. New Phytologist 234: 353–374.

Dobbertin M, Eilmann B, Bleuler P, Giuggiola A, Graf Pannatier E, Landolt W, Schleppi P, Rigling A. 2010. Effect of irrigation on needle morphology, shoot and stem growth in a drought-exposed Pinus sylvestris forest. Tree Physiology 30: 346–360.

Docherty EM, Gloor E, Sponchiado D, Gilpin M, Pinto CAD, Junior HM, Coughlin I, Ferreira L, Junior JAS, da Costa ACL, et al. 2023. Long-term drought effects on the thermal sensitivity of Amazon forest trees. Plant, Cell & Environment 46: 185–198.

Drake JE, Tjoelker MG, Vårhammar A, Medlyn BE, Reich PB, Leigh A, Pfautsch S, Blackman CJ, López R, Aspinwall MJ, et al. 2018. Trees tolerate an extreme heatwave via sustained transpirational cooling and increased leaf thermal tolerance. Global Change Biology 24: 2390–2402.

Epron D, Dreyer E, Breda N. 1992. Photosynthesis of oak trees [Quercus petraea (Matt.) Liebl.] during drought under field conditions: diurnal course of net CO2 assimilation and photochemical efficiency of photosystem II. Plant, Cell and Environment 15: 809–820.

Fang L, Martre P, Jin K, Du X, van der Putten PEL, Yin X, Struik PC. 2023. Neglecting acclimation of photosynthesis under drought can cause significant errors in predicting leaf photosynthesis in wheat. Global Change Biology 29: 505–521.

Fauset S, Freitas HC, Galbraith DR, Sullivan MJP, Aidar MPM, Joly CA, Phillips OL, Vieira SA, Gloor MU. 2018. Differences in leaf thermoregulation and water use strategies between three co-occurring Atlantic forest tree species. Plant, Cell & Environment 41: 1618–1631.

Gagne MA, Smith DD, McCulloh KA. 2020. Limited physiological acclimation to recurrent heatwaves in two boreal tree species. Tree Physiology 40: 1680–1696.

Genty B, Briantais J-M, Baker NR. 1989. The relationship between the quantum yield of photosynthetic electron transport and quenching of chlorophyll fluorescence. Biochimica et Biophysica Acta (BBA) - General Subjects 990: 87–92.

Gimeno TE, Camarero JJ, Granda E, Pías B, Valladares F. 2012. Enhanced growth of Juniperus thurifera under a warmer climate is explained by a positive carbon gain under cold and drought. Tree Physiology 32: 326–336.

Gimeno TE, Pías B, Lemos-Filho JP, Valladares F. 2009. Plasticity and stress tolerance override local adaptation in the responses of Mediterranean holm oak seedlings to drought and cold. Tree Physiology 29: 87–98.

Grant OM, Tronina Ł, Ramalho JC, Kurz Besson C, Lobo-do-Vale R, Santos Pereira J, Jones HG, Chaves MM. 2010. The impact of drought on leaf physiology of Quercus suber L. trees: comparison of an extreme drought event with chronic rainfall reduction. Journal of Experimental Botany 61: 4361–4371.

Grossiord C, Buckley TN, Cernusak LA, Novick KA, Poulter B, Siegwolf RTW, Sperry JS, McDowell NG. 2020. Plant responses to rising vapor pressure deficit. New Phytologist 226: 1550–1566.

Gunderson CA, O’hara KH, Campion CM, Walker AV, Edwards NT. 2010. Thermal plasticity of photosynthesis: the role of acclimation in forest responses to a warming climate. Global Change Biology 16: 2272–2286.

Herzog C, Steffen J, Pannatier EG, Hajdas I, Brunner I. 2014. Nine Years of Irrigation Cause Vegetation and Fine Root Shifts in a Water-Limited Pine Forest. PLOS ONE 9: e96321.

Hikosaka K, Ishikawa K, Borjigidai A, Muller O, Onoda Y. 2006. Temperature acclimation of photosynthesis: mechanisms involved in the changes in temperature dependence of photosynthetic rate. Journal of Experimental Botany 57: 291–302.

Jung M, Reichstein M, Margolis HA, Cescatti A, Richardson AD, Arain MA, Arneth A, Bernhofer C, Bonal D, Chen J, et al. 2011. Global patterns of land-atmosphere fluxes of carbon dioxide, latent heat, and sensible heat derived from eddy covariance, satellite, and meteorological observations. Journal of Geophysical Research: Biogeosciences 116.

Kitudom N, Fauset S, Zhou Y, Fan Z, Li M, He M, Zhang S, Xu K, Lin H. 2022. Thermal safety margins of plant leaves across biomes under a heatwave. Science of The Total Environment 806: 150416.

Knight CA, Ackerly DD. 2002. An ecological and evolutionary analysis of photosynthetic thermotolerance using the temperature-dependent increase in fluorescence. Oecologia 130: 505–514.

Knight CA, Ackerly DD. 2003. Evolution and plasticity of photosynthetic thermal tolerance, specific leaf area and leaf size: congeneric species from desert and coastal environments. New Phytologist 160: 337–347.

Kumarathunge DP, Drake JE, Tjoelker MG, López R, Pfautsch S, Vårhammar A, Medlyn BE. 2020. The temperature optima for tree seedling photosynthesis and growth depend on water inputs. Global Change Biology 26: 2544–2560.

Kunert N, Hajek P, Hietz P, Morris H, Rosner S, Tholen D. 2022. Summer temperatures reach the thermal tolerance threshold of photosynthetic decline in temperate conifers. Plant Biology 24: 1254–1261.

Leigh A, Sevanto S, Ball MC, Close JD, Ellsworth DS, Knight CA, Nicotra AB, Vogel S. 2012. Do thick leaves avoid thermal damage in critically low wind speeds? New Phytologist 194: 477–487.

Leigh A, Sevanto S, Close J d., Nicotra A b. 2017. The influence of leaf size and shape on leaf thermal dynamics: does theory hold up under natural conditions? Plant, Cell & Environment 40: 237–248.

Limousin J-M, Bickford CP, Dickman LT, Pangle RE, Hudson PJ, Boutz AL, Gehres N, Osuna JL, Pockman WT, Mcdowell NG. 2013. Regulation and acclimation of leaf gas exchange in a piñon–juniper woodland exposed to three different precipitation regimes. Plant, Cell & Environment 36: 1812–1825.

Limousin J-M, Longepierre D, Huc R, Rambal S. 2010. Change in hydraulic traits of Mediterranean Quercus ilex subjected to long-term throughfall exclusion. Tree Physiology 30: 1026–1036.

Marchin RM, Backes D, Ossola A, Leishman MR, Tjoelker MG, Ellsworth DS. 2022. Extreme heat increases stomatal conductance and drought-induced mortality risk in vulnerable plant species. Global Change Biology 28: 1133–1146.

Marias DE, Meinzer FC, Woodruff DR, McCulloh KA. 2017. Thermotolerance and heat stress responses of Douglas-fir and ponderosa pine seedling populations from contrasting climates. Tree Physiology 37: 301–315.

Monteith JL, Unsworth MH. 2013. Principles of environmental physics: plants, animals, and the atmosphere. Amsterdam ; Boston: Elsevier/Academic Press.

Muller JD, Rotenberg E, Tatarinov F, Oz I, Yakir D. 2021. Evidence for efficient nonevaporative leaf-to-air heat dissipation in a pine forest under drought conditions. New Phytologist 232: 2254–2266.

Ogaya R, Peñuelas J, Asensio D, Llusià J. 2011. Chlorophyll fluorescence responses to temperature and water availability in two co-dominant Mediterranean shrub and tree species in a long-term field experiment simulating climate change. Environmental and Experimental Botany 71: 123–127.

O'sullivan OS, Heskel MA, Reich PB, Tjoelker MG, Weerasinghe LK, Penillard A, Zhu L, Egerton JJG, Bloomfield KJ, Creek D, et al. 2017. Thermal limits of leaf metabolism across biomes. Global Change Biology 23: 209–223.

Pachauri RK, Mayer L, Intergovernmental Panel on Climate Change (Eds.). 2015. Climate change 2014: synthesis report. Geneva, Switzerland: Intergovernmental Panel on Climate Change.

Panek JA, Goldstein AH. 2001. Response of stomatal conductance to drought in ponderosa pine: implications for carbon and ozone uptake. Tree Physiology 21: 337–344.

Peguero-Pina JJ, Vilagrosa A, Alonso-Forn D, Ferrio JP, Sancho-Knapik D, Gil-Pelegrín E. 2020. Living in Drylands: Functional Adaptations of Trees and Shrubs to Cope with High Temperatures and Water Scarcity. Forests 11: 1028.

Perez TM, Feeley KJ. 2020. Photosynthetic heat tolerances and extreme leaf temperatures. Functional Ecology 34: 2236–2245.

Ribeiro RV, Machado EC, Oliveira RF. 2004. Growth- and leaf-temperature effects on photosynthesis of sweet orange seedlings infected with Xylella fastidiosa. Plant Pathology 53: 334–340.

Rotenberg E, Yakir D. 2010. Contribution of Semi-Arid Forests to the Climate System. Science 327: 451–4.

Santos VAHF dos, Ferreira MJ, Rodrigues JVFC, Garcia MN, Ceron JVB, Nelson BW, Saleska SR. 2018. Causes of reduced leaf-level photosynthesis during strong El Niño drought in a Central Amazon forest. Global Change Biology 24: 4266–4279.

Sastry A, Barua D. 2017. Leaf thermotolerance in tropical trees from a seasonally dry climate varies along the slow-fast resource acquisition spectrum. Scientific Reports 7: 11246.

Sastry A, Guha A, Barua D. 2018. Leaf thermotolerance in dry tropical forest tree species: relationships with leaf traits and effects of drought. AoB PLANTS 10: plx070.

Schindelin J, Arganda-Carreras I, Frise E, Kaynig V, Longair M, Pietzsch T, Preibisch S, Rueden C, Saalfeld S, Schmid B, et al. 2012. Fiji: an open-source platform for biological-image analysis. Nature Methods 9: 676–682.

Schönbeck L, Grossiord C, Gessler A, Gisler J, Meusburger K, D'Odorico P, Rigling A, Salmon Y, Stocker BD, Zweifel R, et al. 2022. Photosynthetic acclimation and sensitivity to short- and long-term environmental changes in a drought-prone forest. Journal of Experimental Botany 73: 2576–2588.

Schreiber U, Berry JA. 1977. Heat-induced changes of chlorophyll fluorescence in intact leaves correlated with damage of the photosynthetic apparatus. Planta 136: 233–238.

Sendall KM, Reich PB, Zhao C, Jihua H, Wei X, Stefanski A, Rice K, Rich RL, Montgomery RA. 2015. Acclimation of photosynthetic temperature optima of temperate and boreal tree species in response to experimental forest warming. Global Change Biology 21: 1342–1357.

Slot M, Winter K. 2017. In situ temperature response of photosynthesis of 42 tree and liana species in the canopy of two Panamanian lowland tropical forests with contrasting rainfall regimes. New Phytologist 214: 1103–1117.

Smith NG, Dukes JS. 2017. Short-term acclimation to warmer temperatures accelerates leaf carbon exchange processes across plant types. Global Change Biology 23: 4840–4853.

Sperlich D, Chang CT, Peñuelas J, Sabaté S. 2019. Responses of photosynthesis and component processes to drought and temperature stress: are Mediterranean trees fit for climate change? Tree Physiology 39: 1783–1805.

Still CJ, Page G, Rastogi B, Griffith DM, Aubrecht DM, Kim Y, Burns SP, Hanson CV, Kwon H, Hawkins L, et al. 2022. No evidence of canopy-scale leaf thermoregulation to cool leaves below air temperature across a range of forest ecosystems. Proceedings of the National Academy of Sciences 119: e2205682119.

Still CJ, Rastogi B, Page GFM, Griffith DM, Sibley A, Schulze M, Hawkins L, Pau S, Detto M, Helliker BR. 2021. Imaging canopy temperature: shedding (thermal) light on ecosystem processes. New Phytologist 230: 1746–1753.

Tan Z-H, Zeng J, Zhang Y-J, Slot M, Gamo M, Hirano T, Kosugi Y, da Rocha HR, Saleska SR, Goulden ML, et al. 2017. Optimum air temperature for tropical forest photosynthesis: mechanisms involved and implications for climate warming. Environmental Research Letters 12: 054022.

Tarvainen L, Wittemann M, Mujawamariya M, Manishimwe A, Zibera E, Ntirugulirwa B, Ract C, Manzi OJL, Andersson MX, Spetea C, et al. 2022. Handling the heat – photosynthetic thermal stress in tropical trees. New Phytologist 233: 236–250.

Teskey R, Wertin T, Bauweraerts I, Ameye M, Mcguire MA, Steppe K. 2015. Responses of tree species to heat waves and extreme heat events: Tree response to extreme heat. Plant, Cell & Environment 38: 1699–1712.

Wahid A, Gelani S, Ashraf M, Foolad MR. 2007. Heat tolerance in plants: An overview. Environmental and Experimental Botany 61: 199–223.

Wilson KB, Baldocchi DD, Aubinet M, Berbigier P, Bernhofer C, Dolman H, Falge E, Field C, Goldstein A, Granier A, et al. 2002. Energy partitioning between latent and sensible heat flux during the warm season at FLUXNET sites. Water Resources Research 38: 30-1-30–11.

Wittemann M, Andersson M, Ntirugulirwa B, Tarvainen L, Wallin G, Uddling J. 2022. Temperature acclimation of net photosynthesis and its underlying component processes in four tropical tree species. Tree Physiology 42.

Wright IJ, Dong N, Maire V, Prentice IC, Westoby M, Díaz S, Gallagher RV, Jacobs BF, Kooyman R, Law EA, et al. 2017. Global climatic drivers of leaf size. Science 357: 917–921.

Yamori W, Hikosaka K, Way DA. 2014. Temperature response of photosynthesis in C3, C4, and CAM plants: temperature acclimation and temperature adaptation. Photosynthesis Research 119: 101–117.

Zhang P, Yang X, Chen Y, Wei Z, Liu F. 2021. Dissecting the combined effects of air temperature and relative humidity on water-use efficiency of barley under drought stress. Journal of Agronomy and Crop Science 207: 606–617.

Zhu L, Bloomfield KJ, Hocart CH, Egerton JJG, O'Sullivan OS, Penillard A, Weerasinghe LK, Atkin OK. 2018. Plasticity of photosynthetic heat tolerance in plants adapted to thermally contrasting biomes. Plant, Cell & Environment 41: 1251–1262.

A3.8 Supporting figures

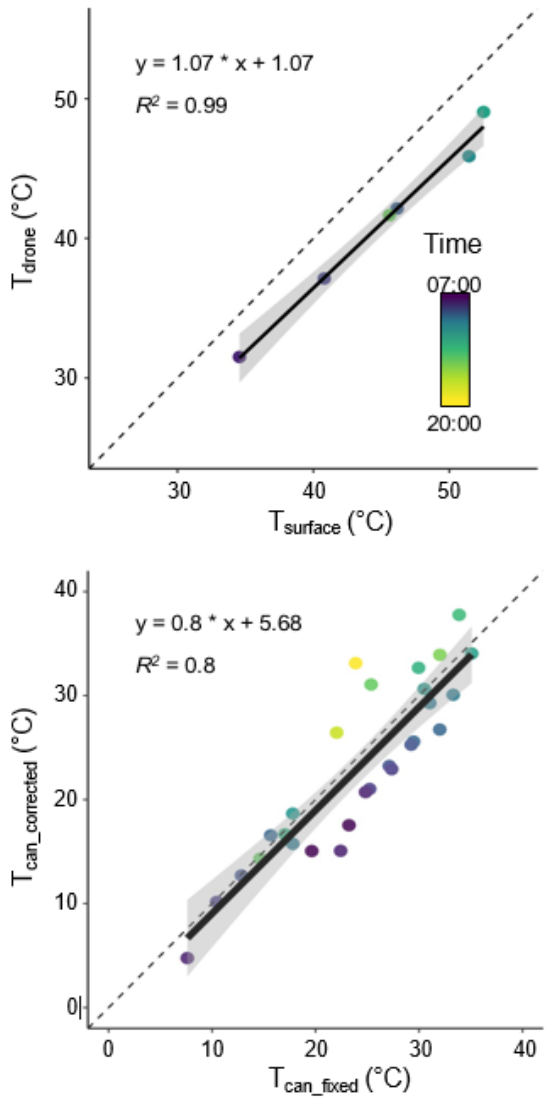

Fig. SA3.1: Relationship between the black reference plate surface temperature recorded with contact temperature sensor (*Tsurface*) and with the drone (*Tdrone*) at the different time during the day (top panel). Relationship between the temperature measures with the fixed IR cameras (*Tcan_fixed*) and the corrected temperature measured with the IR camera from the drone (*Tcan_corrected*) at the different time during the day (bottom panel). The bold line represents the linear regression, and the shaded part are the confidence intervals of the regression. The dotted line represents the 1:1 line. For each regression, the equation, and the coefficient of determination (R^2) is reported on the graph.

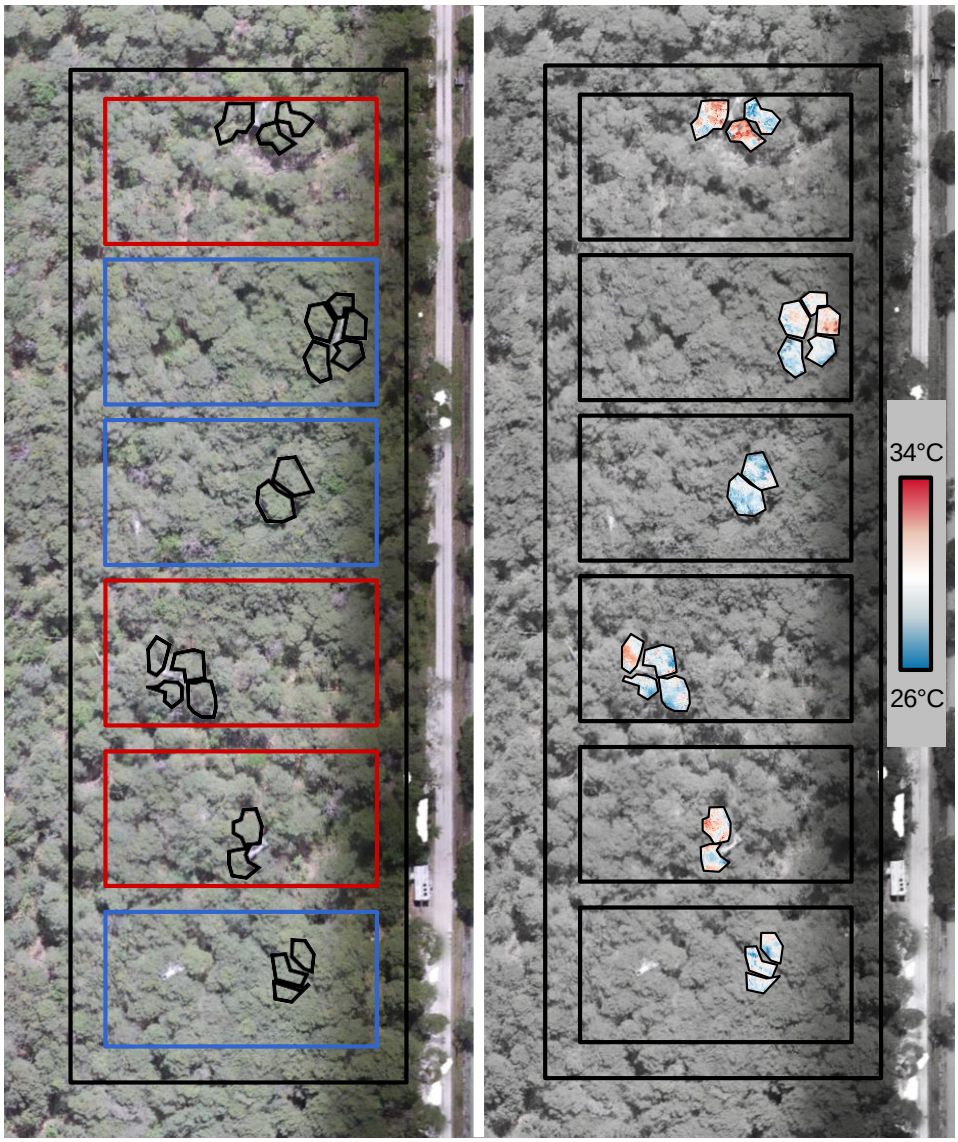

Fig. SA3.2: Experimental field site of Pfynwald forest showing on the left panel, the irrigated (blue) and control (red) plots with the measured trees (polygons). Right panel shows thermal imaging of canopy temperature in these plots in August 2022 at 1pm.

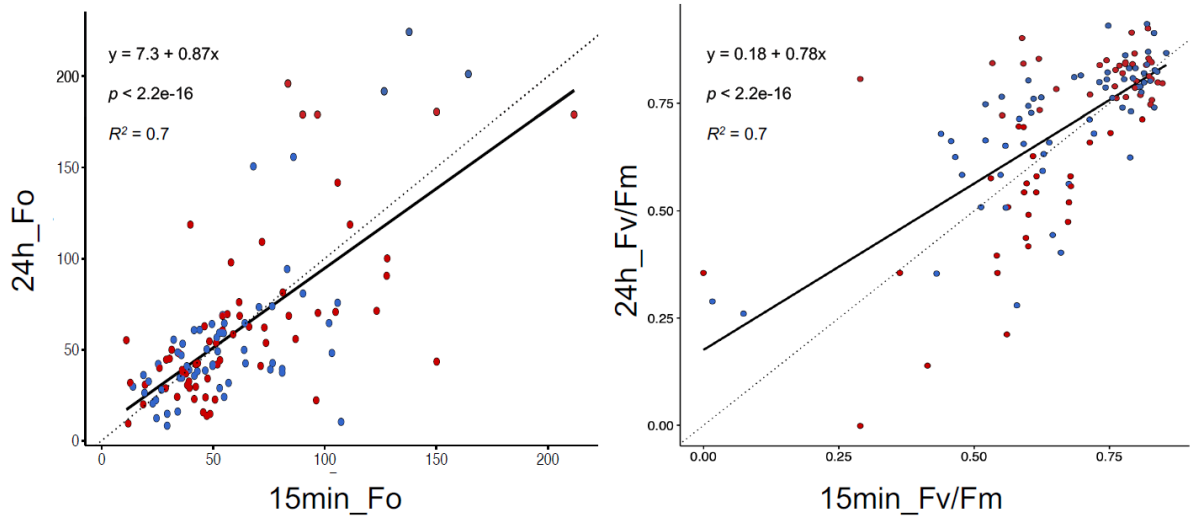

Fig. SA3.3: Relationship between fluorescence measurements taken on dark-acclimated needles 15min and 24h after exiting the water bath.

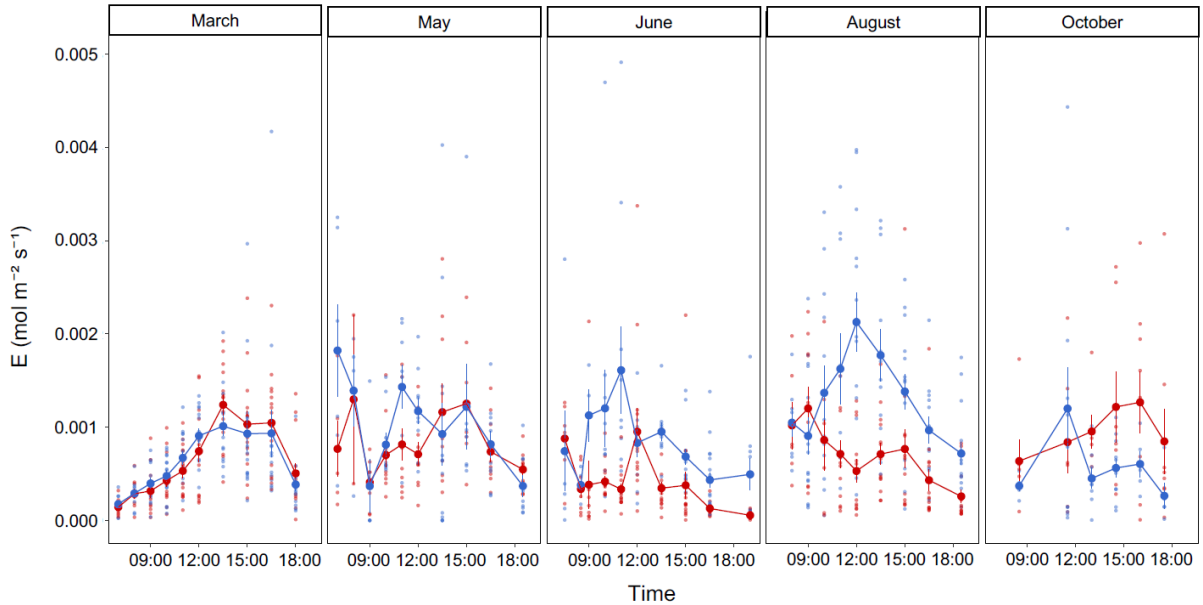

Fig. SA3.4: Mean diurnal variation of leaf-level transpiration rate (E, mol m^{-2} s^{-1}) over the course of the year, in March, May, June, August and October, for control (red) and irrigated (blue) trees. N=30, error bars represent SE.

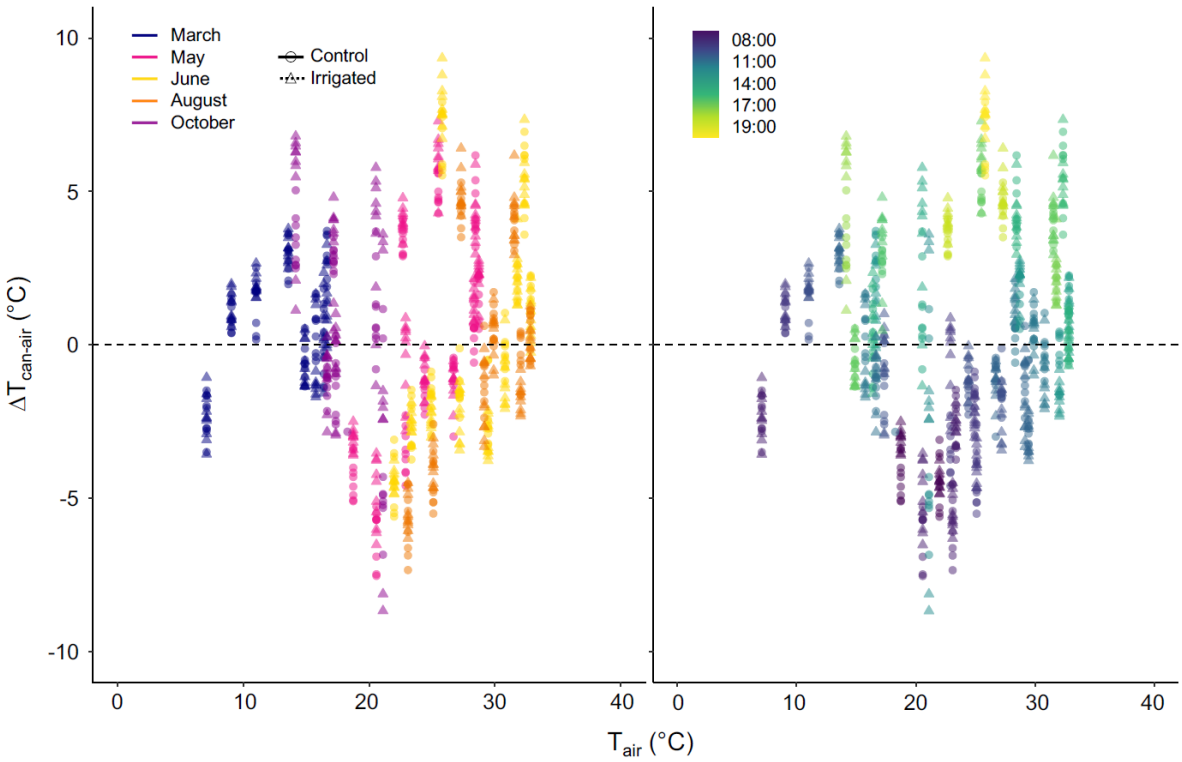

Fig. SA3.5: Difference between canopy and air temperatures ($\Delta T_{can\text{-}air}$) in function of the air temperature (T_{air}), at different months (left) and at different hours of the day (right).

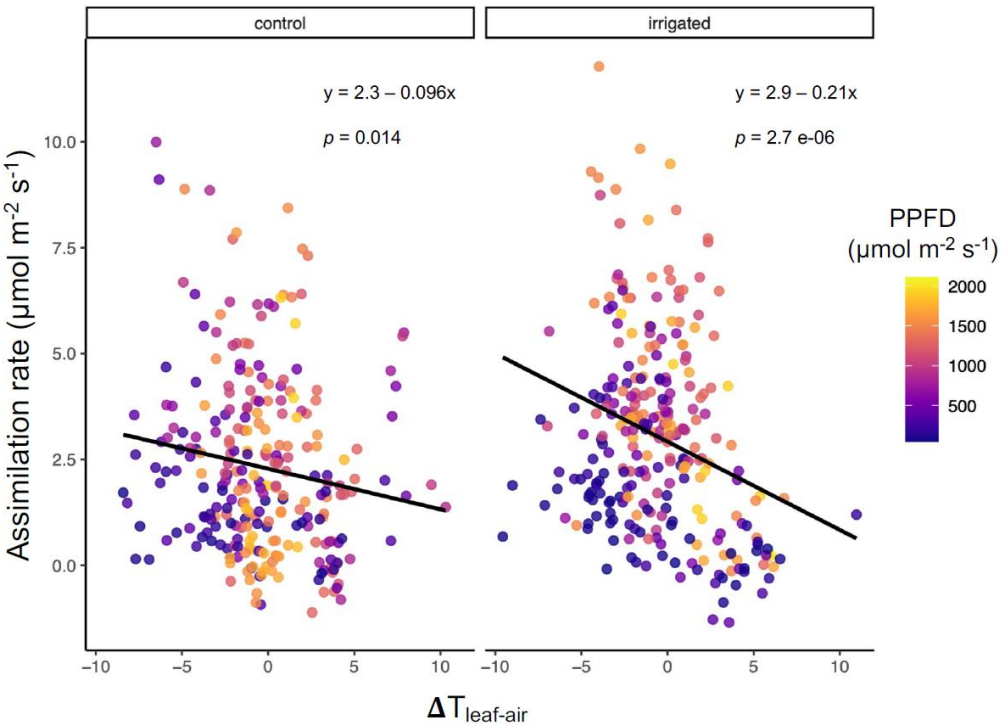

Fig. SA3.6: Relationship between photosynthesis and difference of temperatures between leaf and air in irrigated and control trees. Each point represents one tree and is colored by the photosynthetic photon flux density at the time of measurement.

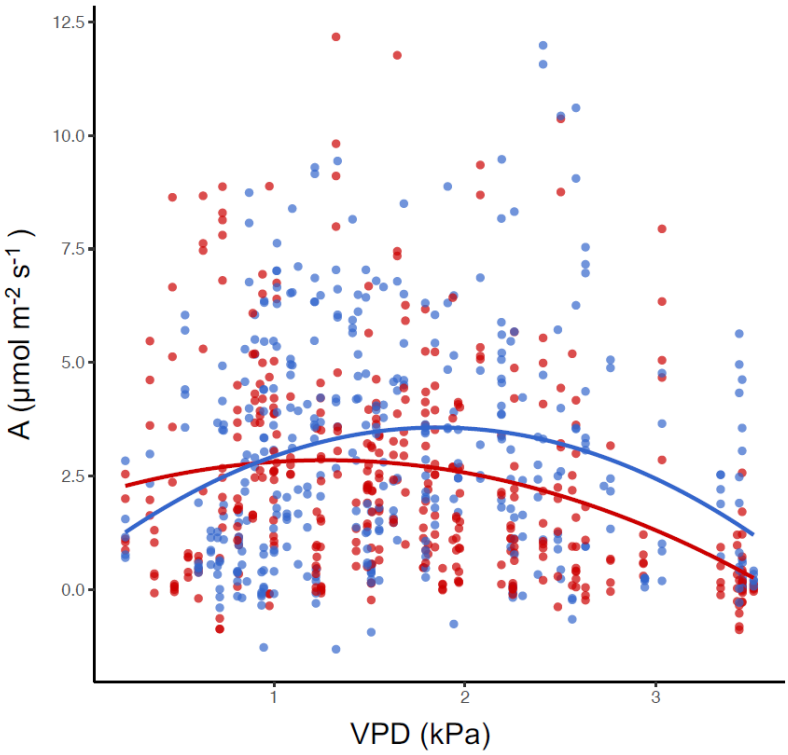

Fig. SA3.7: Relationship between photosynthesis (*A*) and vapor pressure deficit (*VPD*) for irrigated (blue) and control (red) trees.

Curriculum vitae

Eugénie Mas

Plant Ecology Research Laboratory, EPFL & Swiss Federal Institute for Forest, Snow, and Landscape Research WSL, Lausanne, Switzerland

eugenie.mas@epfl.ch; +33 (0)67 978 46 78

https://orcid.org/0009-0008-1615-7738

https://scholar.google.com/citations?user=aSt7UxIAAAAJ&hl=fr&oi=ao

Education

Feb 2024: Ph.D. in tree ecophysiology at EPFL & WSL, Lausanne (Switzerland). Title: *Role of biodiversity on the water relations of trees under warmer and drier climate*. Supervisors: Prof. C. Grossiord & Prof. F. Valladares

Sep 2019: Master of Agronomy, Environment, Landscape, Territory, and Forest at AgroParistech, Nancy (France)

Sep 2017: Bachelor of Biological and Geological Sciences at the University of Paris Cité, Paris (France)

Professional experience

Mar 2020-Feb 2024: Ph.D. student at EPFL & WSL, Lausanne (Switzerland)

Apr 2022-Jul 2022: Visiting scientist at CEAM (host: Dr. A. Vilagrosa), University of Alicante (Spain)

Sep 2020: Visiting scientist at INRAE (host: Dr. H. Cochard), Clermont-Ferrand (France)

Oct 2019-Jan 2020: Research intern at WSL, Birmensdorf (Switzerland)

Mar 2019-Aug 2019: Graduate intern at WSL, Birmensdorf (Switzerland)

Apr 2018-Jun 2018: Graduate intern at INRAE, Nancy (France)

Publication list

- Schönbeck L.C., Schuler P., Lehmann M.M., **Mas E.**, Mekarni L., Pivovaroff A.L., Turberg P., Grossiord C.(2022), Increasing temperature and vapor pressure deficit lead to hydraulic damages in the absence of soil drought, *Plant, Cell & Environment* 45 (11), 3275-3289, https://doi.org/10.1111/pce.14425
- Grossiord C., Bachofen C., Gisler J., **Mas E.**, Vitasse Y., Didion-Gency M. (2022), Warming may extend tree growing seasons and compensate for reduced carbon uptake during dry periods, *Journal of Ecology* 110 (7), 1575-1589, https://doi.org/10.1111/1365-2745.13892
- Gauthey, A., Bachofen, C., Deluigi, J., Didion-Gency, M., Gisler, J., **Mas, E.**, Schaub, M., Schuler, P., Still, C. J., Tunas, A., & Grossiord, C. (2023). Absence of canopy temperature variation despite stomatal adjustment in Pinus sylvestris under multidecadal soil moisture manipulation. *New Phytologist*, *240*(1), 127-137, https://doi.org/10.1111/nph.19136
- **Mas E.**, Cochard, H., Deluigi J., Didion-Gency M., Martin-StPaul N., Morcillo L.J., Valladares F., Vilagrosa A., Grossiord C. (2023), Interactions between beech and oak seedlings can modify the effects of hotter droughts and the onset of hydraulic failure, *New Phytologist*, https://doi.org/10.1111/nph.19358

Under review or close to submission:

- **Mas E.**, Vilagrosa A., Morcillo L., Saurer M., Valladares F., Grossiord C., Droughts in Mediterranean forests are not alleviated by diversity-driven water source partitioning, under review at *Journal of Ecology. Authorea.* October 25, 2023., DOI: 10.22541/au.169825330.00810725/v1
- **Mas E.**, Vilagrosa A., Morcillo L., Valladares F., Grossiord C., Mixing oak and pine trees in Mediterranean forests increases hydraulic dysfunctions, under review at *Plant Biology*
- Gauthey A., Bachofen C., Chin A., Cochard H., Gisler J., **Mas E.**, Meusburger K., Peters R.L., Schaub M., Tunas A., Zweifel R., Grossiord C., Twenty years of drought acclimation is driven by sparser canopies and not by hydraulic plasticity in a *Pinus sylvestris* forest. under review at *Journal of Experimental Botany*

Awards & Grants

- **ECR travel grant** to attend the 5th Xylem International Conference in Germany (**€ 300**), Mar 2022.
- **EDCE Mobility Award**, travel grant (**CHF 2'000**), Nov 2021.

Invited talks & conferences

- Oct 2023: Mas E., Droughts in Mediterranean forests are not alleviated by diversity-driven water source partitioning. Swiss Forest Lab Science Day, ETH Zurich, Switzerland **(oral presentation)**
- Sept 2023: Mas E., Vilagrosa A., Morcillo L., Saurer M., Valladares F. Grossiord C., Can biodiversity make our forest more resilient to climate change?, ENAC Research Day & EDCE Research Day, EPFL Lausanne, Switzerland **(poster presentation)**
- Aug 2023: Mas E., Cochard H., Deluigi J., Didion-Gency M., Martin-St-Paul N., Morcillo L., Valladares F., Vilagrosa A., Grossiord C., The power of diversity: does mixing tree species boost heat and drought tolerance?, Annual meeting of the Ecological Society of America (ESA), Portland, USA **(oral presentation)**
- Apr 2023: Mas E., Mixed forests, a wise choice for the future? A study in the Mediterranean forest, Doctoral day of forest, Blois, France **(oral presentation)**
- Jun 2022: Mas E., Impact of tree species interactions on tree water relations under a warmer and drier climate, Seminar on Ecology, University of Alicante, Spain **(oral presentation)**
- Oct 2022: Mas E., Didion-Gency M., Valladares F., Vilagrosa A., Grossiord C., Soil drought has a more decisive impact than temperature on leaf hydraulic traits in temperate trees, the 5th Xylem International Conference (XIM5), Würzburg, Germany **(oral presentation)**

Teaching

- Mar 2020-Jun 2023: Fundamental of Ecology (ENV-220), Teaching assistant, Bachelor degree, EPFL, Lausanne (Switzerland)
- Apr 2021-Aug 2021: Supervised one master student at EPFL, Lausanne (Switzerland)

Research Experiences & Skills

- Experience using Plant Biology instrumentation including portable photosynthesis analysers (LI6800 & 6400, LICOR), Fluorometers, Scholander Pressure Chambers, Sap flow sensors (Heat Ratio & Thermal Dissipation Methods), datalogger programming (Campbell CR1000), hydraulic techniques (i.e., flowmeters for measuring xylem hydraulic conductivity), cryogenic water extraction (to determine plant water uptake depth using soil isotopic profiling), Leaf Area Index meters (LAI600, LICOR).
- Experience in biogeochemical (i.e., soil ammonium and potassium content) and biochemical measurements (i.e., wood nitrate content)
- Experience in collecting and processing plant material (e.g., wood cores, forest inventories) for numerous scientific projects of WSL, EPFL, and INRAE in Mediterranean (Spain), alpine (Switzerland), and temperate forests (France)
- Skilled in the use of statistical programs (R software), including the use of large datasets

Media & community outreach

- Jul 2023: Short video: "Tree's geopolitics: how to create peaceful forests", *Popscience Heidi news*, https://www.heidi.news/sciences/geopolitique-des-arbres-comment-avoir-des-forets-harmonieuses-video
- Mar 2023: Finalist at the "My thesis in 3 minutes" contest, EPFL, Lausanne (Switzerland), https://www.youtube.com/watch?v=9ncyCX5BOH0
- Dec 2021: Short video to advertise STEM science to young girls, EPFL, Lausanne (Switzerland)

Languages

French: Native
English: Fluent
Spanish: Basic

References

- Prof. Charlotte Grossiord (EPFL, Switzerland), charlotte.grossiord@epfl.ch
- Prof. Fernando Valladares (MNCN-CSIC, Spain), valladares@ccma.csic.es
- Dr. Alberto Vilagrosa (CEAM, Spain), a.vilagrosa@ua.es
- Dr. Hervé Cochard (INRAE, France), herve.cochard@inrae.fr